Genetic mapping and molecular characterisation of Russian wheat aphid resistance loci in wheat

By

Surendran Selladurai

B.Sc in Agriculture (1st Class); PG. Dip. (Biotech. and Mol. Biol.)

The thesis is presented in fulfilment of the requirements for the degree of Doctor of Philosophy

School of Veterinary and Life Sciences,

Murdoch University, Western Australia

April 2016

This thesis was supported by Murdoch University (Western Australia) providing infrastructure at the State Agricultural Biotechnology Centre (SABC) and funds through Murdoch University Research Scholarship. A co-contribution was provided by a Grains Industry Research and Development Corporation.

Declaration

I declare that this thesis is my own account of my research and contains as its main content work which has not been previously submitted for a degree at any tertiary education institute.

Surendran Selladurai

Date:

Abstract

The Russian wheat aphid (RWA, *Diuraphis noxia* Kurdmojov) is considered as one of the most destructive pest of wheat around the world, causing significant yield loss in wheat cultivation. A continuous process of searching for novel resistance loci (*Dn*) to combat evolving new RWA biotypes has been successful in providing RWA resistance to breeding programs. Australia was declared as a RWA free country but Infestation of RWA was first time reported in Tarlee, South Australia in April, 2016. A novel resistance source, PI94365 with expressing resistance to several biotypes found in other countries was selected to incorporate its resistance into the Australian cultivar EGA Gregory. A double haploid (DH) population developed through the microspore technique was phenotyped in South Africa, Turkey and Morocco with respective biotypes. A genetic linkage map was constructed with 4053 molecular markers including simple sequence repeats (SSR), genome by sequencing (GBS) and Diversity array technology (DArT) molecular markers. Major QTLs to RWA resistance were mapped on 1DS, 7DS and 7BL and minor QTLs were mapped on 3BL, 4AS and 4DL. POPSEQ genetic map distances for the QTLs identified on chromosomes 1DS and 7DS were determined by comparative genomics studies with published consensus and POPSEQ maps. A large number of molecular markers have been identified in the region of RWA resistance loci for the marker assisted plant breeding.

Proteomics studies in the absence of live aphids (due to quarantine restriction in Australia) were carried out in order to reveal the resistance mechanism driven by constitutive genes. Ten proteins were significantly differentially expressed between resistance and susceptible lines selected from the double haploid population that was mapped in detail through haplotype analysis. These proteins were annotated using the current wheat genome assembly and functional annotation in relation to RWA resistance.

Studies identified several induced proteins with RWA infestations. Differentially expressed genes identified in these studies annotated to the wheat genome together with their genetic map location assigned some of the genes to major RWA resistance QTLs and thus this study provided some new insights into RWA resistance.
Over all, the work carried out in this study delivered RWA resistant wheat lines for breeding resistance cultivars that are well characterized by a broad range of molecular markers in the regions of the RWA resistance loci. The high density of new molecular markers provides for the efficient tracking of RWA resistance loci in the pipe-line of cultivar development within the framework of quarantine restrictions.

Publications and presentations

Publications in preparation

Selladurai, S., Appels, R., Diepeveen, D., Tolmay, V. and EI Bouhssini, M. Genetic mapping of Russian wheat aphid resistance loci in a doubled haploid mapping population.

Selladurai, S., Appels, R. and Diepeveen, D. A proteomic approach to unravel host plant resistance mechanism to Russian wheat aphid in double haploid lines derived from double haploid mapping populations.

Presentations

Oral Presentation:

Royal Society of Western Australia – Postgraduate Symposium 2015
Title: Molecular interaction between Russian wheat aphid and wheat and its control via host plant resistance.

Poster Presentation:

Selladurai, S., Appels, R., Cakir, M., Webster, H., Tolmay, V., Turanli, V., EI Bouhssini, M., Berryman, D. and O'Hara, G. Genetic mapping of Russian wheat aphid resistance genes in a Double haploid population derived from Australian wheat cultivar. International Wheat conference Sydney Australia (IWC2015), 20-25 September 2015, pp142.

Selladurai, S., Appels, R., Cakir, M., Tolmay, V., Turanli, V. and EI Bouhssini, M. Genetic mapping of Russian wheat aphid resistance genes in wheat. Veterinary and Life Sciences poster day, Murdoch University, November 2014.

Acknowledgements

The goals achieved by this thesis were made possible by collaboration and contribution from many individuals. First and foremost I would like to thank my supervisors Professors Rudi Appels and Dean Diepeveen for their support and encouragement. My sincere gratitude goes to my principal supervisor Professor Rudi Appels for sharing his research wisdom and providing valuable advice, tireless effort and constant encouragement. I am also grateful to Rudi for adopting me (he always says) as his PhD student showing me the respect as a research colleague rather PhD student and also sharing his office and nibbles. It is unforgettable Rudi, your constant guidance, support and encouragement that you have shown me even in the difficult times you faced. There are not enough words to express my appreciation. I would like to thank Dean who joined with me as a team member in the latter part of my PhD career. Your help on statistical analysis, thesis correction and providing moral support and strength were valuable.

I would like to thank Dr. Mehmet Cakir, and Professor Michael G. K. Jones for initially giving me the opportunity to change my carrier from private research to PhD research. Special thanks to Mehmet for providing seed materials and valuable advice and helping me to conduct experiments with overseas collaborators. Dr. Hollie Webster's contributions at the early stages of my thesis production are gratefully acknowledged.

Valuable contributions from Dr. Vicki Tolmay (ARC-Small Grain Institute, South Africa), Professor Ferit Turanli (Ege University, Istanbul, Turkey) and Dr. Mustapha EL-Bouhssini (International Centre for Agricultural Research in the Dry Areas (ICARDA) to conduct Russian aphid screening experiments in overseas were greatly appreciated.

Thanks to A/P Graham O'Hara and Dr. David Berryman for their advice towards my PhD project.

The financial support provided by Murdoch University is kindly acknowledged.

I would like to thank Dr. Reetinder Gill and Mirza Nazim Ud Dowla for their help to conduct field experiments here in Australia.

My sincere thanks go to Ms Bee Lay Addis (SABC administrative officer) for processing my purchase orders and Ms Frankie DeRousie (Academic support & Streaming Coordinator, College of Veterinary Medicine) for facilitating seminar room each week.

I also thank SABC staff members Professor Michael G. K. Jones (SABC Director), Dr. David Berryman (SABC Manager) and Ms Frances Brigg (SABC Officer) for providing excellent facilities to carry out my research at the State Agricultural Biotechnology Centre (SABC), Murdoch University.

To my friends at the State Agricultural Biotechnology Wujun Ma, Steve Wylie, John Fosu-Nyarko, Mike Frankie, Shahid Islam, Rongchang Yang, Chris Florides, Rowan Maddern, Karl Benton, Mirza Nazim Ud Dowla, Samier Dilipkhot, Jamie Ong, Shu Hui, Sadia Iqbal, Sharon Wescott, Xiaolong Wang, I say thank you all for having helpful discussion and social gatherings.

Lastly my family, I wouldn't hold this without you. To my wife, Vathani your love, constant encouragements and tireless support during this bumpy long journey with hurdles are unforgettable and I am forever indebted. My beautiful daughters Asmitha and Lakshana, your dedication and sacrifice in your childhood life and

staying with me patiently while I was working was marvellous. I offer big thank you and heartfelt kiss. You have made this whole journey fruitful.

List of abbreviation

Abbreviations	Description
AAMPs	Aphid-associated molecular pattern(s)
ABA	Abscisic acid
ABS	Australian Bureau of Statistics
ADP	Adenosine diphosphate
AFLP	Amplified Fragment Length Polymorphism
ANT	Adenine nucleotide translocator
ARC	Agricultural Research Council
ATP	Adenosine triphosphate
AUD	Australian dollar
BMV	Brome mosaic virus
BSA	Bovine serum albumin
BYDV	Barley yellow dwarf virus
CC-NB LRR	Coiled-coil nucleotide-binding domain leucine-rich repeat
CIMMYT	International Maize and Wheat Improvement Centre
cM	Centimorgan
cMap	Comparative map
CPO	Corproporphyrinogen
DAFWA	Department of Agriculture and Food Western Australia
DArT	Diversity Array Technology
ddRAD	double digest Restriction-Site Associated DNA sequencing
DH	Double haploid
Dn	*Diuraphis noxia*
DNA	Deoxyribonucleic acid
EDU	Education
EPG	Electrical penetration graph
ET	Ethylene
ETI	Effector-triggered immunity
FAO	Food and Agriculture Organisation of the United Nations
FDR	False discovery rate
GA	Gibberellic acid
GBS	Genotyping-by-sequencing
GDC	Glycine decarboxylase dehydrogenase complex
GMOD	Generic model organism database
GST	Glutathione transferases
GWAS	Genome wide association study
HR	Hypersensitive response
HR-CD	Hypersensitive response cell death
HSP	Heat shock protein

IAA	Indole-3-acetic acid
ICIM	Inclusive composite interval mapping
IEF	Isoelectric focussing
IPG	Immobilized pH gradient
IPM	Integrated pest management
iTRAQ	isobaric Tags for Relative and Absolute Quantification
IWGSC	International Wheat Genome Sequencing Consortium
JA	Jasmonic acid
LOD	Logarithm of odds
LRR	Leucine rich repeats
MAMP	Microbes associated molecular pattern
MAPK	Mitogen-activated protein kinase
MAS	Marker assisted selection
Mb	Megabyte
MeJA	Methyl jasmonate
MIPS	Munich Information Centre for Protein Sequence
M RWA biotype	Moroccan Russian wheat aphid biotype
MS	Mass spectrometry
MTI	MAMP triggered immunity
MYA	Million years ago
NADPH	Nicotinamide adenine dinucleotide phosphate
NCBI	National Centre for Biotechnology Information
NGS	Next generation sequencing
NO	Nitrous oxide
PAGE	Polyacrylamide gel electrophoresis
PCD	Programmed cell death
PCR	Polymerase chain reaction
PDC	Pyruvate dehydrogenase complex
PEP	Phosphoenolpyruvate
POPSEQ	Population sequencing
PR	Pathogenesis related
PVE	Phenotypic variation explained
QTL	Quantitative trait loci
RADseq	Restriction-Site Associated DNA sequencing
RAPID	Random Amplified Polymorphic DNAs
RF	Recombination frequency
RFLP	Restriction Fragment Length Polymorphism
RH	Relative humidity
RhPV	Picorna like virus
RLKs	Receptor like kinase
RNA	Ribonucleic acid
ROS	Reactive oxygen species

RT	Reverse transcription
RWA	Russian wheat aphid
SA	Salicylic acid
SA RWA biotype	South Africa Russian wheat aphid biotype
SABC	State Agricultural Biotechnology centre
SAR	Systemic acquired response
SDS	Sodium dodecyl sulphate
SEs	Sieve elements
SNP	Single nucleotide polymorphism
SSR	Simple sequence repeat
TIR-NB LRR	Toll-interleukin-1 receptor domain leucine-rich repeat
TMV	Tobacco mosaic virus
T RWA biotype	Turkey Russian wheat aphid biotype
UCDAVIS	University of California, Davis
UROD	Uroporphyrinogen
US$	United States of America Dollar
USA	United States of America
USDA	United States Department of Agriculture
USSR	Union of Soviet Socialist Republics
Z	Zadoks growth stage scale

Table of Contents

Chapter 1: General introduction

Australia is unique in being characterised by its ocean barrier to the movement of numerous pests and diseases found in other countries. In the twenty first century, natural bio-security provided this physical barrier which has now been threatened by intervention of human activities. Agriculture is one of the key resources of the Australian economy. Pests and diseases cause significant losses in agriculture through the destruction of crops. This thesis focuses on wheat since it is the 3rd highest cultivated crop around world utilising 222 million hectares (ha) of land in 2014/2015 (Ronald, 2015) and providing stable food for 35% of the world's population (Stankova et al., 2015). Estimated annual production wheat in 2014/15 was 725 million metric tons next to rice and maize (Ronald, 2015). Australia's wheat export volumes are expected to increase 2% to 16.9 million tonnes in 2015-16 because of the higher demand of Australian wheat in overseas countries (ABARES, 2015).

Pre-emptive plant breeding research plays a key role for Australian biosecurity and agricultural research in order to prevent production losses caused by the introduction of pests and diseases to Australia. Molecular technology provides the basis for a fast track approach by shortening the time to move the available genetic resources to the development of new germplasm and improved crop varieties.

The Russian wheat aphid (RWA), *Diuraphis noxia* Kurdjomov has been reported in Tarlee, South Australia in 2016. It causes significant damage on wheat and barley production in North America, several regions of North and Central Africa and South Africa. Unlike other aphid species, RWA can cause significant yield losses and hence the introduction of RWA resistance into the susceptible agricultural crops, especially wheat and barley Australian agricultural industry would prevent major production losses.

In this thesis, a resistant land race PI 94365 from USDA was phenotyped against RWA biotypes found in South Africa, USA, Turkey, Morocco and Kenya. The resistance gene(s) identified in wheat from this resource has been selected to be incorporate into the Australian local cultivar EGA Gregory which is susceptible to RWA. Double haploid (DH) lines (180) created from these parents (EGA Gregory x PI94365) were phenotyped against South African biotypes 1, 2 and 3, Turkey and Moroccan biotypes. These breeding lines were genotyped with simple sequence repeat markers (SSRs), DArT and genotype by sequencing markers (GBS) and a high density genetic map with QTLs for the RWA was created using both genotype and phenotype data.

Based on the association of RWA resistance as a phenotype, this was then used to define genome regions in the DH population with distinctive haplotypes for more detailed study.

The association studies included identifying differentially expressed genes for RWA infestation (from the literature) which were located in RWA resistance genome region. In addition a bulk segregant analysis approach was deployed for identifying proteins encoded by genes located in RWA resistance genome regions. Building on the available wheat genome sequence information the overall data set was interpreted in terms of gene networks influencing RWA resistance.

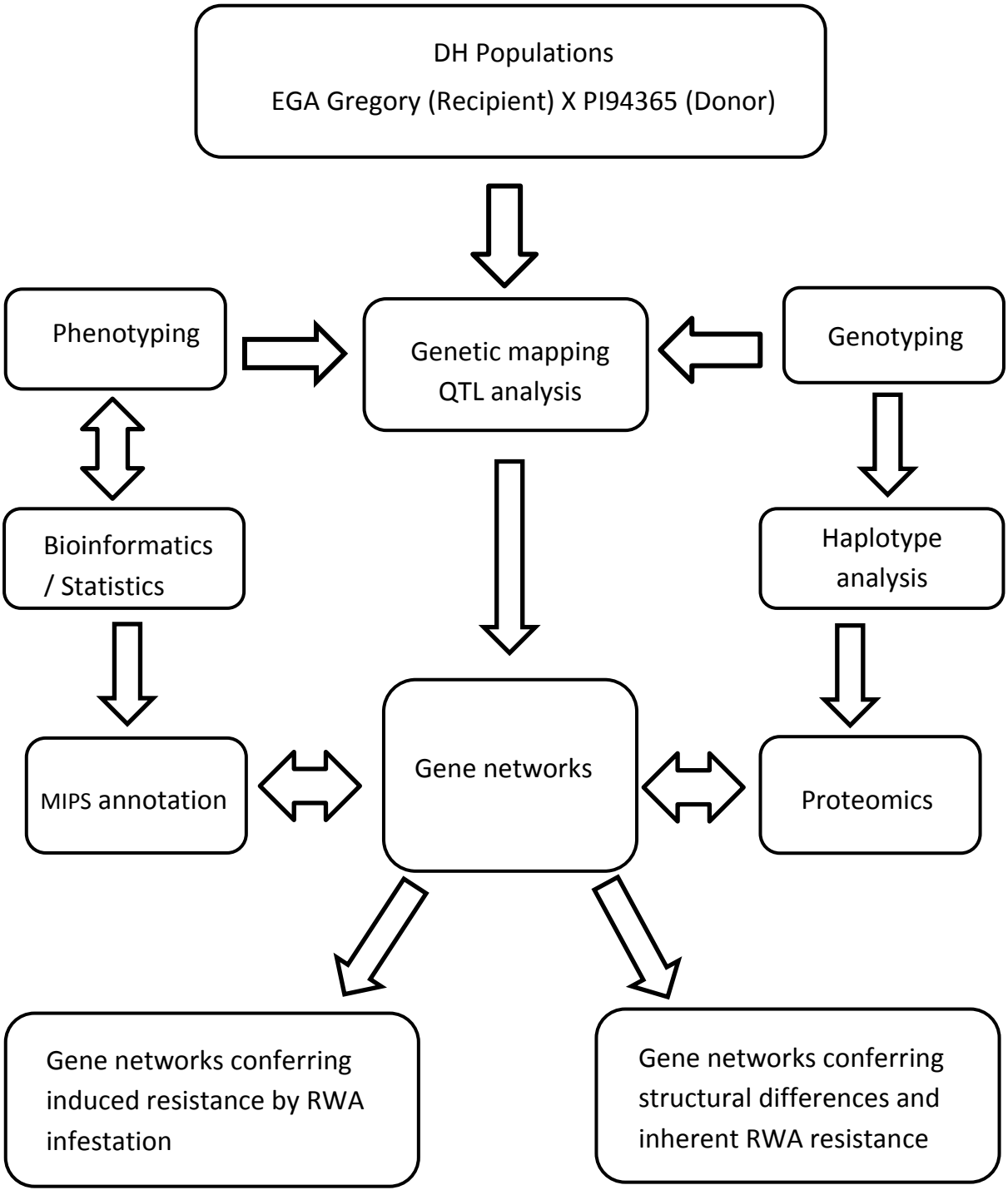

Figure 1.1 summarises the overall experimental approach used in the thesis to investigate the nature of RWA resistance in the DH population derived from the cross between EGA Gregory and PI94365.

This thesis concludes by identifying suites of molecular markers that can be used in pre-emptive plant breeding for RWA.

Chapter 2: Literature review

2.1 Russian wheat aphid

2.1.1 History of RWA

Pests and diseases are a major threat to crop cultivation due to the yield penalties they impose (Ratnadass et al., 2011). Aphid (Order: Hemiptera; Suborder: Homoptera) attack causes significant yield loss due to their effect in removing photo assimilates and vectoring numerous harmful plant viruses (Dogimont et al., 2010). Among the insect pests the Russian wheat aphid (RWA), *Diuraphis noxia*, has been identified as one of the most invasive, particularly in cereal crops such as wheat (*Triticum aestivum* L.) and barley (*Hordeum vulgare* L.). It has caused significant direct and indirect losses of over US$ 800 million in the western United States of America (USA) from 1987 to 1993 (Lapitan et al., 2007; Morrison & Peairs, 1998).

The RWA is believed to originate from the Iranian-Turkestanian mountain range and it extends to Southern Russia, the Middle East and central Asia (Zhang et al., 2012). RWA was treated as a minor pest in these countries because they co-evolved with their host in that region. As per Robinson (1994) report, Kovalev et al. (1991) detailed the history of *D. noxia* spread in Russia beyond the mountain range. Alfaro (1947) firstly reported the pest status of *D. noxia* outside of Russia and documented *D. noxia* as a pest of wheat, *Triticum aestivum* L., and barley, *Hordeum vulgare* L. in Spain. Subsequently RWA was first reported in South Africa in 1978 (Walters et al., 1980), Mexico in 1980 (Gilchrist et al., 1984) and in Texas in the USA 1986 (Webster & Starks, 1987) (Figure 2.1). It reached Chile in 1987 (Zerene et al., 1988) and in Canada in 1988 (Morrison & Peairs, 1998). Its distribution also includes Ethiopia (Haile & Megenasa, 1987), North Africa, the Middle East, Central Asia, southern Europe (Blackman & Eastop, 1984) , and areas as far east as Xinjiang Autonomous Region in north western China (Zhang, 1991). In these countries the population numbers increased rapidly and spread throughout the major wheat growing regions.

The cause of proliferation in these countries was that the climate was, and continues to be, very conducive for the establishment of RWA. RWA has been found in one north-western region of the Republic of China for about 70 years and a study conducted with microsatellite and mitochondrial markers by Zhang et al. (2012) indicated a long term existence and expansion of RWAs in China. Australia was RWA free country (EI Bouhssini et al., 2012) but RWA was first time reported in Tarlee, South Australia in April, 2016.

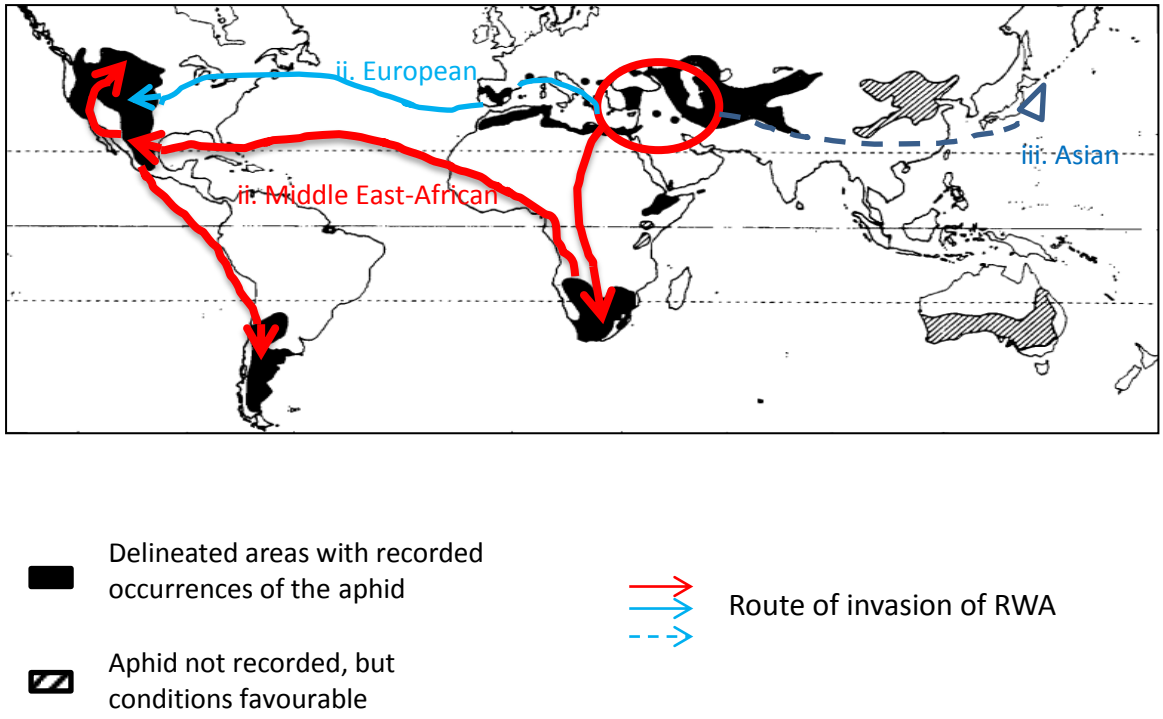

Figure 2.1: Route of invasion and global spread of *D.noxia* (Hughes & Maywald, 1990; Liu et al., 2010)

In the USA, RWA was first reported in Texas in 1986 and subsequently spread throughout most of the other states comprising the major wheat growing regions within a year (Thomas, 1986; Thompson, 1987). It rapidly became a major pest in these regions and caused significant yield losses in grain production in 1980s (Figure 2.2).

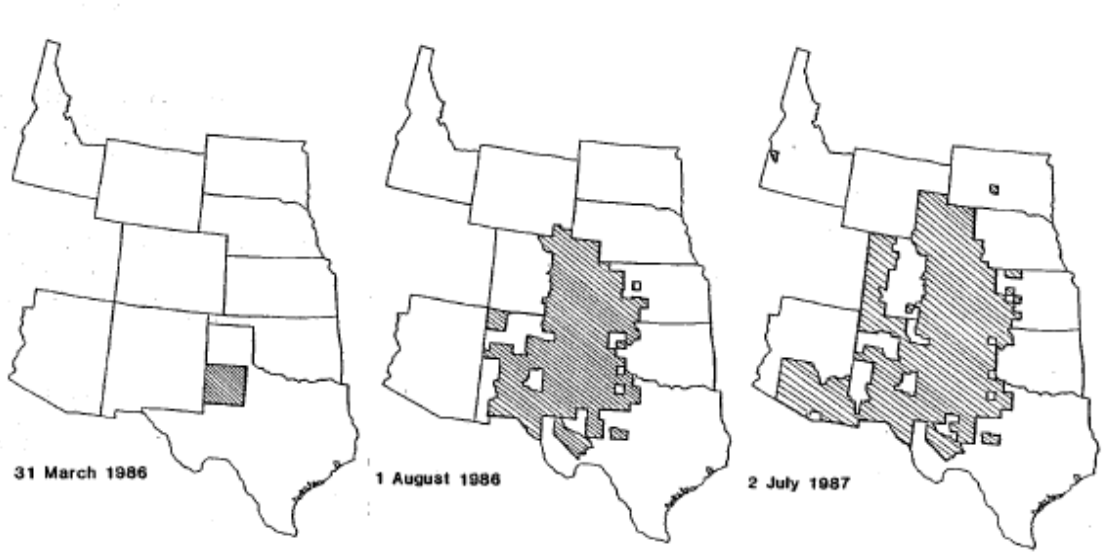

Figure 2.2: Spread of RWA in USA (Thomas, 1986; Thompson, 1987)

Wheat and barley are the most RWA susceptible crops among the cereal grains, followed by rye and triticale (Zhang et al., 2012). Oats also act as a host for RWA, but damage caused by the pest in this crop is marginal. The RWA have not been observed to attack or injure corn, rice, or sorghum (Summers & Godfrey, www.ipm.ucdavis.edu). The RWA does however colonize many native and introduced grasses (Summers & Godfrey, www.ipm.ucdavis.edu).

Although the Australian wheat belt is not yet infested, the drier inland parts of the Australian wheat belt would be very favourable for RWA growth and survival (Hughes & Maywald, 1990). Based on modelling proposed by Thomas (1986) and Thompson (1987) the projected RWA yield loss would be approximately 65% and 75% in eastern in western regions of Australia respectively.

Since RWA has resulted in severe economic damage, especially in wheat and barley industry worldwide (El Bouhssini et al., 2011; Liu et al., 2011), there is an eminent threat to Australia once RWA is introduced in wheat growing areas.

2.1.2 RWA biology, biotype development and symptoms on wheat plant following RWA infestation

Adult RWA (*Diuraphis noxia*, Order: Hemiptera, Family Aphididae, Synonyms: Kurdjumov) are small in size (1.6 to 2.1 mm long), have short antennae, elongated bodies and are pale green in colour. Features that differentiate RWA from cereal aphids commonly found in wheat include their possession of pair of supracaudal appendages (tail like structure) and the absence of siphuncles (Figure 3 and 4) (Amulaka et al., 2013; Robinson, 1994). RWA preferentially colonize areas deep in the whorl or beneath the leaf sheath. However when the aphid number increases the entire plant may be colonized. Infestation of wheat plants by RWA can occur as early as the two leaf stage of development (Jankielsohn, 2011). (http://www.ipm.ucdavis.edu/PMG/r730300211.html).

Figure 2.3: Russian wheat aphid

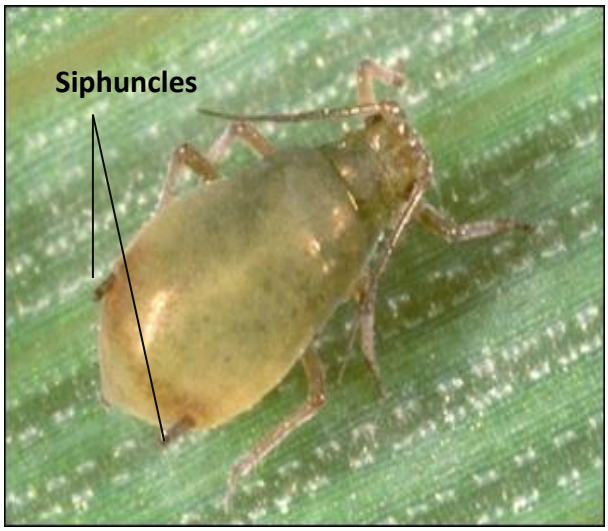

Figure 2.4: Cereal aphid

(Pictures provided by Dr. Vicki Tolmay, ARC-Small Grain Institute, Bethlehem, South Africa)

Two forms of RWA exist, a wingless female and a winged male. Both asexual and sexual reproduction is observed among RWA (Goggin, 2007). Wingless females asexually produce nymphs from spring through to summer. Also there is evidence that biotypes evolve without sexual reproduction but chromosomal rearrangement. The aphid has holocentric chromosomes (chromosomes without centromeres)

making chromosomal breakage and rearrangement easier (Novotna et al., 2011). As winter approaches some of the wingless females turn into males with wings, thus enabling them to disperse to other areas. During the winter period eggs are sexually produced. Sexual reproduction, through the mechanism of DNA recombination and selection, enables new biotypes to evolve. Production of eggs is an avoidance mechanism which enables RWA to escape harsh winter periods. However RWA is tolerant of cold weather and it can survive sub-freezing temperatures (Summers & Godfrey, www.ipm.ucdavis.edu).

RWA are a phloem feeding insect species that target specific tissues to feed on nutrients from the sieve tube elements found in the phloem tubes (Smith & Boyko, 2007). These structures are accessed by RWA as they penetrate their stylets through the mesophyll tissues where a large number of the chlorophyll molecules are found. Toxic compounds excreted by RWA during feeding of photo assimilate break down the chlorophyll molecules found in tissues (Liu et al., 2011). Signs of the RWA feeding damage are evident as white, yellow or purple streaks longitudinally along the leaves and leaf sheaths. Other symptoms may also be present such as (i) leaf rolling, (ii) spikes that are bleached in colour, (iii) grains that do not mature properly or failure for grain head development, (iv) awns trapped by the rolled leaf giving distorted head morphology, and (v) reduced plant height (Burd & Burton, 1992; El Bouhssini et al., 2011; Peng et al., 2007; Tolmay et al., 2012). These symptoms are most strongly evident in instances when RWA density is high and the cultivars are susceptible (Walters et al., 1980).

Figure 2.5a: Leaf chlorosis

Figure 2.5b: Head bleach and distortion

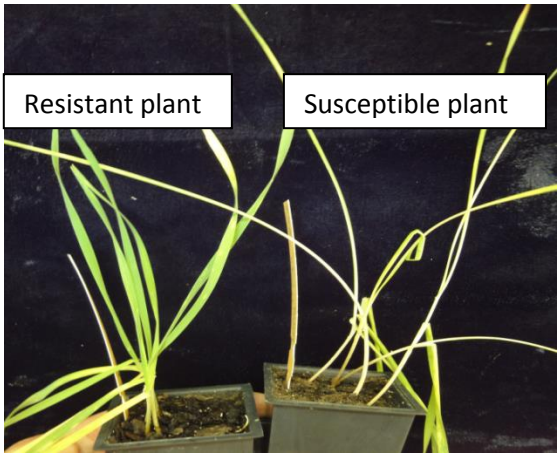

Figure 2.5c: Leaf rolling

Figure 2.5d: Stunted growth

(Pictures provided by Dr. Vicki Tolmay, ARC-Small Grain Institute, Bethlehem, South Africa)

2.1.3 Global impact of RWA on wheat grain production

Bread wheat (*Triticum aestivum* L.) belongs to the family Poeacea (gramineae), genus *Triticum* and it contributed more than 35% world's human grain consumption in 2009-2010 (Wright, 2012). RWA infestation in 10 fields in Texas and Oklahoma, USA brought winter wheat grain yield down by 50.2% to 82.9% and biomass by 55.4 to 76.5% in 2004, 2005, and 2006 (Mirik et al., 2009). In South Africa, wheat grain yield loss on individual susceptible plants has been reported to be as high as 90% (Tolmay & Booyse, 2016) and in Kenya, up to 90 % yield loss in wheat grains was due to RWA infestation (Amulaka et al., 2013). In Australia, wheat is the most important

agricultural crop both in terms of economic value and area planted. Approximately 65% of Australia wheat is exported overseas, making it a significant player in the world market (Harvey, 2011). However, the yield of wheat could be significantly reduced by emerging pest and disease. Decreased quality of the wheat grains is often accompanied pest infestation and disease infection. According to the *2006 Revision*, the global population will likely increase by 2.5 billion over the next 40 years and it will reach 9.2 billion in 2050 (United Nations Press Release - POP/952). Rapid population growth will raise serious questions about the adequacy of food supply (Hopfenberg & Pimentel, 2001). To overcome shortage of food supply, the development of higher yielding cultivars with improved tolerance to biotic and abiotic stresses is essential.

2.1.4 Control measures of RWA

Infestation of RWA causes direct economic losses attributed to reduced grain set and size. Indirect economic losses are due to the associated cost of pest management through the application of insecticide. At present, insecticides are the main and most effective option available to grain producers to combat the RWA infestations. However extensive use of pesticide also brings environmental and social costs. Non chemical RWA management strategies are essential including utilising bio-control agents such as the natural aphid parasitoid wasp *Aphelinus spp*, parasitoid *Diaeretiella rapae* and lady bird beetle (Tanigoshi et al., 1995) as well as the development of new resistant and tolerant cultivars (Turanli et al., 2012). In addition to considering economic costs and impact on environmental and social factors, the application of insecticides can lead to the possibility of emerging insecticide resistant aphids (Burd et al., 2006). Combined with the leaf rolling habitat of the insect, the application of insecticide is less effective for the long term control of RWA infestation. Biological control is not considered an efficient method of control due to the mortality factors of biological control agents and the lack of refuges. Management of aphids in cultivated crops through application of

insecticides and via biological control measures is further compromised because of their short life cycles and the extremely high reproductive rate of RWA (Dogimont et al., 2010). Therefore development and deployment of resistant cultivars is increasingly being seen as the preferred option for excluding RWA infestations in Australia.

Biotype variation in RWA population exists in several countries (Liu et al., 2010). The term biotype refers to a group of individuals that emerge within a population of an insect species and have an ability to break the protective barrier which exists in resistant plants (Smith et al., 1992). The US biotype 2, the most virulent biotype (Burd et al., 2006) among the eight known biotypes identified in the USA (Liu et al., 2010; Peng et al., 2007) remains a major threat to wheat and barley production in the USA (Randolph et al., 2009).

Plant mechanisms conferring resistance to RWA include: (i) tolerance, (ii) antixenosis, or (iii) antibiosis (Painter, 1951, 1958; Smith & Chuang, 2014). Tolerance is the ability of the plant to grow when infested with aphids. RWA tolerance is measured by vegetative and yield parameters of the plant. Antixenosis refers to non-specific features of a plant that prevent pest colonisation, including the aphids, and it is measured by the number of adult aphids per plant (Castro et al., 2001; Castro et al., 2005; Painter, 1951, 1958). Antibiosis refers to the capacity of the adult aphid to produce young aphids when they are feeding the host (Castro et al., 2004; Painter, 1951, 1958). It is measured by number of nymphs per aphids during infestation. Antibiosis resistance can occur alone or concomitantly with tolerance or antixenosis and it has been found in many plants against aphids and arthropod more generally (Painter, 1951, 1958; Smith & Clement, 2012). Therefore gene stacking of a suite of genes each conferring different types of resistance would provide wider protection against RWA in new wheat cultivars (Anderson et al., 2003).

2.1.5 Russian wheat aphid interaction with plant hosts

Aphids are a major insect pest of plants and cause mechanical damage as a result of depletion of metabolizable energy through probing and phloem sap sucking. Aphids feed specifically from the plant sieve element causing them to damage tissue as well as draining plant nutrients. Many aphids act as vectors for the transfer of harmful micro-organisms to plants, especially viruses. Viruses are transmitted to the plants while aphids feed from the sieve element. Symptoms developed by RWA infestation on the wheat plant can look very similar to viral or drought associated symptoms. In fact, Tanigoshi et al. (1995) suggested brome mosaic virus (BMV), barley yellow dwarf virus (BYDV), barley stripe mosaic virus and a picorna like virus (RhPV) were transferred by RWA but this has been disputed by number of authors (Hewitt et al., 1984; Kriel et al., 1984). Instead, it is now evident that RWA injects cytotoxin or eliciting agent into the host plant while they are feeding (Zaayman et al., 2009). The toxic saliva destroys chlorophyll, resulting in white, yellow or purple longitudinal steaks on the stems and leaves (Saheed et al., 2006). The toxin also causes leaves to twist and curl and often displays a prostrate growth habit (Jyoti et al., 2006).

2.2 Molecular genetics of wheat

2.2.1 Wheat

Cereals including wheat, barley, rice, maize and sorghum evolved from a common ancestor about 70–55 million years ago (Kellogg, 2001) but differs greatly in genome size despite their shared lineage. Common bread wheat is an allohexaploid containing three distinct but genetically related (homoeologous) copies of chromosomes (2*n*=6x=42, AABBDD). Each of the three copies was derived from three ancestral diploid progenitors (Martínez-Pérez et al., 1999). Approximately 0.5 million years ago, the first hybridisation event is thought to have occurred when the wild grass *Aegilops speltoides* (2n=2X=14, most closely related to the B genome) spontaneously crossed with the wild diploid wheat, *Triticum urartu* (2n= 2x=14, AA genome) (Huang et al., 2002). The resultant hybrid was tetraploid wheat, *Triticum*

turgidum (2n=28, AABB). Domestication of tetraploid wheat led to the evolution of the durum wheat *Triticum turgidum* var. *durum* (Nesbitt, 2001). Hybridisation of tetraploid durum wheat with the diploid wild goat grass, *Aegilops tauschii,* (2n=2x=14, DD genome) led to the evolution of hexaploid wheat about 8000 years ago (Ozkan et al., 2001). Among agricultural plant species bread wheat (*Triticum aestivum* L.) has the largest 17,000 Mb genome composed of approximately 80% repeats, primarily retroelements, with an gene density of between 1 per 87 kilobase pairs and 1 per 184 kilobase pairs (Brenchley et al., 2012). Bread wheat genome is about 8-fold larger than that of maize and 40-fold larger than that of rice (Arumuganathan & Earle, 1991). The genome space comprises approximately 1% genes, interspersed by large amount of repetitive elements which account for roughly 80% (Simkova et al., 2011). Variation in the numbers of transposable and retrotransposable elements, and duplicated chromosome segments in bread wheat contributes to the complexity of the wheat genome and is a major impediment to genetic improvement for identifying markers when breeding for new cultivars (Feuillet et al., 2012).

2.2.2 Genetic control of host plant resistance in wheat against RWA infestation

To date, fourteen RWA resistant genes (*Dn*) have been identified in wheat germplasm accessions including: These include *Dn1* from common wheat accession PI 137739, Iran (Du Toit, 1987); Dn2 from common wheat accession 262660, Russia (Du Toit, 1989); dn3 in the *Aegilops tauschii* line SQ24 (Nkongolo et al., 1991b); *Dn4* from the Russian bread wheat accession PI 372129 (Nkongolo et al., 1991a); *Dn5* from the Bulgarian wheat accession PI 294994 (Du Toit, 1987; Marais & Du Toit, 1993); *Dn6* from the Iranian wheat accession PI 243781 (Saidi & Quick, 1996); *Dn7*, a gene derived from the 1RS.1BL translocation in wheat "Gamtoos" (Marais et al., 1994; Marais et al., 1998); *Dn8* and *Dn9* from the near-isogenic wheat lines derived from the PI294994 (Also source for the *Dn5*) (Liu et al., 2001); *Dnx* from the PI

220127 (Liu et al., 2001); *Dny* from RWA resistant 'Stanton' (Smith et al., 2004); *Dn2414* from the USDS-ARS RWA resistance wheat line 2414-11 (Peng et al., 2007); *Dn626580* from the Iranian wheat landrace accession PI626580 (Valdez et al., 2012) and *Dn2401* from Iranian wheat accession CI2401 (Fazel-Najafabadi et al., 2014). The RWA resistance genes *Dn1*, *Dn2*, *Dn5*, *Dn6*, *Dn8* and *Dnx* resistance genes are located in chromosome 7D (Liu et al., 2005). The Dn4 gene is located in chromosome 1DS (Arzani et al., 2004). A resistant PI 94365 line was identified by Smith et al. (1991) against Russian wheat aphid and was considered to contain a single dominant gene (Dong et al., 1997). The PI94365 line has not yet been introduced in any breeding programme in Australia. The resistance loci have also not been mapped or characterised in any population either in Australia or internationally.

2.2.3 Significance of host plant resistance

Management of RWA is challenging on account of the aphids having a very high multiplication rate due to their capacity for both asexual and sexual reproduction (Zhang et al., 2012). RWA also have a short life cycle and leaf rolling habitat impacting on pesticide control. High pesticide application rates have led to increased production costs with side-effects on beneficial insects (predators, parasitoids and pollinators) including consequences to ecosystems and environment. Of particular concern is the increased incidence of pesticide resistance in RWA populations. RWA biotype variations occur in different countries (EI Bouhssini et al., 2011; Peng et al., 2007) and therefore developing host plant resistance is an efficient and environmentally safe method of tackling the threat of RWA entry to Australia (El Bouhssini et al., 2011). An extensive breeding program in wheat is required to introduce novel resistance genes into susceptible germplasm in order to provide RWA resistance cultivars for commercial production. This effort requires molecular markers to assist breeding programs during screening of RWA resistance because the resistance phenotype cannot be assessed in Australia with live aphids due to

biosecurity risks. The markers also facilitate tracking the resistance genes in complex backcrossing programs.

Development of host plant resistance to RWA requires a source of resistance in the first instance. Host plant resistance is a heritable trait in plants. RWA resistance sources against aphids are usually identified by screening germplasm for response to aphid attack. New aphid resistance sources are usually limited to unimproved landraces, wild accessions or in some cases in unrelated species. Hence the breeding process to introduce resistance gene(s) into new varieties requires several years. However the process can be made more efficient if there was a better (i) understanding of the genetic and molecular bases of RWA resistance and (ii) availability of molecular markers to assist breeding programs to screen for the resistance gene loci in several stages of the breeding program. In soybean, 3500 soybean germplasm lines were screened to identify eleven aphid resistant accessions (Hill et al., 2004; Mensah et al., 2008). Over 40000 accessions of wheat and wheat related species have been used to screen seedling stage plant against RWA but only 300 accessions have shown resistance or moderately resistance to RWA (Dogimont et al., 2010). Though many accessions have shown resistance to RWA, the genetic studies still need to be performed to determine if the resistance sources carry novel resistance genes. For example, there are many resistant sources with over 50 accessions to the melon-cotton aphid, *Aphid gossypii*. However, the majority of them carry the same resistance allele *Vat*, although some of the accessions from these geographically different resistance sources carry a distinct allele for the respective locus (Dogimont et al., 2008).

A novel landrace resistance source, PI94365 from the USDA germplasm collection was screened at the seedling stage to RWA biotypes in different countries that includes USA, France, South Africa, Turkey, Morocco and Kenya (Personal communication-Dr Mehmet Cakir). Unimproved landrace PI94365 has been

identified as a good resistance source for several biotypes. This landrace line was the focus in this thesis to develop host plant resistance to RWA biotypes in Australian cultivars.

2.2.4 Behavioural pattern of phytophagous insects

Aphids are phloem feeders and are spread throughout the world because of their efficient colonisation and settlement (Liu et al., 2010). Parthenogenesis, an asexual form of reproduction in aphids, produces multiple generations during spring and summer when secondary hosts are readily available and they enter a sexual life stage during autumn, especially when the days become shorter and temperature falls (Jaouannet et al., 2014). Some aphid species are unable to develop any sexual stages and reproduce exclusively by parthenogenesis (Nibouche et al., 2014). The winged form of the adult is able to migrate and colonise new plants whereas the wingless form of adult is involved in reproduction (Powell et al., 2006). Survival of phloem sap feeding insects depends on liquid dietary nutrients drawn from the sieve elements.

Sieve tubes are formed by longitudinally arranged elongated cells called sieve elements (SEs). SEs lack a nucleus and vacuole and contain only an intact plasma membrane, phloem plastid and SE endoplasmic reticulum (Sjolund & Shih, 1983). The terminal walls of elongated cells are transformed into sieve plates to connect adjacent SE (Evert, 1990). The arrangement of SEs enables the transport of plant nutrients which are produced in the mesophyll tissues to the different parts of the plant (Will et al., 2009).

Insects access the SEs for their food and keep SEs alive while withdrawing the nutrients. To search for the sieve tube, aphids have a flexible stylet which possesses two outer mandibles and two inner maxillae capable of entering between two epidermal cells and penetrating through the cell wall apoplasm between the cells and eventually reaching the vascular bundles (Figure 2.6). Electrical penetration

graph (EPG) technology was used to understand the behavioural pattern of the stylet during penetration (Tjallingii, 2006). The EPG study by Tjallingii (2006) showed that most of the cells along the pathway are briefly punctured and the stylet is withdrawn a few seconds later. A small amount of watery saliva is injected into the cells (Martin et al., 1997) and the puncture made by the stylet has little or no effect on the cell. Aphids puncture the sieve tubes with their stylets and subsequently ingest the nutrient rich sieve tube contents. During inter-cellular penetration, aphids continuously secrete gelling saliva which reacts with oxygen and forms a sheath around the stylet (Tjallingii, 2006). Following penetration of the cytoplasm, the ingestion of saliva and cytoplasm mixture from the SEs is facilitated by the watery saliva of the aphids (Tjallingii, 2006; Tjallingii & Hogen Esch, 1993). The purpose of intracellular probing by the aphids is to assess the plant as a food source and the stylet location within the plant tissue (Powell et al., 2006).

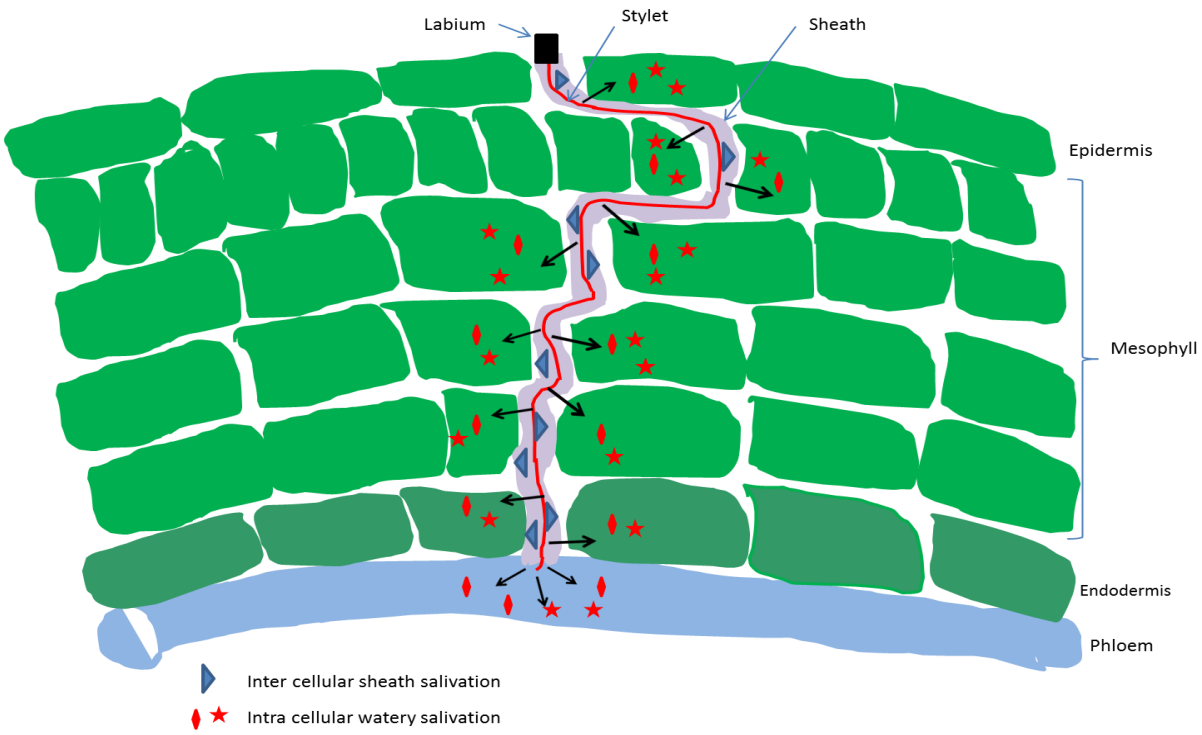

Figure 2.6: Aphids' stylet penetration and salivation

Gelling saliva which is primarily composed of proteins that includes phenoloxidases, peroxidases, pectinases, beta glucosidases, phospholipids, and conjugated carbohydrates shares a common composition between different species of aphids (Anna Urbanska et al., 2002; Cherqui & Tjallingii, 2000; Miles, 1999). In contrast, watery saliva composition differs between aphid species and even within the same aphid species (Elzinga & Jander, 2013). It depends on the feeding of the aphid. Pectinase, pectin methyl-esterase, polygalacturonase and cellulase enzymes have been found in several aphid species (Carolan et al., 2009; Cherqui & Tjallingii, 2000; Will et al., 2009). Therefore it suggests that aphids can have a specific range of host plant species which is determined by the aphid's composition of watery saliva.

Active compounds found in aphid saliva modulate, suppress or circumvent the sieve tube occlusion mechanism in order to continuously ingest the phloem sap. The occlusion mechanism is a Ca^{2+} dependant mechanism that prevents aphids from ingesting the phloem sap as well as blocking the invasion of the pathogen. It includes dispersion forisomes that are observed in the Fabaceae family (Knoblauch, 2001), coagulation of soluble proteins in Cucurbitaceae family (Will & van Bel, 2006) and induction of callus (Beta 1,3 glucan polymer) occlusion in most of the plant family (Kauss, 1983). Influx of Ca^{2+} is due to aphid probing. However aphid survival depends on continuous feeding of nutrients rich phloem sap. Therefore aphids have developed a strategy to bind Ca^{2+} by injecting Ca^{2+} binding watery saliva into the SEs (Tjallingii, 2006; Will et al., 2007) and thus provide the basis for a compatible interaction between aphids and host plants.

2.2.5 Defence mechanism involved in host plant resistance

Biotic stresses cause significant impact on growth and development of the agricultural crops and eventually yield reduction. Unlike mammals, plants lack a circulatory immune system to protect against pests and diseases. Instead, plants possesses cell-autonomous immune systems and systemic signalling cascades to

transfer the signal from infection sites (Coll et al., 2011). There are two different interactions occurring between the plant and aphid when the aphid is trying to break the plant defence mechanism. In an incompatible interaction, the insect is unable to break the plant defence and therefore it is unable to take up any plant nutrients or cause damage to the host (Botha et al., 2005). This incompatible interaction appears to be considered non-host resistance (Mysore & Ryu, 2004). In a compatible interaction, the insect is able to break the plant defence and that allows the aphids to cause physical damage to the host plant and draw nutrients from the host (Botha et al., 2005).

In an incompatible interaction, plants protect themselves by passive and active defensive mechanisms. Passive defences are provided by having preformed or constitutive physical barriers (eg.: thick cuticles, trichomes, thorns) and chemical barriers (eg.: phenolics and alkaloids) (Agrawal, 2007; Nicholson et al., 2012). For instance, glandular trichomes found in *Solanum berthautii* are defensive traits against green peach aphid and potato leaf hopper (Tingey & Laubengayer, 1981). Plants also exhibit phenotype plasticity to defend against insects herbivory such as aphids. For example, the number of trichomes differs in plants, but in most cases, pathogens or pests are able to evade these protective barriers and deliver elicitors or effectors (Coll et al., 2011). These elicitors may be from insect oral secretions and oviposition fluids. Phloemophagous insects such as aphids are able to successfully ingest photoassimilates by injecting saliva which prevents or inactivates sieve tube's normal occlusion during feeding. Plants go one step further by switching on active defensive system to protect themselves against invading pathogens or pests. Active defence systems include: cell wall reinforcement such as callose, suberin or cell wall proteins deposition, lignification of cell wall, accumulation of phytoallexin, production reactive oxygen species such as hydrogen peroxides and peroxynitrite, hypersensitive response (HR) through cell death, synthesis of pathogenesis related protein (PRs) and acquiring systemic acquired resistance (SAR) (Botha et al., 2005).

In compatible interactions, proteins in the elicitors bind to the targeted host proteins, form protein complexes and therefore break the basal defence level. Active defensive system by the plant is triggered by recognizing plant protein complexes which are altered by the elicitors (Jeffery & Jonathan, 2001)(Figure 2.7). Absence of recognition leads to the sign of stress, which is then followed by symptoms associated with aphid feeding (Botha et al., 2005). An early line of defence within the recognition of target/elicitors complex protein is protein phosphorylation or activation of plasma membrane proteins which generates a diverse set of signalling molecules such as free calcium, nitric oxide and reactive oxygen species (ROS) (Smith & Chuang, 2014). These chemicals regulate many biological processes and interconnecting pathways and can activate physiological responses through transcriptional and metabolic changes.

The first line of defence by the plant to aphid probing is recognition by membrane receptors (Botha et al., 2005). Receptor-like kinase is a membrane localised protein and has an ectodomain of leucine-rich repeats (LRR) which recognises molecules associated with a threat to the biological system and an intracellular kinase domain which is involved in signal transduction. Increased phosphorylation activity in tobacco cells infected by *Phytophthora crytogea* was observed with an influx of Ca^{2+} which induced a plant response by activation of protein kinases or inhibition of protein phosphatases (Lecourieux-Ouaked et al., 2000). Influx of Ca^{2+} triggers MAPK activation, ROS and nitric oxide production, anion effluxes and plasma membrane depolarisation, glucose import inhibition, microtubule depolarisation. However aphids can evade this recognition and inject elicitors into the cells. Therefore a second line of defence [effector-triggered immunity (ETI)] is activated by another set of receptors called nucleotide-binding leucine rich repeats (NB-LRRs, (Botha et al., 2005). NB-LRRs contain a variable N-terminus, a central nucleotide-binding site and leucine rich repeats (LRR). The NB-LRR disease resistance proteins are able to

recognise effector proteins which are delivered into the host cytosol by the aphids and the signal transduction pathway to the nucleus where defence genes are activated.

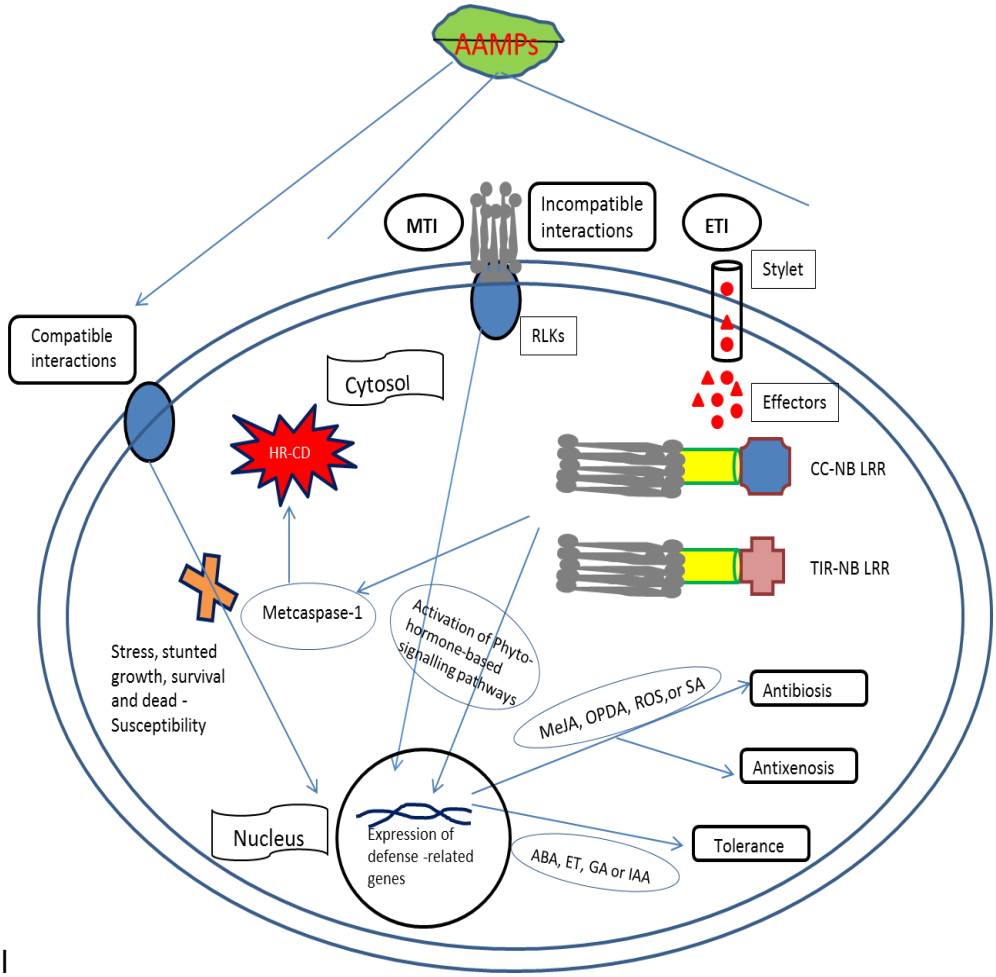

Figure 2.7: Elucidating the mechanism behind the insect herbivore resistance

AAMPs: Aphid-associated molecular pattern; MTI: MAMP (Microbes associated molecular pattern) triggered immunity; ETI:Effectors triggered immunity; RLKs- Receptor –like kinase; CC-NB LRR:Coiled-coil nucleotide-binding domain leucine –rich repeat; TIR-NB LRR:Toll-interleukin-1 receptor domain leucine –rich repeat; HR-CD:Hypersensitive response cell death; MeJA: Methyl jasmonate; OPDA: 12-Oxo-phytodienoic acid; ROS: Reactive oxygen species; SA: Salicylic acid; ABA: Abscisic acid; ET:Ethylene; GA:Gibberellic acid; IAA:Indole-3-acetic acid. Figure modified from Botha et al. (2005)

2.2.6 Identification of closely linked markers for RWA resistance gene

Introducing novel genes into crops facilitates the creation of new cultivars that can withstand pests and diseases or harsh environments. Plant breeding methodology is a long term process requiring 10 to 15 years for a new cultivar or hybrid to be available for sale to grain producers. Also the outcome from improved varieties often remains uncertain because confirmation that the novel gene is present in the plant during the breeding/selection process is based on phenotypic evidence that is greatly influenced by the environment (Gupta et al., 1999). Traditional searches for a gene responsible for a particular trait require plants that have been phenotyped or identified by visible or measurable traits with the offspring from crossing phenotyped for observable characteristics from the desired gene. New technology such as the availability of linked molecular markers can improve the selection process and speed up the breeding process.

Molecular markers have been extensively used in the development of genetic and physical chromosome maps in several plants and animal species including bread wheat (Feuillet et al., 2012). One of the main objectives in plant breeding is the introgression of one or more targeted genes from a donor parent into the background of an elite cultivar or breeding lines which carries desirable characters. Knowing the location of molecular markers linked to the major genes, Quantitative trait loci (QTLs) associated with new traits in elite germplasm offers the possibility to apply marker assisted selection into early screening and selection of plants for desirable traits. Screening the plants for desirable traits with molecular marker technologies can be carried out at any stage of plant growth and also this technology is more beneficial to those traits whose selection depends on specific environments or developmental stages that influence the expression of the target phenotype (Xu & Crouch, 2008).

Isozymes were used to speed up the introgression of monogenic traits from exotic germplasm into a cultivar background before the application of molecular marker tools in plant breeding and genetics (Tanksley, 1983; Tanksley & Rick, 1980). Isozymes are multiple forms of a single enzyme in which one of the forms is linked to a trait of interest (Poehlman & Sleper, 1995; Weining & Langridge, 1991). However, compared to recent developments in molecular markers, isozyme markers are limited in availability, generally offer lower level of polymorphism, labour intensive and less throughput.

Restriction Fragment Length Polymorphisms (RFLPs), a hybridisation based molecular marker technology, were initially used for human genome mapping (Botstein et al., 1980). Later, RFLPs technology were used for mapping plant genomes (Helentjaris et al., 1985) that includes RFLP markers for the wheat genome developed by Chao et al. (1989). The technology uses particular restriction enzyme and probe combinations to identify single or low copy sequences of DNA and subsequently generate specific banding patterns. Restriction enzymes recognise a specific nucleotide sequence and cleave at the particular site. Any mutation or deletion which alters DNA sequence resulting in a failure of recognition by restriction enzymes will produce an alternate banding pattern. The unique banding pattern for the individual is separated and visualised with a specific radioactively labelled probe. RFLP markers have been developed and widely used for several plant and animal species because of the co-dominant nature and unlimited polymorphism observed between species or individuals. With the advent of RFLP technology, a new era has been created in the genetic mapping of both qualitative and quantitative traits in a range of crop plants. However the technology itself has a limitation on its application because its time consuming, utilizes radio-actively labelled probes and require large amounts of DNA and therefore applying RFLP technology in a commercial breeding program where large numbers of progeny are commonly handled is difficult (Gupta et al., 1999). This technology has been found relatively useful when small numbers

of progeny are used in a selection process that involves mapping specific genes derived from wild relatives (Jia et al., 1996; Koebner et al., 1988). RFLP markers have now been replaced with high-throughput and more cost effective technologies.

With the discovery of the polymerase chain reaction by Mullis and Faloona in 1987, PCR based molecular markers such as: Random Amplified Polymorphic DNAs [RAPDs- (Williams et al., 1990)]; Amplified Fragment Length Polymorphisms [AFLP; (Vos et al., 1995)]; microsatellite markers [SSR- (Gupta & Varshney, 2000)]; and single nucleotide polymorphic markers (SNP- (Poland & Rife, 2012)] became available. These technologies have greatly influenced linkage map construction and marker assisted selection (MAS) in plant breeding programs. This is because of their high-throughput and relatively low cost (Mammadov et al., 2012). Though PCR based markers have their own advantages and disadvantages, selection of molecular markers have been primarily driven by the throughput, level of detection and reproducibility (Mammadov et al., 2012).

RAPD markers are able to simultaneously detect polymorphic loci in various regions of the genome (Williams et al., 1990). However, RAPD marker technology is medium throughput and its level of reproducibility is very low due to the non-specific binding of random primers. AFLP technology is still very useful in molecular genetics research in crops with little or zero reference genome sequence available (Zhang et al., 2011). Though the level of reproducibility is very high in AFLP technology, the technology itself is lengthy and labour intensive and it is not amenable to automation (Mammadov et al., 2012).

The discovery of microsatellite markers in plant genomes has eliminated most of the drawbacks faced by the above marker technologies (Gupta & Varshney, 2000). Microsatellites, or simple sequence repeats (SSRs) are stretches of repeated sequences consisting two, three or four nucleotides (Gupta et al., 1999). The

number of repeats often varies between individuals showing high levels of inter and intra species polymorphism. This variation in numbers can be detected by the PCR process using unique sequences (primers) annealing to flank regions of microsatellite loci (Gupta & Varshney, 2000). Amplified polymorphic fragments then can be separated by gel based systems or fluorescent detection methods if the primers are labelled with fluorescent dyes. Despite the cost of detection remaining high, SSR markers are co-dominant, highly polymorphic, reproducible and amenable to automation (Mammadov et al., 2012).

High-resolution genetic mapping has been hampered in many plant species because of insufficient numbers of genetic markers available to undertake effective research and the cost to assay many DNA markers (Xu & Crouch, 2008). This limitation is significant when more than one gene controls a trait and the quantitative trait loci (QTLs) may remain undetected or their contribution on the phenotypic variation may be underestimated because the marker density is very low (Xu & Crouch, 2008). Identification of polymorphic markers at high resolution from individuals is essential for constructing a linkage disequilibrium map (LD) and for association mapping.

Marker assisted selection (MAS) in plant breeding also requires abundant markers for integration of novel genes into modern cultivars. Hexaploid wheat is a self-pollinating species that has relatively low level of intraspecific polymorphism hence requiring large numbers of markers to identify polymorphisms (Plaschke et al., 1995; Roder et al., 1995). Therefore construction of high resolution maps especially for the complex genome needs cost effective technologies to integrate as many DNA markers as possible.

Since the advances in genotyping and sequencing technology are proven technology in human and animal genetics, single nucleotide polymorphism (SNP) markers are being increasingly adapted to cereal molecular genetics (Juliana et al., 2015). SNPs

are abundant and provide a rich source of potential DNA markers and may also directly contribute to phenotypic variation if they are in an intragenic or promoter region (Beales et al., 2005; Konishi et al., 2006).

Despite the low levels of polymorphism observed in SNPs, due to their bi-allelic nature, compared to SSRs markers, SNPs are found in abundant forms as genetic variation among individuals of the same species. They are also amenable to high throughput automation and because of the adaptation of SNPs technologies to genetic mapping, map-based cloning and marker assisted selection in crops (Hayashi et al., 2004).

High through-put assays and genotyping platforms such as Illumina's BeadArray technology based on Infinium assays (Steemers & Gunderson, 2007), Life technologies' based on TaqMan assay (Livak et al., 1995), KBiosciences' based on Competitive Allelic Specific PCR (KASPar) assay (http://www.kbioscience.co.uk) have emerged to detect SNPs in human, animal and plant genomes. Detection of SNPs in wheat genome is more complex than the genomes with less complex in ploidy or with less repetitive in nature. More than 80 per cent of the hexaploid wheat genome contains repetitive sequences (Simkova et al., 2011). A genome such as wheat requires an efficient technology to detect SNPs in a high-throughput and cost effective way. Prior to the discovery of efficient SNP typing technology, different experimental strategies in SNP discovery have been adapted to avoid repetitive sequences (Morozova & Marra, 2008). These include the discoveries of SNPs by re-sequencing of single genes derived amplicons using Sanger sequencing (Wright et al., 2005), *in silico* SNP discovery through the mining of SNPs within EST databases followed by PCR based validation (Bately et al., 2003), transcriptome re-sequencing using Next Generation Sequencing (NGS) technology (Morozova & Marra, 2008) and by NimbleGen sequence capture technology (Hodges et al., 2007). All these approaches are able to discover SNPs in coding regions (gene based) where SNP

frequency is generally low. In this way SNPs in coding regions are a powerful tool for MAS in plant breeding.

Amplicon re-sequencing is unable to use in MAS since it is an expensive and labour intensive procedure (Ganal et al., 2009). *in silico* SNPs through EST data base mining is able to discover large number of non-allelic SNPs (paralogous SNPs) and it is considered suboptimal for application of MAS in plant breeding (Choi et al., 2007). Transcriptome re-sequencing using NGS technology is a rapid approach to characterise SNPs within the genes and is less expensive because it focusses only the transcribed region of the genome (Morozova & Marra, 2008). This technology has been successfully applied in several plant genomes including wheat (Lai et al., 2012). NimbleGen sequence capture technology involved with exon sequence capture, enrichment with microarray and followed by NGS for targeted resequencing allows the detection of SNPs in coding regions with high throughput and at a larger coverage level (Hodges et al., 2007). However this technology can be applied with an available reference genome sequence or larger transcriptome (EST) sets in order to design capture probes.

The development of Next Generation Sequencing (NGS) technology has eliminated most of the problems associated with the discovery of SNPs. However before applying NGS technologies, SNP discovery in complex and larger genomes requires a genome wide study to cover the entire genome including non-coding regions and reduction in genome size as a starting material in order to reduce the number of repetitive sequences and minimise the time involved in data handling (Mammadov et al., 2012).

Complexity reduction technology primarily involves digesting the genome with restriction enzymes and selects the fragments with specific adapters. The adapter is designed to recognise the site of the restriction enzyme and therefore captures only

the fragments that have the respective recognition site. Several technologies using the principle of genome complexity reduction have been developed to discover the SNPs in larger and complex genomes. Restriction–Site Associated DNA sequencing (RADseq) uses a single restriction enzyme (rare cutter) digest followed by secondary random fragmentation and broad size selection to generate reduce representation libraries consisting of all genomic regions adjacent to the restriction site (Baird et al., 2008). To eliminate random shearing and broad size selection in RADseq method, the double digest RADseq (ddRAD) method has been developed by Peterson et al. (2012). ddRADseq uses two restriction enzymes namely a rare cutter and common cutter to double digest the genome followed by precise size selection that excludes the region flanked by either very close or very distant restriction sites. Reduced representation libraries consist almost entirely of expected size targets. DArTseq technology developed by DArT Pty Ltd uses the principle of ddRADseq to make reduce representation libraries and then uses the NGS platform to sequence the library.

Novel Two-Enzyme Genotyping-by-Sequencing methodology developed by Poland and Rife (2012) also uses a rare cutter and a common cutter restriction enzymes coupled with a forward adapter which ligate to the 5'end via barcode and a reverse adapter which ligates to the 3'end of the digested genomic DNA. This allows amplification of fragments with rare cutter sites at the 5' end and common cutter sites at the 3' end site. This technology enables the subsequent use of Illumina assay or the Ion Torrent sequencing platform to sequence the reduce representation library.

Linkage studies followed by gene characterisation require high resolution genetic maps. Resolution in mapping can be increased by analysing greater numbers of progeny and increasing number of genetic markers (Collard & Mackill, 2008). Despite genome wide association studies (GWAS) becoming increasingly popular in

genetic research (Hall et al., 2010), markers in large numbers are still required for increased resolution to detect linkage between the marker and phenotypic variation (Mammadov et al., 2012).

Advances in sequence technologies should allow GWAS studies to provide better approaches for studying the genetics of natural variation and traits of agricultural importance. This technology is effective when using inbred or double haploid lines because the information derived from genotyping these lines by GWAS has structured genetic diversity. Combining genome wide reduction with genotyping-by-sequencing (GBS) may be an ultimate deliverable to identify linked markers to the trait of interest. At present, considering a genome wide approach, the ability for high through-put and low costs, and to engage both microsatellite and SNP markers to construct a genetic map, is an ideal methodology to reach the goal set in this project.

Molecular markers technologies have been applied to map the RWA resistance loci in the wheat genome and to identify molecular markers to link to the RWA resistance loci (Fazel-Najafabadi et al., 2014; Liu et al., 2002; Liu et al., 2001; Liu et al., 2005). Majority of the RWA resistance genes (*Dn*) were mapped in chromosome 7D and 1D (Liu et al., 2001). RWA resistance genes, *Dn1*, *Dn2*, *Dn6* and *Dnx* were mapped near centromeric region of the short arm of chromosome 7D (7DS) and *Dn8* gene was mapped to the distal region of the 7DS centromere (Liu et al., 2005). Although a RWA resistance gene was mapped on chromosome 7DS by Liu et al., 2005, a later study found the RWA resistance gene *Dn5* to be located on long arm of chromosome 7D (7DL) (Marais et al., 2007). RWA resistance gene loci *Dn4* was mapped in proximity to the IDS centromere and RWA resistance gene *Dn9* was mapped on long arm of 1D (Liu et al., 2002). RWA resistance genes *Dn1*, *Dn2*, *Dn5*, *Dn6* and *Dnx* are appears to be in a cluster and are located near to the centromere region of 7D. These genes are either allelic at the same locus on wheat chromosome arm 7DS or

are tightly linked to one another (Liu et al., 2005). To date, molecular markers that were mapped near to the *Dn* resistance loci in different mapping population are provided in the table 2.1.

Table 2.1: Chromosomal location of molecular markers that linked to Russian wheat aphid resistance gene loci

Gene	Chromosomal location	Molecular Marker	Marker type	Linkage distance (cM) to the gene	Reference
Dn1	7DS	*Xgwm111*	SSR	3.82±0.20	Liu et al., 2001
Dn2	7DS	*Xgwm111*	SSR	3.05±0.18	Liu et al., 2001
Dnx	7DS	*Xgwm111*	SSR	1.52±0.15	Liu et al., 2001
Dn6	7DS	*Xgwm111*	SSR	3.0	Liu et al., 2002
Dn6	7DS	*Xgwm44*	SSR	14.6	Liu et al., 2002
Dn8	7DS	*Xgwm635*	SSR	<3.20	Liu et al., 2001
Dn626580	7DS	*Xgwm214*	SSR	1.8	Valdez et al., 2012
Dn626580	7DS	*Xgwm473*	SSR	5.0	Valdez et al., 2012
Dn2401	7DS	*Xbarc214*	SSR	1.1	Fazel Najafabadi et al., 2014
Dn2401	7DS	*Xgwm473*	SSR	1.8	Fazel Najafabadi et al., 2014
Dn5	7DL				Heyns et al., 2005, Marais et al., 2013
Dn4	1DS	*Xgwm106*	SSR	7.4	Liu et al., 2002

Dn4	1DS	*Xmwg77*	RFLP	Between *Xgwm106* and *Xgwm337*	Roder et al., 1998
Dn4	1DS	*Xgwm337*	SSR	12.9	Liu et al., 2002
Dn9	1DL	*Xgwm642*	SSR	<3.20	Liu et al., 2001
Dn7	1RS/1BL	*Xksud14*	RFLP	1.4	Anderson et al., 2003

2.2.7 Comparative genomics

Comparative genomics enables the cross-genome comparisons of structure and function to estimate similarity of biological organisation (Sorrells et al., 2003). Grasses originated approximately 55-75 million years ago (Gill et al., 2004) and rice, maize and wheat have evolved from a common ancestor ancestor approximately 40 million years ago (MYA) and today contribute most of the food for humans. About 3 million years ago, progenitors of AA, BB and DD genome of allohexoploid *T.aestivum* (bread wheat) diverged from a common ancestor (Figure 2.8). This history of plant evolution allows comparative biological analyses to link genes, proteins, genomes, and traits across species and genera. The wheat genome is 40 times larger than the rice genome with 25% to 30% of gene duplication as well as containing as much as 80% highly repetitive sequence content and it is often associated with gene free segments of the sequence (Choulet et al., 2010). Polyploidization, amplification of transposable elements and duplication of chromosome segments contributed expansion of wheat genome (Gill et al., 2004). Genes are distributed in the wheat genome in small gene islands which are interspersed between the transposable elements (Feuillet et al., 2012). Although the major cereals, rice, maize and wheat diverged 40 MYA, comparative mapping of cereal genomes showed extensive conservation in gene content and order at a low resolution genetic map level (Gill et al., 2004). Genomics projects do require a model species to provide genomic

information that can be used with other species. Wheat is a member of Poaceae family and it shares substantial gene similarity and synteny with other cereals species such as maize, barley, sorgum and rice (Wheat Genome Database – J. Craig Venter Institute (jcvi.org/wheat). Rice is one of the major cereal groups and the genome of rice has been fully sequenced (International Rice Genome Sequencing Project, doi: 10.1038/nature03895) and an ordered draft sequence of the more complex allohexaploid bread wheat genome has been recently completed (International Wheat Genome Sequencing Consortium, 2014; plants.ensembl.org/Triticum_aestivum). The nature of the hexaploid wheat genome comparative genomics studies with rice genome provides a powerful tool for de novo prediction of genes and identification of non-coding functional elements (Gill et al., 2004).

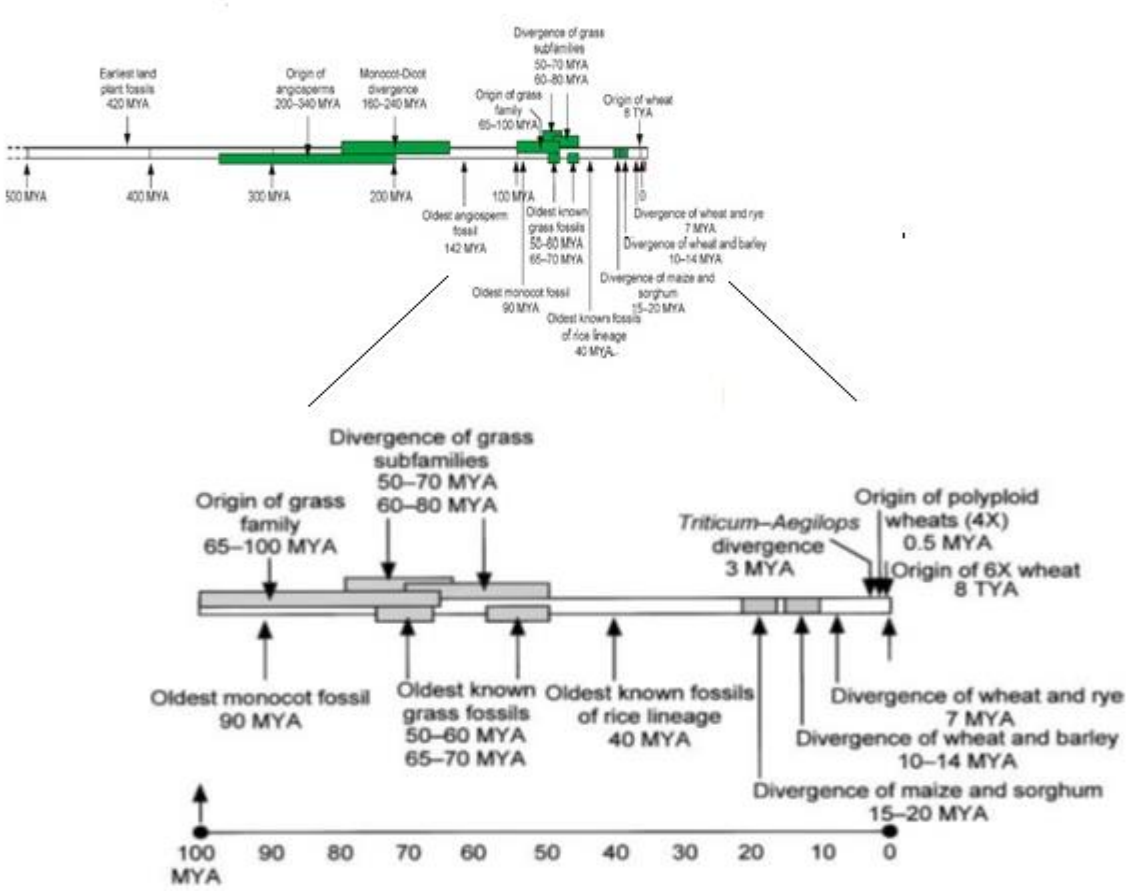

Figure 2.8: Time line of wheat evolution [P.F. Byrne (Colorado State University (CSU), Ft Collins), P. Gornicki (University of Chicago); (Gill et al., 2004)]

2.2.8 Proteomics of plant and aphid interaction

Proteins are the products of gene expression and responsible for expressed phenotypes. Studies conducted at the genome level provide the first step for elucidating the mechanism behind the resistance against pests and diseases.

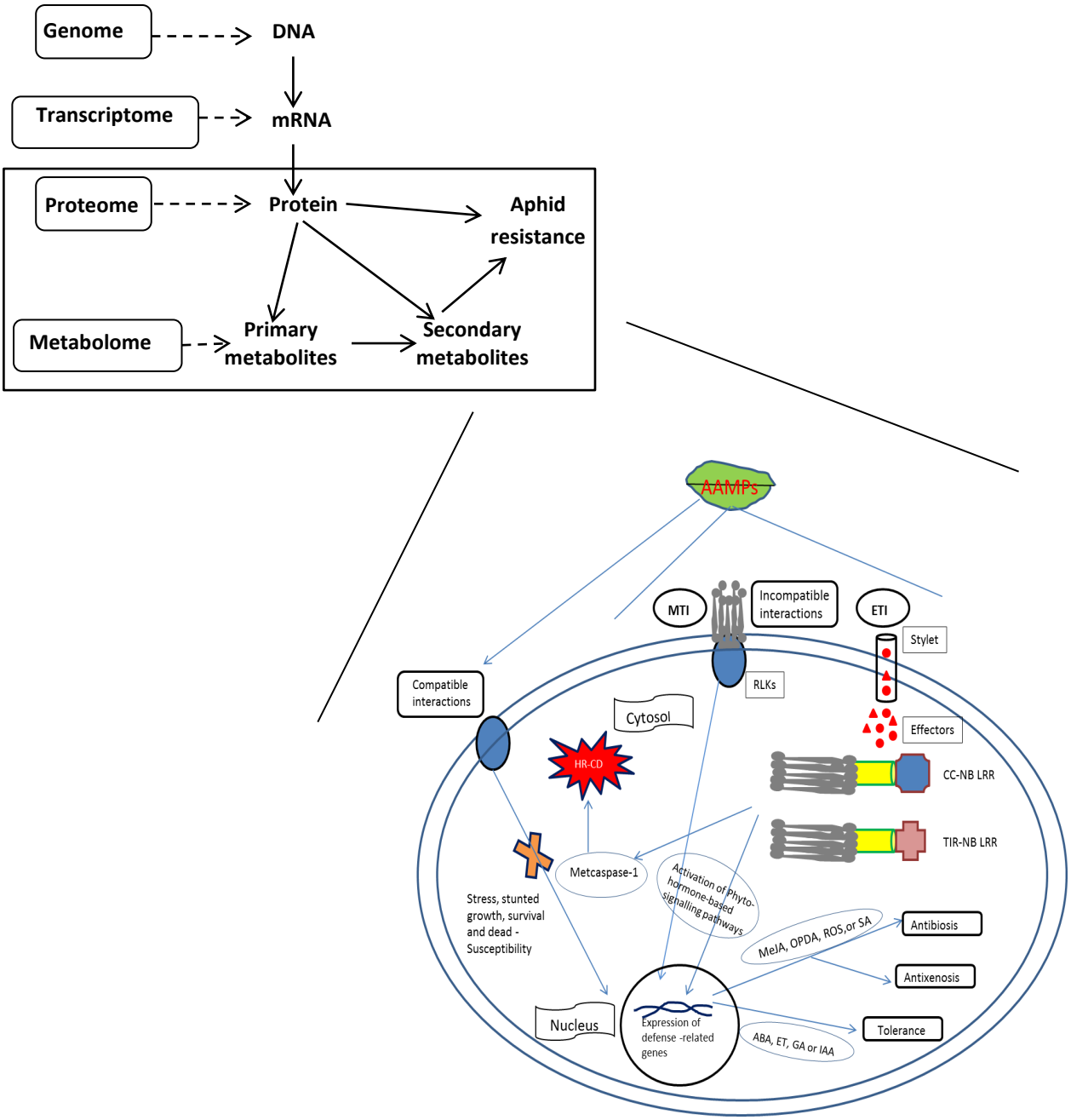

Figure 2.9: Cellular processes for aphid resistance (Modified from Figure 2.7)

AAMPs: Aphid-associated molecular pattern; MTI: MAMP (Microbes associated molecular pattern) triggered immunity; ETI:Effectors triggered immunity; RLKs- Receptor –like

kinase; CC-NB LRR:Coiled-coil nucleotide-binding domain leucine –rich repeat; TIR-NB LRR:Toll-interleukin-1 receptor domain leucine –rich repeat; HR-CD:Hypersensitive response cell death; MeJA: Methyl jasmonate; OPDA: 12-Oxo-phytodienoic acid; ROS: Reactive oxygen species; SA: Salicylic acid; ABA: Abscisic acid; ET:Ethylene; GA:Gibberellic acid; IAA:Indole-3-acetic acid.

Unlike the genome of an organism which has a fixed number of genes, the levels of protein expressed by the cells (the proteome) are highly dynamic (Corthals et al., 2000). QTL studies of biotic or abiotic resistance often describe only single genes or multiple genes involved in the resistance but rarely provide any other information as to how the resistance is achieved by the resistant plants. Studies at the genome level provide the foundation to do cross correlation of data generated from transcriptomes and proteomes. However a linear relationship between transcriptome and proteome does not exist (Corthals et al., 2000). This is firstly due to formation of isoforms due to post transcriptional control in the form of alternate splicing, poly-adenylation and mRNA editing (Park et al., 2006) and secondly due to post translational modification of proteins such as phosphorylation and glycosylation (Choe et al., 2007). The mRNA concentration in the cells also depends on both the synthesis and degradation rate. The variation in mRNA stability is thus an additional factor contributing to the absence of a linear relationship between transcriptomes and proteomes (Perez-Ortin et al., 2007).

Genetic interaction between plants and aphids requires resistance gene (R gene) products of the host plant and the elicitors or effectors released by the aphids (Botha et al., 2006). In incompatible interactions, R gene products recognise the effectors and trigger the chain of signal transduction events that induce defence genes and prevent the host from aphid infestation. With the advancement in protein technology, protein studies have been widely used for many different applications in plant sciences that include the study of proteins of biosynthetic pathways leading to secondary metabolites (Jacobs et al., 2000; Tanksley, 1983).

Unlike mammals which have circulatory immune systems, plant cells possess inbuilt immunity (Coll et al., 2011). The inbuilt immunity systems in plants against the pests and diseases consist of tiers of receptors. These receptors recognise and respond to the invaders and often provide signals to the rest of the plant. Aphid's sheath and watery saliva primarily composed of proteins (Cherqui & Tjallingii, 2000; Tjallingii, 2006). R gene products from the resistant plants are also composed of proteins. Interaction between these two proteins decides whether the host plant is compatible or incompatible to the aphid. A strong resistance response is expressed by the host when the R gene protein matches the avirulence (Avr) gene protein (Botha et al., 2006). Several functional R genes identified so far encode for resistance to bacteria, fungus, virus, oomycete, nematode and insects and they were found in several crop species (Zhang et al., 2011). Despite the wide range of pathogen taxa and their respective pathogenicity of effector molecules, R genes encode for only 5 classes of proteins (Jeffery & Jonathan, 2001): (i) Xa21 and (ii) Cf-X proteins carry transmembrane domains and extracellular LRRs; (iii) *RPW8* gene product carries a putative signal anchor at the N terminus; (iv) *Pto* gene encodes a cytoplasmic Ser/Thr kinase but may be membrane associated through its N-terminal myristoylation site; and (v) the largest class of R proteins NB-LRRs are cytoplasmic and carry distinct N-terminal domains (Jeffery & Jonathan, 2001).

As the first line of defence (ie a general defence) by plants, receptors recognise the aphid attack and transfer the signal from the cellular membrane to defence genes which are in the nucleus. The second internal defence system induced by delivery of effectors inside the cells is achieved by activating defence proteins or enzymatic pathways which activates a hypersensitive response (HR) or systemic acquired response (SAR) by the plant (Ni et al., 2001). HR leads to programmed cell death (PCD) and SAR leads to giving signal or immunity to the remainder of the plant. Several proteins are up regulated or down regulated, both in susceptible and

resistant plants as a result of aphid attack (Ciepiela & Sempruch, 1999; Haley, 2004; Smith et al., 2010).

The ability of plants to defend themselves against aphid attack depends on the expression of constitutive genes or induced genes or both. Proteins are the products of gene expression and proteomics is the systemic analysis of the proteins expressed by the genome (Jacobs et al., 2000) involving identification, quantification and characterisation of proteins in order to elucidate their function and interaction with other proteins. Many plant proteins are well documented in databases such as UniProt Viridiplantae (www.uniprot.org); Plant Protein Phosphorylation Database (www.p3db.org); National Center for Biotechnology Information (NCBI) database (www.ncbi.nlm.nih.gov) and therefore proteomes of resistant and susceptible plant tissues can be compared to identify resistance related proteins through proteomics (Jacobs et al., 2000).

With the aim of protein profiling in biological samples, the proteomics has utilized techniques of two-dimensional sodium dodecyl sulphate - polyacrylamide gel electrophoresis (2D SDS-PAGE) developed by O'Farrell (1975) and mass spectrometry (MS) (Shevchenko et al., 1996). In the first dimension of 2D SDS –PAGE, proteins are separated according to their isoelectric point (pI) by isoelectric focussing (IEF). Development immobilized pH gradients strips (IPG) used in the first dimension separation has overcome many technical issues such as reproducibility and resolution and allowed to detect many protein spots in the second dimension of SDS-PAGE separation where proteins are separated with their mass (Park, 2004).

Comparing the proteins of two biological samples requires sensitive and accurate quantification. Though the 2D SDS-PAGE technique has proven technology to do the proteome analysis the technology has limitation in high through-put application (Corthals et al., 2000; Gygi et al., 2000). Two dimension protein profiling utilizes gels

to separate and image-analysis to profile the proteins and therefore it limits the loading capacity and reproducibility of the results (Issaq & Veenstra, 2008). Poor staining techniques and variation in concentration among the proteins in the protein samples may hamper to visualise entire protein profiling resulting in inaccurate quantification (Fuller & Morris, 2012; Park, 2004).

Further development in mass spectrometry (MS) and bioinformatics allows identification and quantification of protein in a higher level of sensitiveness and throughput. This technology has been improved further by the development of stable isotope labelling by amino acids in cell culture (SILAC) (Ong et al., 2002), Isotope Coded Affinity Tags (ICAT) (Gygi et al., 1999) and isobaric Tags for Relative and Absolute Quantification (iTRAQ^{TM}) (Choe et al., 2007; Ross et al., 2004) . The two methods, SILAC and ICAT involve isotope labelling of proteins. iTRAQ^{TM} method has overcome some of the major limitation faced by the isotope tagging. iTRAQ^{TM} method involves labelling the digested proteins with isobaric tags. With the availability of the 8-plex kit (Choe et al., 2007), simultaneous multiplex analysis can be carried out for up to 8 samples. This technique increases the sensitivity of the detection of proteins and the level of through-put.

2.2.9 In-silico analysis expressed proteins by RWA infestation

Plants and aphids are involved in a series of molecular interactions for their survival. As a result, plants have evolved a sophisticated defensive mechanism to aphid attack which are referred to as the aphid-associated molecular patterns (AAMPs) (Liu et al., 2011) and is followed by activation of defensive mechanism (Garcia-Brugger et al., 2006). This association can be mapped to the up or down regulations of genes associated with defensive signal cascades (Goggin, 2007; Liu et al., 2011; Smith et al., 2010; Wittstock & Gershenzon, 2002). In compatible interactions, the plant shows direct or indirect resistance responses to insects' herbivory attack (Liu et al., 2011). Direct defensive systems against phloem feeding insects such as RWA may arise

through the expression of (i) constitutive genes and (ii) induced genes. Expression of both constitutive and induced genes may result in antibiosis, antixenosis or tolerance in plants (Smith & Clement, 2012).

Constitutive defenses include structural barriers and allelochemical barriers. Presence of structural barriers such as glandular and non-glandular trichomes, tissues toughness, cell wall compositions and cuticles provides repellent or deterrent effects to aphids (Garcia-Brugger et al., 2006; Smith & Chuang, 2014). Allelochemical barriers such as flavonoids, phenoloics, alkaloids, organic acids (Hydroxamic, chlorogenic, isochlorogenic acids), wax sterols, esters, alkanes and triacontanol provides toxic, repellent, deterrent or growth inhibition effects to aphids (Botha et al., 2005; Smith & Chuang, 2014).

Induced defence in plants are initiated by the mechanical damage caused by the aphid or signalling compounds such as oral secretions, saliva or oviposition fluid from the aphids (Liu et al., 2011). Several studies show differential expression of large and diverse ensembles of genes by AAMPs (Smith et al., 2010; Boyko et al., 2006; Park et al., 2006; Studham & MacIntosh, 2013). Annotation of differentially expressed genes in susceptible and resistant plant by herbivore attack to the wheat genome can be done with the recently of wheat genome sequence [International Wheat Genome Sequencing Consortium, 2014; plants.ensembl.org/Triticum_aestivum; (Brenchley et al., 2012)].

2.3 Overview and aims of thesis

Russian wheat aphid (RWA), *Diuraphis noxia*, has been identified as a major pest of wheat (*Triticum aestivum*) and barley (*Hordeum vulgare)* and the cause of major economic loss worldwide. RWA exhibits biotype variations in several countries and has not been reported in Australia. The leaf rolling caused by the injected RWA-toxin creates an enclosure that protects the insect from harsh environment, natural

enemies and insecticides. Therefore developing host plant resistance is an efficient and environmentally safe method of tackling the threat of RWA entry to Australia. The main objective of this thesis is to generate well characterized germplasm to incorporate novel RWA resistance into Australian cultivars and identify a suite of molecular markers that can be used in the germplasm development in lieu of using live aphids.

Historically, several RWA resistance genes from resistance resources were identified and they have been utilised in wheat breeding programs for the production and deployment of cultivars to withstand against aphid infestation. For example, hard red winter cultivar "Halt" containing the *Dn4* gene was released in 1994 to tackle RWA biotype 1 in the USA. However emerging RWA biotypes are continuously posing threats to cereal production worldwide. Gene for gene interactions to the biotype by the host plant has been demonstrated to develop a resistance germplasm against emerging biotypes.

Since RWA has been recently reported in Australia and it is paramount to have resistant cultivars against multiple biotypes which are found in several countries in order to face the threat. A novel RWA resistance source, PI94365 (Dong et al., 1997; Smith et al., 1991) was screened for the RWA biotypes found in different countries and it has shown resistance to moderate resistance to several biotypes. Therefore the resistance landrace PI94365 could be a potential resource to develop a resistance germplasm. Recent developments in wheat genome sequencing and high through put screening platforms can now contribute to incorporate genomics and proteomics together in the development of cultivars with RWA resistance.

The specific objectives of thesis are as follows:

1. Map the resistance loci in DH population developed from the EGA Gregory and PI 94365 cross with SSR and SNP markers

2. Identify the potential genes in the regions of resistance loci through the annotation process of published induced genes for use as potential molecular markers in marker assisted selection (MAS) in germplasm development.

3. Understand the gene network involved in RWA resistance by integrating genomics and proteomics

The new approach undertaken in this study is the molecular marker development incorporating the latest information available from the wheat genome sequencing projects. In this way, this study will also further increase the knowledge of the resistance mechanism involved in wheat against the RWA infestation.

Chapter 3: Genetic mapping of Russian wheat aphid resistance loci in a doubled haploid mapping population derived from EGA Gregory x PI94365

Chapter contributors:

Dr. Mehmet Cakir (Former Supervisor): Providing seed materials and valuable advice towards the development of this project

Ms Sue Broughton, Department of Agriculture and Food, Western Australia: Developing Double haploid (DH) population

Dr. Vicki Tolmay, Small Grain Institute, Bethlehem, South Africa: Phenotyping DH population in South Africa

Professor Ferit Turanli, Ege University, Izmir, Turkey: Phenotyping DH population in Turkey

Dr. Mustapa El Bouhssini, International Centre for Agricultural Research in the Dry Areas (ICARDA): Phenotyping DH population in Mexico

Dr. Andrzej Kilian, Diversity Arrays Technology Pty Ltd, Australia: Genotyping DH population with GBS and DArT molecular markers

3.1 Abstract

Diuraphis noxia (Russian wheat aphid, RWA) has a major impact on wheat production in most of the wheat growing countries and has evolved several biotypes which carry virulence against the plant defense genes. Since RWA has been reported in Australia developing host plant resistance via pre-emptive plant breeding are key for Australian biosecurity as it is the most economical and practical means of

controlling the pest. The wheat variety EGA Gregory is highly susceptible to RWA and was used to map RWA resistance derived from PI94365 by generating a double haploid (DH) population from a cross between EGA Gregory and PI94365. The wheat line PI94365 has been shown to have high level resistant ratings against several biotypes around the world. Genotyping was carried out on 188 DH lines with simple sequence repeats markers (SSR), genotyping-by-sequencing markers (GBS) and Diversity Array Technology markers (DArT). A molecular genetic map consisting of 50-60 markers for each chromosome was constructed. Phenotyping studies were undertaken against South African biotypes 1, 2, and 3 in South Africa, Turkey Izmir RWA population in Turkey and Moroccan RWA population in Morocco. QTL analysis using 63 SSR markers and 23650 GBS and DArT data was performed to assign variation in RWA resistance onto the genetic map. The major resistance loci identified were located to chromosomes 1DS and 7DS and accounted for different aspects of resistance to South African biotypes 1, 2 and 3, Moroccan RWA biotype and the Turkey Izmir RWA population. Comparative genomics studies with POPSEQ map allowed the identification of additional molecular markers in the region of RWA resistance. The respective genome regions allowed suites of genes to be identified for developing SNP-arrays to be used in marker assisted selection. Incorporation of multiple resistance genes against RWA biotypes into Australian wheat cultivar is vital to avoid significant yield losses in grain production as any RWA incursion occurs.

3.2 Introduction

Bread wheat (*Triticum aestivum* L.) is the third highest cultivated crop around the world delivering one-fifth of the total calories to the world's population (Ronald, 2015) and provides the major food for 35% of the world's population (Liu et al., 2002). Pests and diseases cause significant yield reduction in cultivated crops with aphids (Order: Hemiptera) being the major insect pest by causing tissue damages, ingesting photo assimilates and vectoring numerous harmful plant viruses (Dogimont et al., 2010).

Russian wheat aphid (*Diuraphis noxia*, Hemiptera: Aphididae) is found in many wheat growing countries (EI Bouhssini et al., 2012) and recently reported in Australia. It causes significant yield losses in the cereal grains, particularly wheat and barley (Liu et al., 2001). Yield losses can be up to 90% possible when RWA infestation is severe (Liu et al., 2010) These insects was first identified in southern part of the former United States of Soviet Republic (USSR) in 1900 and subsequently the pest spread to several Mediterranean and Middle East countries (Zhang et al., 2012). RWA was first reported in South Africa in 1978 and followed by in Texas, North America in 1986. The aphid populations increased rapidly and spread through most of the wheat growing regions of these countries. In the United States of America, the pest was first notified in Texas in 1986 and quickly spread throughout the wheat growing regions within a year causing significant yield losses and also increasing usage of insecticide (Turanli et al., 2012).

RWA is a phloem feeding insect that targets specific tissues (Smith & Boyko, 2007). Most of the aphids feed from the sieve tube elements found in the phloem tubes by penetrating their stylets through mesophyll tissues where large numbers of chlorophyll molecules are found. During this process of probing, aphids secrete reducing agents and enzymes such as pectinases, cellulases, amylases, oxidases, phenolic glucosides, 1, 4 glucosidases and glucose dehydrogenase (Cooper et al., 2010). Enzymes are also secreted by aphids to breakdown glucose, to establish and maintain feeding sites, suppress plant defences and/- or induce changes in plant physiology in order to facilitate aphid feeding (Hughes & Maywald, 1990). Infestations of RWA causes direct and indirect damage on wheat plants (Pathak et al., 2007). Direct affects include damage to leaf tissues and loss of nutrients for the infested plant. Indirect damage is through the injection of elicitors that contain toxic protein and non-protein compounds which breakdown cellular membranes and chlorophyll molecules (Liu et al., 2010). This leads to symptoms such as: longitudinal white, yellow or purple streaks along the leaves and leaf sheaths; rolled up leaves

that stay in an upright position; heads showing a bleached appearance containing grains that do not mature properly or fail to develop; and awns trapped by the rolled flag leaf resulting in distorted heads (Jyoti et al., 2006). The consequences of aphid infection can be: reduction of plant height; sterile heads; low kernel weight; and in severe RWA infestation, death in susceptible cultivars (Walters et al., 1984) . Cultural practices, biological and chemical controls have been used to minimise the impact of RWA on wheat production (Turanli et al., 2012) . Cultural practices include the destruction of volunteer plants to reduce early season infestations. However this practice is often difficult to implement effectively. Biological control practices with combinations of natural predators including wasp, *Aphelinus varipes;* native parasitoids such as *Diaeretiella rapae* and *Aphelinus varipes;* or introduced parasitoids such as *A. albtpodus* and *A. asychis*; or lady bird beetles are not as effective to control RWA since they are in low numbers prior to outbreaks, taking a longer time to establish in the natural environment and encountering high mortality rate (Tanigoshi et al., 1995). While chemical control can be effective, the effectiveness of the measure is limited as a viable option for aphid control when considering the impact on the environment, the likelihood of emerging insecticide resistant aphids (Burd et al., 2006), and the impact of leaf rolling caused by the aphid in reducing the overall effectiveness of insecticides.

Having large numbers of accessions of wheat and wheat relatives from the regions where RWA is endemic, the identification of evolving host plant resistance to combat against RWA is likely to be the best long term solution to aphid control on wheat (Tolmay et al., 2012). To date, fourteen RWA resistance genes (*Dn* genes) have been identified, based on their capacity to provide resistance to a particular biotype of RWA, in wheat and wheat related germplasm. These include *Dn1* from common wheat accession PI 137739, Iran (Du Toit, 1987); *Dn2* from common wheat accession 262660, Russia (Du Toit, 1989); *dn3* in the *Aegilops tauschii* line SQ24 (Nkongolo et al., 1991b); *Dn4* from the Russian bread wheat accession PI 372129 (Nkongolo et al.,

1991a); *Dn5* from the Bulgarian wheat accession PI 294994 (Du Toit, 1987; Marais & Du Toit, 1993); *Dn6* from the Iranian wheat accession PI 243781 (Saidi & Quick, 1996); *Dn7*, a gene derived from the 1RS.1BL translocation in wheat "Gamtoos" (Marais et al., 1994; Marais et al., 1998); *Dn8* and *Dn9* from the near-isogenic wheat lines derived from the PI294994 (Also source for the *Dn5*) (Liu et al., 2001); *Dnx* from the PI 220127 (Liu et al., 2001) ; *Dn2414* from the USDS-ARS RWA resistance wheat line 2414-11 (Peng et al., 2007); *Dn626580* from the Iranian wheat landrace accession PI626580 (Valdez et al., 2012) and *Dn2401* from Iranian wheat accession CI2401 (Fazel-Najafabadi et al., 2014).

The first successful hard red winter cultivar "Halt" that contained the *Dn4* gene against biotype 1, was released by Colorado Agricultural Experiment station in 1994 (Quick et al., 1996) and was followed by cultivar 'Ankor'- a hard red winter wheat using the line PI 632275 in 2002 (Haley, 2004) and cultivar Prairie – a hard winter wheat using the line PI 605390 (Quick et al., 2001) that also featured the *Dn4* gene resistance to RWA.

Although aphid attack on the plant activates general defence genes in both susceptible and aphid resistance cultivars, plant cultivars with the specific aphid resistance genes are only activated in aphid resistant cultivars (Smith & Boyko, 2007). The level of response given by the resistance gene(s) in different resistance cultivars depends on the genetic background in which the resistant gene is bred (Botha-Oberholster et al., 2004). Biotype variations were also found among RWA collected from different countries (EI Bouhssini et al., 2011; Peng et al., 2007). In the USA, RWA is grouped into five different biotypes (RWA 1, 2, 3/7, 6 and 8) based on biotype and plant interaction (Puterka et al., 2015). The elicitors from the biotypes possess different sizes of proteins and non-protein compounds (Botha et al., 2005) which raise different levels of response from the R gene in resistant cultivars. Therefore, the development of resistant cultivars for several biotypes becomes more difficult

since it is necessary that one cultivar showing resistant to one biotype must also show resistant to other biotypes. A new biotype, *Dn4*-virulant biotype (biotype 2) found in the south eastern Colorado in 2003, has overcome all the resistant cultivars which are carrying *Dn4* resistance gene (Haley, 2004). This breakdown of *Dn4* by RWA biotype 2 has raised the awareness of having gene for gene interactions with diverse resistance sources to develop resistant wheat cultivars against RWA biotypes. A gene pyramiding approach as used for plant breeding for yield traits, incorporating more than one gene into the wheat cultivars may be a suitable option to create multiple resistances against several RWA biotypes.

Australia has been declared a RWA free country. However the drier inland parts of the Australian wheat belt would be more vulnerable for RWA growth and survival (Hughes & Maywald, 1990). Based on the model proposed by Thomas (1986) and Thompson (1987), Australia will face grain yield loss between 65% in Eastern Australia to over 75% in Western Australia if RWA enters into Australia. Therefore the deployment of resistant cultivars in Australia is paramount for combating invading RWA from overseas countries. Pre-emptive plant breeding research plays a key role for the Australian bio-security for agricultural research to prevent production losses from introduced species such as RWA. This research using molecular technology provides a fast track approach by shortening the time frame for deploying genetic resources to the development of new or improved crop varieties.

The objectives of this study were to incorporate novel genes from RWA resistance germplasm sources into an Australian local cultivar and characterize a set of loci associated with RWA resistance genes through genetic mapping.

3.3 Material and methods

3.3.1 Genetic materials

Seeds from the resistant wheat PI94365 were provided by USDA/ARS National Small Grains Research facility in Aberdeen, Idaho (Appendix: Supplementary Document I) and screened against several RWA biotypes found in different countries including South Africa, Turkey, Morocco and Kenya (Personal communication – Dr Mehmet Cakir). PI94365 was used to cross with a susceptible Australian wheat cultivar EGA Gregory (Pelsart/2*Batavia doubled haploid line) as a male parent to create mapping population. Four of the F1 seeds (Donor seeds D1, D2, D3, and D4) from four successful crosses were selected to develop double the haploid population (DH). DH lines were created by Ms Sue Broughton, DAFWA using the microspore culture technology (Broughton, 2011). A mapping population of 200 DH lines covering all four crosses were selected to carry out the phenotyping and genotyping study. Five seeds were planted in 1 meter short row with 30 cm interval in between rows and with 50 cm interval between columns in a complete randomised block design to increase seed amounts and for collection of leaf tissue. For genotyping, leaf samples were collected from one month old leaf seedlings in duplicates, frozen in liquid nitrogen and stored at- 80^{o}C until DNA extraction was performed.

3.3.2 Phenotyping study of doubled haploid (DH) populations in South Africa, Turkey and Morocco

A phenotyping study against RWA biotypes was carried out in 3 different countries, South Africa, Turkey and Morocco with the DH population.

South Africa

In South Africa, 189 DH lines were phenotyped against South Africa RWA biotype 1 (RWASA1), South Africa RWA biotype 2 (RWASA2) and South Africa RWA biotype 3 (RWASA3) by Dr. Vicki Tolmay, Small Grain Institute, Bethlehem, South Africa. These phenotyping studies were conducted in a glasshouse with 3 replications along with

parental lines, 2 differential checks and 3 controls. Differential checks on controls (Gariep and PAN3144) were used to check the correct biotype for the evaluation during phenotyping. Gariep is resistant to RWASA1 and susceptible to RWASA2 and RWASA3. PAN3144 is resistant to RWASA1 and RWASA3 and susceptible to RWASA2 (Personal communication – Dr. Vicki Tolmay). The controls used in the experiment included: Hugenoot is susceptible to all the three South African biotypes; CM 14 which is moderately resistant and CITR-2401 is resistant to all three biotypes from United States Department of Agriculture (USDA). Six seeds from each of the DH lines were planted in a randomised complete block design with controls. Aphid infestation of RWASA1, RWASA2 and RWASA3 from clone colonies was carried out at the 2 leaf stage and individual plants were scored after 21 days of infestation. A damage rating score using a 1-10 scale described by Tolmay et al. (2012) was used to rate the damage level caused by RWA (Figure 3.1) with damage scale 1 and 2 were considered extremely resistant and 3 and 4 resistant and 9 and 10 susceptible (Table 3.1).

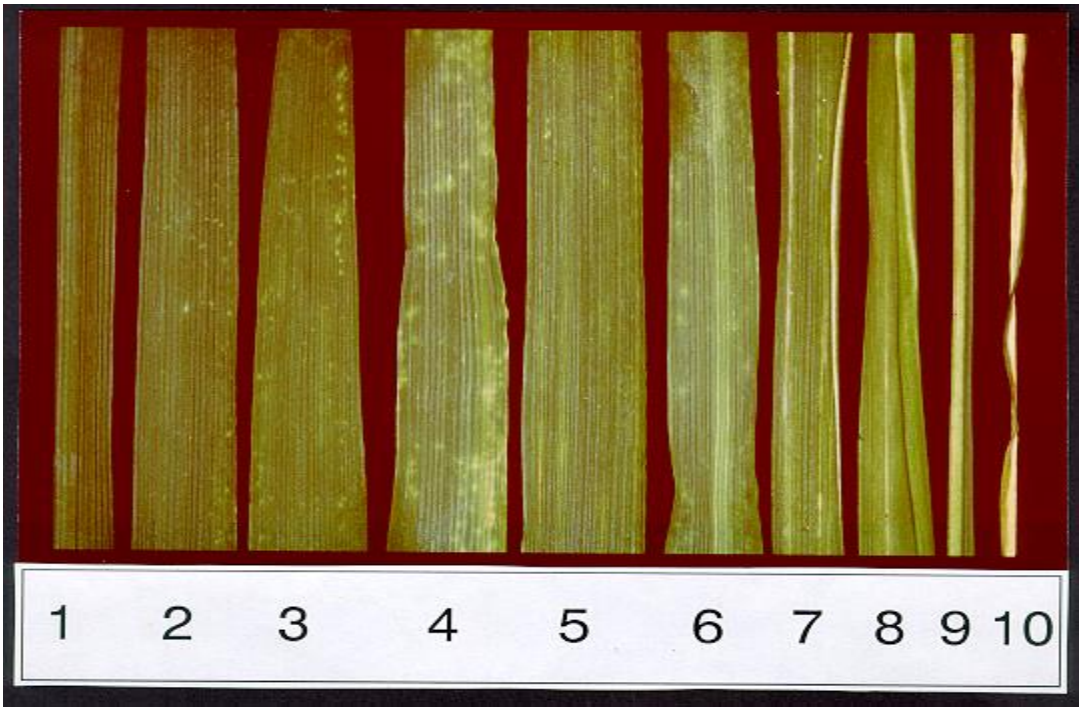

Figure 3.1: RWA damage ratings in wheat leaves (Photo provided by Dr. Vicki Tolmay)

Table 3.1: Descriptions and rating scales used for evaluation of DH population for resistance to Russian wheat aphid in South Africa (Tolmay et al., 2012).

Scale[1]	RWA Damage symptoms
1	small isolated chlorotic spots
2	small chlorotic spot
3	chlorotic spots in rows
4	chlorotic splotches
5	mild chlorotic streaks
6	prominent chlorotic streaks
7	severe streaks, leaves fold con-duplicate
8	severe streaks, leave roll convolute
9	severe streaks, leaves roll tightly
10	plant dying

[1]Scale 1, 2 were referred to as extremely resistant; 3, 4 resistant; 5, 6 moderately resistant; 7, 8 moderately susceptible and 9, 10 susceptible. We note an alternative scoring system is as follows: Scale 1-3: resistant, lesions due to PCD (hypersensitive response – oxidative burst) which is indicative of a strong host defence response; Scale 4-6: intermediate, first visual symptoms of chlorosis (breakdown of chorophyll) and leaf rolling due to decrease in turgor; Scale 7-10: susceptible, clear chlorotic streaks and severe leave rolling, and later death. This alternative system was not followed in this study because the RWA screening was carried out by Dr. V. Tolmay who utilised the scoring system shown in the table.

Turkey

In Turkey, phenotyping experiments were conducted in a complete randomised block design in a controlled greenhouse conditions at 20±1^{o}C, with light/dark photoperiod of 16/8h, and 60±5% relative humidity by Dr Ferit Turanli. The 96 DH lines and differential controls including susceptible Bezostaja variety for comparing a line carrying *Dn7* gene for a resistance were planted in small field plots. Five seeds of each entry were planted in 3 replications. RWA were collected from Izmir wheat growing region in Turkey reared on susceptible barley in the greenhouse under equivalent experiment glasshouse condition. DH lines, parents and controls were infested with five individual RWAs per plant at the two-leaf stage using a paintbrush

by placing the aphids on the first leaf. The RWA damage rating scale 1-6 scale described by Ennahli et al. (2009) for leaf chlorosis and leaf rolling was used to establish a damage level caused by RWA and RWA damage rate was taken after 21 days of infestation. For the leaf chlorosis, plants with 1, 2 and 3 leaf chlorosis values were referred to as resistant and ratings 4, 5 and 6 as susceptible. For the leaf rolling, plants with 1 and 2 were referred to as resistant and with value 3 susceptible. RWA density was determined by counting the number of aphids present on the plant. Zero to 3 scale was used where a score of 0 indicated that no individuals was on the plant, zero to 2 were referred to as resistant and more than 2 was referred to as susceptible (Table 3.2).

Table 3.2: Descriptions and rating scales used for evaluation of DH population for resistance to Russian wheat aphid in Turkey and Morocco (Ennahli et al., 2009)

Scale for Leaf Chlorosis (1-6)	
Scale	Description
1	No chlorosis
2	<1/3 of leaf area chlorotic
3	1/3 - 2/3 leaf area chlorotic
4	>2/3 of leaf area chlorotic
5	Necrosis in at least one leaf
6	Plant death
Scale for Leaf rolling (1-3)	
Scale	Description
1	No rolling
2	Trapping or curling in one or more leaves
3	Rolling in one or more leaves
Scale for Aphid density (1 - 3)	
Scale	Description
0	No individual on the plant
1	1-10 aphids on the plant
2	10-100 individuals on the plant
3	>100 individuals on the plant

Leaf chlorosis: 1, 2 and 3 were referred to as resistant and 4, 5, 6 susceptible

Leaf rolling: 1 and 2 were referred to as resistant and 3 susceptible

Aphid density: Zero to 2 were referred to as resistant and 3 susceptible

Morocco

In Morocco, screening experiment with parents and 200 DH lines was conducted in alpha–lattice design with block of 12 and 3 replications in at the Anoeceur research station where RWA was more prevalence. The RWA damage rating scale (ie 1-6) described by Ennahli et al. (2009) for leaf chlorosis and leaf rolling was used to establish a damage level caused by RWA (Table 3.2). The RWA resistance assessments were carried out by Dr Mustapa El Bouhssini, International Centre for Agricultural Research in the Dry Areas (ICARDA).

3.3.3 Statistical analysis of phenotyping data gathered from the experiments conducted in South Africa, Turkey and Morocco

South Africa

Six measurements for 3 replicates were recorded for screening each DH line in response to SA aphid biotypes. Each replicate (up to 6 measurements) was averaged to get a replicate score which then was assessed (Resistant = <=6; Susceptible = >7) for aphid reaction. The response to DH lines was then combined for an overall Resistant : Susceptible score.

After initial data analysis of the South African biotyping dataset, the results show a significant proportion of DH lines with a score of 6 or 7. Based on the definition of score (6 = prominent streaking; 7 = severe streaking on leaf) we observed from the results that it is very difficult to distinguish the boundary between resistant and susceptible symptoms. This led us to re-evaluate DH lines across the three replicates. When a score of resistance (replicate-average <=7) was consistent across at least 2 replicates, we considered that DH lines as resistant. All other DH lines including indeterminate lines (ie including 2 reps of susceptible, 1 rep of resistant) where considered susceptible. The phenotyping results were evaluated for outliers and these were not included in the analysis. For example, when a replicate include all

but 1 or 2 measures that is very different from the other replicates scores (ie 7,7,7,7,3,2) then these replicates were excluded.

Turkey

Five leaf measurements were taken to assess aphid reaction by leaf chlorosis and leaf rolling. Leaf measurements were carried out in duplicate on each DH line to assess the reaction to the Turkey Izmir biotype. Each replicate (up to 5 measurements) was averaged to get a value for the replicate. Then the two replicates were scored for aphid reaction using the criteria for resistance of (chlorosis <=3; and leaf roll <=2). For aphid susceptible lines, the aphid reaction score used was chlorosis > 3 and leaf roll = 3. In circumstances where replicates showed inconsistent results they were excluded from the analysis (2 removed from a total of 96).

Morocco

In the Moroccan experiment, three leaf measurements were taken from an alpha lattice design using a total of 200 DH lines. Leaf chlorosis was scored from 1-6 with 1-2 as resistant and 3 or more as increasing degree of aphid susceptibility. Leaf roll was scored using a 1-3 scale also with 1-2 as resistant and 3 as susceptible. A final aphid-score was calculated from each replicated and then combined (for all 3 replicates) with both traits (chlorosis and leaf roll) with a score of 1 or 2 to be considered resistant. All other results (other than those for aphid-score for resistant) were considered susceptible including the inconsistent measurements with replicates showing both resistance and susceptibility. Since a reduced population of DH lines was tested in Turkey, a separate analysis was carried out on a subset of 94 DH lines.

3.3.4 Genotyping study of doubled haploid (DH) population

Extraction of DNA from leaf tissues collected from one month old seedlings

Genomic DNA from the leaf tissues was extracted using the Phenol/Chloroform extraction method. Briefly, 1.5 ml Eppendorf tubes contained 3cm size leaf tissues were placed in liquid nitrogen and ground with a plastic pestle. Ground powder was homogenized by adding 400 µL extraction buffer (100mMTris-HCl (pH 8.5); 100mM NaCl; 10mM EDTA; 1% Sarkosyl; and 2% PVPP). Another 400 µL Phenol:Chloroform:Isoamyl alcohol (25:24:1) at pH8 was added to homogenised material. Tubes were inverted several times, left for on ice 5 minutes and then centrifuged at 13000 rpm for 6 minutes. A volume of 40 µL 3M Sodium acetate and 400 µL isopropanol was added to the supernatant. They were incubated on ice overnight after inverting the tubes for several times. Tubes were centrifuged at 13000 rpm for 6 minutes. The pellet was washed with 70% ethanol twice and dried using a speed vacuum (Thermo SCIENTIFIC: Model ISS110P1-115). The pellet was dissolved with 200 µL R40 solution containing 40 µg RNase A in 1 ml 1X TE buffer (10mM Tris-HCl, 1mM EDTA at pH 8). DNA quantification was carried out using a Nanodrop 280 (www.nanodrop.com). Ninety six well plates containing 25 ng/ µL of genomic DNA were made by diluting the stock DNA with ultra-pure nuclease free water.

Parental and doubled haploid (DH) population screening with SSR markers

Parental screening was carried out using a collection of publicly available SSR markers (Sources: John Innes centre (psp), IPK Gatersleben (gwm/gdm), Wheat Microsatellite Consortium (wmc), Beltsville Agricultural Research Station (barc), and INRA collections (cfd/cfa). A total of 252 SSR markers distributed across the 1D, 1B and 7D and 7B wheat genome were chosen to screen the parents to identify polymorphic markers. Polymerase chain reaction with 50ng genomic DNA was

performed in a 10 µL reaction volume containing 2 µL cresol red solution, 1X My Tag Buffer (Bioline), 250nm each primers and 2.5 units MyTaq enzyme (Bioline). PCR conditions were at initially at denaturation at 94^0C for 3 min., then followed by 9 cycles of 94^0C 30 sec., annealing at 60^0C 30 sec with a 1^0C touch down and extension of 72^0C 30sec; 29 cycles of 94^0C 30 sec., annealing at 50^0C 30 sec and extension 72^0C 30sec and with final extension of 72^0C 5 min. PCR amplifications were carried out using a PerkinElmer 384 VT thermocycler. For analysis of the PCR products, 6uL of the amplified fragments were separated with 8% (19:1 Acrylamide:bisacrylamide). Polyacrylamide gel using Biorad Protein xl vertical gel apparatus at 110 voltage for 12 hours. Gels were photographed using the UV mode under the Gel Doc 2000 by staining with ethidium bromide solution (1 µg /ml) for 10 min and destained with deionised water for 2 min. Targeted markers selected to screen the DH population was based on clear polymorphisms and with wider genome coverage with a published consensus map (Somers et al., 2004). Identified polymorphic markers then were used to screen the 188 DH populations and separated either with 8% Polyacrylamide or 2% agarose gel electrophoresis.

Gel electrophoresis with 2% agarose was chosen to screen the DH population with polymorphic SSR markers showing either with presence/absence of allele or the SSR markers possessed polymorphic allele fragments that can be scored without any difficulties in 2% agarose gel. Gelgreen solution was added and mixed with agarose solution before casting the gel. Polyacrylamide gels (8% 19:1 Acrylamide:bisacrylamide) were used to screen DH population with the rest of the markers.

Whole genome scanning with genotyping–by–sequencing (GBS) and DArT molecular markers

To further improve map density, genome wide scanning was carried out by Diversity Arrays Technology Pty Ltd (www.diversityarrays.com), a commercial company

providing genome wide scanning using GBS and DArT markers in Australia. A volume of 10 µL of a 100 ng per µL genomic DNA from the parents and 92 DH lines was sent to Triticarte Pty Ltd for genome wide identification of GBS and DArT polymorphic markers.

3.3.5 Linkage analysis and QTL mapping

Firstly a genetic linkage map for EGA Gregory x PI94365 DH population of 92 was constructed with 1019 genetic markers with known chromosomes that include SSR, GBS and DArT markers with integrated genetic analysis software (Wang et al., 2014) . Linkage map construction involved three general steps: Grouping, Ordering and Rippling. All genetic markers were grouped based on the logarithm of odds (LOD) score which was set at 3.0. After ordering algorithm of SER (SERiation) was applied to the group the marker sequence was rippled for the fine tuning. Recombination frequencies (RF) was converted into genetic linkage distance (cM) using the Kosambi mapping function (Kosambi, 1944). This preliminary linkage map was used as an anchor map to create a complete linkage map with the rest of the markers.
QTL analysis was performed with Inclusive Composite Interval Mapping (ICIM) in QTL IciMapping v4.0 (Wang et al., 2014). ICIM-additive method was used for QTL mapping by choosing "Deletion" command for missing phenotype and with 1cM chromosome walking speed. Stepwise regression model was applied in ICIM software to identify background genetic variation control. LOD threshold was calculated using 1000 permutation with a Type 1 error of 0.05. Significant QTLs for the traits were identified as those with a minimum LOD score of 3.0.

3.3.6 Comparative mapping of the linkage maps derived from DH population of EGA Gregory x PI94365

Comparative mapping study with other publically available linkage maps was useful in order to identify more molecular markers associated with the region of interest. SSR consensus maps for chromosomes (https://ccg.murdoch.edu.au/cmap/ccg-

staging) and Population sequencing maps [POPSEQ maps (Chapman et al., 2015)] were chosen to perform comparative analysis. The comparative mapping analysis was performed with the Generic Model Organism Database Comparative Map (GMOD CMap) software package (https://ccg.murdoch.edu.au/cmap/ccg-staging).

3.4 Results

3.4.1 Phenotyping of doubled haploid (DH) lines in South Africa, Turkey and Morocco

South Africa

Doubled haploid (DH) lines from the cross EGA Gregory x PI94365, the parents and controls plus differential checks were infested with respective biotypes in South Africa, Turkey and Morocco to determine the reaction of individual DH lines to RWA. After inoculation at the two leaf stage, reactions to RWA infestation were assessed 21 days later (Table 3.3, 3.4 and 3.5).

Cultivar Hugenoot and wheat line CIM 14 are used as susceptible and resistant control in the experiment conducted in South Africa. The results show all three biotypes were able to infest and develop symptoms on the susceptible wheat lines. In Table 3.3 Damage ratings 9.0, 9.0 and 9.0 for the biotype 1, 2, and 3 respectively indicates susceptibility to infestation. Damage ratings 5.0, 6.0 and 5.0 indicate no significant damage and hence a classification of resistance to RWA.

Differential checks, cultivar Gariep, line Pan3144 and line CITR 2401 were used to check if any cross contamination occurred in aphid colonies during colony development or during experiment. All three differential checks are resistant to SA biotype 1. Table 3.3 shows differential checks are all resistant to moderately resistant judged from the Damage ratings (6.0, 5.0 and 4.0 respectively). SA biotype 2 was unable to cause significant infestation on CITR2401 (Damage ratings 4.0) but cultivar Gariep (Damage ratings 8.0) and PAN 3144 (Damage ratings 7.0) were

considered susceptible to SA biotype 2 (see legend to Table 3.3). SA biotype 3 caused significant damage on Gariep cultivar which is susceptible and failed to make significant damage on the lines PAN3144 (Damage rating 3.0) and CITR 2401 (4.0). PAN3144 and CITR2401 were defined as resistant to biotype 3. The results show from the control and differential checks that SA biotypes were able to cause significance visible damage on susceptible wheat plant and not to resistant line. The differential checks confirmed that there were no cross contamination in between biotypes during colony culture or during the experiment.

Based on the available controls and differential checks described above, the DH population showed a good range of resistant and susceptible phenotypes after infestation by SA biotype 1 (Damage ratings 4.0 to 9.0), SA biotype 2 (Damage ratings 3.0 to 9.0) and SA biotype 3 (Damage ratings 4.0 to 9.0).

Table 3.3: Mean value of RWA damage ratings from 6 replications after 21 days of infestation of South African biotypes 1, 2, and 3.

Trait	Controls		Differential checks			Parents		DH Population
	Hugenoot	CIM 14	Gariep	PAN3144	CITR 2401	PI94365	EGA Gregory	Range
SA Biotype 1	9.0	5.0	6.0	4.7	4.0	5.0	9.0	4.0 - 9.0
SA Biotype 2	9.0	6.0	8.1	7.0	4.0	6.0	9.0	3.0 - 9.0
SA Biotype 3	9.0	5.0	8.5	3.0	4.0	3.0	9.0	4.0 - 9.0

Damage ratings 1, 2 were referred to as extremely resistant; 3, 4 resistant; 5, 6 moderately resistant; 7, 8 moderately susceptible and 9, 10 susceptible.

Turkey

Resistance check a line carrying *Dn7* gene and susceptible check, Bezoztaja bread wheat were used as a control to check the effectiveness of the aphid infestation on wheat seedlings (Table 3.4). The line carrying *Dn7* gene remained resistant to the Izmir aphid population (Damage ratings - Leaf chlorosis 2.5, leaf rolling 1.0 and RWA density 2.0) and the susceptible wheat remained susceptible (Damage ratings- Leaf chlorosis 5.7, leaf rolling 3.3 and aphid density 0.1). The results show aphids were virulent to infest susceptible DH lines.

Based on the differential checks damage ratings, the DH population showed good range of resistant and susceptible phenotypes after infestation by RWA biotype (Damage ratings for leaf chlorosis, leaf rolling and RWA density 3.0 to 4.0, 1.0 to 3.0 and 0.0 to 3.0 respectively).

Table 3.4: Mean value of RWA damage ratings from 3 replications after 21 days of infestation of Turkey Izmir RWA populations.

Trait	Differential checks (average of 5 replications)		Parents (average of 5 replications)		DH Population (average of 5 replications)
	Resistant check	Susceptible check	PI94365	EGA Gregory	Range
Leaf Chlorosis	3.0	6.0	3.0	6.0	3.0– 4.0
Leaf Rolling	1.0	3.0	1.0	3.0	1.0 -3.0
RWA density	1.0	3.0	2.0	3.0	0.0 - 3.0

Leaf chlorosis: 1, 2 and 3 were referred to as resistant and 4, 5, 6 susceptible

Leaf rolling: 1 and 2 were referred to as resistant and >2 susceptible

RWA density: Unable to define resistance and susceptible group

Morocco

Field experiment with 200 DH lines was conducted in Anoeceur research station, Morocco. The results show the resistant line PI94365 is resistant (Damage ratings Leaf chlorosis 2.0 and leaf rolling 1.0) and EGA Gregory is susceptible (Damage ratings leaf chlorosis 4.0 and leaf rolling 3.0). DH population showed good range damage ratings to RWA infestation (Damage ratings leaf chlorosis 2.0 to 4.0 and leaf rolling 1.0 to 3.0 (Table 3.5).

Table 3.5: Mean value of RWA damage scale from 3 replications after 21 days of infestation of Morocco RWA biotypes.

Trait	Parents (average of 5 replications)		DH Population (average of 5 replications)
	PI94365	EGA Gregory	Range
Leaf Chlorosis	2.0	4.0	2.0 – 4.0
Leaf Rolling	1.0	3.0	1.0 -3.0

Leaf chlorosis: 1, 2 and 3 were referred to as resistant and 4, 5, 6 susceptible
Leaf rolling: 1 and 2 were referred to as resistant and 3 susceptible

3.4.2 Statistical analysis of RWA phenotyping data

Statistical analysis of phenotype data from South Africa, Turkey and Morocco were carried out as described in section 3.3.3. The histogram (Figure 3.2) shows proportion of resistant vs susceptible DH lines for each of the biotypes.

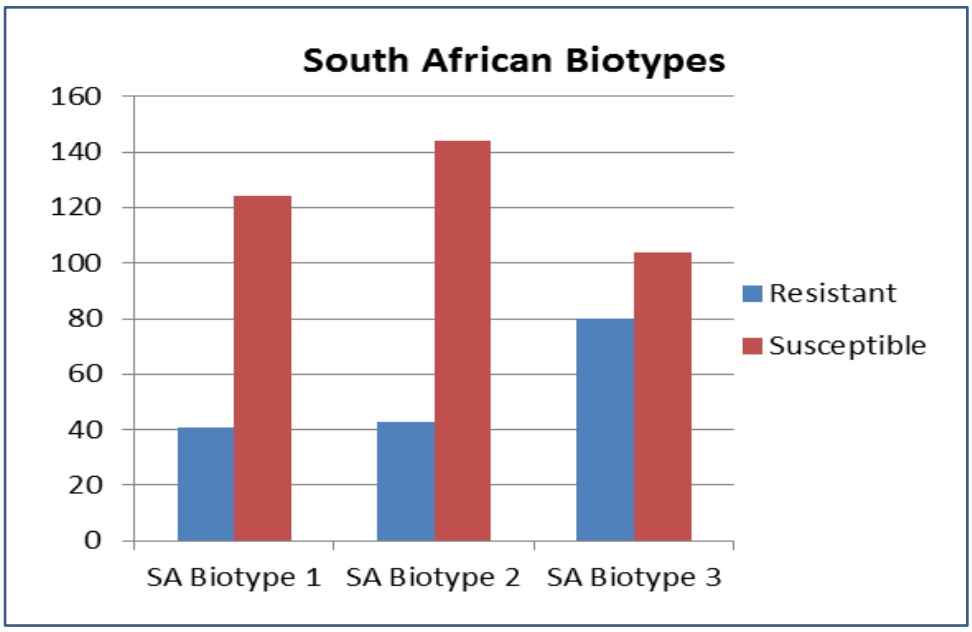

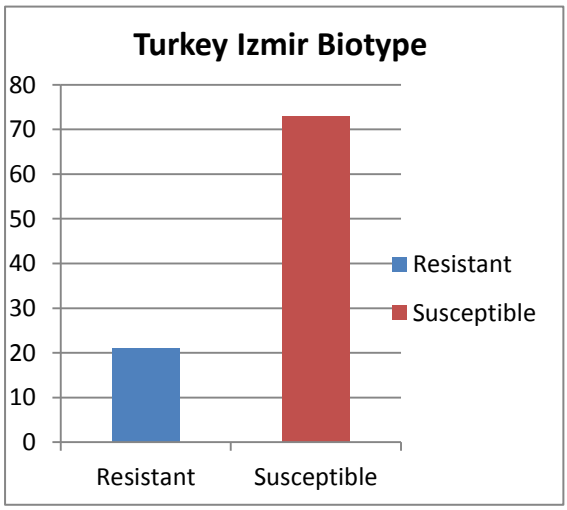

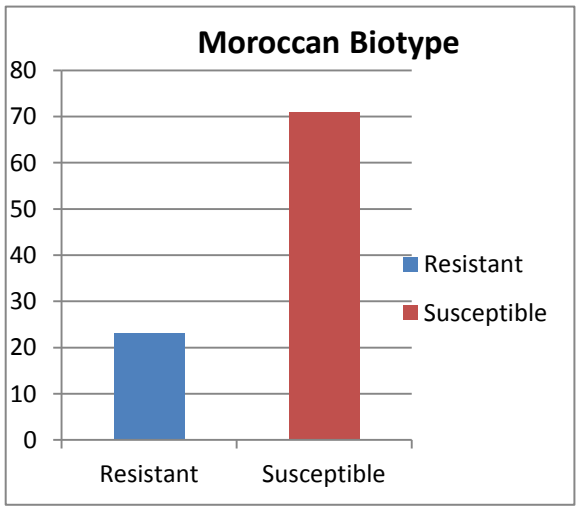

Figure 3.2: Number of DH lines showing resistant and susceptible reaction to the RWA biotype infestation

A chi-squared test was carried out using Genstat version 17 to compare observed measurements with predicted estimates and all the results confirmed the ratios (Table 3.6).

Table 3.6: Chi square test analysis of phenotype data showing observed and predict ratio between resistant and susceptible group.

	Resistant DH lines	Susceptible DH lines	Observed ratio (R:S)	Predict ratio (R:S)	Pearson chi-square value with 1 d.f.	Probability level (under null hypothesis)
South Africa: Biotype 1	41	124	1:3	1:3	0.00	0.975
South Africa: Biotype 2	43	144	1:3	1:3	0.21	0.65
South Africa: Biotype 3	80	104	1:1	1:1	1.57	0.21
Turkey	21	73	1:3	1:3	0.18	0.668
Morocco	23	71	1:3	1:3	0.01	0.933

R: Resistant; S: Susceptible; d.f: degree of freedom

3.4.3 Genotyping of DH lines

Gel fragmentation of amplified PCR products from the SSR markers those distributed on chromosome 1B, 1D, 7B and 7D during parental screening is given in Appendix Supplementary Figure I. The polymorphic SSR marker and the type gels used for further screening of DH population derived from the parents EGA Gregory and PI94365 are detailed in Appendix Supplementary Table II.

Genetic mapping

All the polymorphic SSR markers used to screen the DH population were subjected to Chi-square analysis to test for segregation pattern 1:1. Any markers showing segregation distortion were discarded. Total of 4053 molecular markers included SSR, DArT and GBS markers and were used to create linkage map and followed by GWAS study to underpin the QTL region on the chromosomes for the RWA resistance. A threshold logarithm of the odds to the base 10 (LOD) score of 3 was used for the mapping analysis. Identified chromosomal regions associated with RWA resistance to the different biotypes are shown Table 3.7.

Major resistance gene loci for the SA RWA biotype 1 and 2 were found to be located on short arm of 1D (1DS) and 7D (7DS) chromosomes. A single resistance locus for the SA RWA biotype 3 was mapped on 1DS. The QTLs for the RWA biotype 1 located on 1DS and 7DS were with LOD score of 14 and 19 and with Phenotype variation explained by QTL (PVE, as per the ICIM manual) of 29% and 43% respectively. The QTLs for the RWA biotype 2 located on 1DS and 7DS were with LOD score of 10 and 11 and with PVE of 29% and 36% respectively. Based on these observations, the QTLs on 1DS and 7DS equally contribute to the resistance to the SA biotypes 1 and 2. A QTL for the SA biotype 3 was mapped on 1D with LOD score of 21 and PVE of 66%. The major QTL for the Turkey biotype leaf chlorosis was mapped on long arm of 7B (7BL) chromosome (LOD – 22; PVE – 95%) and minor QTL was in the proximal region of long arm of 7D (7DL) chromosome (LOD - 5; PVE – 16%). The major QTL for Turkey biotype leaf rolling was mapped on 7DS (LOD – 37; PVE – 64%) and minor QTLs were short arm of 4A (4AS) with negative additive effect (LOD – 4; PVE – 13%) and long arm of 7B (LOD- 10; PVE – 8%). Two QTLs on 7BL and 7DS were identified for the RWA density for the Turkey biotype with LOD score of 4.6 and 4.3 respectively and they had negative additive effect.

QTLs for the Morocco RWA biotype leaf chlorosis were mapped on 1DS (LOD – 7; PVE – 17%), 3BL (LOD – 7; PVE – 17%) and 7DS (LOD – 4; PVE – 11%). A QTL for the Moroccan RWA biotype leaf rolling was mapped on 4DL (LOD – 4.5 and PVE – 16%) with negative additive effect.

The results from the genetic analysis shows that chromosomes 1D and 7D are the prominent loci involved in RWA resistance for SA and Turkey biotypes. Manhattan plots (Figure: 3.3) analysis carried out with GBS and DArT markers by DArT Pty Ltd, represents the significance of the association between the chromosomes with their respective biotypes.

South Africa – RWA biotype 1 and 2

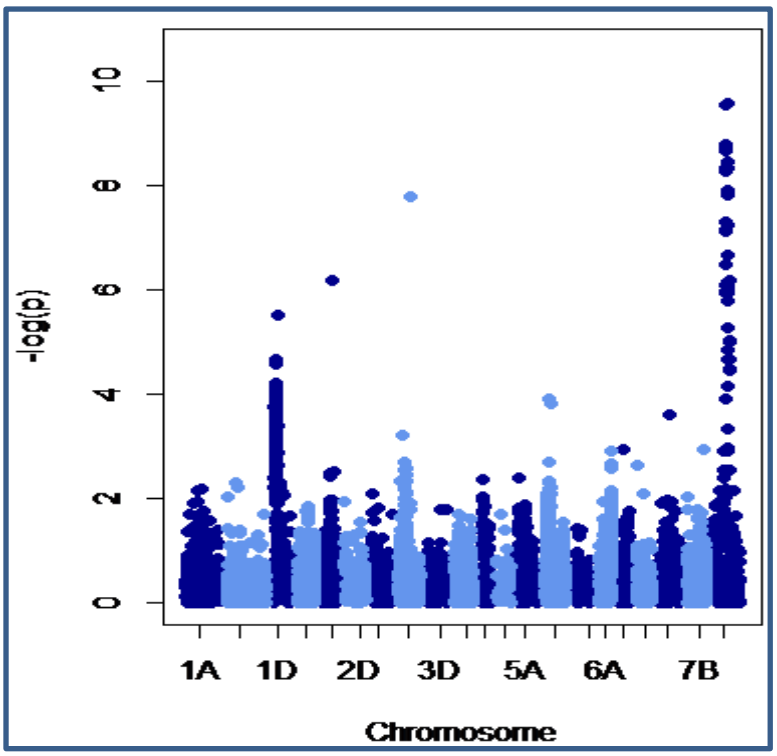

South Africa - RWA biotype 3

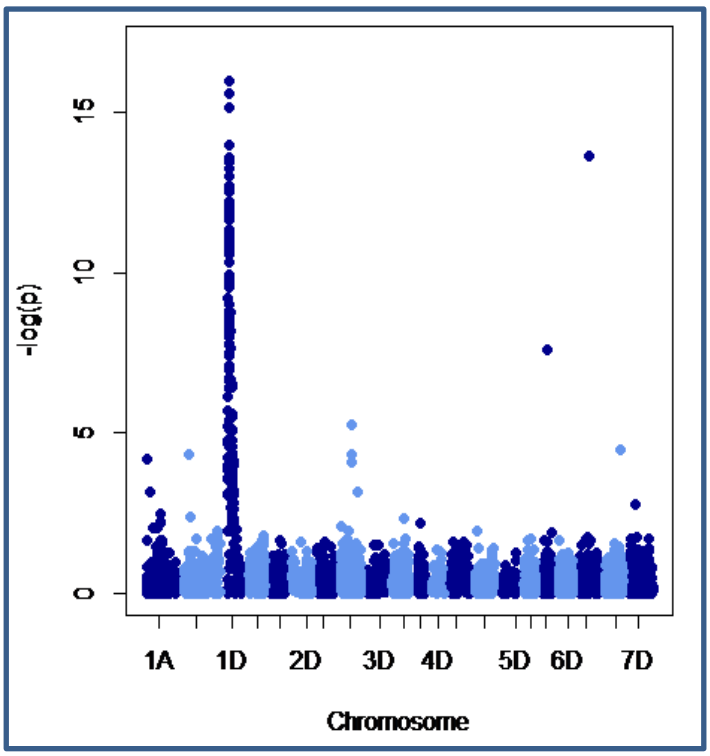

Turkey Izmir – Leaf rolling

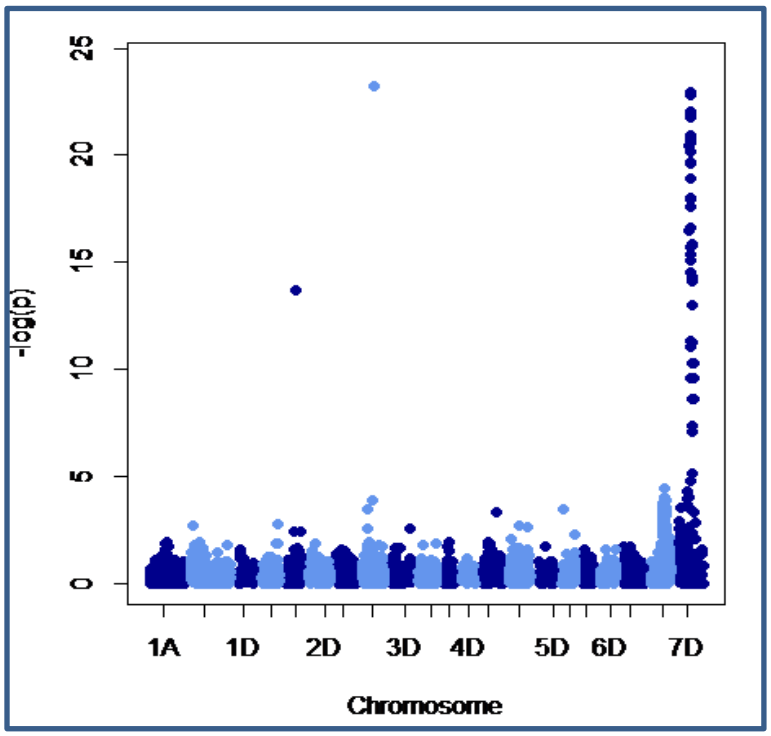

Turkey Izmir – Leaf chlorosis

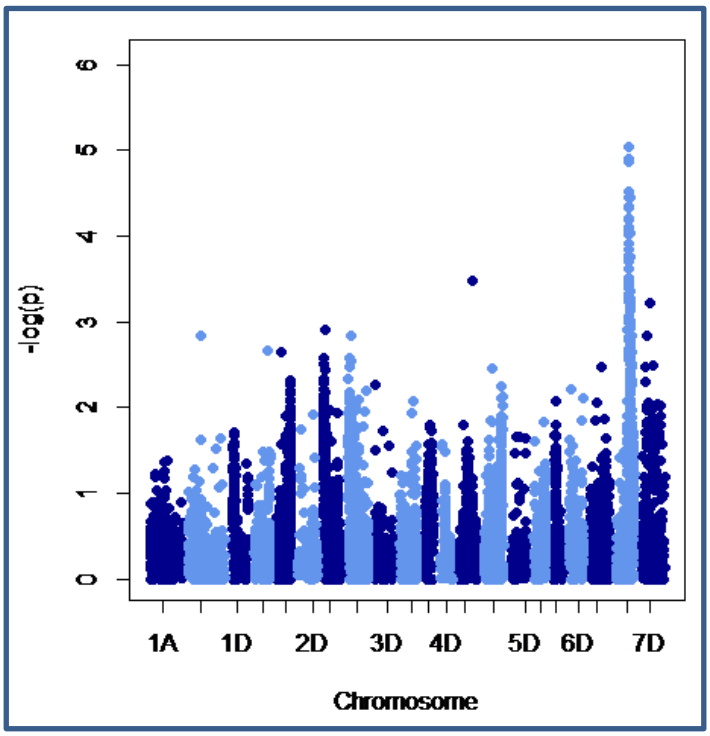

Figure 3.3: Manhattan plots showing chromosome 7D and 1D associated with SA biotype 1 and 2; chromosome 1D associated with biotype 3; Turkey leaf rolling associated with 7D and chromosome 7B associated with Turkey leaf chlorosis. The plots were kindly provided by Dr. Andrzej Kilian (Diversity Arrays Technology Pty Ltd, Australia)

Table 3.7: Summary of Quantitative trait loci (QTL) identified from inclusive interval mapping (ICIM) for the traits associated with RWA resistance

Trait	QTL	Chromosome	Position (cM)	Left Marker	Right Marker	LOD	PVE(%)	ADD
Leaf damage associated with SA RWA biotype 1	QTL_RWA_SAB1_1D	1DS	117	wmc336*	barc152*	14.45	29.00	0.7677
Leaf damage associated with SA RWA biotype 1	QTL_RWA_SAB1_7D	7DS	266	1109327**	1010929**	19.00	43.54	1.0066
Leaf damage associated with SA RWA biotype 2	QTL_RWA_SAB2_1D	1DS	116	wmc336*	barc152*	9.89	28.98	0.5809
Leaf damage associated with SA RWA biotype 2	QTL_RWA_SAB2_7D	7DS	266	1109327**	1010929**	11.43	34.54	0.6843
Leaf damage associated with SA RWA biotype 3	QTL_RWA_SAB3_1D	1DS	116	wmc336*	barc152*	21.28	66.32	1.4604
Leaf chlorosis (Turkey biotype)	QTL_RWA_Tchlorosis_7B	7BL	795	1215832***	2271493***	22.28	95.32	0.7427
Leaf chlorosis (Turkey biotype)	QTL_RWA_Tchlorosis_7D	7DL	1401	1241714**	1026339**	5.08	16.31	0.3129
Leaf rolling (Turkey biotype)	QTL_RWA_Trolling_4A	4AS	80	1000950***	984908***	4.11	12.91	-0.5362
Leaf rolling (Turkey biotype)	QTL_RWA_Trolling_7B	7BL	827	1041538***	1075525***	10.46	8.10	0.2119
Leaf rolling (Turkey biotype)	QTL_RWA_Trolling_7D	7DS	266	1109327**	1010929**	37.34	64.26	0.6487
RWA density (Turkey biotype)	QTL_RWA_Tdensity_7B	7BL	828	1075525***	1113446**	4.64	16.83	-0.2949
RWA density (Turkey biotype)	QTL_RWA_Tdensity_7D	7DS	1407	1026339**	1233310**	4.34	16.48	-0.2939
Leaf chlorosis (Morocco biotype)	QTL_RWA_Mchlorosis_1D	1DS	121	1056487**	988523**	6.70	17.18	0.1643
Leaf chlorosis (Morocco biotype)	QTL_RWA_Mchlorosis_3B	3BL	849	1013062**	989565***	6.77	17.69	0.1641

Leaf chlorosis (Morocco biotype)	QTL_RWA_Mchlorosis_7D	7DS	403	2263161**	100000632**	4.20	10.96	0.1291
Leaf rolling (Morocco biotype)	QTL_RWA_Mrolling_4D	4DL	277	1087762**	982040**	4.55	16.17	-0.1056

Trait: Trait on which data was collected, Chromosome : Chromosome on which the QTL was mapped to, Position: Scanning position in cM on the chromosome, Left marker: Name of the left-side marker of the identified QTL, Right marker: Name of the right-side marker of the identified QTL, LOD: logarithm of Odds score caused of the QTL; PVE%: Phenotype variation explained by QTL at the current scanning position, ADD: Estimated additive effect of the QTL at the current scanning position, *: SSR markers; **:DArt Markers; *:GBS markers**

3.4.4 Comparative genomics analysis

QTLs for the RWA resistance in this mapping population were mapped on Chromosomes 7D, 1D, 7B, 3B, 4A and 4D. Comparative genomic analysis of 7D and 1D maps with corresponding published consensus https://ccg.murdoch.edu.au/cmap/ccg-staging) and with corresponding POPSEQ maps (Chapman et al., 2015) are shown in Figure 3.4 and 3.5. The rest of the maps are shown in appendix. The order of SSR markers are consistent with the published SSR consensus maps (Somers et al., 2004; Roder et al., 1995; https://ccg.murdoch.edu.au/cmap/ccg-staging) and POPSEQ map (Chapman et al., 2015). The comparative wheat 7Dcon Dec 2014 on the left hand side of the Figure 3.4 shows location of *Dn* genes from the previous studies, the middle map shows the reference wheat EGAxPI4054 shows the location of the QTLs of SA biotype 1 and 2, Turkey leaf rolling, Turkey leaf chlorosis and Morocco leaf chlorosis of this study. Comparative mapping studies confirmed that QTLs of SA biotype 1 and 2, Turkey leaf rolling and Morocco chlorosis from this study were in the same region of *Dn* gene cluster on the chromosome 7DS. Comparative mapping study with 7D_POPSEQ_ver2GSS_CMap (map the far right) shows the alignment to several POPSEQ markers in the mapped QTL region.

As in Figure 3.5, the wheat 1D_Con_2015 map on the left shows the location of *Dn4* gene and the middle map wheat EGAxPI4054 shows the QTLs of SA biotype 1, 2 and 3 and the QTL of Morocco chlorosis. The comparison of these two maps confirmed that the QTLs of SA biotype 1, 2 and 3 and the QTL of Morocco chlorosis were in the same region of *Dn4* gene. Many POPSEQ markers are aligned with in the region of resistance on the chromosome 1DS in the comparative mapping study with 7D_POPSEQ_ver2GSS_CMap. The full details of the comparative maps shown in this study can be obtained at higher levels of magnification from the cMap location at the website, https://ccg.murdoch.edu.au/cmap/ccg-staging.

As in Figure 3.6 shows the QTLs of Turkey leaf chlorosis, Turkey leaf rolling and RWA density on 7BL EGAxPI4054 (right). Alignment of the 7BL EGAxPI4054 map with the current 7B_POPSEQ_ver2GSS_CMap (left) resulted in too many ambiguities to allow a clear alignment of markers. This needs to be investigated further.

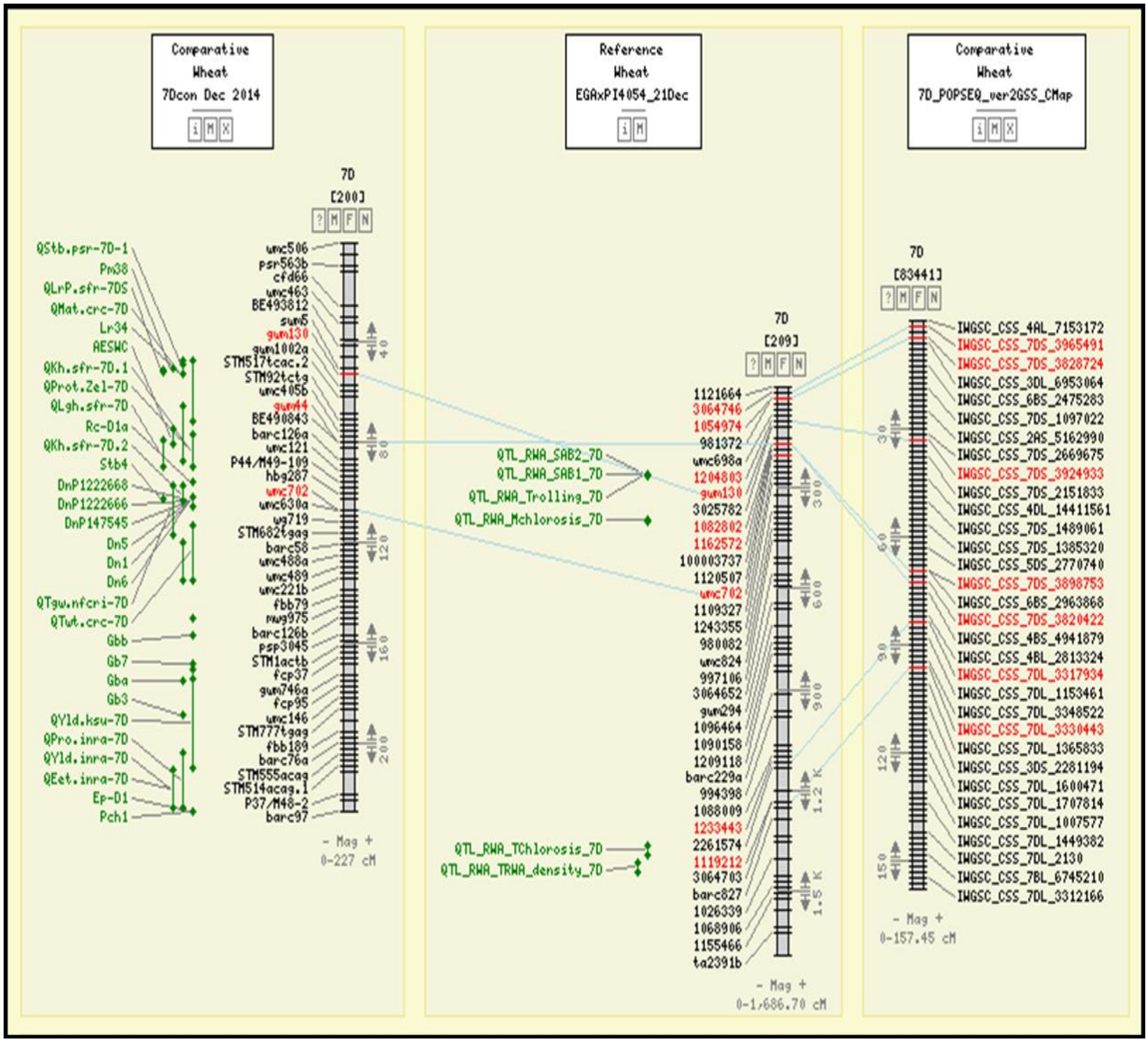

Figure 3.4: Genetic linkage map of EGA Gregory x PI94365 showing RWA QTLs aligned to the RWA QTLs on wheat 7D consensus map December 2014 (left) and corresponding wheat 7D_POPSEQ_ver2GSS_CMap (right). The traits mapped as QTL are: South African RWA biotype 1 and 2; Leaf chlorosis for Moroccan RWA population; leaf chlorosis for Turkey Izmir RWA biotype; RWA density for Turkey Izmir RWA biotype.

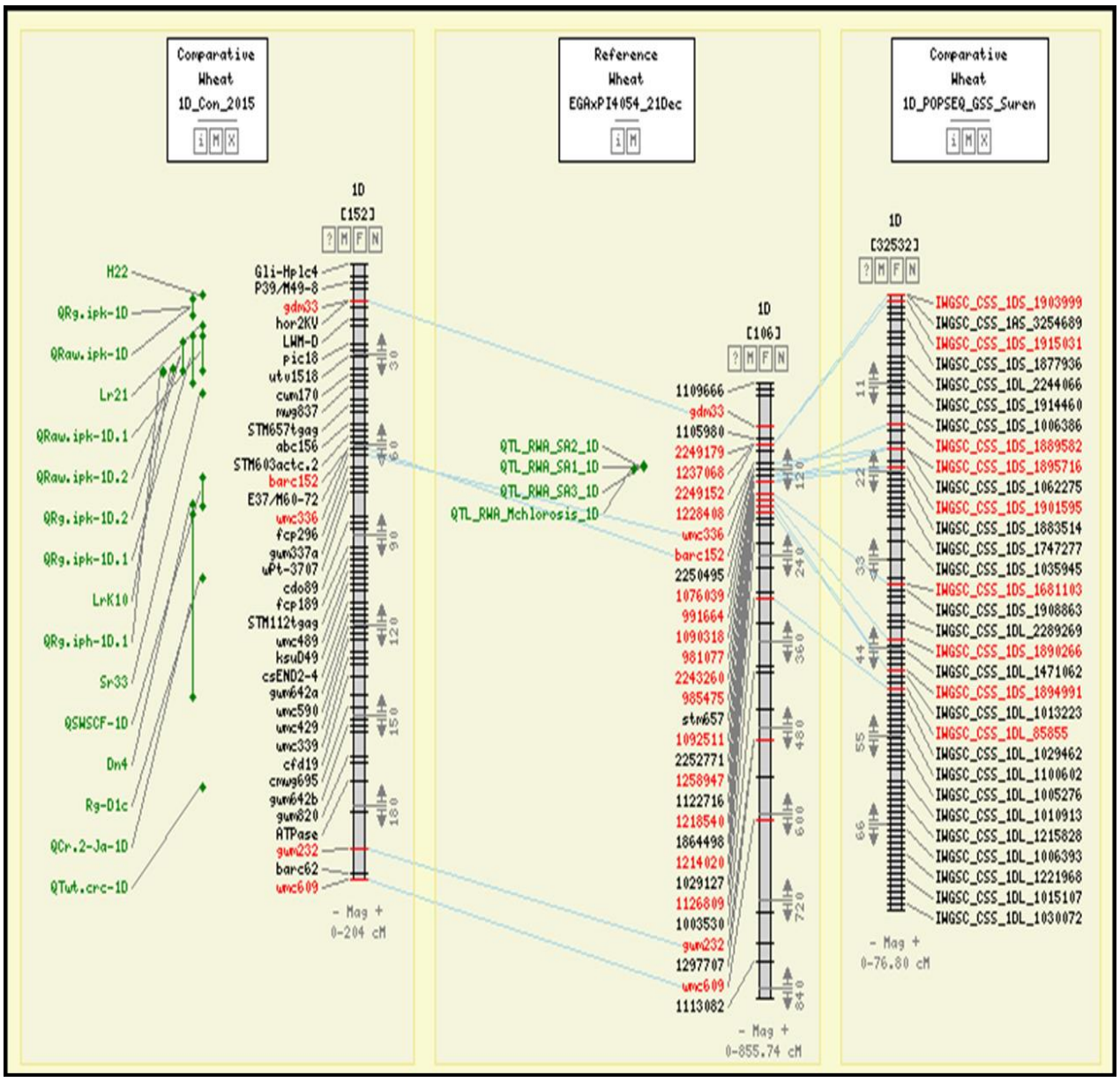

Figure 3.5: Genetic linkage map of EGA Gregory x PI94365 showing RWA QTLs aligned to the wheat 1D_Con_2015 (left) and to the wheat 1D_POPSEQ_GSS_Suren (right). The traits mapped as QTL are: South African RWA biotype 1, 2 and 3; Leaf chlorosis for Moroccan RWA population.

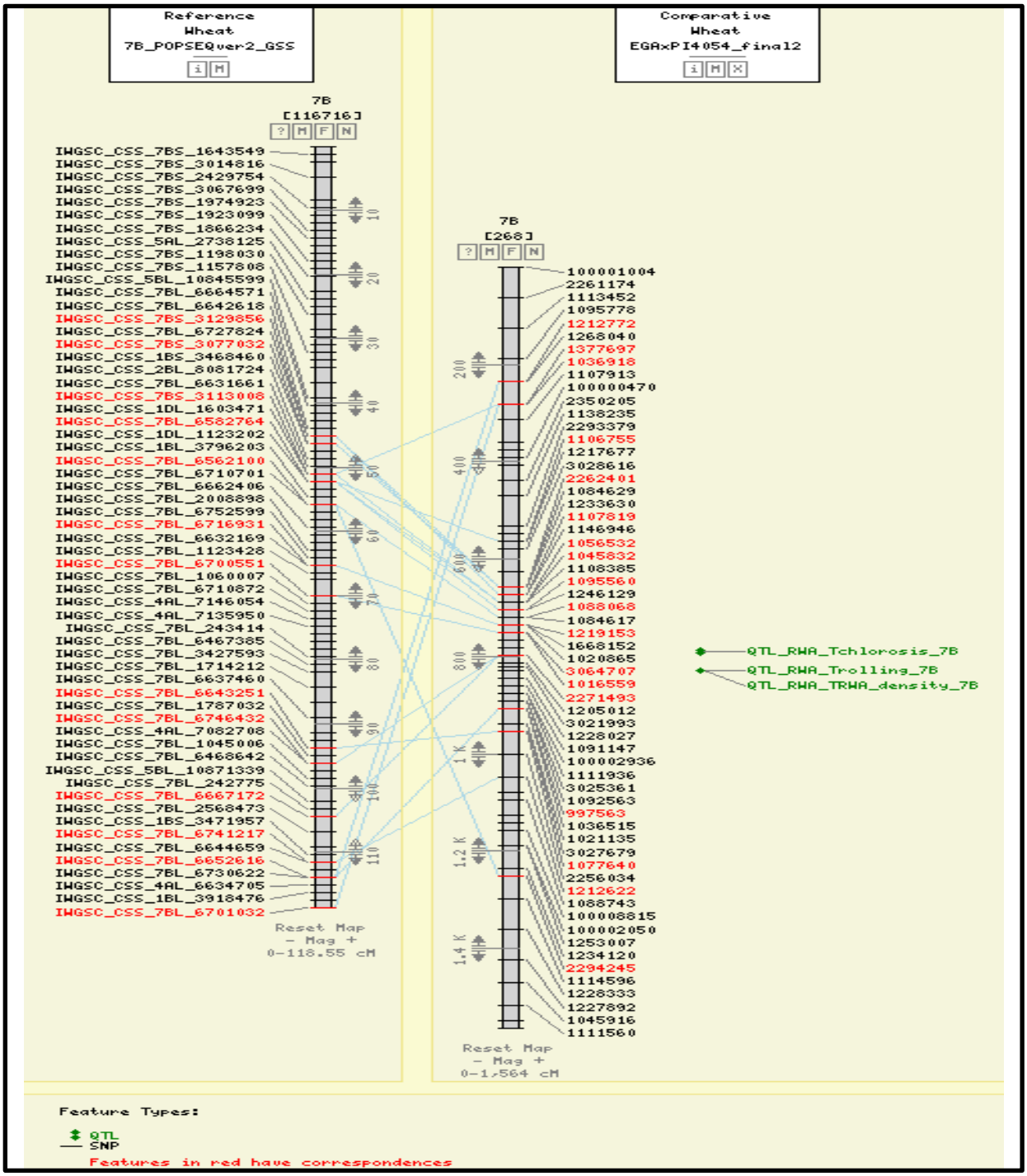

Figure 3.6: Genetic linkage map of EGA Gregory x PI94365 showing RWA QTLs aligned to the wheat 7B_POPSEQ_GSS (left). The traits mapped as QTL are: Leaf chlorosis and leaf rolling for Turkey Izmir RWA biotype; RWA density for Turkey Izmir RWA biotype.

3.5 Discussion

The Russian wheat aphid has caused significant yield losses in susceptible wheat cultivars by injecting toxic substances that break down chloroplasts (Cooper et al., 2010). The occurrences of new and more virulent biotypes require new resources of resistance to broaden the genetic base of the resistance in wheat (Ricciardi et al., 2010). Wheat (*Triticum aestivum* L.) is a hexaploid genome consisting three distinct homoeologous A, B and D genomes. Complexity of the genome in harbouring extensive repetitive elements means that genes tend to occur in clusters called gene islands (Feuillet et al., 2012). RWA resistant loci (*Dn*) from resistant sources were mapped in several mapping populations.

A summary of the RWA resistance loci is described in Figure 3.6 as shown, loci *Dn1*, *Dn2*, Dn5, *Dn6*, *Dn8*, *Dnx*, *Dn626580* and *Dn2401* were located in chromosome 7D (Liu et al., 2005) with SSR markers, *Xgwm111* being closely linked to *Dn1*, *Dn2*, *Dn6* and *Dnx* on chromosome 7DS (Liu et al., 2005). The *Dn4* locus was mapped on chromosome 1DS (Liu et al., 2002) and *Dn9* resistance gene was located on 1DL (Peng et al., 2007). Since the majority of the *Dn* resistance loci were found in chromosomes 7D and 1D (Figure: 3.7), the initial parental screening was carried out with 216 SSR molecular markers distributed through chromosomes 7D, 1D and 1B. Parental screening with 36 chromosome 7B SSR markers was included in the later part of the analysis. Entire genome wide screening of DH population was performed with DArT and GBS markers. Genome-wide association study (GWAS) was chosen to locate chromosome region for the resistance loci in this mapping population since GWAS provided good marker coverage and higher possibilities to identify potential markers in the region of interest (Pozniak et al., 2012). The association study performed with more than 10,000 SNP, DArT and SSR markers and the phenotype score confirmed that chromosome 7DS and 1DS had major association with RWA resistance.

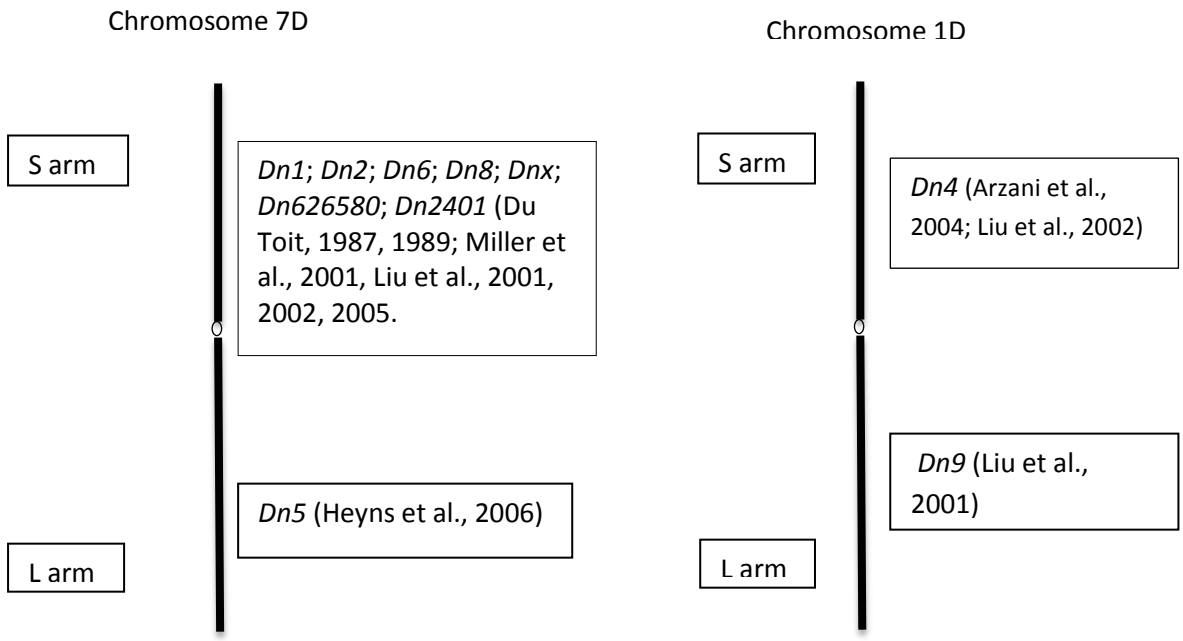

Figure 3.7: Chromosomal region of designated *Dn*-genes that derived from the hexaploid common wheat

3.5.1 Mapping for the South African biotypes

Segregation pattern in DH population following the infestation SA RWA biotypes 1 and 2 was 3:1 susceptible to resistant ratio and 1:1 for the SA RWA biotype 3. This pattern of segregation fits to two genes and single gene model for biotype 1 and 2, and biotype 3 respectively. Mapping results of this study shows RWA resistance on 7D in the same region of other *Dn* genes mapped on 7DS (Figure 3.7). Aphid resistance genes often occur as clusters within specific chromosomal regions (Valdez et al., 2012).

Several studies as in figure 3.7 shows *Dn1*, *Dn2*, *Dn6*, *Dn8*, *Dnx*, *Dn626580*, *Dn2401* genes were mapped in this region from several resistance sources. This study has also confirmed that the same region contributes to acquire resistance towards the biotypes. Liu et al. (2001, 2002, 2005), Miller et al., 2001 and Du Toit (1987) mapped these loci on 7DS and identified they were linked to *Xgwm111*. We hypothesise that

the QTL at the 7DS (near centromere) is controlled by several loci through providing small additive effects from each locus. The loci at the region are tightly linked, segregate together and it is possible that the phenotype association described by QTL_RWA_SAB1_7D, QTL_RWA_SAB2_7D, and QTL_RWA_Trolling_7D on 7DS may in fact be a single locus comprising multiple genes. Multiple genes in a disease resistance QTL region for RWA has been suggested by Fazel-Najafabadi et al. (2014). A well characterized precedent for this possibility has been described by Manosalva et al. (2009) who reported seven of 12 rice germin-like proteins (OsGLPs) coding genes were tightly linked in a QTL in chromosome 8 of Rice (*Oryza sativa*) conferring broad spectrum disease resistance against many races of the pathogen *Magnaporthe oryzae*.

Another QTL for the resistance to the biotype 1, 2 and 3 was mapped in the 1DS in the region of *Dn4* (Figure 3.7). Single land race contributing RWA resistance with 2 major QTLs, one in 7DS and other one in 1DS has not been reported previously. Based on the LOD value (Biotype 1:7DS-19.001, 1DS-14.45; Biotype 2: 7DS-11.43, 1DS- 9.89), it clearly showed that both QTLs were contributing in an equal basis to the RWA resistance.

A QTL from 1DS (LOD - 21.28) could be enough to contribute resistance to the biotype 3 and the QTL was in the same region of *Dn4* gene. It confirmed that region of DNA may possible to have multiple loci at the QTL. This study also confirmed loci at the 7DS are the driving force of RWA resistance in addition to other mapped loci. We hypothesize the QTL at the 7DS may have multiple genes for the resistance and that the resistance to RWA may have been occurred by recruiting any one of the genes or combination of genes at the QTL region. A minor gene effect was not detected in response to SA biotypes. Leaf rolling and leaf chlorosis components were combined to determine the reaction of the DH line in response to the SA biotypes'

infestation. Therefore the scoring methodology may possibly not detect minor gene effects with RWA infestation (Fazel-Najafabadi et al., 2014).

3.5.2 Mapping for the Turkish biotype

The phenotyping study with the Turkey Izmir RWA population revealed the segregation pattern of 1:3 resistant to susceptible ratio fitting a two genes model. The mapping with molecular markers and the quantitative scores to the resistance to RWA shows loci on the 7BL region associated with RWA resistance in addition to loci on 7DS that have been discussed in the SA biotypes. Gene(s) from these two loci appeared to be induced to acquire resistance against the Turkey Izmir RWA population. The additional resistance loci mapped on chromosome 7BL demonstrates that the Turkey Izmir RWA population differs from the SA biotypes 2 and 3. Apart from these two QTLs, 7BL and 7DS another loci involved in the Turkey leaf chlorosis resistance was mapped at the long arm of 7D (7DL). Involvement of 7DL in RWA resistance has been reported by Valdez et al. (2012).

3.5.3 Mapping for the Moroccan biotype

Following the infestation with the Moroccan RWA biotype, the DH population segregated in the ratio of 1:3 resistant to susceptible fitting the two genes model. However there were three loci for the leaf chlorosis on chromosome 1DS, 3BL and 7DS and another locus for the leaf rolling on chromosome 4DL (LOD 4.5). The lines showing resistance to RWA was contributed by all four loci from 1DS, 3BL, 7DS and 4DL and hence indicates more than just two loci contributing to the RWA resistance. We note that in this experiment the RWA assessments were conducted in an open field environment where RWAs were more prevalent and the number of RWA biotypes that were in the experiment was not clearly defined.

3.5.4 Comparative mapping study with consensus and POPSEQ maps

Comparative mapping of EGA Gregory x PI94365 linkage map with relevant consensus and POPSEQ maps show that the marker alignments are in order with few incidences of cross over. Mapped QTLs of SA biotypes 1 and 2, Turkey leaf rolling, Turkey leaf chlorosis and Morocco leaf chlorosis from this study falls in the region of RWA gene cluster on chromosome 7DS. The QTLs, SA biotypes 1, 2 and 3 and the QTL of Morocco chlorosis mapped on short arm of chromosome 1D area falls on the region of the *Dn4* gene. Through the alignment of these regions with POPSEQ map means that it is now possible to access many more of the POPSEQ molecular markers. The number of POPSEQ markers available in the respective regions (1130, for the 1DS region and 14908 for the 7DS region) of the enlarged version of these maps can be accessed through https://ccg.murdoch.edu.au/cmap/ccg-staging. Sequences of these markers are publically available in the so-called survey maps at http://plants.ensembl.org/Triticum_aestivum/Info/Index (see also Chapman et al 2015). The scaffold sequences can be proposed to design markers for screening the parents to identify polymorphic markers.

3.5.5 Proposed model for the locus 7DS

The evidence increasingly support that eukaryotic chromatin is organised as independent loops (Heng et al., 2001; Heng et al., 2004) and smaller loops are formed towards the telomere and larger loops are integrated away from the telomere regions. The loops anchor on the nuclear matrix via a chromatin segment and as a basic unit, they are essential for DNA replication, transcription regulation and chromosomal packaging (Stein et al., 1999; Sumer et al., 2003).

To date, the majority of *Dn* genes for RWA resistance have been mapped in the proximal region of the short arm of chromosome 7D and we proposed that they can be considered to be a cluster of genes tightly linked into an apparently single genetic locus. One of the loci contributing resistance to RWA biotypes from the PI94365

resistance source was also mapped in the same region. *Dn* genes are nearer to the centromere regions and there is a higher possibility of the *Dn* genes in that region to form a larger loop and act as a single locus.

We propose a model based on the principle of nuclear Scaffold/ Matrix attachment regions (SS/MARs) model previously reported by Heng et al. (2004). *Dn* genes conferring RWA resistance at the 7DS locus can be considered to be the loop. The loop is attached to the nuclear matrix with via Structural Scaffold/Matrix attachment region (SS/MARs). SS/MARs is a chromatin segment of the loop which has a specific DNA sequence attached to it. The DNA sequence in the chromatin segment helps the loop anchor into the nucleus matrix. On other hand, each *Dn* gene in the loop is attached to its own Functional Scaffold/Matrix attachment regions (FS/MARs) as described in figure 3.7. These FS/MARS is (active in some cases and in-active in another case) a region for transcription/replication regulation. As in Figure 3.7 this repetitive gene model provides the opportunity for genes in the array to be recruited for resistance to a new RWA biotype and could account for resistance to new biotypes mapping to the same locus.

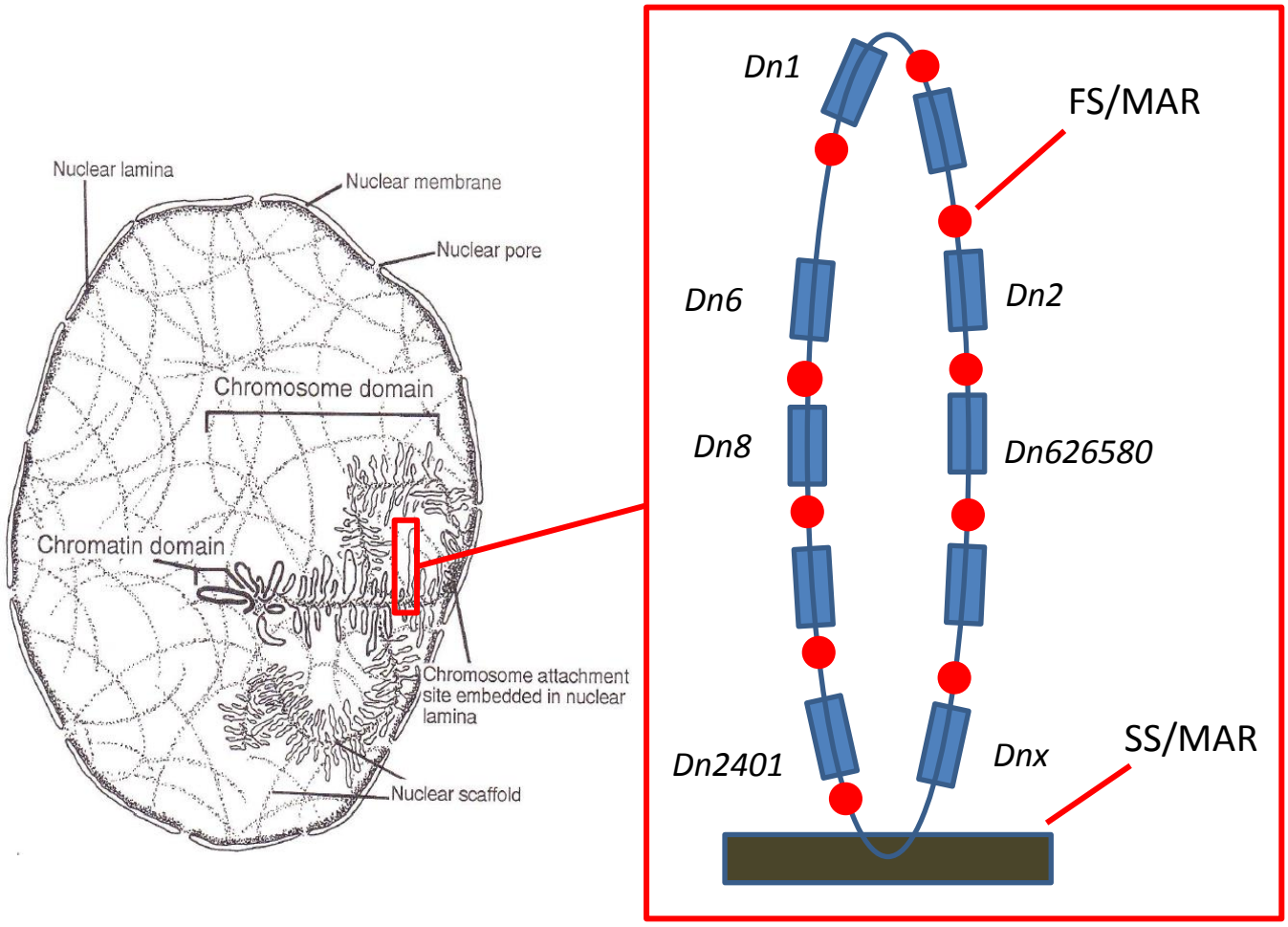

Figure 3.8: Possible structure of 7DS Russian wheat aphid resistance locus. The diagram of the nucleus in the left panel is from Appels et al. (1998)

***Diuraphis noxia* resistance genes: *Dn1*, *Dn2*, *Dn6*, *Dn8*, *Dn 2401*, *Dn 626580*, *Dnx*; SS/MAR-Structural Scaffold/Matrix attachment region; FS/MAR- Functional Scaffold/Matrix attachment region**

3.6 Conclusion

Having host plant resistance to the devastating pest such as RWA is a sustainable solution to mitigate damage caused by the insect and it is also an environmentally safe method to control the pest. Genetic linkage mapping for agricultural pests and diseases and the traits plays a vital role in the cultivar development through the use of molecular markers. Several QTLs controlling RWA resistance have been mapped from RWA resistance sources. However the effectiveness of RWA resistance from

the RWA resistance loci is varied and it depends on the background into which *Dn* genes are transferred and the possible involvement of the modifier genes which may control the expression of resistance genes (Valdez et al., 2012). Hence genetic background can play a vital role in the expression of major RWA resistance genes and the phenotype of individuals. In this study, we have mapped several QTLs for the biotypes and identified several molecular markers closely linked to the resistance loci. These molecular markers can be used to identify polymorphic markers and hence they can be successfully utilised in the pipe-line of RWA-resistant cultivar development. A resistance PI 94365 line was identified by (Smith et al., 1991) against Russian wheat aphid and was argued to contain a single dominant gene (Dong et al., 1997) . The present study demonstrates the value of PI94365 as a source of RWA resistance and in fact showed that the line possesses multiple resistance genes to RWA. DH lines developed through EGA Gregory and PI94365 showed resistance against the several biotypes and we have mapped the chromosomal region of the loci responsible for the resistance. The work in this Chapter identified a large number of new molecular markers linked to the resistance regions through alignment of the EGA Gregory x PI94365 to the POPSEQ maps (Figure 3.4, 3.5, 3.6) (Chapman et al., 2015). This high density of new molecular markers means it is now feasible to always identify polymorphic markers for tracing the RWA loci in a breeding program.

Chapter 4: Relating transcriptome and functional studies of genes induced by phloem feeding Russian wheat aphid to wheat gene model

Additional acknowledgement:

Mr Gabriel Keeble-Gagnère, Bioinformatics, Murdoch University: Providing advice on wheat genome annotation

4.1 Abstract

In a compatible interaction, Russian wheat aphid (*Diuraphis noxia*) is able to deliver elicitors into the host plants and can cause significant yield reduction reported in major wheat growing countries. Several published genes involved in the production of biosynthetic compounds were up regulated or down regulated with infestation of RWA. This study annotated 287 differentially expressed proteins from the published literature to the wheat genome and the genes were annotated into the categories of hydrolases, oxidoreductases, transferases, isomerases, signal transduction, pathogenesis proteins (PR), transport proteins, calcium ion binding proteins, ligase, lyase, replication, protein binding proteins, cytochrome c, antiviral proteins and electron transport proteins. We identified fourteen genes assigned chromosome to 1D, 7D and 7B that were hypothesized to be the gene loci in the RWA resistance loci regions characterised in the chapter 3. Possible protein models for those genes identified in the mapped chromosomes for RWA resistance loci in the generated DH population are presented. Investigation of proteins in the region RWA resistance loci describes potential gene networks involved in RWA resistance.

4.2 Introduction

Aphids are the largest group among the insects damaging the agricultural crops by removing photoassimilates (Smith & Boyko, 2007). Selection of plant tissues by the aphids depends on genetic architecture of both the insects and plants. In a compatible interaction, well-coordinated interactions take place between protein(s) encoded by the attacking insects and the host. When a non-coordinated interaction occurs in between proteins an incompatible interaction results and aphids are unable to cause damage on the plant (Botha et al., 2005). In aphid associated molecular patterns (AAMPs), the compatible vs non-compatible interactions are largely determined by the reactions in the plant to the oral secretions injected by the aphids into the phloem. Factors such as blockage of the point of entry into the phloem as well as the overall reaction to the chemical component of the oral secretions can determine the outcome for the plant aphid interaction (Nicholson et al., 2012). Oral secretions of phloem feeding insects consist of complex mixture of lipoprotein, phospholipids, carbohydrates and enzymes which involve in proteolytic, hydrolytic, oxidative or degradation of cell wall (Cherqui & Tjallingii, 2000; Miles, 1999; Tjallingii, 2006). These signalling compounds from aphid secretions induce plant defence signalling pathways, AAMPs, which lead to the production of several defensive compounds to counter aphid infestation (Ciepiela & Sempruch, 1999).

Plant tissues respond to aphid feeding in as little as 1 hour (Forslund et al., 2000). Following recognition of insects' elicitors, plant cells generate ROS which initiate several signalling cascades involving the activation of defence and metabolic genes as a result of downstream production of defence and de-toxification proteins (Ciepiela & Sempruch, 1999). Defence signalling cascades include production of jasmonic acid (JA), salicylic acid (SA), ethylene (ET), abscisic acid (ABA) and giberellic acid. The signalling cascades associated with metabolic genes include glycolysis, tricarboxilic acid (TCA), pentose phosphate, and amino acid synthesis pathway. Differential expression of many genes involved in these plant pathways as a result of

aphid feeding have been identified by the transcript profiling studies and provided a basis for studying changes in gene expression at the transcription level (Ciepiela & Sempruch, 1999; Smith & Boyko, 2007). The genes and gene networks include genes involved in the oxidative burst and hypersensitive response based cell death, cell wall modification, signalling cascades, transcription factors, photosynthetic regulation and the production of metabolites (Botha et al., 2005). Transcript profiling study conducted in the wheat cultivar containing a resistance (*DnX*) RWA gene and the susceptible cultivar to RWA has shown that many genes were differentially expressed by aphid infestation (Smith et al., 2010). Accurate annotation of the genes involved in RWA resistance in the wheat genome is paramount for downstream bioinformatics analysis and for the design genome wide biological assays. The genome sequence of major crop species are publically available or in the process of completion (Feuillet et al., 2012; plants.ensemble.org). An ordered draft sequence of the more complex allohexaploid bread wheat genome has been recently completed with >124 000 gene loci distributed across of the A, B, and D sub genomes (International Weat Genome Sequencing Consortium, 2014; plants.ensembl.org/Triticum_aestivum; Ross et al., 2004). The availability of sequence information for the wheat genome enables the annotation of genes involved in the defence mechanism against herbivore attack which has not been previously carried out. The objectives of this Chapter are:

(i) to annotate defence genes in the hexaploid wheat genome involved in defence signalling pathways that includes metabolome changes in resistance and susceptible plants against RWA infestation

(ii) to understand the gene-networks involved in RWA resistance in wheat

4.3 Materials and methods

Lists of proteins and their respective gene accession were gathered through publically available data bases including National Centre of Biotechnology Information (NCBI, http://www.ncbi.nlm.nih.gov). Full length cDNAs to those accessions were retrieved through Graingenes (wheat.pw.usda.gov/cgi-bin/graingenes/est_fasta.cgi). The functional protein domains of the full length cDNA sequences were further analysed with NCBI Conserved Domain Search Service (Marchler-Bauer et al., 2009, Marchler-Bauer et al., 2011 and Marchler-Bauer et al., 2015) using default settings and the Pfam 28.0 programme (http://www.pfam.sanger.ac.uk) using protein sequence queries with an E-value cut-off of 1.0 (default). TRAES number for the cDNA sequences which were correctly matched to proteins were retrieved through EnsemblPlants-Tritcum aestivum (plants.ensembl.org/Triticum_aestivum). TRAES numbers were taken to corresponding cDNA sequences with >95% alignment and with the cut of E value of $^{-}$50. Protein structure for the gene model and its function were identified using Phyre 2 annotation [Protein Homology/Analogy Recognition Engine; (Kelley et al., 2015)]. Expression of the genes at the different growth stages of wheat with RNASeq data base (Pingault et al., 2015) and their distances in the POPSEQ map (Chapman et al., 2015) were retrieved through Tritigate website (aestivum.accwi.org.au) at accwi.org.au, user ID: triticum, password: urartu.

4.4 Results

Several genes have been found to be differentially expressed at the significant level in RWA resistant or susceptible wheat plants as a result of interactions between proteins in RWA elicitors and their host proteins (Botha et al., 2005; Boyko et al., 2006; Lacock et al., 2003; Liu et al., 2011; Smith & Boyko, 2007; Smith & Chuang, 2014; Smith et al., 2010). In this study, 287 gene models showing significant differential expression with RWA infestation were annotated with respect to the wheat genome (Appendix: Supplementary Table II).

Although the proteins expressed by the RWA infestation found in literature were annotated to all the wheat chromosomes, this study focussed on the genes that were annotated to chromosomes 1DS, 7DS, 7BL, 3B (long or short arm of the chromosome 3B were not to be distinguished in the data base), 4AS and 4DL since RWA resistance loci in this mapping population were mapped in those chromosomes. Protein structures, RNASeq expression profile and POPSEQ distances were identified for the genes that were mapped in the region of RWA resistance loci (Table 4.1, relevant gene models highlighted in red).

A total of 12 genes were mapped on the short arm of chromosome 1D and among them, genes involved in signalling contributed a major proportion followed by genes involved in hydrolase and membrane proteins. The transcript profiles from the RNASeq data bases showed that the gene involved in membrane protein (Traes_1DS_474BD1144) and the gene involved in protein binding (Traes_1DS_0D10FE51D) were highly up regulated in leaf tissues at the two leaf stage (Zadoks 10). Traes_1DS_0DF78825D, Traes_1DS_CD25033C4, Traes_1DS_BD30088EB, Traes_1DS_27349324C, Traes_1DS_A171C7D59, Traes_1DS_A6733B734 and Traes_1DS_A373E79EA expressed in leaf tissues at the 2 leaf stage. Traes_1DS_A6733B734, Traes_1DS_A373E79EA and Traes_1DS_321E8C254 and Traes_1DS_DBE2058BD show no expression in leaf tissues at the two leaf stage.

A total of 19 genes were mapped on the short arm of chromosome 7D. Genes involved in the hydrolase and transferase activity contributed a major proportion. Among the genes, transcript profile from RNASeq data base showed that a gene (Traes_7DS_309E71F44) involved in transferase and a gene Traes_7DS_52F1E4F62 involved in ribosome were highly expressed in leaf tissues at the two leaf stage. Genes, Traes_7DS_A2F956FD8, Traes_7DS_BCC35B081, Traes_7DS_28E2128F3,

Traes_7DS_546D3927E, Traes_7DS_303EC152F**,** Traes_7DS_351943FD9, Traes_7DS_5A68A26E9, Traes_7DS_E373FDD65, Traes_7DS_EC365BE37, Traes_7DS_3F6DCEAA8 and Traes_7DS_0A968BA86 and Traes_7DS_0B170AFF9 were also expressed in leaf tissues at the two leaf stage. Traes_7DS_E1BFD91BA, Traes_7DS_5A98193E8 and Traes_7DS_10C38526F1 show no expression in leaf tissues at the 2 leaf stage.

A total of 11 genes were mapped in the long arm of chromosome 7B. Genes involved in oxidoreductase activity contributed major proportion. Transcript profiles of the genes involved in oxidoreductase (Traes_7BL_0367BBFE6) and ligase (Traes_7BL_39451C0EC) shows these genes expressed at higher level in leaf tissues at the two leaf stages. Genes Traes_7BL_74071485F, Traes_7BL_CA6B7C9E6, Traes_7BL_580CFC05F, Traes_7BL_660FFDCE2, Traes_7BL_6A2BED3EA, and Traes_7BL_A51BC9795 expressed in leaf tissues at the 2 leaf stage.

A total of 7 genes were mapped in the short arm of chromosome 4A. Genes involved in transcription contributed major proportion in this chromosome. Transcript profiles show the gene (Traes_4AS_2BDA1260C) involved in transcription expressed highly in leaf tissues at the two leaf stages. The genes Traes_4AS_85B580603, Traes_4AS_20EAF4CEC, Traes_4AS_2BDA1260C, Traes_4AS_2D88ED3F8 and Traes_4AS_705FE3DAC expressed in leaf tissues at the 2 leaf stage. Transcript profiles of the Traes_4AS_A79A68739 and Traes_4AS_7258345F9 shows no expression in leaf tissues at the 2 leaf stage.

A total of 10 genes were mapped in the long arm of chromosome 4D. Genes involved in transport proteins contribute the major proportion. Transcript profile shows genes involved in transcription (Traes_4DL_C083C804E) and transport (Traes_4DL_38FBC0AC7) expressed highly in leaf tissues at the 2 leaf stages. Genes Traes_4DL_BE50C5130 and Traes_4DL_4448E934B1 also expressed in leaf tissues at

the two leaf stages. Transcript profiles of Traes_4DL_D41CB81EA, Traes_4DL_CFC191A06, Traes_4DL_B81290546 and Traes_4DL_1184F6F68 show no expression in leaf tissues at the two leaf stage.

In this study, loci contributing to RWA resistance were mapped on the long arm of chromosome 3B. With available information from the genome sequencing database, it is unable to differentiate the genes of the 3B that belongs to long or short arm of the chromosome 3B. Therefore genes expressed differentially could not be allocated to short or long arm of the chromosome 3B. It was also not possible to identify the transcript profiles and the POPSEQ distances of the expressed genes through Tritigate website due to the underpinning database still being under development. A total of 28 genes were mapped on chromosome 3B - their expression in the leaf tissues at the 2 leaf stage could not be determined.

Transcript profile of the mapped genes on the chromosomes 1DS, 7DS, 7BL, 4AS and 4DL were able to identify the expression of the gene in the other tissues of the wheat plant specifically root tissues. Gene transcripts expressed in both leaf and root tissues are Traes_1DS_0DF78825D, Traes_1DS_CD25033C4, Traes_1DS_474BD1144, Traes_1DS_A171C7D59, Traes_1DS_A6733B734 and Traes_1DS_0D10FE51D in 1DS; Traes_7DS_0B170AFF9, Traes_7DS_BCC35B081, Traes_7DS_28E2128F3, Traes_7DS_303EC152F, Traes_7DS_E1BFD91BA, Traes_7DS_351943FD9, Traes_7DS_5A68A26E9, Traes_7DS_E373FDD65, Traes_7DS_EC365BE37, Traes_7DS_52F1E4F62, Traes_7DS_3F6DCEAA8 and Traes_7DS_0A968BA86 in 7DS; Traes_7BL_74071485F, Traes_7BL_CA6B7C9E6, Traes_7BL_580CFC05F, Traes_7BL_39451C0EC, Traes_7BL_6A2BED3EA and Traes_7BL_A51BC9795 in 7BL; Traes_4AS_85B580603, Traes_4AS_20EAF4CEC, Traes_4AS_2BDA1260C and Traes_4AS_705FE3DAC in 4AS; Traes_4DL_B75BA7E6C, Traes_4DL_C083C804E and Traes_4DL_BE50C5130 in 4DL.

The genes expressed only in root tissues are Traes_1DS_A373E79EA in 1DS; Traes_7DS_10C38526F1 in 7DS; Traes_4AS_7258345F9 and Traes_4AS_2D88ED3F8 in 4AS; Traes_4DL_CFC191A06, Traes_4DL_B81290546, Traes_4DL_1184F6F68 and Traes_4DL_4448E934B1.

Table 4.1 provides the details underpinning the above summary of the genes that were identified for further consideration in Chapter 6. We note that the transcript profiles described for the 3B transcripts were not included in the table because the format of the outputs from Wheat-Expression.org was not consistent with the Tritigate format (the inclusion of the Wheat-Expression.org transcription profiles into Tritigate is under development).

The Phyre2 based annotations were generally consistent with annotations from other sources. Although Phyre2 annotations were treated with caution, since they were sometimes based on relatively small sections of the gene models, they were a useful source of possible function based on fundamental structure/function-features of the amino acid sequences.

Table 4.1: Annotation of published RWA induced genes utilising new wheat genome sequence data

Gene models	Amino acid sequences of encoded proteins	Transcript profiles of gene model	Phyre^2 based annotation (Kelley et al., 2015)
Traes_1DS_0DF78825D POPSEQ distance is not available	MLDLADSLTVCSAISSSSGETLNTHHLSPYMKPL GSDYSNGVNFAIAGATATPGDTPFSLDVQIDQFI FYRDRCNDSITRDEPAPLNMLDFERALYTMDIG QNDITSILYLPYDEVLAKLPHFVAEIRKAIEILHKN GARKFWIHGTGALGCLPAKLAMPRASDGDLDE HGCIAKFNNAAKKFNTLLSEACDDLRLLLKKSSIIF VDMFAIKYDLVANHTKHGIEKPLMTCCGHGGP PYNYDPKRSCMGDSKDLCKLGDKFISWDGVHFT DAANSIVASMAISGEYSVPRMKLTSLVKPAKSKA S	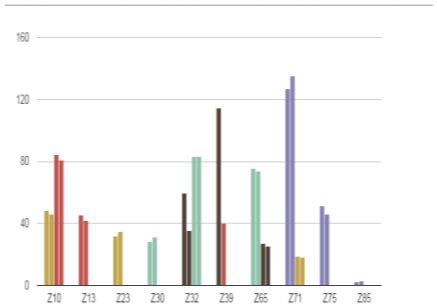	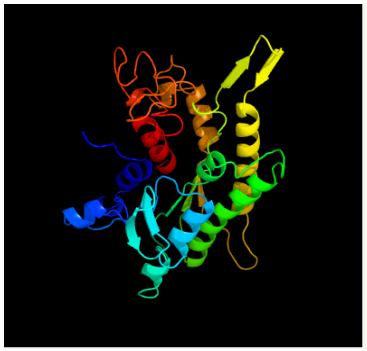 Model (left) based on template c3kvnA_ Top template information **PDB header:**hydrolase **Chain:** A: **PDB Molecule:**esterase esta; **PDBTitle:** crystal structure of the full-length autotransporter esta from2 pseudomonas aeruginosa Confidence and coverage Confidence: 100.0% Coverage: 84% 257 residues (84% of your sequence) have been modelled with 100.0% confidence by the single highest scoring template. 3D viewing Interactive 3D view in JSmol For other options to view your downloaded structure offline see the FAQ
Traes_1DS_CD25033C4 POPSEQ - 1D:7.36cM	MAGGGGRGRGEEEYDYLFKVVLIGDSGVGKSN LLSRFTRNEFCLESKSTIGVEFATRTLHVEEKIIKA QIWDTAGQERYRAITSAYYRGALGAVLVYDVTK PTTFENISRWLKELRDHADANIRIMLVGNKTDLK DLRAVPADDAGGYAEAEGLSYIETSALEAMNVE EAFQLILGDIYRAVSKKAVASEEDRAGAAGVKEG KTINVAAAADNGGEKKQCCSA	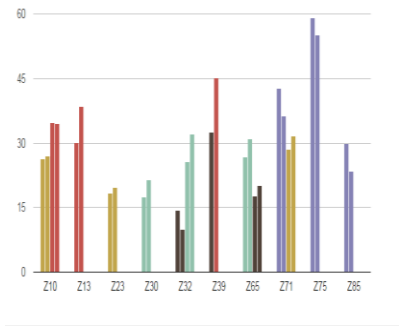	 Model (left) based on template d2bcgy1 Top template information **Fold:**P-loop containing nucleoside triphosphate hydrolases **Superfamily:**P-loop containing nucleoside triphosphate hydrolases **Family:**G proteins Confidence and coverage Confidence: 100.0% Coverage: 85% 189 residues (85% of your sequence) have been modelled with 100.0% confidence by the single highest scoring template. 3D viewing Interactive 3D view in JSmol

Traes_7DS_0B170AFF9 POPSEQ - 7D:13.647 cM	MALDIDQDLSRGEKLLGDLGGLFSKKWKP KKNGAIRGPMLTRDDSFIRKGSHMEQRHK LGLSDRPRRSNARQFLSEPTSELEKVEVEKA KQDDGLSDLSDILTELKGMAIDMGTEIEGQ TKDLGHAEKDFDELNYRVKGANTRTRRLL GR	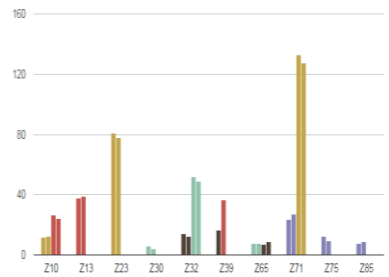	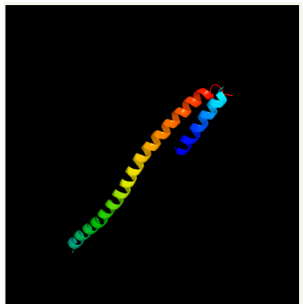 Model (left) based on template c3j99M_ Top template information **PDB header:**hydrolase **Chain:** M: **PDB Molecule:**synaptosomal-associated protein 25; **PDBTitle:** structure of 20s supercomplex determined by single particle2 cryoelectron microscopy (state iiib) Confidence and coverage Confidence: 99.8% Coverage: 56% 84 residues (56% of your sequence) have been modelled with 99.8% confidence by the single highest scoring template. Phyre alarm You may wish to submit your sequence to Phyrealarm. This will automatically scan your sequence every week for new potential templates as they appear in the Phyre2 library. 3D viewing
Traes_7DS_2F5418BA0 POPSEQ – 7D:44.602 cM	MGEIRVLNPRIAWECNYTDGTNSSGLDGLRLDP FHKLSYTKNKLISIGCATLGFIGGITKGENQLLFPIV NSCFSFCTDASSMNGSTKCVGMGCCETAFPGNI SSFRTESRPLTIYNSSTQPSRPCSYTFVAEEDWFK FNHSYIISTNFATKYTDGVPLVLDWVVGNKSCSE ATKMGSQYACQAKNSQCINVSNGPGYRCNCSQ GYEGNPYLQGGCQDINECEPPNQSFYPCKGNC RNTDGNYICLCPSGFRSDDPKSIPCVPADPKKAL KVVLGISFSVVFLMVCIFALRAEYQKR	Profile not available	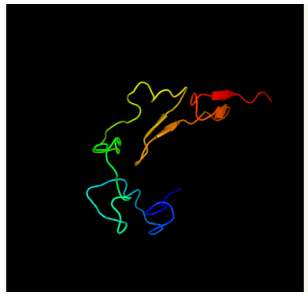 Model (left) based on template c3p5cL_ Top template information **PDB header:**hydrolase/lipid binding protein **Chain:** L: **PDB Molecule:**low density lipoprotein receptor variant; **PDBTitle:** the structure of the ldlr/pcsk9 complex reveals the receptor in an2 extended conformation Confidence and coverage Confidence: 99.0% Coverage: 27% 79 residues (27% of your sequence) have been modelled with 99.0% confidence by the single highest scoring template. Phyre alarm You may wish to submit your sequence to Phyrealarm. This will automatically scan your sequence every week for new potential templates as they appear in the Phyre2 library. 3D viewing
Traes_7DS_A2F956FD8 POPSEQ - 7D: 76.49 cM	MVAGAVTNPFGDGFYQGEREAPLEAATACPGV YGKGAYPGNAGQLLVDGATGASYNAHGAHGR KYLLPALFDPATSACSTLV	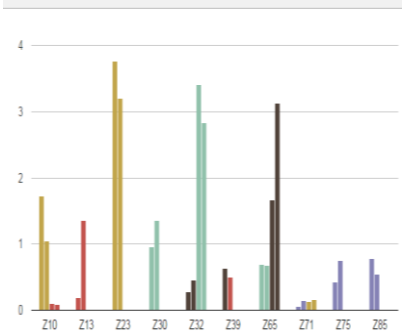	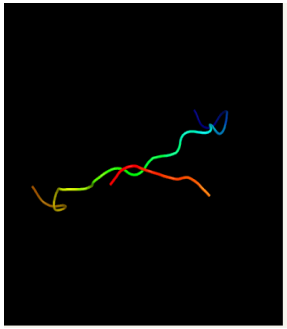 Model (left) based on template c2zxqA_ Top template information **PDB header:**hydrolase **Chain:** A: **PDB Molecule:**endo-alpha-n-acetylgalactosaminidase; **PDBTitle:** crystal structure of endo-alpha-n-acetylgalactosaminidase2 from bifidobacterium longum (engbf) Confidence and coverage Confidence: 59.3% Coverage: 32% 26 residues (32% of your sequence) have been modelled with 59.3% confidence by the single highest scoring template. Phyre alarm You may wish to submit your sequence to Phyrealarm. This will automatically scan your sequence every week for new potential templates as they appear in the Phyre2 library. Please note: You must be registered and logged in to use Phyrealarm. 3D viewing

Traes_7DS_BCC35B081 POPSEQ – 7D:44.602 cM	MGELAIAGHARALLEWHNTAKFCGACGAKAVP TEAGTRKQCSNESCKKRIYPRVDPVVIMLVIDKE NDRALLSRQSRFVPRMWSCLAGFIEPGESLEEA VRRETWEETGIEVGQVIYHSSQPWPVGPNTMP CQLMVGFFAYAKSLDIHVDKKELEDAQWHSCE DVKKALTFAEYEKAQRSSALKVNQICKGAERGQ SASSGLSVESEEPAPMFVPGPYAIAHHLISSWAF EGAPKVPSSFSNL	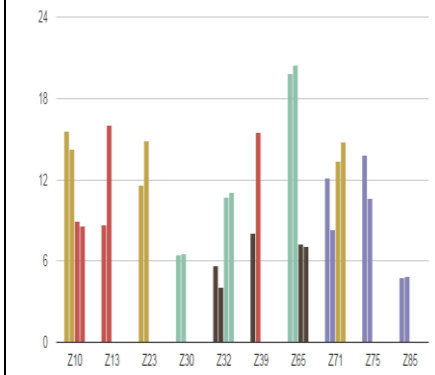	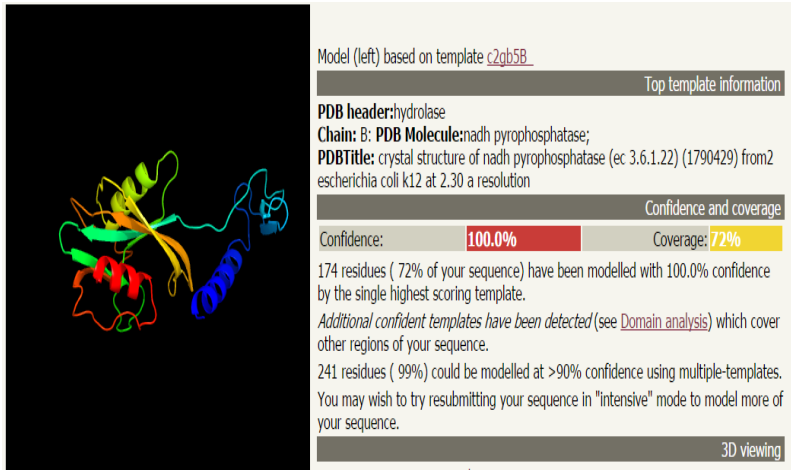
Traes_4AS_85B580603 POPSEQ - 4AS: 61.05 cM	MLTTCCLLTPEAEANATVPEANATDPTKSF LPRRTGDLVITYDVVQAYPTSYLALVTLENN AKLGRLDNWRLSWEWRRGEFIYSMKGAH PLEVDVNGCIYGAPGQYYQSLDFSQVLNC EKKPVILDLPLSRYNDTQMGKIEHCCRNGT ILPKSMDAAQSKSAFQMQVFKMPPDTNR TKLFPPANFKISGGSSLNPDYSCGQPVPVS PTGFPNPSGLDSTTLAVATWQVVCNITTA KGAKPKCCVTFSAHYNDSVIPCNTCACGCP VNRRGPTCSTTAPSMLLPPEALLVPFDNRT QKAQAWAQLKHYNVPRPMPCGDFCGVSI NWHVSSDFNKGWSARVTLFNWGDVDM ANWFAAMVMDKAYDGFEKAYSFNATAE GNNTIFMQGLEGLNYLVKQTNMSGSDYL VPGKQQSVLSFTKKLTPDIDVVAGDGFPTK VFFNGDECAMPQRFPLKSGGFRTHLSSAL AWVLLMASSALLLLQQ	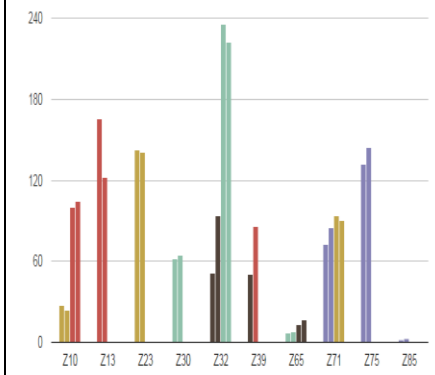	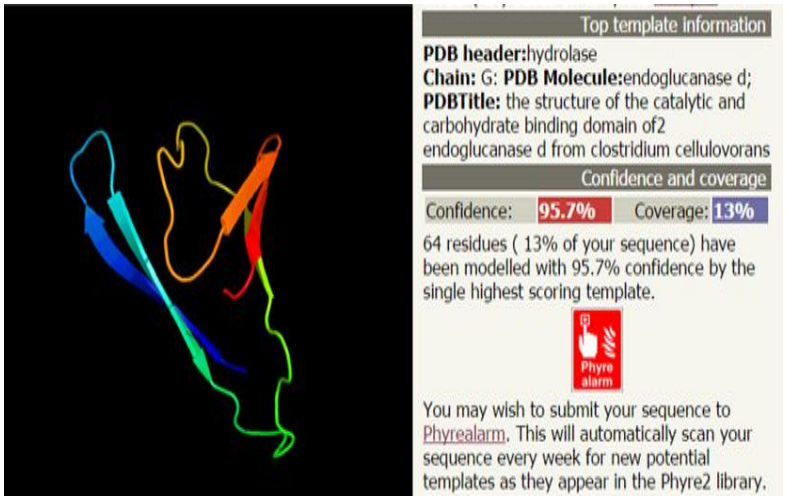

TRAES3BF128500020CFD_g POPSEQ distance is not available	MARPDAASLLSPSPPPFKPRRRGRLLPSILAVLAA AVALFLLAVLRSPPTPSPNLGSLFLSLGSNNTAAS HLRALTLHPHVAGTKANSLTAAYVLHAFSSLSIPS HITPYSVLLSYPVHRSLSLSAGPGRATKSFSLTQD TYPNDPYARAAAEVTPTFFAYSASGSVSAEAVYA NYGREEDFAYLASRGVDVAGKVALARYGRIHCE DIVHNARAAGAAAALVYPDPLEYGGPAGEGSFP DSRWLPPSGVQVGSLFRGVGDPTTPMWASSE GCERVSVEDAMATDDMPGIPALPVSARDAAEI QRVLGGAEAPADWQGRDGSPAYRLGPGPAVL NLTYQGNDTMATIENVFAVIEGAEEPDRYVILG NHRDAWTFGAADPNSGTAAMIELAQRFSMLQ KQGWRPRRTIIFCSWDAEEYGLTGSTEWVEENR EMLSSRAVAYLNIDVSVVGPVLLPSTTPQLDELLL ETIKLVQDPDNSSQTVYDSWVKSSASPKIQRLG NGGSDYAAFVQHVGIPSTNLIFGEGPGYPVYHSL YDDFVWVEKFADPGFRRHVAAASIWGIMALRL ADEEIIPFDYMSYTTELEAYTKVVEKETEGTAVSC SPLYNSIRALKKAATKVNSERKDIERALSSKQLSK DSTKIRGLNDRLMQAERAFTNREGIFKQAWYKH LIYGPSEQNDWDTASYPGIADAIATARSSNTSAS WKLVQHEVHRVARAVAQASAVLSGSLT	RNASeq profile is not available	 Model (left) based on template c3rbuA_ Top template information **PDB header:**hydrolase/hydrolase inhibitor **Chain:** A: **PDB Molecule:**glutamate carboxypeptidase 2; **PDBTitle:** n-terminally avitev-tagged human glutamate carboxypeptidase ii in2 complex with 2-pmpa Confidence and coverage Confidence: 100.0% Coverage: 90% 654 residues (90% of your sequence) have been modelled with 100.0% confidence by the single highest scoring template. 3D viewing Interactive 3D view in JSmol For other options to view your downloaded
TRAES3BF043600090CFD_g POPSEQ distance is not available	MAGNRACMFSVALALLGVLLASIPTTVQSIGVCY GVNGDGLPSASDVVQLYQSNGITGMRIYFPDA NALQALSGSNIGLIVDVANEDLASLASDRSAATA WVQTNVQAYQGLNIKYIAAGNEVGDQGGDTG NILPAMQNLDAALSAAGLGGIKVSTSVSQGVTT GYPPSQGTFSAGYMGPIAQYLASTGAPLLANVY PYFSYVDNQAQIDINYALFTSPGTVVQDGANAY QNLFDALVDTFYSALESAGAGSVNVVVSESGWP SAGGTAATTDNAQTYNQNLIKHVGQGTPKRPS AIEAYVFAMFNEDKKGPAEIEKHFGLFNPDKSPA YPISF	RNASeq profile is not available	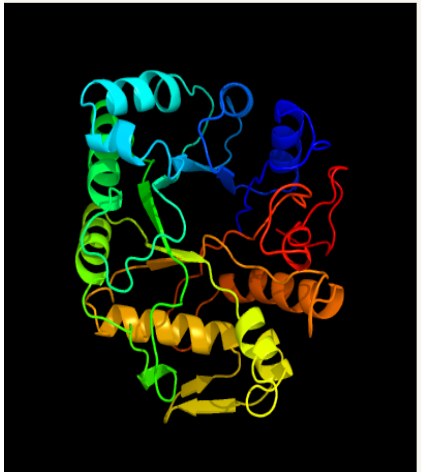 Model (left) based on template c3f55A_ Top template information **PDB header:**hydrolase, allergen **Chain:** A: **PDB Molecule:**beta-1,3-glucanase; **PDBTitle:** crystal structure of the native endo beta-1,3-glucanase (hev b 2), a2 major allergen from hevea brasiliensis (space group p41) Confidence and coverage Confidence: 100.0% Coverage: 91% 303 residues (91% of your sequence) have been modelled with 100.0% confidence by the single highest scoring template. 3D viewing Interactive 3D view in JSmol For other options to view your downloaded

TRAES3BF168400230CFD_g POPSEQ distance is not available	MGMKRCIVPSILLMLSLEAALLIADRPSVDDEVG TILLPSQGQVADQQAAMAAPRPWKCCDRPRCT RSIPPICTCVDEAFECASTCKACVPSTRNPSLQVC QDQYVGDPGPICRPWECCDSAACTKTDPPTCR CGDEVEQCAPTCKSCEASTSNPSLNVCKDAFTG AIPPTCTPPEALAAGGN	RNASeq profile is not available	 Top template information **PDB header:**hydrolase/protein binding **Chain:** J: **PDB Molecule:**bowman-birk type trypsin inhibitor; **PDBTitle:** trypsin:bbi complex Confidence and coverage Confidence: 100.0% Coverage: 62% 113 residues (62% of your sequence) have been modelled with 100.0% confidence by the single highest scoring template. *Additional confident templates have been detected* (see Domain analysis) which cover other regions of your sequence. 154 residues (84%) could be modelled at >90% confidence using multiple-templates. You may wish to try resubmitting your sequence in "intensive" mode to model more of your sequence.
Traes_1DS_27349324C POPSEQ – 1D: 0.0 cM	MPALATSVPQHIHEELTMAERGGLLTFLLLGLFL GLAGSSPPPEPVECAHGTSDCTVTNVYGSFPDR TVCRAANATFPRTEEELVAAVAAAAAAKRKVKV ATRHSHSFTKLACPGGRDGTIISTKRLNKTVSLDA AKGLMTVESGMVLKDLIQAAAEAGLALPHSPY WYGVTIGGLLATGAHGSSLWGKGSAVHEYIVG MRIVTPALASQGFAVVRELSVGDPDLDAVKVSL GVLGVVSQVTLALQPMFKRSVTFETRDDMDLP AQAAVWGRLHEFGDMAWLPWQGKVIYRKDN RVPVSTKGHGLNDYLGYRSNPTLALITDRATEER LEEDNSDIARCLAARVPSALFELQGYGFTNDGSF FTGWPVIGFQNRIQASGTCISSPEDGLLSTCTWD PRIRSPFFYSSSFSIALSKAPSFIAEMQKLRDLKPC AFCGLDATLGVLLRYVKASSAYLGKSEDSIDFDFT YYRSYTQGEPRANSDVVDELEQLALCKYDAVPH WGKNRNFAFDGVIAKYPKAAEFLKVKARYDPD GIFSSEWSDQVLGAKGSSNMAEKSCGIEGICICS DDSHCAPEKGYFCHPGKVFTDARVCSTRRTFGD DLLKEQ	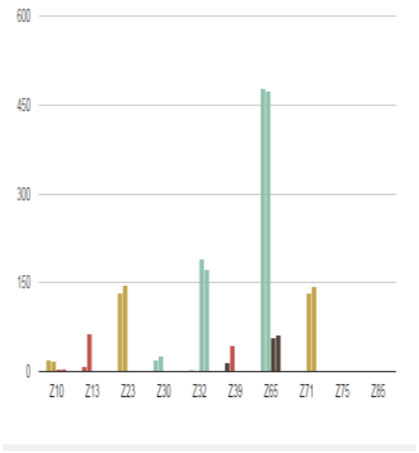	**PDB header:**oxidoreductase **Chain:** C: **PDB Molecule:**cytokinin oxidase 2; **PDBTitle:** structure of maize cytokinin oxidase/dehydrogenase 2 (zmcko2) Confidence: 100% ; % ID: 13 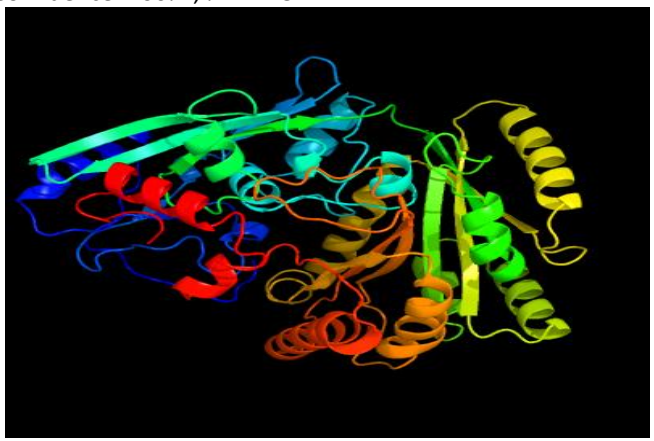

Traes_7DS_28E2128F3 POPSEQ - 7D: 75.353cM Protein models with similar designation but no RNASeq profiles include: Traes_7DS_0467D80FB Traes_7DS_2BF9F77 Traes_635FA1D7E Traes_72929F5D3 Traes_7DS_8990E8E56	MVYSKPRQLLTNEIPLIVDDFRRAARNAIEAGFD GVEIHGAHGYLLEQFMKDSSNDRTDEYGGSLEN RCRFAVEVIDAIINEIGADRVGIRLSPFVDYMDCF DSNPHALGMYMVQQLNKHQGFVYCHMVEPR MAIVDGRRQIPHGLLPFRKAFKGTFIAAGGYDRE EGNKVVADGYADLVAYGRIFLANPDLPKRFELDS PLNKYDRKTFYTQDPIVGYTDYPFLEGGSNAE	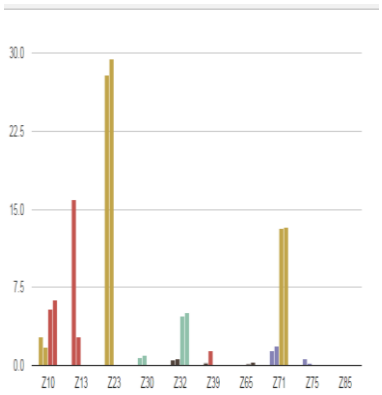	 Model (left) based on template d1qwja_ Top template information **Fold:**TIM beta/alpha-barrel **Superfamily:**FMN-linked oxidoreductases **Family:**FMN-linked oxidoreductases Confidence and coverage Confidence: 100.0% Coverage: 97% 226 residues (97% of your sequence) have been modelled with 100.0% confidence by the single highest scoring template. 3D viewing Interactive 3D view in JSmol For other options to view your downloaded structure offline see the FAQ
Traes_7DS_546D3927E POPSEQ - 7D: 68.529cM	SLDCNIKHFSVIQDIDGKNVSLSKFKGKALLIVNV ASQCGLTTANYTELSHLYEKYKTQGFEILAFPCN QFGFQEPGSNTQIKQFACTRFKAEFPIFDKVDVN GPFTAPIYKFLKSSAGGFLGDIVKWNFEKFLVDK NGKVVERYPPTTSPFQIEVREVSLWLY	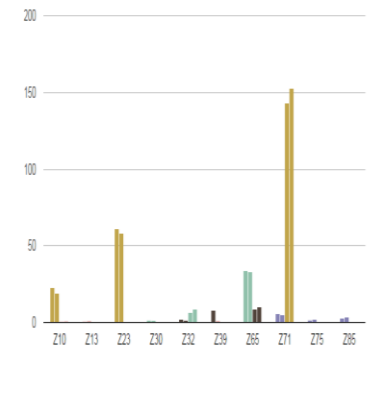	 Model (left) based on template c2p5qA_ Top template information **PDB header:**oxidoreductase **Chain:** A: **PDB Molecule:**glutathione peroxidase 5; **PDBTitle:** crystal structure of the poplar glutathione peroxidase 5 in2 the reduced form Confidence and coverage Confidence: 100.0% Coverage: 96% 158 residues (96% of your sequence) have been modelled with 100.0% confidence by the single highest scoring template. 3D viewing Interactive 3D view in JSmol For other options to view your downloaded structure offline see the FAQ
Traes_7BL_63C1B410D POPSEQ distance is not available	SRKLEMLGWKTKPLEETLRDSVESYKAAAV LN	RNASeq profile is not available	Protein model wasn't identified

Traes_7BL_0367BBFE6 POPSEQ - 7B:51.193 cM	MISNHLLFKLASGEVFGQDQPIALKLLGSER SLQALEGVAMELEDSLYPLLREVSIGIDPYVI FEDADWALLIGAKPRGPGVERAALLDING QIFAEQGKALNAVASRNVKVIVVGNPCNT NALICLKNAPNLPAKNFHALTRLDENRAKC QLALKAGVFYDKISNMTIWGNHSTTQVPD FLNAKINGTPVKEVIKDTKWLEEDFTITVQK RGGVLIQKWGRSSAASTAVSIVDAMRSLV TPTPEGDWFSTGVYTTGNPYGIAADIVFS MPCRSKGDGDYELVKDVAMDDFLWGRIK KSEAELIAEKRCVAHLTGEGNAFCDLPGDT MLPGEM	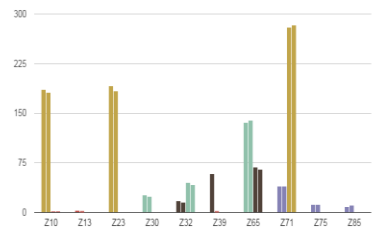	 Model (left) based on template c7mdhA_ Top template information **PDB header:**chloroplastic malate dehydrogenase **Chain:** A: **PDB Molecule:**protein (malate dehydrogenase); **PDBTitle:** structural basis for light acitvation of a chloroplast enzyme. the2 structure of sorghum nadp-malate dehydrogenase in its oxidized form Confidence and coverage Confidence: 100.0% Coverage: 98% 328 residues (98% of your sequence) have been modelled with 100.0% confidence by the single highest scoring template. 3D viewing Interactive 3D view in JSmol For other options to view your downloaded
Traes_4AS_20EAF4CEC POPSEQ - 4A:57.601cM	MFWALFVLGHDCGHGSFSSNPKLNSVVG HILHSSILVPYNGWRISHRTHHQNHGHVE KDESWHPLPQRLYNSLDNMTKKLRFSMPF PMLAFPLYLFARSPGKEGSHFNPNSDLFQP NEKKDVLTSTASWLAMIGVLAGLTFVMGP LKMLKLYAVPYVIFVMWLDFVTYLHHHGH EDKVPWYRGKEWSYLRGGLTTLDRDYGLI NNIHHDIGTHVIHHLFPQIPHYNLVEATEA AKPVLGKYYKEPEKSAPLPFHLLQVLSRSLK EDHYVSDTGDIVYYQSESETSTSGQSSD	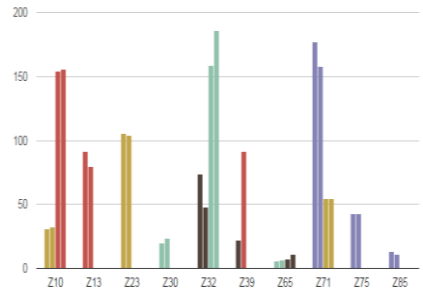	 Model (left) based on template c4zyoA_ Top template information **PDB header:**oxidoreductase **Chain:** A: **PDB Molecule:**acyl-coa desaturase; **PDBTitle:** crystal structure of human integral membrane stearoyl-coa desaturase2 with substrate Confidence and coverage Confidence: 99.8% Coverage: 80% 234 residues (80% of your sequence) have been modelled with 99.8% confidence by the single highest scoring template. 3D viewing Interactive 3D view in JSmol For other options to view your downloaded
Traes_4DL_B75BA7E6C POPSEQ – 4D:54.756 cM	MSYVLRDVLVXGLAAAAARADSWLVWPL YWAAQGTMFWALFVLGHDCGHGSFSSN PKLNSVVGHILHSSILVPYNGWRISHRTHH QNHGHVEKDESWHPLPQRLYNSLDNMTK KLRFSMPFPMLAFPLYLFARSPGKEGSHFN PNSDLFQPNEKKDVLTSTASWLAMIGVLA GLTFVMGPLKMLKLYAIPYVIFVMWLDFV TYLHHHGHEDKVPWYRGKEWSYLRGGLT TLDRDYGLINNIHHDIGTHVIHHLFPQIPHY HLVEATEAAKPVLGKYYKEPEKSAPLPFHLL QVLSRSLKEDHYVSDTGDIVYYQSESETSTC AQSSD	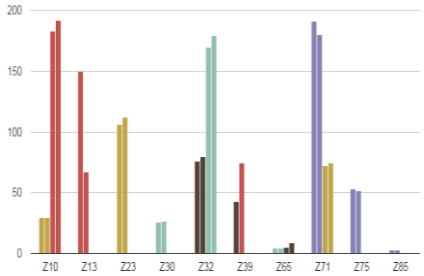	 Model (left) based on template c4zyoA_ Top template information **PDB header:**oxidoreductase **Chain:** A: **PDB Molecule:**acyl-coa desaturase; **PDBTitle:** crystal structure of human integral membrane stearoyl-coa desaturase2 with substrate Confidence and coverage Confidence: 99.9% Coverage: 82% 267 residues (82% of your sequence) have been modelled with 99.9% confidence by the single highest scoring template. 3D viewing Interactive 3D view in JSmol For other options to view your downloaded

Traes_4DL_8DBE42AE9 POPSEQ distance is not available	MLTLQMKDAPLIRDPLSRAGCGHASRGVS GGTPPILDQKTNSWKKLVNVSVTGATGMI SNHLLFKLASGEVFGQDQPIALKLLGSESSV HALEGVVMELQDSLYPLLREVSIGIDPYVIF EDADWALLIGAKPRGPGMERAGIVDING QIFAEQGKALNAVASRNVKVIVVGNPCNT NALICLKNAPNLPAKNFHALTRLDENRAKF QLALQAGVFYDKVSNMTIWGNHSTTQVP DFLNAKISGRPVKEVIKDTKWLEEDFTITVQ KRGGVLIEKWGRSSAASTAVSIVDAMRSLV TPSSEGDWFSTAVYTTGNPYGIAEDLVFS MPCRSKGDGDYELVQHVAMDDFLWDRIK KSEAELIAE	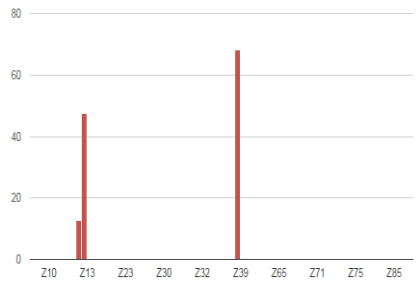	
TRAES3BF041000020CFD_g POPSEQ distance is not available	MVVIAIKCPTIEVVVVDISKPRIHAWNNDTLPIYE PGLDDVVKACRGKNLFFSTDVEKHIAEADIIFVSV YTPTKTRSLGAGKVADLTYWESAARMIAGVSNS DKIDVDESTVPSFLAEGTATDDLFKPDRVLIGGRE TPEGRKAVQAIKEVYAYWVSEENIVTTNMWSD ELSKLAANAFLA	RNASeq profile is not available	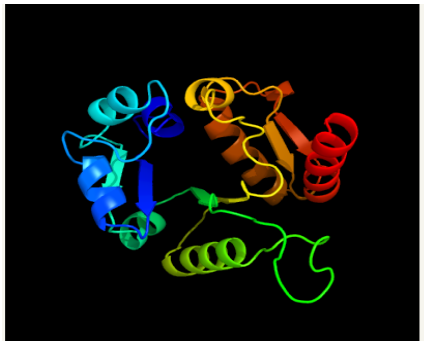
TRAES3BF047400040CFD_g POPSEQ distance is not available	MAALTGAALLLASLLALAAIASGNTEGDILYSQR QVWKDPNNVLQSWDPTLVNPCTWFHVTCNNI NSVIRVDLGNAGLSGALVPGLGRMVNLQYLELF GNNISGPIPATLGNLTRLVSLDLYDNRLTGAIPAS LGNIGTLRFLRLHGNKLAGGIPASLGNLTKLQTLE LQENMLTGTVPLEVLSLVLLGHLTELNVAKNSLA GTVKSSKPRVATVIQDTLKTTRL		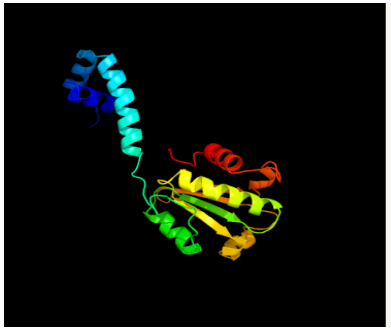

Traes_1DS_321E8C254 POPSEQ distance is not available	MAKLMCLCFIILTIAVAVSADECEGDRRAMIKEC AKYQQWPANPKLDPSDACCAVWQKANIPCLC AGVTKEKEKIYCMEKVAYVANFCKKPFPHGYKC GSYTFPPLAY	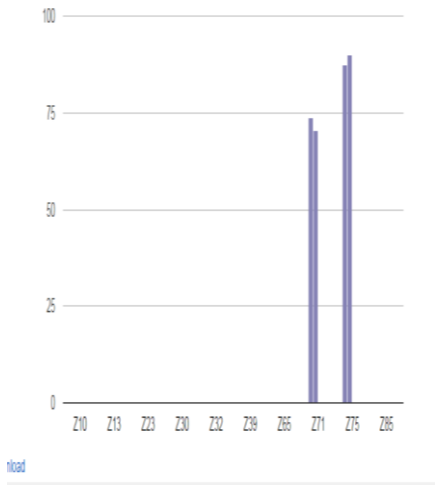	 Model (left) based on template c2rknA_ Top template information **PDB header:**signaling protein, lipid transport **Chain:** A: **PDB Molecule:**dir1 protein; **PDBTitle:** x-ray structure of the self-defense and signaling protein dir1 from2 arabidopsis taliana Confidence and coverage Confidence: 99.5% Coverage: 69% 75 residues (69% of your sequence) have been modelled with 99.5% confidence by the single highest scoring template. 3D viewing Interactive 3D view in JSmol For other options to view your downloaded structure offline see the FAQ
Traes_1DS_9696ADD50 POPSEQ – 1D: 9.09cM	MQILHFDIKPHNILLDSNFVPKVADFGLAKLYPR GDSFVPLSAMRGTVGYVAPEMISRSFGVISSKSN VYSFGMLLLEMAGGRRNADPNMGSSSQAYYPS WVYDQLTQEEAGEISPVAADMHELEKKLCVVGL WCIQMRSRDWPTMGEVIEILEAGADGLQMPS RPFFCDEGHIHVEDSYQFTSELTAVSEEEFSAVSE EDDV	Profile not available	 Model (left) based on template c3qa8H_ Top template information **PDB header:**immune system, signaling protein **Chain:** H: **PDB Molecule:**mgc80376 protein; **PDBTitle:** crystal structure of inhibitor of kappa b kinase beta Confidence and coverage Confidence: 99.9% Coverage: 69% 141 residues (69% of your sequence) have been modelled with 99.9% confidence by the single highest scoring template. 3D viewing Interactive 3D view in JSmol For other options to view your downloaded structure offline see the FAQ

Traes_1DS_BD30088EB POPSEQ: 1D: 9.09 cM	MQILHFDIKPHNILLDSNFVPKVADFGLAKLYPR GDSFVPLSAMRGTVGYIAPEMISRSFGVISSKSD VYSFGMLLLEMAGGRRNADPNMGSSSQAYYPS WVYAKLTREEAGEEISPVAADMHELEKKLCVVG LWCIQMRSCDRPTMGEVIEILEAGTDSLQMPSR PFFCDEGHIHVEDSYHFTSELTVVSEEESTAVSEE DNV	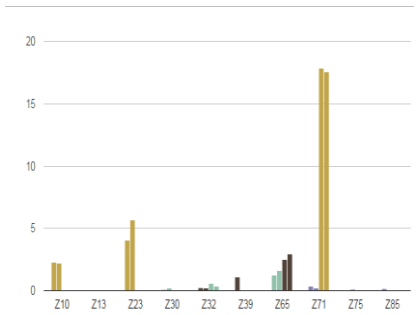	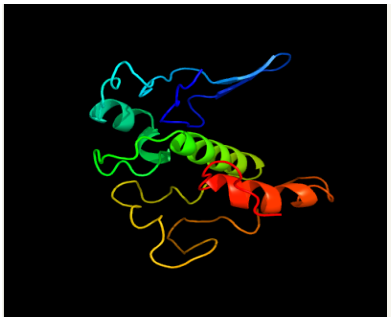 Model (left) based on template c3qa8H_ Top template information **PDB header:**immune system, signaling protein **Chain:** H: **PDB Molecule:**mgc80376 protein; **PDBTitle:** crystal structure of inhibitor of kappa b kinase beta Confidence and coverage Confidence: 99.9% Coverage: 69% 141 residues (69% of your sequence) have been modelled with 99.9% confidence by the single highest scoring template. 3D viewing Interactive 3D view in JSmol For other options to view your downloaded structure offline see the FAQ
Traes_1DS_DBE2058BD POPSEQ distance is not available	MAKLMCLCFIILTIAVAVSADECEGDRQAMIKEC AKYQQWPANPKLDPSDACCAVWQKANIPCLC AGVTKEKEKIWCMEKVAYVANFCKKPFPHGYKC GSYTFPPPA	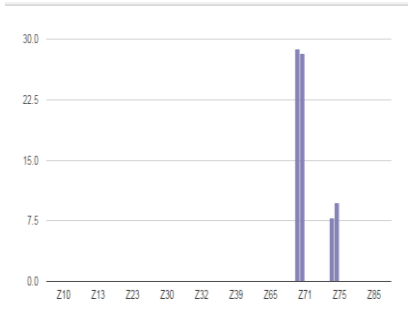	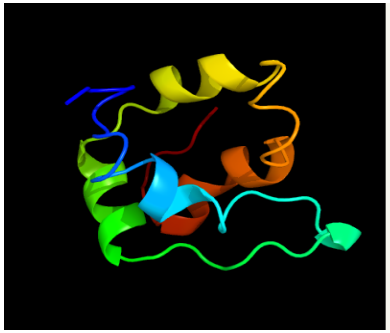 Model (left) based on template c2rknA_ Top template information **PDB header:**signaling protein, lipid transport **Chain:** A: **PDB Molecule:**dir1 protein; **PDBTitle:** x-ray structure of the self-defense and signaling protein dir1 from2 arabidopsis taliana Confidence and coverage Confidence: 99.7% Coverage: 69% 74 residues (69% of your sequence) have been modelled with 99.7% confidence by the single highest scoring template. 3D viewing Interactive 3D view in JSmol For other options to view your downloaded structure offline see the FAQ
Traes_7DS_303EC152F POPSEQ – 7D:44.602 cM	MAWPGCPDKCGNVNIPYPFGTREGCFREPFNV TCNETGAYLASTEVKVLDINLTVGEIRVLNPHISW ECNYTNGTSGNGSDGLSLDPFHKLSNTKNKLISI GCATLGLILGVTKGKNQLEFPIVNTCYSVCTDAN SVDDSTKCIGMGCCQTPLPGNISSFNTVSSSLTF TNSASQSFSPCSYSFVAEEDRFKFNRSYVSSTNFL NKYTDGVPLVLDWVVGNESCSEATKMGSQYAC KDMNSKCVDVSNGPGYRCNCSEGYEGNPYLQG GCQDINECEPPNQSLYPCQGKCTNTVGNYTCFC PSGFRSDDPKSIPCVPADPKKALKVVLGISFSAIFL MVCIFALRAEYQKRKLAKEKDKFFDQNGGQILY RQIMSKQVDTLKIFTQEDLKKATNDFDKSRELGR GGHGTVYKGILKDDRVVAVKRSKIMNV	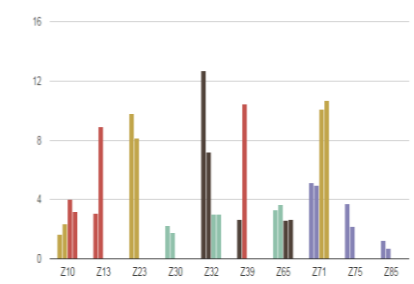	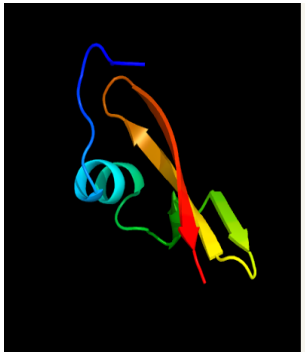 Model (left) based on template c4l68A_ Top template information **PDB header:**signaling protein **Chain:** A: **PDB Molecule:**leucine-rich repeat protein kinase-like protein; **PDBTitle:** structure of the pseudokinase domain of bir2, an immune regulator of2 the rlk/pelle family Confidence and coverage Confidence: 99.5% Coverage: 12% 50 residues (12% of your sequence) have been modelled with 99.5% confidence by the single highest scoring template. Phyre alarm You may wish to submit your sequence to Phyrealarm. This will automatically scan your sequence every week for new potential templates as they appear in the Phyre2 library. 3D viewing

Traes_7DS_E1BFD91BA POPSEQ distance is not available	SGVIGVSPINCVWRNGEIPYSRRKQIFVIYP FAVLDFILFYVGPNGSYQLLGHCLTGQTLLL LVVATLTLQHSATAYESESSGSIRMARPDC PDKCGSVSIPYPFGTGKGCFQEPFDVTCNA TGPYLASTRVRILDINLAMGEIRVLNPHIA WECNYTNGTNSSGSDGLTLDPFHKLSNTK NKLISIGCATLG	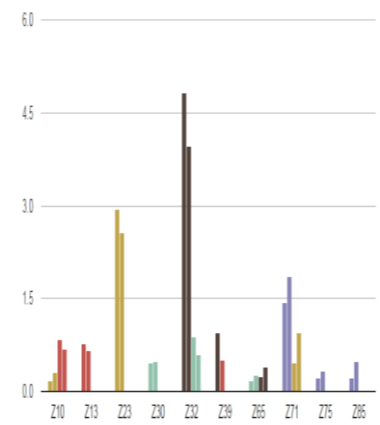	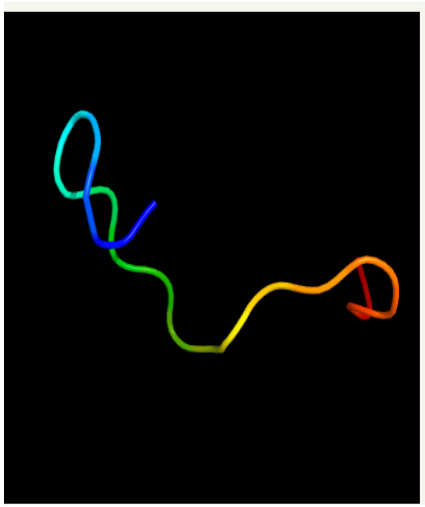 **Fold:**Bifunctional inhibitor/lipid-transfer protein/seed storage 2S albumin **Superfamily:**Bifunctional inhibitor/lipid-transfer protein/seed storage 2S albumin **Family:**Plant lipid-transfer and hydrophobic proteins Confidence and coverage Confidence: 28.2% Coverage: 9% 18 residues (9% of your sequence) have been modelled with 28.2% confidence by the single highest scoring template. Phyre alarm You may wish to submit your sequence to Phyrealarm. This will automatically scan your sequence every week for new potential templates as they appear in the Phyre2 library. Please note: You must be registered and
TRAES3BF050800220CFD_g POPSEQ distance is not available	MKQQGFGGLRFESQRFRLLSIVVGCFLISVTFLLS TRPDSTVFDTLSPKMAWLEETRSTPARSAVKTV KPSSSSSPRGLGRDFLVDVAPKQGDAHGRQPEQ SAGEKTETEWVKDTVIIQESSAVAAERAEQEEAE QGHSADAGAGAGEDAMPGATEEEVRDAAVPT RAAAITARPAVETTPTPATTTRHDQDQLLPERAT GGRMMKLQAEPATTEQQQLPTPGRLETAEPER AARDQPQQPLPPLCDFSDRRSDVCDFTGDIRME ANTSSFVVVVDAATAAQSHKVRPYPRKGDQTC MGRVPEITVRTASSSSTPPPPQCTRTHSVPAVTF SIGGYTGNIFHDFSDVLVPLYNTVHRYRGDVQLV MANVVPWWLVKYDKLLRELSRHAPLDLAVAAA KGETHCFRHAVVSLRAHRELIIERDRSPDGLATP DFTRFIRRALSLPRDAPTRLADGMGRKPRLLIIAR HRTRILLNLGDMLRVAEEAGFEAAVSESDVGDSI SRVGAEINSADVLLGVHGAGLTNMMFLAPGAT LVQVVPWGGLQWIARMDYGDPAEAMGLRYV QYEIGVEESSLKDTYPRGHKIFTDPTSLHKKGFGF MRRTLMDGQNITLDLGRFRGVLHQALGNYLVQ	RNASeq profile is not available	 Top template information **Fold:**NAD kinase/diacylglycerol kinase-like **Superfamily:**NAD kinase/diacylglycerol kinase-like **Family:**Diacylglycerol kinase-like Confidence and coverage Confidence: 94.6% Coverage: 15% 93 residues (15% of your sequence) have been modelled with 94.6% confidence by the single highest scoring template. Phyre alarm You may wish to submit your sequence to Phyrealarm. This will automatically scan your sequence every week for new potential templates as they appear in the Phyre2 library. 3D viewing

Traes_1DS_474BD1144 POPSEQ – 1D : 47.767 cM	MAACRGFFECLLRLLNFFLTVAGLAMVGYGIYLL VEWMRISGGGGGAPPSPPPPAELLTFGRPMLT VVALGEGGSFFDKLPKAWFIYLFIGVGAVIFIVSLF GCIGAGTRNTCCLCCYSFLVILLILAEAGGAAFIFF DHSWKDVIPVDKTQNFDAMYDFLNENWKIAR WVALGVVVFEVLLFLLALAVRAMNKPAEYDSDD EIIGTARSTSIRQPLIHSQNAPATGVPVPTLDQRA SRNDAWSQRMREKYGLDTSQFTYNPSDATRYQ QNGAPPAEERSRCTVM	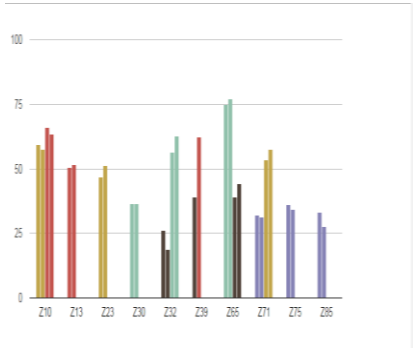	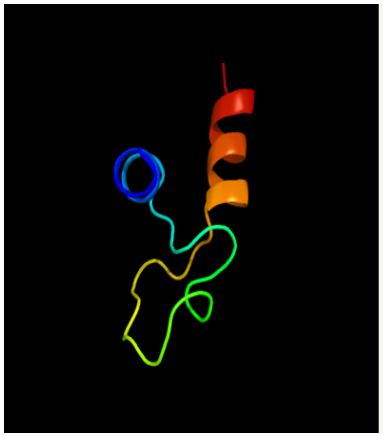 Top template information **PDB header:**membrane protein **Chain:** A: **PDB Molecule:**cd63-like protein sm-tsp-2; **PDBTitle:** smtsp2ec2 Confidence and coverage Confidence: 97.0% Coverage: 15% 42 residues (15% of your sequence) have been modelled with 97.0% confidence by the single highest scoring template. Phyre alarm You may wish to submit your sequence to Phyrealarm. This will automatically scan your sequence every week for new potential templates as they appear in the Phyre2 library.
Traes_1DS_A171C7D59 POPSEQ - 1D: 47.767 cM	MAANGNDGLCVAEPRSAADPLNWGKAAEELS GSHLDAVKRMVEEYRRPVVVMEGASLTIAQVA AVAAAGGARVELDESARGRVKESSDWVMASM ANGTDSYGVTTGFGATSHRRTKEGGALQRELIR FLNAGAFGTGSDGHVLPAATTRAAMLVRVNTLL QGYSGIRFEILETIATLLNANVTPCLPLRGTITASG DLVPLSYIAGLVTGRPNAVAVAPDGTKVNAAEA FKIAGIQHGFFELQPKEGLAMVNGTAVGSGLASI VLFEANILAVLAEVLSAVFCEVMNGKPEYTDHLT HKLKHHPGQIEAAAIMEHILEGSSYMMLAKKLG ELDPLMKPKQDRYALRTSPQWLGPQIEVIRAAT KSIEREINSVNDNPLIDVSRGKAIHGGNFQGTPIG VSMDNTRLAIAAIGKLMFAQFSELVNDFYNNGL PSNLSGGRNPSLDYGFKGAEIAMASYCSELQFLG NPVTNHVQSAEQHNQDVNSLGLISSRKTAEAIDI LKLMSSTFLVALCQAIDLRHLEENVKNAVKNCVT RVARKTLITNDMGGLHNARFCEKDLLQTIDREA VFAYADDPCSANYPLMKKMRAVLVEHALANGE AERNKETSVFAKVATFEQELCAALPQEVEAARG AVENGTAAEPNRIADCRSYPLYRFVRKELGTVYL TGEKTRSPGEEVDKVFIAMNQGKHINALLECLKE WNDEPLPIC	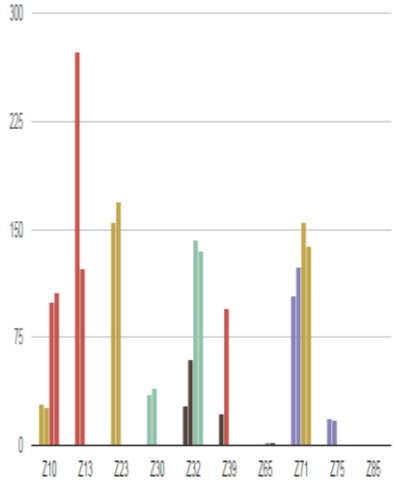	**PDB header:**lyase (C=100, ID= 47) **Chain:** A: **PDB Molecule:**phenylalanine ammonia-lyase; **PDBTitle:** crystal structure of a taxus phenylalanine aminomutase Confidence: 100% ; % ID: 47 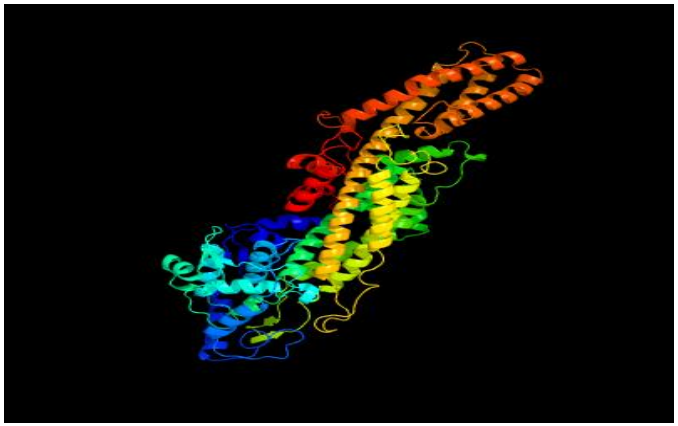

TRAES3BF040500030CFD_g POPSEQ distance is not available	MAVRLTLVAALLCAAAAAAAAAQQASNVRATY HYYRPAQNNWDLGAPAVSAYCATWDASKPLS WRSKYGWTAFCGPAGAHGQAACGKCLRVTNP ATGAQVTARIVDQCANGGLDLDWDTVFTKIDT NGVGYQQGHLNVNYQFVDCRD	RNASeq profile is not available	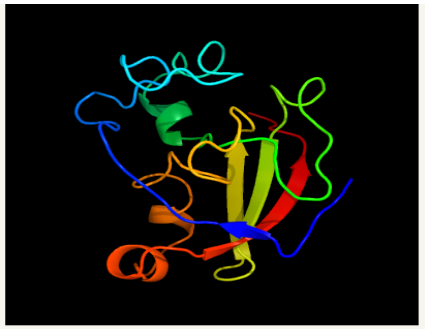 Model (left) based on template d1bw3a_ Top template information **Fold:**Double psi beta-barrel **Superfamily:**Barwin-like endoglucanases **Family:**Barwin Confidence and coverage Confidence: 100.0% Coverage: 85% 125 residues (85% of your sequence) have been modelled with 100.0% confidence by the single highest scoring template. 3D viewing Interactive 3D view in JSmol For other options to view your downloaded structure offline see the FAQ
Traes_1DS_A6733B734 POPSEQ – 1D:46.631cM	MSSSTGSLDHAGFTFTPPPFITSFTELLSGSGAGD AERSPRGFNRGGRAGAPKFKSAQPPSLPISSPFS CFSIPAGLSPAELLDSPVLLNYSHILASPTTGAIPA RRYDWQASADLNTFQQDEPCRGDSGLFGFSFH AVKSNATVNAQANCLPLFKEQQQQQQQQVVE VSNKSSSGGGNNKQVEDGYNWRKYGQKQVKG SENPRSYYKCTYNNCSMKKKVERSLADGRITQIV YKGAHDHPKPLSTRRNSSGCAAVVAEDHANGS EHSGPTPENSSVTFGDDEADNGLQLSDGAEPVT KRRKEHADNEGSSGGTGGCGKPVREPRLVVQTL SDIDILDDGFRWRKYGQKVVKGNPNPRSYYKCT TVGCPVRKHVERASHDNRAVITTYEGKHSHDVP VGRGRALPATSSSDSSGVIWPAAVPAPYTLEML TNPAAGHRGYAAGGAFQRTKDEPRDDMFVESL LC	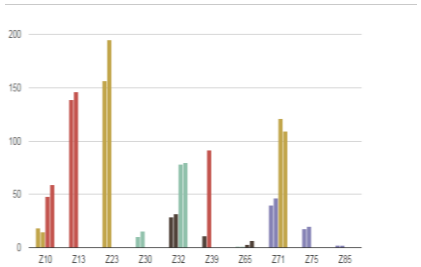 	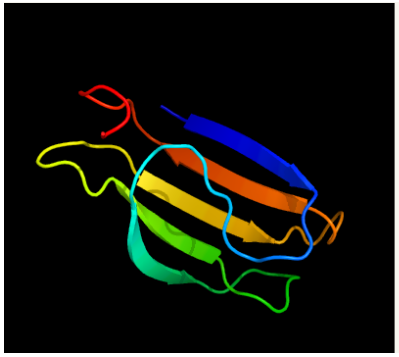 **PDB header:**transcription **Chain:** A: **PDB Molecule:**wrky transcription factor 1; **PDBTitle:** crystal structure of the c-terminal wrky domainof atwrky1,2 an sa-induced and partially npr1-dependent transcription3 factor Confidence and coverage Confidence: 100.0% Coverage: 16% 75 residues (16% of your sequence) have been modelled with 100.0% confidence by the single highest scoring template. Phyre alarm You may wish to submit your sequence to Phyrealarm. This will automatically scan your sequence every week for new potential templates as they appear in the Phyre2 library.
Traes_7BL_74071485F POPSEQ - 7B:51.193 cM	MVCADAALETPLILPVRSVEMISHGVLTLLS HVITSLSWTSFQRYVPMNASSSITLLQMFF ERALLAYRVFLVPAGHGESTGNSGRDGLS DCRLMDLKSGTELVLTYEDKDGDWMLVG DVPWRMFTDSCRRMRIMKGSDAVGLAP RAAEKSKNQKWQKG	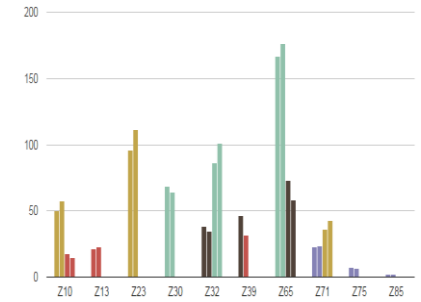 	 Model (left) based on template c2mukX_ Top template information **PDB header:**transcription **Chain:** X: **PDB Molecule:**auxin-responsive protein iaa17; **PDBTitle:** 1h, 13c, and 15n chemical shift assignments for aux/iaa17 Confidence and coverage Confidence: 100.0% Coverage: 71% 113 residues (71% of your sequence) have been modelled with 100.0% confidence by the single highest scoring template. 3D viewing Interactive 3D view in JSmol For other options to view your downloaded structure offline see the FAQ

Traes_4AS_A79A68739 POPSEQ – 4A:9.1 cM	MIPAVACVGYDRTDAMEVPSPIKTGSWSPEED ALLVALVRQHGARRWSVISASVPGRTGKSCRLR WCNQLSPAVQHRPFTVQEDALIIAAQARYGNK WADIARLLPGRTDNSVKNHWNSNLRRCQRRAK AMAAATAARVAASSSSSGSAVRAKMQQEEQV MVMNRSPPAVVHGAVTAVIDDPMPMLSLTLSL GLPQMAADKASEEAKAKAKEKTPPPVGVGGND VRLMAAIRQVVREEVERQAGQLLYSVVMATTA ARVDGASSSDHPTNGHH	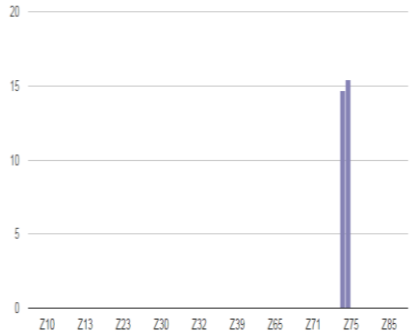	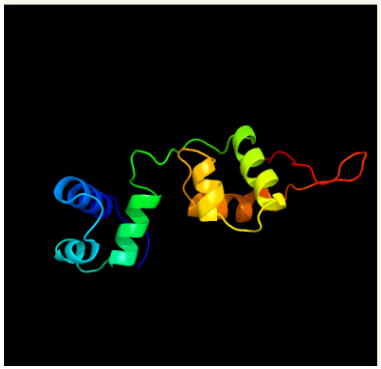 **PDB header:**transcription/dna **Chain:** G: **PDB Molecule:**myb3; **PDBTitle:** structure of the trichomonas vaginalis myb3 dna-binding2 domain bound to a promoter sequence reveals a unique c-3 terminal beta-hairpin conformation Confidence and coverage Confidence: 100.0% Coverage: 43% 117 residues (43% of your sequence) have been modelled with 100.0% confidence by the single highest scoring template. Phyre alarm You may wish to submit your sequence to Phyrealarm. This will automatically scan your sequence every week for new potential templates as they appear in the Phyre2 library.
Traes_4AS_2BDA1260C POPSEQ - 4A:61.015 cM	MMGGGLLMDQGMAFSGVHNFVDLLQQ NGADKNLGFGSLMPQTSSGDQCVMGEG DLVDPPTNNFPDAGEDDSDDDVDDIEELE RRMWRDRMKLKRLKELQQSRGKEQAAG GGGAGDGLKPRQSQEQARRKKMSRAQD GILKYMLKMMEVCRAQGFVYGIIPEKGKP VSGASDNLRAWWKEKVRFDRNGPAAIAK YQADNAVPGSESELASGTASPHSLQELQD TTLGSLLSALMQHCDPPQRRFPLEKGISPP WWPSGDEEWWPELGIPKDQGPPPYKKP HDLKKAWKVSVLTAVIKHMSPDIEKIRRLV RQSKCLQDKMTAKEISTWLAVVKQEEELF MRLHPGVRPPASAGGIASAISFNASSSEYD VDLADDCKGDEAGTHKMAMDDPTAFNL GAAILNDKFLMQAPMKEETGDMEYVQKR SAVAAEPELMLNNRVYTCNNVQCPHSDY GYGFLDRNARNSHRYTCKYNDPLPPSAEN KATPPAPPQVFPAAYNQQNHGLNNLDFG LPMDGQRSIAELMNMYDTTFPATNKNM GNDDVTIIERPNAITPVMDEGFFGQGNGI GGNGDSMFSDVSNMMQQQQAQQPQQ QQQQQQQAPAQQQFFIGDDAQAQFGN QMGSISGASDFRFGSGFNMSGTVDYPQK NDGPNWYY	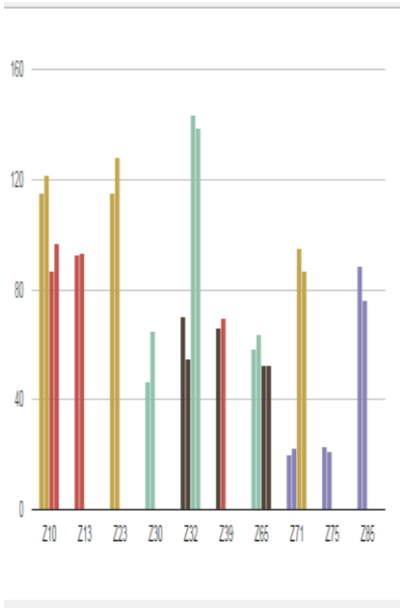	 **Fold:**LEM/SAP HeH motif **Superfamily:**DNA-binding domain of EIN3-like **Family:**DNA-binding domain of EIN3-like Confidence and coverage Confidence: 100.0% Coverage: 20% 127 residues (20% of your sequence) have been modelled with 100.0% confidence by the single highest scoring template. Phyre alarm You may wish to submit your sequence to Phyrealarm. This will automatically scan your sequence every week for new potential templates as they appear in the Phyre2 library. Warning: 52% of your sequence is predicted disordered. Disordered regions cannot be meaningfully predicted.

Traes_4DL_D41CB81EA POPSEQ- 4D:61.58 cM	MEMPAPIKTGSWSPEEDALLVALVRQHG ARRWSVISAGVPGRTGKSCRLRWCNQLSP AVQHRPFTAQEDALIIAAQARYGNKWADI ARLLPGRTDNSVKNHWNSNLRRCQRRAK AMAAAAAARAAASSSSSSGSAARAKTQQ QEQ	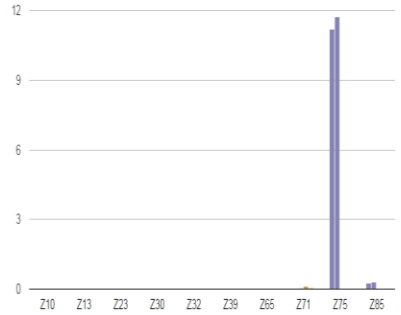	 Model (left) based on template c3zqcG_ Top template information **PDB header:**transcription/dna **Chain:** G: **PDB Molecule:**myb3; **PDBTitle:** structure of the trichomonas vaginalis myb3 dna-binding2 domain bound to a promoter sequence reveals a unique c-3 terminal beta-hairpin conformation Confidence and coverage Confidence: 100.0% Coverage: 81% 117 residues (81% of your sequence) have been modelled with 100.0% confidence by the single highest scoring template. 3D viewing Interactive 3D view in JSmol For other options to view your downloaded structure offline see the FAQ
Traes_4DL_C083C804E POPSEQ – 4D: 54.756 cM	MMGGGLLMDQGMAFSGVHNFVDLLQQ NGADKNLGFGSLMPQTSSGDQCVMGEG DLVDPPTDNFPDAGEDDSDDDVDDIEELE RRMWRDRMKLKRLKELQQSRGKEQAAA GGGVGDGLKPRQSQEQARRKKMSRAQD GILKYMLKMMEVCRAQGFVYGIIPEKGKP VSGASDNLRAWWKEKVRFDRNGPAAIAK YQADNAVPGSESELASGTASPHSLQELQD TTLGSLLSALMQHCDPPQRRFPLEKGISPP WWPSGDEEWWPELGIPKDQGPPPYKKP HDLKKAWKVSVLTAVIKHMSPDIEKIRRLV RQSKCLQDKMTAKEISTWLAVVKQEEELF MRLHPGARPPASAGGIASAISFNASSSEYD VDLADDCKGDEAGTHKMAMADPTAFNL GAAILNDKFLMQAPMKEETADMEYVQKR SAVAAEPELMLNNRVYTCNNVQCPHSDY GYGFLDRNARSSHQYTCKYNDPLPPSAEN KAAPPAPPQVFPAAYNQQNHGLNNLDFG LPMDGQRSIAELMNMYDTAFPATNKNM GNDDVTIIERPNAITPGAQMDEGFFGQGN GIGGNGDSMFSDVSNMMQQQQQQQA QQPQQQQAPAQQQFFIRDDAQAQFGNQ MGSISGASDFRFGSGFNMSGTVDYPQKN DGPNWYY	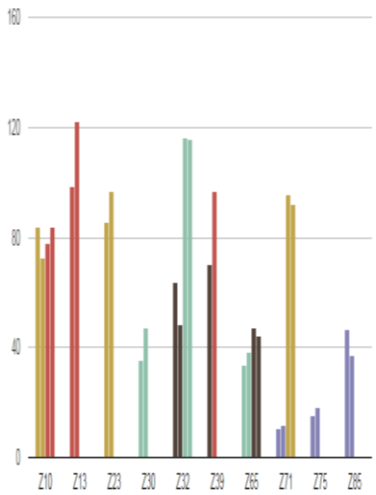	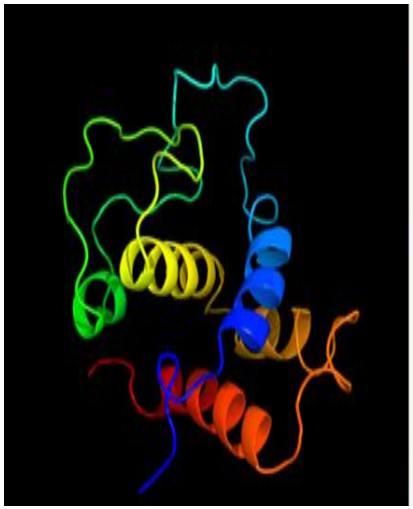 **Fold:**LEM/SAP HeH motif **Superfamily:**DNA-binding domain of EIN3-like **Family:**DNA-binding domain of EIN3-like Confidence and coverage Confidence: 100.0% Coverage: 20% 127 residues (20% of your sequence) have been modelled with 100.0% confidence by the single highest scoring template. Phyre alarm You may wish to submit your sequence to Phyrealarm. This will automatically scan your sequence every week for new potential templates as they appear in the Phyre2 library.

TRAES3BF109900090CFD_g POPSEQ distance is not available	MVRKLDGGRGRLAEAVEAVKDHGAGALHLAAS GQNLEVCEYLVEDVGVNVDAVDEAGRTPLVWA IIVKGGQVDIVKYLLDHGANPDNADRTGITPLHE AVERGHCEVVELLLSRGAYVDPFSTIDGTPLHVA AEHKQEWAMKILLDHHADCNKILRGFLTPLNIAI ESRSVKCVKLLVKAGADVKGPRNATPLQGAARL GLTDALKCLLDAGADPNDRDEHGHWPIQLAAY FGTRKDVEILFGVTSRIPAVHDWSVDGIISYVKA QPKLEDLPLSKMTVAELKKEGSKAMYKQDYKAA LEIYNMAITLDHDNIDPVIIGNRGFCRLILHRDGA LNDAQICRQIQPDCPHACWLEGYSYLLLQEFEKA CDSFLDAVKLDPGHVGIEKALREALRLLTESDAD KKNGVEGPGYRPVYLYH	RNASeq profile is not available	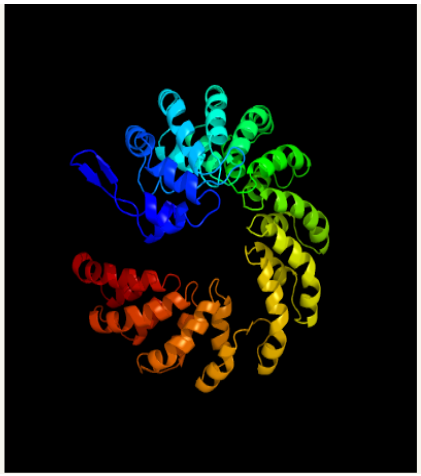 Model (left) based on template c4cj9A_ Top template information **PDB header:**transcription **Chain:** A: **PDB Molecule:**burrh; **PDBTitle:** burrh dna-binding protein from burkholderia rhizoxinica in2 its apo form Confidence and coverage Confidence: 100.0% Coverage: 97% 404 residues (97% of your sequence) have been modelled with 100.0% confidence by the single highest scoring template. 3D viewing Interactive 3D view in JSmol For other options to view your downloaded structure offline see the FAQ
TRAES3BF117700060CFD_g POPSEQ distance is not available	MLPEIREEGGGAGTSATKAMSVSLSGKRGRYVR QVTGRHNDTDLHVAARAGDAAALRRALDEAAV VVAVGEGGEQLEAVRRAVAAEANEAGETPLLA AAERGHLEVVVELLRHLDAQGVAAKNRSGYDAL HVAAREGHHAVLQEMLRHDRMFAKTFGPANT TPLISAATRGHAEVVKLLLEQDDFGLGEMAKDN GKNALHFAARQGHMEIVKALLEKDPQLARRND KKGQTALHMAVKGTNCDVLRALVDADPAIVML PDKNGNTALHVATRKKRAEIVIVLLRLPDTHVNA LNRDHKTAFDIAEGLPHCEESSEIKDILSQHGALR SRELNQPRDELRKTVTEIKKDVHTQLEQTRKTNK NVHGIAKELRKLHREGINNATNSVTVVAVLFATV AFAAIFTVPGGNENNGVAIVVQTASFRIFFIFNAI ALFTSLAVVVVQITVVRGETKSERKVVEVINKLM WLASVCTTISFIASCYIVLGRHFQWAAILVSLIGG VTMTGVLGTMTYFVVKSKRMRKIRKKEKMSRR SGSSSWVDNTEISETELNQVYAL	RNASeq profile is not available	 Top template information **PDB header:**transcription **Chain:** A: **PDB Molecule:**burrh; **PDBTitle:** burrh dna-binding protein from burkholderia rhizoxinica in2 its apo form Confidence and coverage Confidence: 100.0% Coverage: 50% 277 residues (50% of your sequence) have been modelled with 100.0% confidence by the single highest scoring template. *Additional confident templates have been detected* (see Domain analysis) which cover other regions of your sequence. 505 residues (91%) could be modelled at >90% confidence using multiple-templates. You may wish to try resubmitting your sequence in "intensive" mode to model more of your sequence.

TRAES3BF267200010CFD_g POPSEQ distance is not available	MSSYSSLLSVSPGEQIGGYADGGDHDDMAAAA NYLSSFCFDFGEEYYSLAEAATASYPLHAQQQQP PTQADSHHSGKAASTTSSSQGLDNINTSLTSSDA RSKGSKIAFKTRSEMEVLDDGYRWRKYGKKMV KNSPNPRNYYRCSSEGCRVKKRVERDRDDERFVI TTYDGVHDHLAPLPPRGCAGYSLSLAQTRVDEG SSPLPVQGRRCFLDTMKMHAAGSQQGCTPVP QPRKLERDN	RNASeq profile is not available	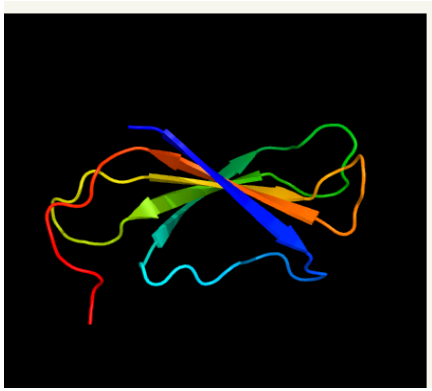 **PDB header:**transcription **Chain:** A: **PDB Molecule:**wrky transcription factor 1; **PDBTitle:** crystal structure of the c-terminal wrky domainof atwrky1,2 an sa-induced and partially npr1-dependent transcription3 factor Confidence and coverage Confidence: 100.0% Coverage: 31% 75 residues (31% of your sequence) have been modelled with 100.0% confidence by the single highest scoring template. Phyre alarm You may wish to submit your sequence to Phyrealarm. This will automatically scan your sequence every week for new potential templates as they appear in the Phyre2 library. Warning: 72% of your sequence is predicted
TRAES3BF001100080CFD_g POPSEQ distance is not available	MPPAAMAPPQAPSAGDPLYDELWHACAGPLV TVPRVGDLVFYFPQGHIEQVEASMNQVAGNQ MRLYDLPSKLLCRVINVELKAEADTDEVYAQVM LMPEPEQNEMAVDKSTSTTGATPPRPAVRSFCK TLTASDTSTHGGFSVLRRHADECLPPLDMTQSP PTQELVAKDLHGMDWRFRHIFRGQPRRHLLQS GWSVFVSSKRLVAGDAFIFLRGESGELRVGVRR AMRQLPNVPSSVISSHSMHLGVLATAWHAINT KSMFTVYYKPRTSPSEFIIPYDQYMESVKNNYSIG MRFRMRFEGEEAPEQRFTGTIVGSENLDQLWP ESNWRSLKVRWDEPSTIPRPDRVSPWKIEPASS PPVNPLPLSRVKRPRPNVPPVSPESSVLTKEGAT KIDMDSAQAQQRNQNNMVLQGQEHMTLRTN NLTASNDSDATVQKPMMWSPSPNIGKNHASA FQQRPSMDNWMQLGRCDASSGAQSFGDSQG FFMQTFDEAPNRHGSFKNQFQDHSSARHFSDP YTKMQTEANEFHFWNSQSTVYGNPRDQSQGF RFEEHPSNWLRQQQFSPVEQPRVIRPHASIAPV DLEKAREGSGFKIFGFKVDTTSTPSNHLSSSMAAI HEPVLQIQASASLTQLQHTHADCIPELSVSTAGT TENEKSIQQAPHSSKDVQSKSHGASTRSCTKVH KQGVALGRSVDLSKFGDYDELTAELDRMFEFDG ELMSSNKDWQIVYTDPEGDMMLVGDDPWEEF CNIVRKIFIYTKEEVQKMNSKSSAPRKEEGSGDA DGANEKAHLATSSHLDN	RNASeq profile is not available	 Model (left) based on template c4ldxB_ Top template information **PDB header:**transcription/dna **Chain:** B: **PDB Molecule:**auxin response factor 1; **PDBTitle:** crystal structure of the dna binding domain of arabidopsis thaliana2 auxin response factor 1 (arf1) in complex with protomor-like sequence3 er7 Confidence and coverage Confidence: 100.0% Coverage: 42% 335 residues (42% of your sequence) have been modelled with 100.0% confidence by the single highest scoring template. *Additional confident templates have been detected* (see Domain analysis) which cover other regions of your sequence. 443 residues (56%) could be modelled at >90% confidence using multiple-templates. You may wish to try resubmitting your sequence in "intensive" mode to model more of your sequence. Warning: 62% of your sequence is predicted

Traes_7BL_CA6B7C9E6 POPSEQ: 7B: 64.839 cM	MLRCSSASGCHWERVSMSGPRQGSSQP QFMTSVGQNNNLSNGPGTPLIDSIDVDQI VIPEKNSWKNLFSYIGPGFLVSIAYIDPGNF ETDLQAGAQYKYELLWIILIASCAALVIQSL AASLGVVTGKHLAEHCRAEYPKVTNFILWI LAELAVVACDIPEVIGTAFALNMLFKIPIWC GVLITGLSTLMLLFLQQYGVRKLEFLIAFLVF LIATCFLVELGYSKPNSSEVVRGLFVPEIKGD GATGLAISLLGAMVMPHNLFLHSALVLSRK VPRSVHGIKEACRFYMIESAFALTVAFLINIS IISVSGAVCSADNLNPEDRMNCNDLDLNK ASFLLKNVLGNWSSKVFSIALLASGQSSTIT GTYAGQYVMQGFLDLRMTPWLRNLLTRS LAIVPSLIVSLIGGSSAAGKLIIIASMILSFELP FALVPLLKFTSSKTKMGPHTNSRFISVLTW AIGSFIMVINIYFLITSFVRLLLHSGLSTVSQV FSGIFGFLGMLIYIAAILYLVFRKNRKCTLPLL ECDAKLGDAGHTEGEGSLGHLPREDISSM QLPHQRPASDLD	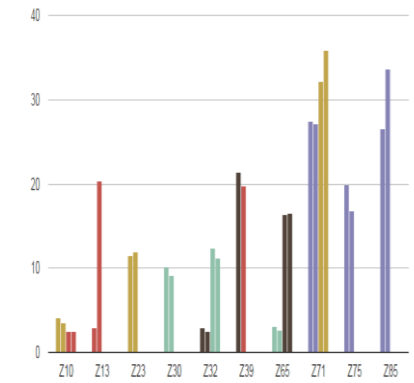	 Top template information **PDB header:**transport protein **Chain:** C: **PDB Molecule:**divalent metal cation transporter mnth; **PDBTitle:** crystal structure of staphylococcus capitis divalent metal ion2 transporter (dmt) in complex with nanobody Confidence and coverage Confidence: 100.0% Coverage: 69% 389 residues (69% of your sequence) have been modelled with 100.0% confidence by the single highest scoring template. *Additional confident templates have been detected* (see Domain analysis) which cover other regions of your sequence. 499 residues (88%) could be modelled at >90% confidence using multiple-templates. You may wish to try resubmitting your sequence in "intensive" mode to model more of your sequence.
Traes_4AS_7258345F9 POPSEQ: 4A: 57.601 cM	MPGGGFAVSAPSGVEFEAKITPIVIISCIMA ATGGLMFGYDVGISGGVTSMDDFLREFFP AVLRRKNQDKESNYCKYDNQGLQLFTSSLY LAGLTATFFASYTTRRLGRRLTMLIAGVFFII GVIFNGGAQNLAMLIIGRILLGCGVGFANQ AVPLFLSEIAPTRIRGGLNILFQLNVTIGILFA NLVNYGTSKIHPWGWRLSLSLAGIPAAML TLGALFVTDTPNSLIERGHLEEGRAVLKRIR GTDNVEPEFNEIVEASRIAQEVKHPFRNLL QRRNRPQLVIAVLLQIFQQFTGINAIMFYA PVLFNTLGFKSDASLYSAVITGAVNVLATLV SVYAVDRAGRRALLLEAGVQMFLSQVVIA VVLGIKVTDRSDNLGHGWAILVVVMVCTY VASFAWSWGPLGWLIPSETFPLETRSAGQ SVTVCVNLLFTFLIAQAFLSMLCHLKFAIFIF FSAWVLVMSVFVLFFLPETKNVPIEEMTDK VWKQHWFWKRYMDDDDHHHHNIANG KNATV	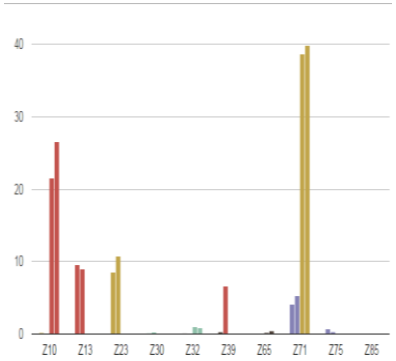	 Top template information **PDB header:**transport protein **Chain:** A: **PDB Molecule:**solute carrier family 2, facilitated glucose transporter **PDBTitle:** structure of the human glucose transporter glut3 / slc2a3 Confidence and coverage Confidence: 100.0% Coverage: 88% 453 residues (88% of your sequence) have been modelled with 100.0% confidence by the single highest scoring template. *Additional confident templates have been detected* (see Domain analysis) which cover other regions of your sequence. 506 residues (98%) could be modelled at >90% confidence using multiple-templates. You may wish to try resubmitting your sequence in "intensive" mode to model more of your sequence.

Traes_4DL_CFC191A06 POPSEQ: 4D: 54.756 cM	MPGGGFAVSAPSGVEFEAKITPIVIISCIMA ATGGLMFGYDVGISGGVTSMDDFLREFFP AVLRRKNQDKESNYCKYDNQGLQLFTSSLY LAGLTATFFASYTTRRLGRRLTMLIAGVFFII GVIFNGAAQNLAMLIIGRILLGCGVGFANQ AVPLFLSEIAPTRIRGGLNILFQLNVTIGILFA NLVNYGTSKIHPWGWRLSLSLAGIPAAML TLGALFVTDTPNSLIERGHLEEGKAVLKRIR GTDNVEPEFNEIVEASRIAQEVKHPFRNLL QRRNRPQLVIAVLLQIFQQFTGINAIMFYA PVLFNTLGFKSDASLYSAVITGAVNVLATLV SVYAVDRAGRRALLLEAGVQMFLSQVVIA VVLGIKVTDKSDNLGHGWAILVVVMVCTY VASFAWSWGPLGWLIPSETFPLETRSAGQ SVTVCVNLLFTFLIAQAFLSMLCHLKFAIFIF FSAWVLVMSVFVLFFLPETKNVPIEEMTDK VWKQHWFWKRFMDDDDHHHNIANGK NATV	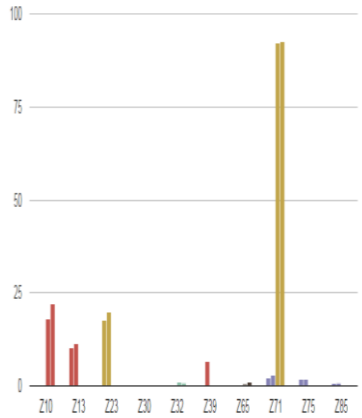	 Model (left) based on template c4ybqB_ Top template information **PDB header:**transport protein/immune system **Chain:** B: **PDB Molecule:**solute carrier family 2, facilitated glucose transporter **PDBTitle:** rat glut5 with fv in the outward-open form Confidence and coverage Confidence: 100.0% Coverage: 88% 451 residues (88% of your sequence) have been modelled with 100.0% confidence by the single highest scoring template. 3D viewing Interactive 3D view in JSmol For other options to view your downloaded
Traes_4DL_38FBC0AC7 POPSEQ distance is not available	MASRTFSAACLLALLVANTFLAGDACGSCK HKTPPPASPSPPPPSPSTTPCPPPSSGGGTS CPTDTLKLGACANVLGLVNVGVGKPPSGG GDKCCSLLGGLADLEAAVCLCTALKANVLG IVLNIPVKLSLLLNYCGKTAPKGFQCA	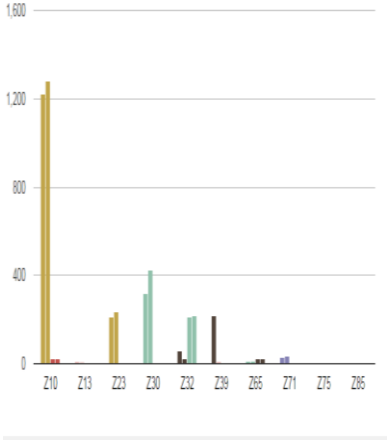	 **Fold:**Bifunctional inhibitor/lipid-transfer protein/seed storage 2S albumin **Superfamily:**Bifunctional inhibitor/lipid-transfer protein/seed storage 2S albumin **Family:**Plant lipid-transfer and hydrophobic proteins Confidence and coverage Confidence: 100.0% Coverage: 48% 71 residues (48% of your sequence) have been modelled with 100.0% confidence by the single highest scoring template. Phyre alarm You may wish to submit your sequence to Phyrealarm. This will automatically scan your sequence every week for new potential templates as they appear in the Phyre2 library.

Traes_4DL_B81290546 POPSEQ distance is not available	GQCSIDALKLRVCANVLGGLLGLKVGVPAH DECCPLLQGLVDLDAAVCLCTAVRANVLGI HLNVPVDISLLLNHCGKTCPSEFTCPAH	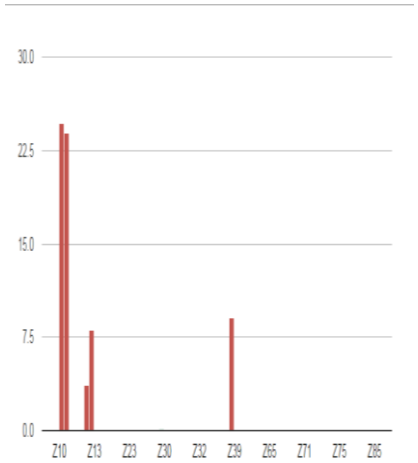	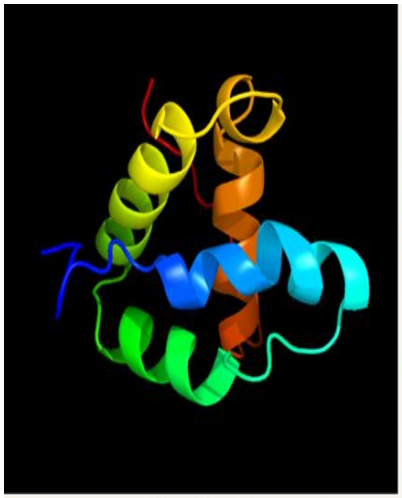 Model (left) based on template d1hypa_ Top template information **Fold:**Bifunctional inhibitor/lipid-transfer protein/seed storage 2S albumin **Superfamily:**Bifunctional inhibitor/lipid-transfer protein/seed storage 2S albumin **Family:**Plant lipid-transfer and hydrophobic proteins Confidence and coverage Confidence: 100.0% Coverage: 83% 73 residues (83% of your sequence) have been modelled with 100.0% confidence by the single highest scoring template. 3D viewing Interactive 3D view in JSmol For other options to view your downloaded structure offline see the FAO
TRAES3BF063600170CFD_g POPSEQ distance is not available	MATPALPNPSPPLDDPPPPEPKPRRETKVWKPK VRDPDAREPPAAAQDPEEDAPEEPEPDQDEGP EPPPLPTDAIEPTPSGAEEEDADDSSSVSSVSSAA AATDAATATGGKTERPFPAATDLLHISYNQDYG CFAAGTKTGFRIYNCDPFREIFRRDLGPSPPAAP GEEAAQAIHQPPAAASGGGGGIGVVEMLFRCN ILALVGGGDAPHYPPNKVMIWDDHQSRCIGELS FKSPVRGVRLRRDRIVVVLENKIFVYNFADLKLV QQIETAPNPKGLCSVSQQPGSIVLVCPGAQKGQ IRVEHYGARKTKFINAHASRVACFALSQDGRLIA TASTKGTLVRIFNAAEGNLLQEVRRGADRAEIYS LAFSNNLQYLAVSSDKGTIHVFNLKINVGLTTND KPLPAPDADVPHMSPSFSFIKGVLPKYFHSEWSV AQFRLHEGEQYIVAFGHEKNTVAVVGMDGSFY RCQFDPVNGGEMQQLECHNFLKPSDQP	RNASeq profile is not available	 Top template information **PDB header:**transport protein **Chain:** K: **PDB Molecule:**coatomer subunit alpha; **PDBTitle:** the structure of the copi coat linkage i Confidence and coverage Confidence: 100.0% Coverage: 51% 252 residues (51% of your sequence) have been modelled with 100.0% confidence by the single highest scoring template. *Additional confident templates have been detected* (see Domain analysis) which cover other regions of your sequence. 377 residues (76%) could be modelled at >90% confidence using multiple-templates. You may wish to try resubmitting your sequence in "intensive" mode to model more of your sequence.

TRAES3BF088300030CFD_g POPSEQ distance is not available	MARGAATQLVLVAMVAAMLLVASDAAISCGQ VTSALSPCISYARGNGANPPAACCSGVRSLAGA ARSTADKQAACKCIKSAAGGLNAGKAAGIPSKC GVSVPYAISSSVDCSKIR	RNASeq profile is not available	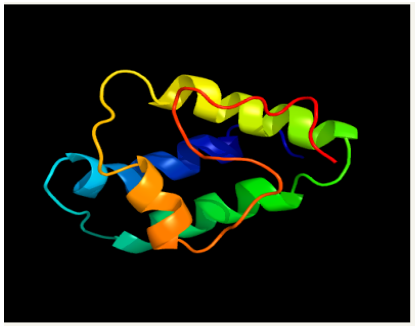 Model (left) based on template c2ljoA_ Top template information **PDB header:**lipid transport **Chain:** A: **PDB Molecule:**non-specific lipid-transfer protein 2; **PDBTitle:** 3d solution structure of lipid transfer protein lc-ltp2 Confidence and coverage Confidence: 100.0% Coverage: 77% 89 residues (77% of your sequence) have been modelled with 100.0% confidence by the single highest scoring template. 3D viewing Interactive 3D view in JSmol For other options to view your downloaded structure offline see the FAQ
TRAES3BF042900030CFD_g POPSEQ distance is not available	MASYDKAMESYKKAVTTAASLAASAMLVRGVV NELVPYEVRDLLFSGMGYLRSHMSSQHTIIIAETE GWANNQLYDAARAYLATRINTDMQRLRVSRV DETKSMMFSMEEGEEMADVHEGTEFKWRLVC RDNSSASSSNGNGRGGSGNFKLEVRSFEMSFHR KHKDKALTSYLPHILAVAKKIKEQNRTLKIYMNEG ESWFAIDLHHPSTFSTLAMDHKLKQSVMDDLER FVKRKEYYKKIGKAWKRGYLLYGPPGTGKSSMIA AMANYLKFDVYDLELTEVNWNSTLRRLLIGMTN RSILVIEDIDCTVELQQREEGQEGTKSNPSEDKVT LSGLLNFVDGLWSTSGEERIIIFTTNYKERLDPALL RPGRMDMHIHMGYCCPESFRILASNYHSKITMS HTRRSKK	RNASeq profile is not available	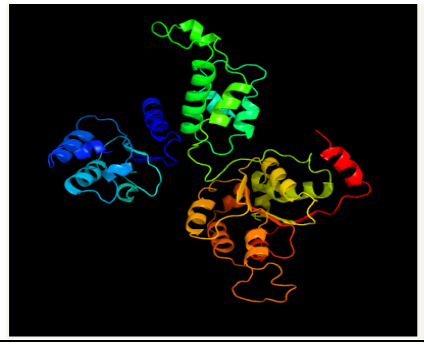 Model (left) based on template c3cf1C_ Top template information **PDB header:**transport protein **Chain:** C: **PDB Molecule:**transitional endoplasmic reticulum atpase; **PDBTitle:** structure of p97/vcp in complex with adp/adp.alfx Confidence and coverage Confidence: 100.0% Coverage: 94% 384 residues (94% of your sequence) have been modelled with 100.0% confidence by the single highest scoring template. 3D viewing Interactive 3D view in JSmol For other options to view your downloaded structure offline see the FAQ
TRAES3BF111500010CFD_g POPSEQ distance is not available	MGRGVLEVHLVDAKGLFGSDFLGKIDPYVIVQY RSQERKSSTSRDEGRNPSWNEVFRFQINSSAAN GQHKLFLRIMDHDNFSSDDFLGQATINVTDLIST GMESGASQLNAAKYSVVSADNSYHGEIRVGLTF TATKVEEDGGQVGGWTHSSRE	RNASeq profile is not available	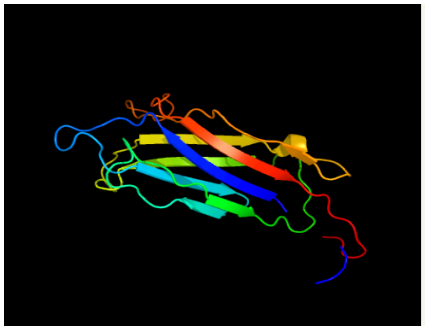 Model (left) based on template c2dmhA_ Top template information **PDB header:**lipid binding protein **Chain:** A: **PDB Molecule:**myoferlin; **PDBTitle:** solution structure of the first c2 domain of human myoferlin Confidence and coverage Confidence: 100.0% Coverage: 89% 137 residues (89% of your sequence) have been modelled with 100.0% confidence by the single highest scoring template. 3D viewing Interactive 3D view in JSmol For other options to view your downloaded structure offline see the FAQ

Traes_1DS_A373E79EA POPSEQ – 1D:46.631cM	MPAVAHRCFVVNQSLLPHLFFNSPDPHTGIHRL NQESNQSASRGSLPVLPILALALRSPSSIAAELVSP MASAQPWKSMFCCVGAGAAVDEEGPSPSSTP RRRRGERRTLLPSSSASTASRVSLSSLGSTGTLTPE DLSLTLSGSNLHAFTYAELKAATAGFSRSRYLGCG GFGPVYKGQLAAELRPGLEAQTVAVKYLDLDSSS QGHNEWLAEVFFLGQLRHRNLVKLVGYCYEEE HRMLAYEFMGTGSLEKHLFRSIDGPMPWMTR MKIAVGAAKGLAFLHGADTPVIFRDLKASNILLD SDYTAKLSDFGLAKDGPNGDATHVTTRIMGTH GYAAPEYIMTGHLTAKSDVYSFGVVLLELLSGRR SIDRARRSREQSLVDYARPYLKKQDKLHRVMDP ALECQYSSQGAELAARVAYKCLSQNSKLRPTMK EVVQALEPILKMDDYLQVGTFVFTVVVENTDKS VENKGKLIDDEWKADMKVEKIVEDKHQSHQDR HRQKFPNSTIHADILLQRDGAIGPYTTALQRHRR ASSYTEERGA	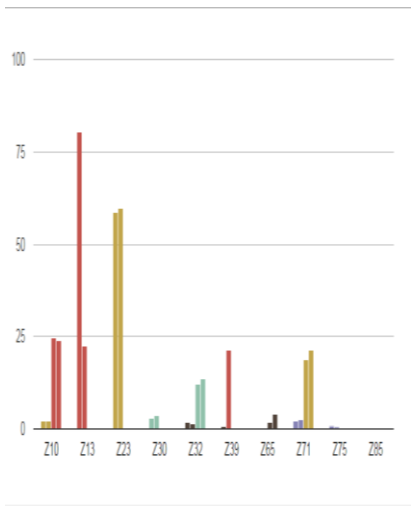	 **PDB header:**transferase **Chain:** A: **PDB Molecule:**proto-oncogene tyrosine-protein kinase abl1 (1b isoform); **PDBTitle:** organization of the sh3-sh2 unit in active and inactive forms of the2 c-abl tyrosine kinase Confidence and coverage Confidence: 100.0% Coverage: 48% 262 residues (48% of your sequence) have been modelled with 100.0% confidence by the single highest scoring template. *Additional confident templates have been detected* (see Domain analysis) which cover other regions of your sequence. 328 residues (60%) could be modelled at >90% confidence using multiple-templates. You may wish to try resubmitting your sequence in "intensive" mode to model more of your sequence.
Traes_7DS_351943FD9 POPSEQ - 7D: 77.626cM	MMGSGKSTVGKILAEVLGYSYFDSDSLVEQAVG MPSVAQIFKVHSEAFFRDSESSVLRDLSSMHRLV VATGGGAVIRPVNWRYMKKGLSIMLDVPLDAL AKRIAQVGTASRPLLDQPSADPYTAAFTKLSVLA EQRGDAYANADVRVSLEELAAKKGHDDVSQLT PTDIAVEALQKIKNFVTEHSMASGPFDDL	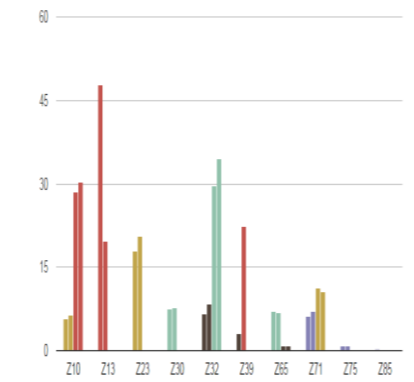	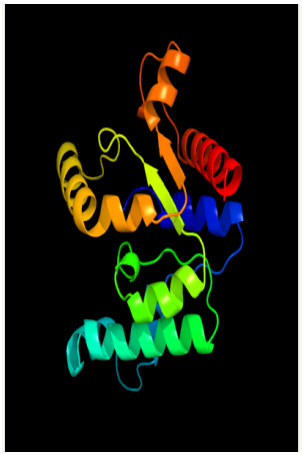 Model (left) based on template c3nwjB Top template information **PDB header:**transferase **Chain:** B: **PDB Molecule:**atsk2; **PDBTitle:** crystal structure of shikimate kinase from arabidopsis thaliana2 (atsk2) Confidence and coverage Confidence: 99.9% Coverage: 86% 167 residues (86% of your sequence) have been modelled with 99.9% confidence by the single highest scoring template. 3D viewing Interactive 3D view in JSmol For other options to view your downloaded structure offline see the FAQ

Traes_7DS_5A68A26E9 POPSEQ – 7D: 1.137 cM Protein models with same annotation but no RNASeq profiles include: Traes_7DS_D01759F78	QQCVQHYSDPILLSVCVLCVQSIPRTVELDEKTRT NLIQWPVEELDTLRINTTDLSGITVGAGSVVSLPL HQTSQLDIEASFRINASVIEALNEVDVSYNCTMT SGAATRGALGPFGILVLANAALTEQTAVYFYVSK GLDGVLRTHFCHDELRSTHATDVAKEVVGSTVP VLDGEDFSVRVLVDHSIVQSFVMGGRMTATSR AYPTEAIYAAAGVYLFNNATSATITAEKLIVHDM DSSYNRIFTDADLVVLD	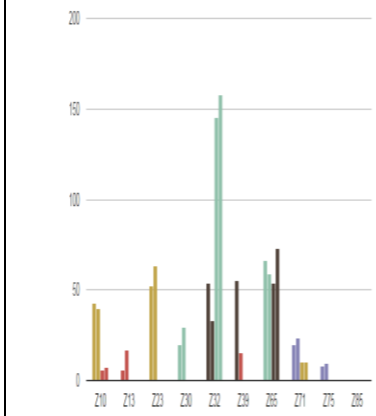	 Model (left) based on template c3ugfB Top template information **PDB header:**transferase **Chain:** B: **PDB Molecule:**sucrose:(sucrose/fructan) 6-fructosyltransferase; **PDBTitle:** crystal structure of a 6-sst/6-sft from pachysandra terminalis Confidence and coverage Confidence: 100.0% Coverage: 84% 214 residues (84% of your sequence) have been modelled with 100.0% confidence by the single highest scoring template. 3D viewing Interactive 3D view in JSmol For other options to view your downloaded structure offline see the FAQ
Traes_7DS_E373FDD65 POPSEQ : 7D: 0.5685 cM	MLHVLKASMDDERHDYYSLGTYDSAANTWTPI DPDLDLGIGLRYDWGKFYASTSFYDPAKKRRVL MGYVGEVDSKRADVVKGWASIQSVPRTIALDE KTRTNLLLWPVEEIETLRLNATELSDVTMNTGSV IHIPLRQGTQLDIEATFHLDASAVAALNEADVGY NCSSSGGAVNRGALGPFGLLVLAAGDRRGEQT AVYFYVSRGLDGGLHTSFCQDELRSSRAKDVTKR VIGSTVPVLDGEAFSMRVLVDHSIVQGFAMGG RTTMTSRVYPMEAYQEAKVYLFNNATGASVMA ERLVVHEMDSAHNQLSNMDDYSYVQ	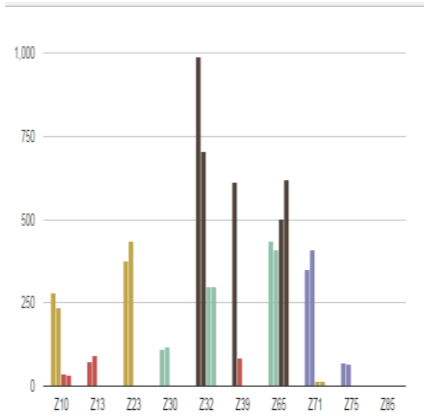	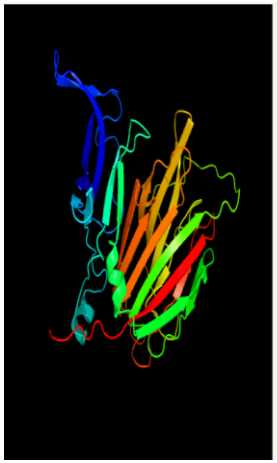 Model (left) based on template c3ugfB Top template information **PDB header:**transferase **Chain:** B: **PDB Molecule:**sucrose:(sucrose/fructan) 6-fructosyltransferase; **PDBTitle:** crystal structure of a 6-sst/6-sft from pachysandra terminalis Confidence and coverage Confidence: 100.0% Coverage: 93% 299 residues (93% of your sequence) have been modelled with 100.0% confidence by the single highest scoring template. 3D viewing Interactive 3D view in JSmol For other options to view your downloaded structure offline see the FAQ

Traes_7DS_EC365BE37 POPSEQ : 7D: 82.173 cM	MCYILRHSAVFLPIKKSDYFQVTGVPLNIVLHKPI FASTMARKQQSRSTKVKCPMCHVLRNAKMKL NITGGNRGNSSDSAFYCSDNTQKCDALQSSGSC DAERVIKPNCSSDGCNCSNCFTRKPRKRKRLYS WQRCSKQKQFCNEDNLTELSKLNDSNYALCNLL SDGSAAGVNGQTHSLKRTADNISIGMNNGEFV SQTEEPCNVPVLSLKKPPSSVLDTSPSQDLLCGYS KSGVQCTSPKVGPSSYSQLNSGSICFNCLMLNAS KCVSVDSLIPRQAIFYNKEISENVFHRSNLTNKRK GPDALSLLKRIFGIKECCIKFFQCDCHGSSRPNSN CLYHWMLQLVKNLVRNSKRCQYKKLFLKHCSVK SKQVAKDGLPSGNIQYSTGGKSAYCGESFAQLE AYSTHQQVVSFVWAVLTRIIPQPLLGNPSSKRSL RVNIWKFIRLRRFETFQVTDCIRELKAPEYSWLSK IGFTSCFCSVLLGEETGLSNGTEEQKQNNLLHCW ISWLFSDIVIPLISTYFYVTERETKRYDVFYYPKSV WRNLTSNTIASLNAQSFKILRGTSRRAIKHLYRSS RVRFLPKAKDIRPLVNFKAQSKDGILYKCHLVIKKI RDDNPEMFGSSVFDYDGVYKNLSSFMSSVRRQ LKESKIYIVVADVSKAFDCVNHDVLLKIMDDVLK GDEYALRKCTKVIYSRSKNVAYRFDSNVSVSNGN GINDFSIQPSSGGGILVDQGTVSTIRKEELQRVLF EQVKCNILKIGHNFYLQQVGIAQGNKLSPNLCSL YYGHLENSVILNFLHDGNSGDAISEPEFLMMRFI DDFMFISLSKKHALNFFNRMRRGFVYYNTYMN DSKYGFNFNIGDNEQCDNRLYRGDDGVTFIPW SGLLINCENLEIQADYTRYVCQFLVLVC	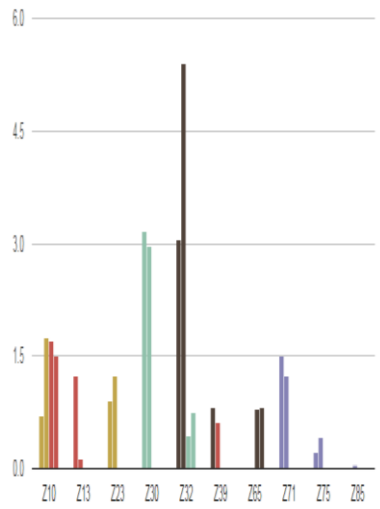	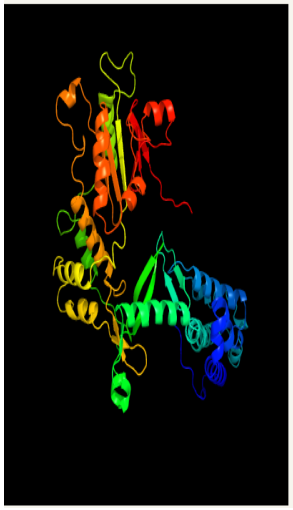 Model (left) based on template c3du6A Top template information **PDB header:**transferase **Chain:** A: **PDB Molecule:**telomerase reverse transcriptase; **PDBTitle:** structure of the catalytic subunit of telomerase, tert Confidence and coverage Confidence: 100.0% Coverage: 44% 396 residues (44% of your sequence) have been modelled with 100.0% confidence by the single highest scoring template. *Additional confident templates have been detected* (see Domain analysis) which cover other regions of your sequence. 505 residues (56%) could be modelled at >90% confidence using multiple-templates. You may wish to try resubmitting your sequence in "intensive" mode to model more of your sequence. 3D viewing Interactive 3D view in JSmol
Traes_7DS_309E71F44 POPSEQ : 7D: 83.31cM	MDLSSLARPQALRGGXXXHAARRRSVQLLRPRR PTFRCSVEAAKQQVQGTLAAEAEAARKECFGVF CTTYDLEADEKTKSWKKLVNVSVSGAAGMISNH LLFKLASGEVFGQDQPIALKLLGSERSLQALEGVA MELEDSLYPLLREVSIGIDPYVIFEDADWALLIGA KPRGPGVERAALLDINGQIFAEQGKALNAVASR NVKVIVVGNPCNTNALICLKNAPNLPAKNFHAL TRLDENRAKCQLALKAGVFYDKISNMTIWGNHS TTQVPDFLNAKINGRPVKEVIKDTKWLEEDFTIT VQKRGGVLIQKWGRSSAASTAVSIVDAMRSLVT PTPEGDWFSTGVYTTGNPYGIAEDIVFSMPCRS KGDGDYELVKDVAMDDFLWGRIKKSEAELIAEK RCVAHLTGEGNAFCDLPGDTMLPGEM	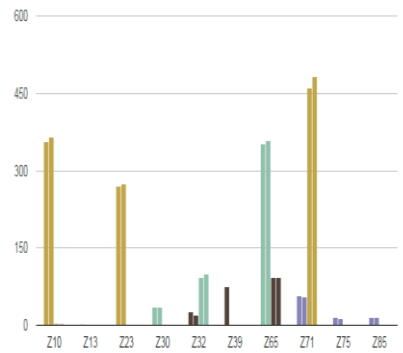	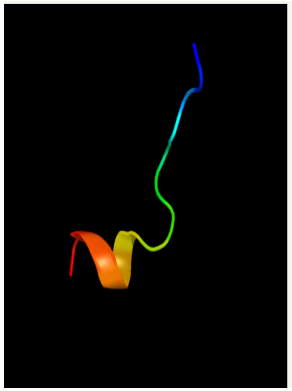 Model (left) based on template c3gliO Top template information **PDB header:**transferase/dna **Chain:** O: **PDB Molecule:**dna polymerase iii subunit psi; **PDBTitle:** crystal structure of the e. coli clamp loader bound to primer-template2 dna and psi peptide Confidence and coverage Confidence: 10.7% Coverage: 29% 14 residues (29% of your sequence) have been modelled with 10.7% confidence by the single highest scoring template. Phyre alarm You may wish to submit your sequence to Phyrealarm. This will automatically scan your sequence every week for new potential templates as they appear in the Phyre2 library. Please note: You must be registered and logged in to use Phyrealarm. 3D viewing

Traes_7BL_580CFC05F POPSEQ : 7B: 52.33 cM	MAANLEDVPSVDLITEVLRRAKCSSKPDKR IILIGPPGSGKGTQSPLIKDEYCLCHLATGD MLRAAVAAKTPLGIKAKEAMNKGELVSDD LVVGIIDEAMKKPSCQKGFILDGFPRTVVQ AQKLDDMLAKQGAKVDKVLNFAIDDAILE ERITGRWIHPSSGRSYHTKFAPPKTPGVDD VTGEPLIQRKDDTAAVLKSRLEAFHMQTEP VIDYYSKNGLVANLHAEKPPKEVTVEVQKA LQ	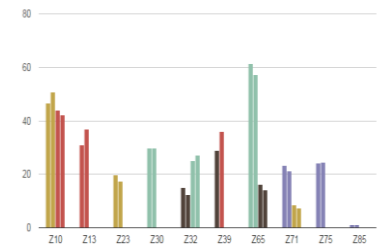	 Model (left) based on template c3tlxA_ Top template information **PDB header:**transferase **Chain:** A: **PDB Molecule:**adenylate kinase 2; **PDBTitle:** crystal structure of pf10_0086, adenylate kinase from plasmodium2 falciparum Confidence and coverage Confidence: 100.0% Coverage: 97% 234 residues (97% of your sequence) have been modelled with 100.0% confidence by the single highest scoring template. 3D viewing Interactive 3D view in JSmol For other options to view your downloaded structure offline see the FAQ
Traes_7BL_660FFDCE2 POPSEQ: 7B: 55.744 cM	WTLPLGDCVVERVNRSALPLSLIRGDTIQD GDEGVEEERGGEGPGAPVPVAGARRXPLC LWLALVAATLVLAQGKKSNLSEVTHKVYFD IEIDGKPAGRVVMGLFGKAVPKTAENFRAL CTGEKGMGNSGKPLHYKGSSFHRIIPSFMI QGGDFTLGDGRGGESIYGTKFADENFKLK HTGPGYLSMANAGRDTNGSQFFITTVTTS WLDGKHVVFGKVLSGMDVVYKVEAEGKQ NGTPKSKVVIADSGEVPL	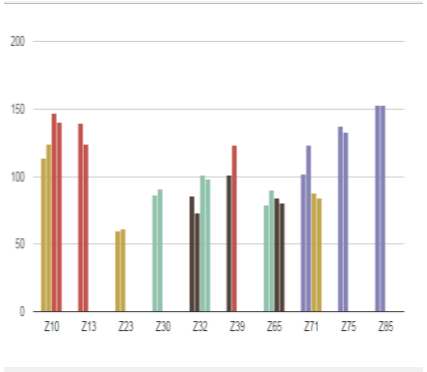	 Model (left) based on template c1hfgA_ Top template information **PDB header:**isomerase **Chain:** A: **PDB Molecule:**cyclophilin 40; **PDBTitle:** bovine cyclophilin 40, monoclinic form Confidence and coverage Confidence: 100.0% Coverage: 71% 180 residues (71% of your sequence) have been modelled with 100.0% confidence by the single highest scoring template. Phyre alarm You may wish to submit your sequence to Phyrealarm. This will automatically scan your sequence every week for new potential templates as they appear in the Phyre2 library.
Traes_4DL_1184F6F68 POPSEQ distance is not available	AELIAEKRCVAHLIGEGNALSDLPGDT MLPGEM	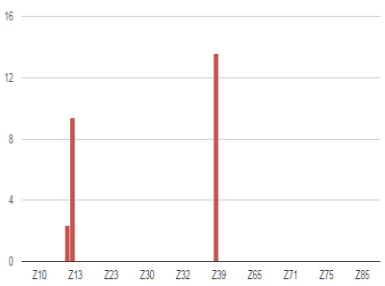	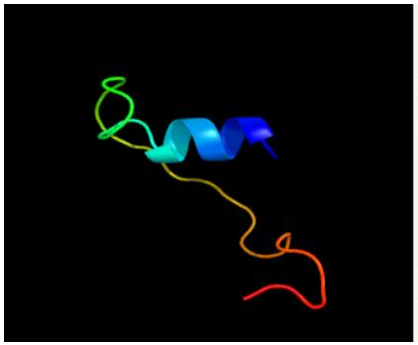 Model (left) based on template d1civa2 Top template information **Fold:**LDH C-terminal domain-like **Superfamily:**LDH C-terminal domain-like **Family:**Lactate & malate dehydrogenases, C-terminal domain Confidence and coverage Confidence: 98.9% Coverage: 97% 32 residues (97% of your sequence) have been modelled with 98.9% confidence by the single highest scoring template. 3D viewing Interactive 3D view in JSmol For other options to view your downloaded structure offline see the FAQ

TRAES3BF089500140CFD_g POPSEQ distance is not available	MAGTTHLLALFALTQLYSVAASTSDAHAHGHDNDTAS SFCHPDQAAALLQLKQSFILDYSTTTLPSWQPGTDCCL WEGVGCDGVSGSSSSSVTVLDLGRRGLYSYSCHAALFN LTSLRYLDLSMNDFGGSRIPGDGFERLSKLTHLNLSYSGF YGQIPIAIGKLKSLVSLDLSSLHNIESAEITNLYAIMDGYN FLVLREPSFKTLLANLNNLRELYLDGVDISSSGEEWSSDL AKAVPRLHVFSMAYCKLNGPIHSSLSSLRSLTVVNLKLN GGISGAVPEFFTDFLNLSVLQLSYNNFSGWFPWKIFQLK NIRVLDVSHNERLSGRLPEFPSRASLETLILQYTNFSGVRL SSFNNLLSLRELGELAPFFSWIRSLKNLTSLHLSDCYSSKL TPPMIGNLTNLTSLEITYCGFVGQIPSSIGNLNKLTSLRIS DCAFSGTIPSSIGNLKKLRRLEISYTELSCPITTDFGHLNKL MNDLRGDIPTYLFTLPAMLQLDLSSNQLSGPIQEFGTLH SHMIIVYLSQNQISGQIPRSFFQLTSLIDLDLSSNNLTGLV ELNLLWKLRKLASLDLSNNRLSVLDGEGNKSTVPLLSKLS YLILVSCNMTTMPRFLMHINHIDTLDLSNNIIQGTIPQW IWETWDDSLTQLNLSNNMFTDMQLTSYLLPYSRLDSLD LSSNRLQGQAPMPNLFKEVDYSNNRFSSIMPNFTAYLS QTVYLKLSRNNISGHIPDSTIDLHGNNIRGKLPRSLSNCA GLGILDIGNNRMVGTFPFWLGRLSDLCIIVLGSNLFYGSL TYPARDRKSREYFSKIQIVDIASNNFSGNLDPQWFGRFA SMMAKFSETGNILRHQIYGDYHDTVAITYKGQYVTFEE VLTTLTAIDFSNNALEGDIFESVGSLVSLHILNMSHNAFK GRIPAQIGEMRQLESLDLSWNKLSGEIPQELTNLTFLSTL NLSGNRLDGRIPQSSQFATFEYTSYEGNAGLCGPPLSKP CGNSSNPNEAQVSISKDHVDVILFLFAGWALALDSRQV FC	RNASeq profile is not available	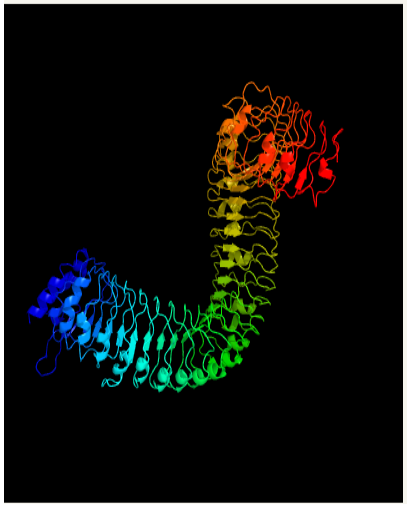 Top template information **PDB header:**transferase/transferase receptor **Chain:** A: **PDB Molecule:**Irr receptor-like serine/threonine-protein kinase fls2; **PDBTitle:** crystal structure of flg22 in complex with the fls2 and bak12 ectodomains Confidence and coverage Confidence: 100.0% Coverage: 73% 755 residues (73% of your sequence) have been modelled with 100.0% confidence by the single highest scoring template. *Additional confident templates have been detected* (see Domain analysis) which cover other regions of your sequence. 990 residues (96%) could be modelled at >90% confidence using multiple-templates. You may wish to try resubmitting your sequence in "intensive" mode to model more of your sequence.
TRAES3BF111600230CFD_g POPSEQ distance is not available	MANPSMAAGGGVPWAEGARAVGAQIRNRLR VAPVDRRWLWRRPEGRAASEAVRQWSDRLRA ILQRDKQNQGPGSPDASAAAAAKPSSSAFKFYR KKVGKEVNGVEDSVIFRSLQALAVPLIGNACHVF MHGLNSVQIYGAEKLQQALQERPKDKPLLTVSN HVAAMDDPFVIASLLPPSVMLEAQKLRWTLCAT DRCFTNPVLSTFFRSVKVLPVNRGEGIYQKGMD MALSKLNNGGWVHIFPEGSRSRDGGKTIAPAKR GVGRLIMDADSLPVVVPFVHTGMQDIMPVGKR IPRTGKRVIVVVGDPINFDDLMAENSNDSQHISR GDLYDKVTERIGQRLQQLKVEVDRLAAEQKAEL QNRHVANDTVNDGYKVWQQVDWESFGIGN MLSSAEHSSAQEPPPKQIQHEVLLAEQSASPAK QAEPEPRLEEEQSVFSPISRVPHWFSRRTDASEL MGFAARGLVGNGRSMQEGYRQFQEPSVFSAW WEAQTSSAMMPRWSTA	RNASeq profile is not available	 Top template information **Fold:**Glycerol-3-phosphate (1)-acyltransferase **Superfamily:**Glycerol-3-phosphate (1)-acyltransferase **Family:**Glycerol-3-phosphate (1)-acyltransferase Confidence and coverage Confidence: 99.2% Coverage: 39% 194 residues (39% of your sequence) have been modelled with 99.2% confidence by the single highest scoring template. Phyre alarm You may wish to submit your sequence to Phyrealarm. This will automatically scan your sequence every week for new potential templates as they appear in the Phyre2 library.

TRAES3BF154700050CFD_g POPSEQ distance is not available	MATSATAARHMVALPYPGRGHINPMLAVCRLL VAADGALTVTVVVTEEWHGLLASAGVTPTLPDR VHLATIPNVIPSEHGRGADHGGFIEAVNCKMGE PVERLLDRLALELGRRPDAIVADTYLQWAVAAG ARRGIPVCSLWTQPATFFLALCHLDLWQPAVEG VSDKELSCKSLEQYVPGLSSVRLSDIKIFLAWKGPI KIAAEAFVNVRKAQGVLFTSFHELEPSSMSKIAEL LPCPIYPIGPSILRAPDNEEKARDEEHRRWLDAQ PENSVLYVSFGSFVAMPPKQFEEIAVGLRDSAVR FFWVARDRATDGLREMCGDRGLPVPWCDQQE VLRHPSVGGFLSHCGWNSVLEAVCAGVPVLGFP VAWDQLVNARMVADEWKAGIDLREQRGKDGI VSRAAVSAAARKLMDLDSGAGQEMRTRAAQL REASRGAVIEGGSSHRSLTGFLEDLGKGKLDVPE SSA	RNASeq profile is not available	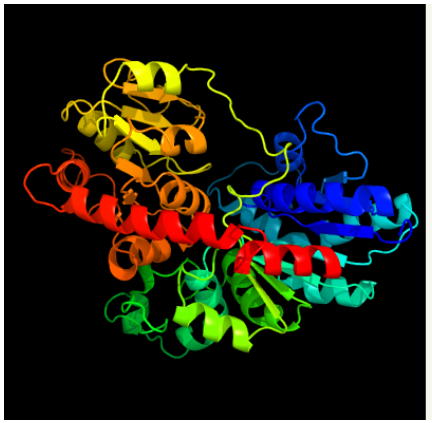 Model (left) based on template c3hbjA_ Top template information **PDB header:**transferase **Chain:** A: **PDB Molecule:**flavonoid 3-o-glucosyltransferase; **PDBTitle:** structure of ugt78g1 complexed with udp Confidence and coverage Confidence: 100.0% Coverage: 94% 438 residues (94% of your sequence) have been modelled with 100.0% confidence by the single highest scoring template. 3D viewing Interactive 3D view in JSmol For other options to view your downloaded structure offline see the FAQ
TRAES3BF021800050CFD_g POPSEQ distance is not available	MTFAGSGDGQSGSARAHFVLVPMMAQGRTIP MTDMACLLAEHGAQVSFITTPVNAARLEGFAA KVEAAGLVVQLVELHFPSVEFGLPDGCENLDMI QSKNLFFNFMKACAALHEPLMAYLREQQRSPPS CIISDMAHWWTGDIARELGIPRLTFSGFCGFSSL VRYIVFHNNVLENVTDDNELITIPGFPTPLELTKA KLPGGTLCIPGMEQIREKMFEEELRCDGEITNSF KELETLYIESYEQITRKKVWTIGPMCLCHRNSNRT AARGNKASMDEAQCLQWLDSRKPGSVIFVSFG SLACTTPQQLVELGLGLEASKKPFVWVIKAGAKL PEVEEWLADGFEERVKDRGLIIRGWAPQLMILQ HQAVGGFVTHCGWNSTIEGICAGVPMITWPHF GEQFLNEKLLVDVLQIGMEVGVKGVTQWGSEN QEVMVTRDAVETAVNTLMGEGEATEELRMRA EDCAIKARRAFDEEGSSYNNVRLLIQEMGNKTN ACG	RNASeq profile is not available	 Model (left) based on template d2vcha1 Top template information **Fold:**UDP-Glycosyltransferase/glycogen phosphorylase **Superfamily:**UDP-Glycosyltransferase/glycogen phosphorylase **Family:**UDPGT-like Confidence and coverage Confidence: 100.0% Coverage: 90% 446 residues (90% of your sequence) have been modelled with 100.0% confidence by the single highest scoring template. 3D viewing Interactive 3D view in JSmol For other options to view your downloaded structure offline see the FAQ

TRAES3BF038300120CFD_g POPSEQ distance is not available	MAAKSSHTMTIPTDAELVQAQADLWRHSLSYL TPMALRCAIQLGIPTAIHRHGGAASLIDLVTTLSL PPSKAPFLSRLLRLLSTTGVLASNEVGIYSLVPLSYL LVDGVLVDGDASQAALVLCLTSRYHMEAAMGL ADWFKKDIAQPLPSPFEDVHGATLFEESMAVLD PESDKLFNEALAAHDHMGIGTILRECHGLFNGL QSLTDCCGGDGTTAKAIVKAFPHIKCNVLDLPKV VDKAPSDGLVNYVAGDMFHSIPPAQAIMVKLVL HFWSDDDCINILAQCKKAIPSREAGGKVIVIDMV VDSSSPMFETQLLMDVAMMVCTRGRQRDEND WNAIFMKAGFSDYKIVKKLGARGVMEVYP	RNASeq profile is not available	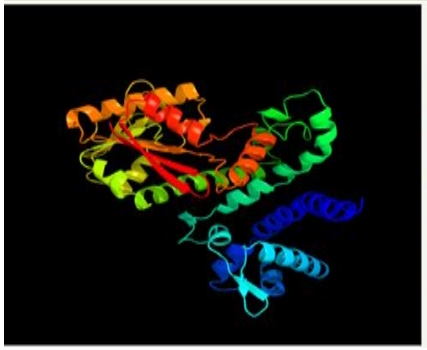 Model (left) based on template c1zgaA_ Top template information **PDB header:**plant protein, transferase **Chain:** A: **PDB Molecule:**isoflavanone 4'-o-methyltransferase'; **PDBTitle:** crystal structure of isoflavanone 4'-o-methyltransferase complexed2 with (+)-6a-hydroxymaackiain Confidence and coverage Confidence: 100.0% Coverage: 94% 342 residues (94% of your sequence) have been modelled with 100.0% confidence by the single highest scoring template. 3D viewing Interactive 3D view in JSmol For other options to view your downloaded
TRAES3BF044100020CFD_g POPSEQ distance is not available	MASKKMAQIMIQGQGETSYARNSSIQNAEQKK TKPWIEAVIVELCSSTGTLQPGKMVIADLGCSTG PNALALVSIAVEAIHAHCLQFQQLPPECVVLNDL PENNFNTVVKSRITLRQSNDPVVMTGITPGSFYE RLFTTESLHLVCLSNSMHWLSKAPEDLTRNLIPA YDIDEHSRSERLPIVLEAYAKQYRKDFTLFLELRAK ELVSGGRMIVSLVGRRSDAMTTKFSYILEIVAQIL CVMVSEGVIGKEKFDSFYGLLYEPSSEELREIIQE GASFSIREMRAHDPRTDMNNALSTPGRFAGFLR ALFEPVLVQHFGDAMDEFVRTAERRWILEGSLQ EERVRCPYAMLVVSLTKA	RNASeq profile is not available	 Model (left) based on template d1m6ex_ Top template information **Fold:**S-adenosyl-L-methionine-dependent methyltransferases **Superfamily:**S-adenosyl-L-methionine-dependent methyltransferases **Family:**Salicylic acid carboxyl methyltransferase (SAMT) Confidence and coverage Confidence: 100.0% Coverage: 96% 344 residues (96% of your sequence) have been modelled with 100.0% confidence by the single highest scoring template. 3D viewing Interactive 3D view in JSmol For other options to view your downloaded
TRAES3BF061700020CFD_g POPSEQ distance is not available	MSTPAAVRVIGAFDSPFSHRAEVALRLKGVPYEL ILEELHNKSELLLTSNPVHKKVPVLLHGDRTICESL IIVEYVDETFDGPALLPTDPYDRATARLWSRFIDD KCSKPFWLAMWTDGEAQKGFTKEIKENFALLEA QLEGKRFFGGGTIGLVDIAACGFAHWLTVCEEV SGVTLVTAEEFPRLCRWAKEYASDEKVRACLPDR AQMLAHFTANKEMFMAMAKSMLPK	RNASeq profile is not available	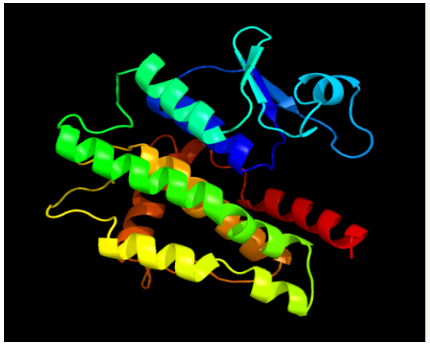 Model (left) based on template c4j2fA_ Top template information **PDB header:**lyase, transferase **Chain:** A: **PDB Molecule:**glutathione s-transferase; **PDBTitle:** crystal structure of a glutathione transferase family member from2 ricinus communis, target efi-501866 Confidence and coverage Confidence: 100.0% Coverage: 93% 214 residues (93% of your sequence) have been modelled with 100.0% confidence by the single highest scoring template. 3D viewing Interactive 3D view in JSmol For other options to view your downloaded

Traes_7BL_39451C0EC POPSEQ - 7B: 63.702 cM	MLRSGKAPGVGLLHAPFALLPMSFPKVYW EQALELAPLFNELVHRVSLDGDFLQQTLAR TKEVDPFTRRLLDIHSKMMELNKKEDIQLG LTRSDYMVDGATDKLLQVELNTISTSSNGL ACGVSELHRNLIRHHERELGLDPASVVGNT AITQHAEALATAWAEYNNQSAVVLVVVQ AEERYMYDQYWITVALREMYGVTTIRKTM AEIEAEGDLRPDGTLVINGRPVAVVYFRAG YSPADYPSEAEWRARLLIERSSAVKCPSIAH HLVGTKKIQQELAKEKVLERFLDNKSDIENV RKCFAGLWSLENDNIVNSAIKSPELFVLKP QREGGGNNIYGDNLRETLIRLRKDGSNEIA AYILMQRIFPPASPSYLVREGTFVRDNVVSE FGIFGAYLRNKDKVIINDQCGYLLRTKAASL NEGGVVAGYAFLNSIFLT	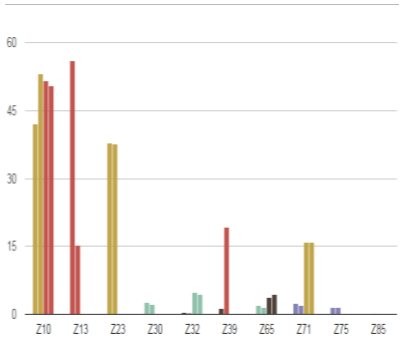	 Model (left) based on template c3kalB_ Top template information **PDB header:**ligase **Chain:** B: **PDB Molecule:**homoglutathione synthetase; **PDBTitle:** structure of homoglutathione synthetase from glycine max in2 closed conformation with homoglutathione, adp, a sulfate3 ion, and three magnesium ions bound Confidence and coverage Confidence: 100.0% Coverage: 98% 429 residues (98% of your sequence) have been modelled with 100.0% confidence by the single highest scoring template. 3D viewing Interactive 3D view in JSmol For other options to view your downloaded structure
TRAES3BF234900010CFD_g POPSEQ distance is not available	MLIVTEACAVDKVLEYAAGKGLPVVTVDGKRDG CVEFSELIAGEELPEAEEAGIHPDDVVALPYSSGT TGLPKGVMLTHRSLITSVAQQVDGENPNLYFSK EDVLLCLLPLFHIYSLNSVLLAGLRAGSAMVIMRK FDIGALVELVRAHGITIAPFVPPIVVEIAKSPQVTA GDLASIRMVMSGAAPMGKELQDAFMAKIPNA VLGQGYGMTEAGPVLAMCLAFAKEPFKVKSGS CGTVVRNAALKIVDPDTGASLGRNQPGEICIRGE QIMKGYLNDPESTKNTIDKDGWLHTGDIGLVDD DDEIFIVDRLKEIIKYKGFQVAPAELEALLITHPEIK DAAVVSLKDDLAGEVPVAFVMRIEGSEITEDDIK KFVAKEVVFYKRIHKVFFTDSIPKNPSGKILRKDLR ARLAAGIPS	RNASeq profile is not available	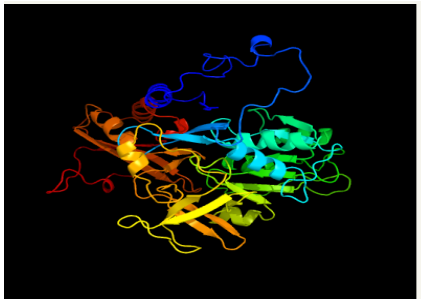 Model (left) based on template c5es8A_ Top template information **PDB header:**ligase **Chain:** A: **PDB Molecule:**linear gramicidin synthetase subunit a; **PDBTitle:** crystal structure of the initiation module of lgra in the thiolation2 state Confidence and coverage Confidence: 100.0% Coverage: 93% 387 residues (93% of your sequence) have been modelled with 100.0% confidence by the single highest scoring template. 3D viewing Interactive 3D view in JSmol For other options to view your downloaded structure offline see the FAQ
TRAES3BF078400030CFD_g POPSEQ distance is not available	MARTAATTTTAAAAALLLLALVATSAGADAVDA AAGGYEMTAAAAAGGRRGPAGLTQCMGGCG TRVTSCLLDCYNTSTGGTLPICFLGCTNNAVFCAT DCTTKGL	RNASeq profile is not available	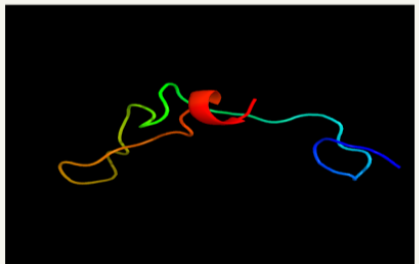 **PDB header:**lyase **Chain:** B: **PDB Molecule:**hydroxymethylglutaryl-coa lyase, mitochondrial; **PDBTitle:** crystal structure of human hmg-coa lyase: insights into2 catalysis and the molecular basis for3 hydroxymethylglutaric aciduria Confidence and coverage Confidence: 19.4% Coverage: 36% 38 residues (36% of your sequence) have been modelled with 19.4% confidence by the single highest scoring template. You may wish to submit your sequence to Phyrealarm. This will automatically scan your sequence every week for new potential templates as they appear in the Phyre2 library.

Traes_7DS_52F1E4F62 POPSEQ - 7D: 83.31cM	MVKYSRDPSNPTKSAKACGKDLRVHFKNTRETA FALRRMPLGKAKRYLEDVLAHKQAIPFRRYCRG VGRTAQVKNRQPNGQGRWPAKSAQFVLDLLK NAESNAEVKGLDVDNLYISHIQVNQAQKQRRRT YRAHGRINRKFSRVLY	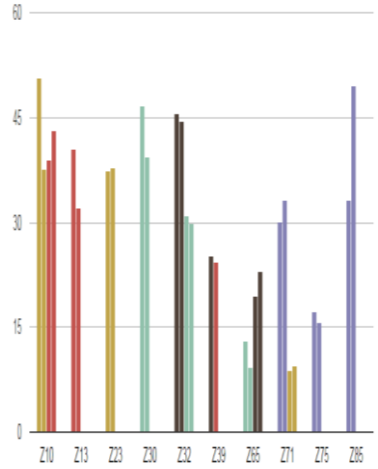	 Model (left) based on template c3jz5V_ Top template information **PDB header:**ribosome **Chain:** V: **PDB Molecule:**60s ribosomal protein l17 (l22p); **PDBTitle:** localization of the large subunit ribosomal proteins into a 5.5 a2 cryo-em map of triticum aestivum translating 80s ribosome Confidence and coverage Confidence: 100.0% Coverage: 100% 146 residues (100% of your sequence) have been modelled with 100.0% confidence by the single highest scoring template. 3D viewing Interactive 3D view in JSmol For other options to view your downloaded
Traes_7BL_54CCDE40A POPSEQ – 7B:51.193 cM	NIPHLRPTEYKKSRLSRNRRIVNRPYHGVLSGQA VRERIIHAFLVEEKKIVKKVLKIQKTKEKQLSG	RNASeq profile is not available	 Model (left) based on template c3zf7j_ Top template information **PDB header:**ribosome **Chain:** J: **PDB Molecule:**ribosomal protein; **PDBTitle:** high-resolution cryo-electron microscopy structure of the trypanosoma2 brucei ribosome Confidence and coverage Confidence: 100.0% Coverage: 93% 62 residues (93% of your sequence) have been modelled with 100.0% confidence by the single highest scoring template. 3D viewing Interactive 3D view in JSmol For other options to view your downloaded structure offline see the FAQ

Traes_4AS_2D88ED3F8 POPSEQ -4A:57.601 cM	MQLVRWHGTSVYTVVVLAKFVWHPAFSS SSGLGRTMAGGFRVLHLVRPFLGFLPEVQS ADRRIPFREKLIYTVISLFIFLVCSQLPLYGIHS TTGADPFYWLRAILASNRGTVMELGITPIV TSGMVMQLLVGSKIIEVDNSVREDRALLN GAQKLLGILIAIGEAVAYVLSGMYGSVSQL GTGNAILIILQLFFAGIIVICLDELLQKGYGLG SGISLFIATNICENIIWKAFSPTTINSGRGAE FEGAVIGLFHLLITRTDKVRALREAFYRQNL PNVTNLLATVLVFLIVIYFQGFRVVLPVRSR NARGQQGSYPIKLFYTSNMPIILHSALITNL YFISQLLYKKFSGNFLVNLLGIWKESEYSGH SIPVGGLAYYVTAPSSLADVVANPFHALFY VVFMLSACALFSKTWIEVSGSSARDVARQL KEQQMVMPGHRESNLERELNRYIPTAAAF GGVCIGALTVLADFMGAIGSGTGILLAVTII YQYFETFEKERATELGFFGF	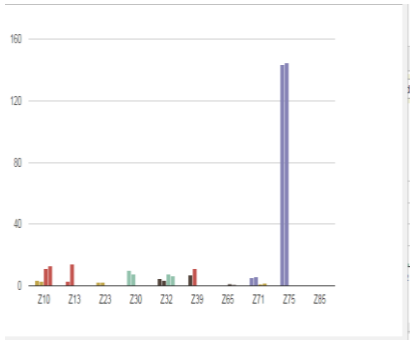	 Model (left) based on template c2wwbA_ Top template information **PDB header:**ribosome **Chain:** A: **PDB Molecule:**protein transport protein sec61 subunit alpha isoform 1; **PDBTitle:** cryo-em structure of the mammalian sec61 complex bound to the2 actively translating wheat germ 80s ribosome Confidence and coverage Confidence: 100.0% Coverage: 92% 471 residues (92% of your sequence) have been modelled with 100.0% confidence by the single highest scoring template. 3D viewing Interactive 3D view in JSmol For other options to view your downloaded
Traes_4DL_BE50C5130 POPSEQ is not available	MAGGFRVLHLVRPFLGFLPEVQSADRRIPF REKLIYTVISLFIFLVCSQLPLYGIHSTTGADP FYWLRAILASNRGTVMELGITPIVTSGMV MQLLVGSKIIEVDNSVREDRALLNGAQKLL GILIAIGEAVAYVLSGMYGSVSQLGTGNAIL IILQLFFAGIIVICLDELLQKGYGLGSGISLFIA TNICENIIWKAFSPTTINSGRGAEFEGAVIG LFHLLITRTDKVRALREAFYRQNLPNVTNLL ATVLVFLIVIYFQGFRVVLPVRSRNARGQQ GSYPIKLFYTSNMPIILHSALITNLYFISQLLY KKFSGNFLVNLLGIWKESEYSGHSIPVGGL AYYVTAPSSLADVVANPFHALFYVVFMLSA CALFSKTWIEVSGSSARDVARQLKEQQMV MPGHRESNLERELNRYIPTAAAFGGVCIGA LTVLADFMGAIGSGTGILLAVTIIYQYFETFE KERATELGFFGF	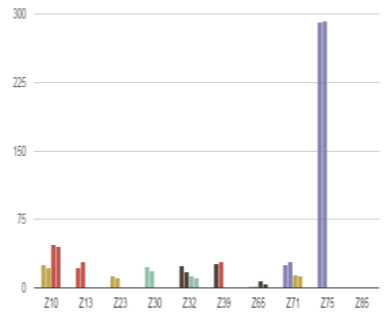	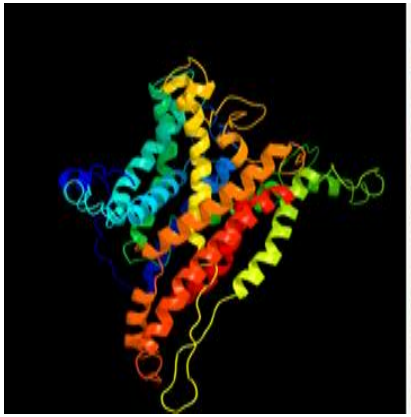 Model (left) based on template c2wwbA_ Top template information **PDB header:**ribosome **Chain:** A: **PDB Molecule:**protein transport protein sec61 subunit alpha isoform 1; **PDBTitle:** cryo-em structure of the mammalian sec61 complex bound to the2 actively translating wheat germ 80s ribosome Confidence and coverage Confidence: 100.0% Coverage: 97% 462 residues (97% of your sequence) have been modelled with 100.0% confidence by the single highest scoring template. 3D viewing Interactive 3D view in JSmol For other options to view your downloaded

Traes_7BL_6A2BED3EA POPSEQ - 7B:52.33 cM	PYFNIAQKVRPTVPGNQDASARRKTSKYFAPKTEKDAD VAEKSSSKRKLQKSSEDLEDDIKPFAANKALKDEEDDDD DFVVPSKKKTPVKPPPLKKLKAASNDDDQDERMDEDA ETPSKAAGRGRGRGRGGRGAGAAHGKTTSHDDDGGE DRMDEDAKTPSKAAGRGRGRGRGRVGRGGGTAHGK TTTGLDDDGEEDRMDEDDKTPSKAAGRGRGGRGAGA TPGGRGRGGGGRGFMNFGERKDPPHKGEKEVPEGAP DCLAGLTFVISGTLDSLEREEAADLIKRYGGRVTGSISKKT SYLLADEDIGGVKSNKAKDLGVPFLTEDGLFDMIRKSKP AKAPVNKHEGNSNSEKLQKSQTKSSPVKPERRAVDQV GTMGKSTPSKSNKESNSTNNQKVKVVDRGSLQWTEKY RPKVPNDIVGNQSMVKQLHDWLKSWENQFLHSGQK GKGKKQVDGGAKKAVLLSGPPGIGKTTTAKVVSQMLG LQAIEVNASDSRGKADSKIEKGVGGSTSNSIKELISNATL NYSDNRIKKPKAVLIMDEVDGMSAGDRGGVADLIASIK ISKIPIVCICNDRYSQKLKSLVNYCLLLNFRKPTKQQMGK RLMEIARKEGIQAQENAMEELAERVHGDIRMALNHLQ YMSLSQSVVKYDDIRLRLNSSSKDEDISPFTAVDKLFGFN GGRLRMDERIDLSMSDPDLVPLIIQENYINYRPSAVGKD DSGVKRMNYLARAAESIADGDIVNVQIRRYRQWQLSQ AACLASSIVPAALMHGNREVLEAGERNFNRFGGWLGK YSTTNKNKRLLEDVHSHILASQQANLDREALRLDYLTLLL RQLTDPLKTMPKEEAVQKVVEFMDTYSLSQEDFDTLVE LSKFKGHPNPMDGIQPAVKSALTKAYKQGSSSRVVRSA DLINIPGMKKTLKKRVAAILEPLDESLPEETGVASAEGDE EELSDAENDDELVPGDSKPKLDLQSDNKKGIQVQLNLK SNGNGSXXXXXXXXXXXXXXXXXEGRRRLRREAEE	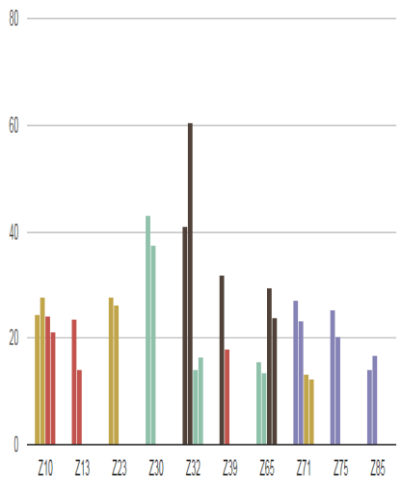	 **PDB header:**replication **Chain:** A: **PDB Molecule:**activator 1 95 kda subunit; **PDBTitle:** crystal structure of the eukaryotic clamp loader (replication factor2 c, rfc) bound to the dna sliding clamp (proliferating cell nuclear3 antigen, pcna) Confidence and coverage Confidence: 100.0% Coverage: 38% 388 residues (38% of your sequence) have been modelled with 100.0% confidence by the single highest scoring template. *Additional confident templates have been detected* (see Domain analysis) which cover other regions of your sequence. 451 residues (44%) could be modelled at >90% confidence using multiple-templates. You may wish to try resubmitting your sequence in "intensive" mode to model more of your sequence.
Traes_7DS_3F6DCEAA8 POPSEQ 7D: 76.49 cM	RAIRKHYADTYGEELLRSITDEISGDFERAVILWTL DPAERDAVLANETAKKWHPGNPVLVEIACARG SKQLFAARQAYHDRFKRSLEEDVAAHVTGDFRK LLVPLVSSHRYEGPEVNTRLAHSEAKLLHEKIEHK AYGDDEVIRILTTRSKAQLLATFNNYNDTFGHPIT KDLKADPKDEFLKTLRAVIRCFTCPDRYFEKVARL AIAGNGTDENSLTRVITTRAEVDLKLIKEAYQKRN SVPLEKAVAGDTSGDYESMLLALLGKE	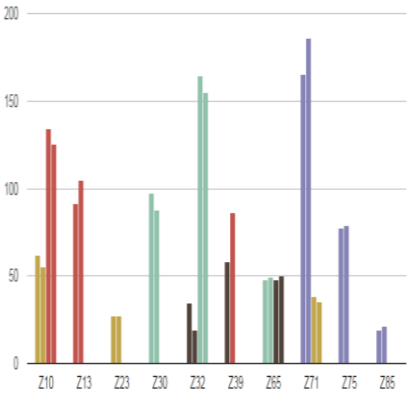	 Model (left) based on template c1avcA Top template information **PDB header:**calcium/phospholipid-binding protein **Chain:** A: **PDB Molecule:**annexin vi; **PDBTitle:** bovine annexin vi (calcium-bound) Confidence and coverage Confidence: 100.0% Coverage: 100% 267 residues (100% of your sequence) have been modelled with 100.0% confidence by the single highest scoring template. 3D viewing Interactive 3D view in JSmol For other options to view your downloaded structure offline see the FAQ

Traes_7DS_5A98193E8 POPSEQ -7D: 83.31 cM	MADDMERIFKRFDTNGDGKISLTELTDALRTLGS TSADEVQRMMAEIDTDGDGFIDFSEFISFCNAN PGLMKDVAKVF	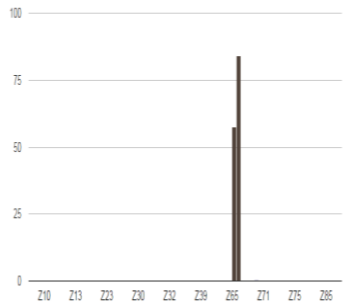	 Model (left) based on template d1k9ua_ Top template information **Fold:**EF Hand-like **Superfamily:**EF-hand **Family:**Polcalcin Confidence and coverage Confidence: 99.7% Coverage: 97% 76 residues (97% of your sequence) have been modelled with 99.7% confidence by the single highest scoring template. 3D viewing Interactive 3D view in JSmol For other options to view your downloaded structure offline see the FAQ
Traes_7BL_AABF91B01 POPSEQ 7B: 109.456 cM	ITPASLRRTLSRLGSHELGVEECRAMICRFD LDGDGKLSFDEFRVMMMA	RNASeq Profile is not available	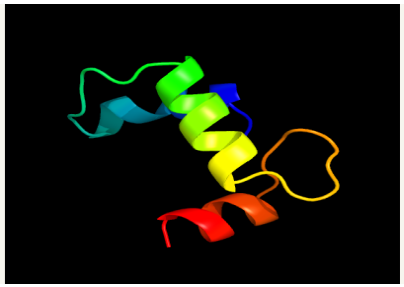 Model (left) based on template c3h4sE_ Top template information **PDB header:**motor protein/calcium binding protein **Chain:** E: **PDB Molecule:**kcbp interacting ca2+-binding protein; **PDBTitle:** structure of the complex of a mitotic kinesin with its2 calcium binding regulator Confidence and coverage Confidence: 99.2% Coverage: 98% 48 residues (98% of your sequence) have been modelled with 99.2% confidence by the single highest scoring template. 3D viewing Interactive 3D view in JSmol For other options to view your downloaded structure offline see the FAQ
Traes_1DS_0D10FE51D POPSEQ- 1D:18.2 cM	GMEYGVERARGDRDWKNALIGGIATGALVSAV SNNKGNKIAQDAITGGAIATAVEFINYLT	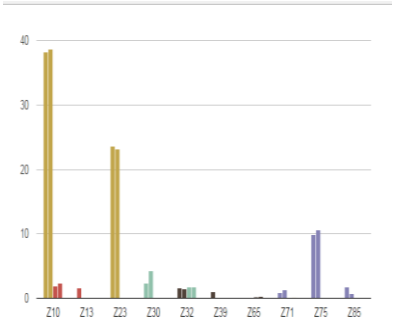	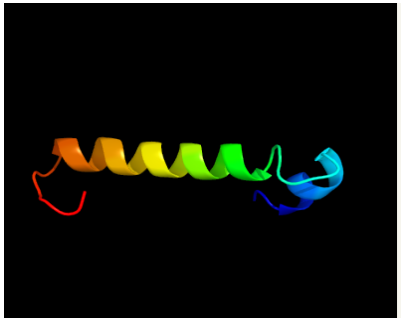 **PDB header:**structural genomics, unknown function **Chain:** B: **PDB Molecule:**hypothetical protein pf1176; **PDBTitle:** crystal structure of a singleton protein pf1176 from p. furiosus Confidence and coverage Confidence: 28.2% Coverage: 62% 38 residues (62% of your sequence) have been modelled with 28.2% confidence by the single highest scoring template. Phyre alarm You may wish to submit your sequence to Phyrealarm. This will automatically scan your sequence every week for new potential templates as they appear in the Phyre2 library.

Traes_7DS_80767C575 POPSEQ – 7D - 54.835 cM	YSVPFVSPPFFIPILHGLFFLQSIILWSCRHVTEAG LVALVNKCLELECINVGGMRVSPESFAGLQSISP ALRIRSIPQILNADVQVA	RNASeq Profile is not available	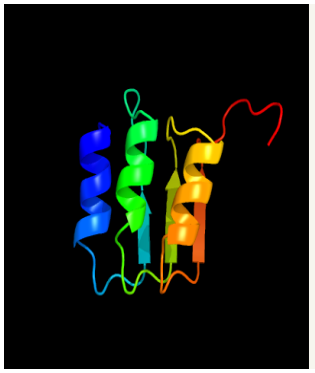 Model (left) based on template c3oglD_ Top template information **PDB header:**protein binding **Chain:** D: **PDB Molecule:**coronatine-insensitive protein 1; **PDBTitle:** structure of coi1-ask1 in complex with ja-isoleucine and the jaz12 degron Confidence and coverage Confidence: 99.7% Coverage: 91% 80 residues (91% of your sequence) have been modelled with 99.7% confidence by the single highest scoring template. 3D viewing Interactive 3D view in JSmol For other options to view your downloaded structure offline see the FAQ
Traes_7BL_A51BC9795 POPSEQ – 7B - 55.74 cM	MAPRPPSSLLLVGAALLLGLAAGAARASNE EGDALYALRMRLSDPNGVLQSWDPTLVN PCTWFHVTCDSASRVVRLDLGNSNVSGSI GPELSRLVNLQYLELYRNNLNGEIPKELGKL KNLISLDLYANKLTGRIPKSLSKLSSLRFMRL NNNKLAGSIPRELAKLSNLKVIDLSNNDLC GTIPVDGPFSSFPLRSFENNSRLNGPELQGL VSYDFGC	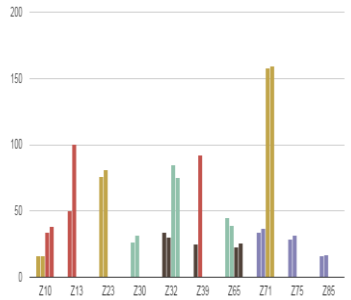 	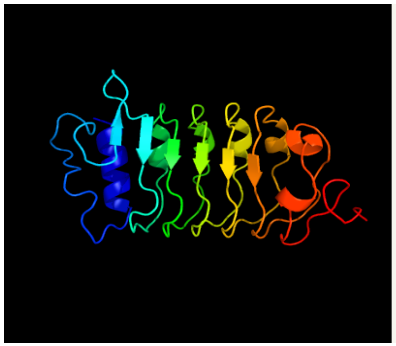 Model (left) based on template c4lscA_ Top template information **PDB header:**protein binding **Chain:** A: **PDB Molecule:**somatic embryogenesis receptor kinase 1; **PDBTitle:** isolated serk1 co-receptor ectodomain at high resolution Confidence and coverage Confidence: 100.0% Coverage: 85% 185 residues (85% of your sequence) have been modelled with 100.0% confidence by the single highest scoring template. 3D viewing Interactive 3D view in JSmol For other options to view your downloaded structure offline see the FAQ
TRAES3BF186700010CFD_g POPSEQ is not available	MSAAAGKPSRSASAIVASTVSGYHLLKVDGYSRT KGVPTGERIKSRPFTLGGHRWHIEYYPNGQKPE YAEYISVFLNLDASVATAVKAQQKFSFADEETNQ APSLISTVNSYSSQQGWGVATFIKRADLEKSEHL KDDSFTIRCDIIVIGDYRAEDLLEETPPAFVTVAPS DLHQHLGDLLNTEKGADVVFEEGDAAGVVHRD EMEAEVFKALLCFAYTDSLPVTEKEDEDVMYQH LLVAADRYNMERLKSICEEKLCKFINAATIATILTL AEQHHCEGLKKACLNFLRFPANLRALLDSDGFD HLSRSCPSVIKNLIAMSALV	RNASeq profile is not available	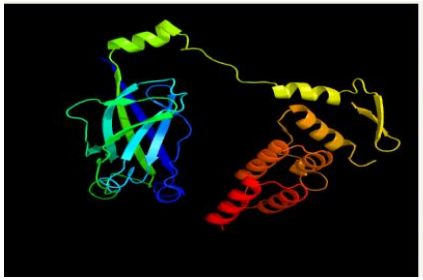 Model (left) based on template c3hu6B_ Top template information **PDB header:**protein binding, ligase **Chain:** B: **PDB Molecule:**speckle-type poz protein; **PDBTitle:** structures of spop-substrate complexes: insights into2 molecular architectures of btb-cul3 ubiquitin ligases:3 spopmathx/btb/3-box-pucsbc1 Confidence and coverage Confidence: 100.0% Coverage: 79% 258 residues (79% of your sequence) have been modelled with 100.0% confidence by the single highest scoring template. 3D viewing Interactive 3D view in JSmol For other options to view your downloaded

Traes_7DS_0A968BA86 POPSEQ is not available	MHGACLKGEYCEFSHDWSDQANNVCTFY QRGSCSYGNRCRYDHVKVSRNNPVPPLPS SSTATRNSPVRLPPSSSTATHVASTSPQLLS SGRPLHLGHQTNSSNQRQQISMDKLAVSE SKPAWRNEVQLDSVSEDGIGWSSIQTAQ NQTSMKLADMPICSFAAGGNCPYGEECP HMHGDLCAFCGKMCLHPYRPDERQEHIK LCEKNHKRLEALKRSQEIECSVCLDRVLSKP TAAERKFGLLSECDHPFCISCIRNWRGNSP TSGMDVNSALRACPICRKLSYYVIPSVLWY FSKEEKLEITENYKAKLKSIDCKYFDFGTGTC PFGTSCFYKHAYRDGRLEEVVLRHLDCDD GSTLIAKNIRVVRLPRPVASLGTCGCIYIELIR RHQFKSRHLGKLLLYLQFIGGCFVAKHTKKI RSSLPDTWMTL	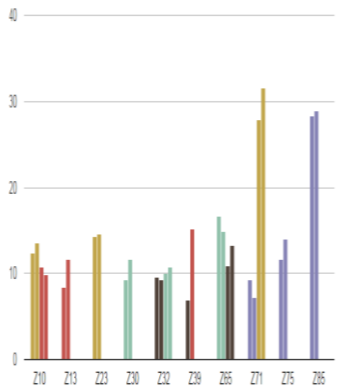	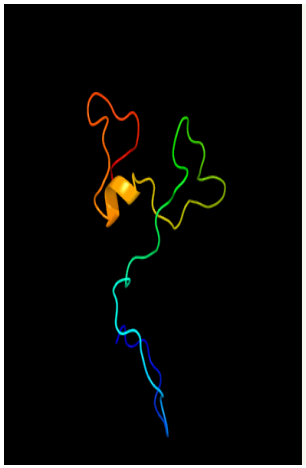 Model (left) based on template c3u9gA Top template information **PDB header:**antiviral protein **Chain:** A: **PDB Molecule:**zinc finger ccch-type antiviral protein 1; **PDBTitle:** crystal structure of the zinc finger antiviral protein Confidence and coverage Confidence: 99.1% Coverage: 15% 65 residues (15% of your sequence) have been modelled with 99.1% confidence by the single highest scoring template. *Additional confident templates have been detected* (see Domain analysis) which cover other regions of your sequence. 256 residues (60%) could be modelled at >90% confidence using multiple-templates. You may wish to try resubmitting your sequence in "intensive" mode to model more of your sequence. 3D viewing Interactive 3D view in JSmol
Traes_7DS_10C38526F1 POPSEQ – 7D:71.94cM	MQTPKLAILLALAMSAAMANLSQAQNSPQDYL SPHNAARAAVGVGAVTWSTKLQGFAQSYANQ RINDCKLQHSGGPYGENIFWGSAGADWKAAD AV	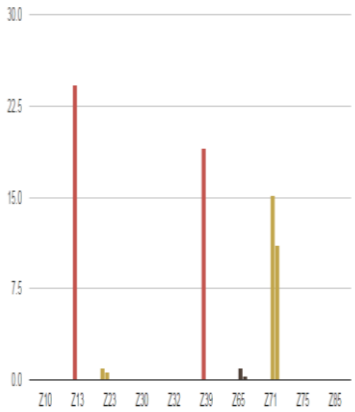	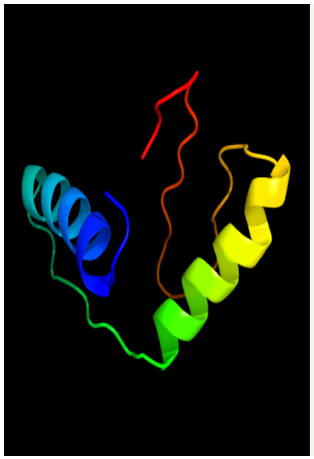 Model (left) based on template d1cfea Top template information **Fold:**PR-1-like **Superfamily:**PR-1-like **Family:**PR-1-like Confidence and coverage Confidence: 99.6% Coverage: 66% 63 residues (66% of your sequence) have been modelled with 99.6% confidence by the single highest scoring template. 3D viewing Interactive 3D view in JSmol For other options to view your downloaded structure offline see the FAQ

Traes_4AS_705FE3DAC POPSEQ - 4A:43.941 cM	MPLHQPISLGAWLYIKAHGSTSTAATPAPA KHQPSTSSALHSSFQFQPQSMAAMKITLL AVAAISALLLGTASAATYGVGEPGGSWTL NTDYSNWVSNKKFHPGDEIVFKYSTPAHD VVEVSKAGYDSCSTDGAINTLTSGNDVISL NATGTRYFICGVPSHCSPTAAASMKVTIEV VPGASSPSSPMPAAGPGATNPPPPSSTAT SVGAAAGFGLVALLAAGLMA	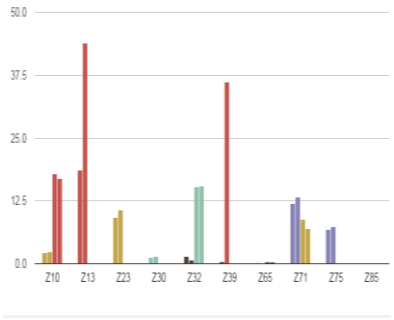	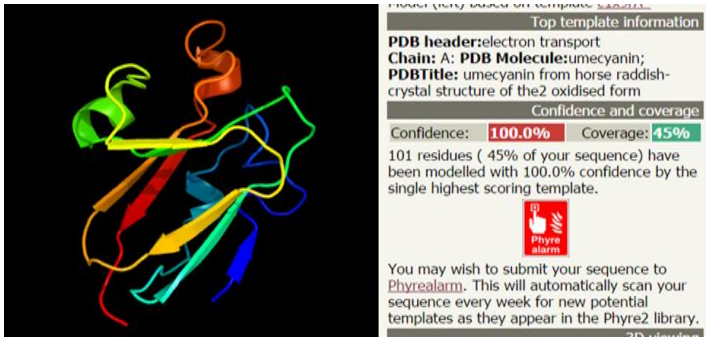
Traes_4DL_4448E934B POPSEQ – 4D:53.619 cM	MAAMKITLLAVAAISAVLLGTASAATYGVG EPGGSWTLNTDYSNWVSNKKFHPGDEIVF KYSTPAHNVVEVSKAGYDSCSTDSAINTLT SGNDVVAINATGTRYFICGIPGHCSPTAAA SMKVVIDVVPSSSSPSSPMPAAGPGASNL PPPSSTATSAGATAGFGLVVLLAASLMA	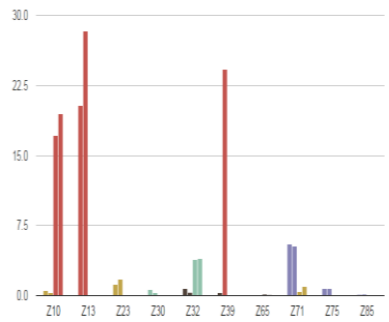	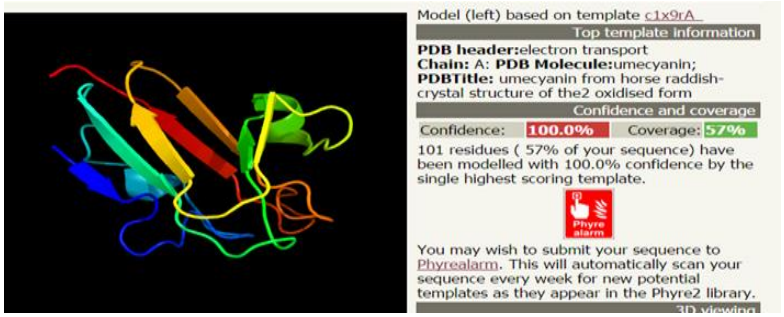
TRAES3BF086900030CFD_g POPSEQ distance is not available	MAARLAQLRTKAAQAAEFASKHGGAYYKEAME KNKQYVVQPPSVEKCQELSKQLFYTRLASLPGRY EALWKEVDGVKQLWKNRKELRVEDLGIATLFGV ELYAWFCIGEIAGRGFTLTGYKV	RNASeq profile is not available	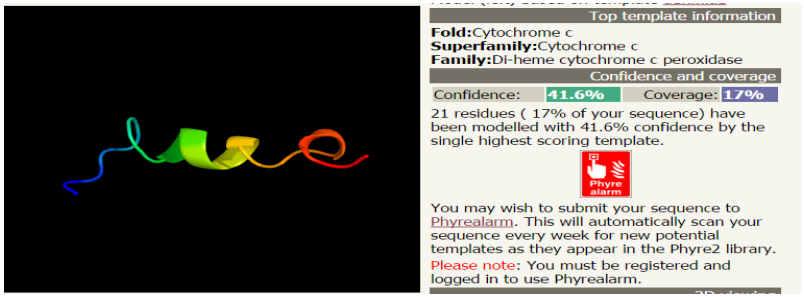

TRAES3BF086900030CFD_g POPSEQ distance is not available	MAARLAQLRTKAAQAAEFASKHGGAYYKEAME KNKQYVVQPPSVEKCQELSKQLFYTRLASLPGRY EALWKEVDGVKQLWKNRKELRVEDLGIATLFGV ELYAWFCIGEIAGRGFTLTGYKV	RNASeq profile is not available	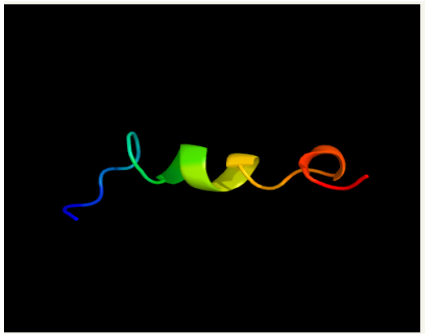 Top template information **Fold:**Cytochrome c **Superfamily:**Cytochrome c **Family:**Di-heme cytochrome c peroxidase Confidence and coverage Confidence: 41.6% Coverage: 17% 21 residues (17% of your sequence) have been modelled with 41.6% confidence by the single highest scoring template. Phyre alarm You may wish to submit your sequence to Phyrealarm. This will automatically scan your sequence every week for new potential templates as they appear in the Phyre2 library. Please note: You must be registered and logged in to use Phyrealarm.
TRAES3BF082100020CFD_g POPSEQ distance is not available	MATKLAALVVLVAFLAGPAACEGAFICFNGWLR LPIICPRGSGTPREPVPSTSGSGLSYGYYTTSCPSA ETIVTEAVRKAVVVDKNPGIGAGLIRLFFHDCFV RGCDASVLLNTTNSKNSDTEREGPPNKNSLRGF EVIYEAKTAIEAACKNTVSCADIVAFAARDASYFL SDGSINIPMPGGRYDGRESFASETDQLPGPFSN VPQLQASFAAKGLNPVEMVTLSGAHTIGRARC MFFSSRFSEMNQTYAASLMAECGDNGNTNVN QDYVTSNVLDKQYYQNVIDNKVLFTSDAVLNST EETRTEVMQNANTAGAWERKFEKAMEKMGKI KSDQQSVEIRKVCWKVNNNYK	RNASeq profile is not available	 Model (left) based on template d1bgpa_ Top template information **Fold:**Heme-dependent peroxidases **Superfamily:**Heme-dependent peroxidases **Family:**CCP-like Confidence and coverage Confidence: 100.0% Coverage: 84% 294 residues (84% of your sequence) have been modelled with 100.0% confidence by the single highest scoring template. 3D viewing Interactive 3D view in JSmol For other options to view your downloaded structure offline see the FAQ

4.5 Discussion

The literature to date has identified a broad range of genes in wheat that are modified in expression as result of RWA infestation (Botha et al., 2005; Boyko et al., 2006; Lacock et al., 2003; Liu et al., 2011; Smith & Boyko, 2007; Smith & Chuang, 2014; Smith et al., 2010). The genes identified by these studies are related to incompatible interactions between wheat and aphid. It includes genes belong to ROS, signalling, PR defence, synthesis of allelochemicals and the production of physical barriers. In this Chapter, this broad range of expressed proteins under the influence of RWA have been re-examined in light of major advances in wheat genome sequencing.

Advances in wheat sequencing have established high density molecular genetic maps (see Chapter 3), extensive data bases of survey sequence for all the chromosomes (NCBI, http://www.ncbi.nlm.nih.gov; wheat.pw.usda.gov/cgi-bin/graingenes) and RNA Seq based transcriptome data (wheat-urgi.versailles.inra.fr/seq-repository/Expression). The new knowledge at the wheat genome level has provided a valuable basis from which to investigate the QTLs associated with agronomic traits of interest (Feuillet et al., 2012). In Chapter 3 of this study, RWA resistance loci were identified in molecular marker maps based on wheat genome sequence information. The data in this chapter indicated that this approach is feasible for the mapped loci on chromosome 1DS, 7DS, 7BL, 3BL, 4AS and 4DL and thus contribute to identifying a core suite of genes for used in marker assisted selection in the development of RWA resistance cultivars.

Proteins expressed at significantly different levels in resistance and susceptible wheat plants were studied at the two leaf stage (Z10) to RWA infestation. Z10 stage was of particular interest since RWA infestation can occur as early as this stage in wheat development, as discussed in Chapter 2. The genes were annotated utilising Ensembl plants (Trticum aestivum), UniProtkb and Phyre 2. The gene models for proteins in wheat were identified as Traes numbers with Ensembl plants (*Triticum aestivum*). Due to the fragmented nature of the current wheat genome sequence

some gene models overlapped. Phyre2 software was used to validate the annotation provided in literature because the software includes potential 3D structure in its processes. In addition, RNA Seq information provided expression data at different wheat growth stages and different tissues (Zadoks) to help interpreting the data. The annotation processes allowed the following broad categories of gene identified: Hydolases, oxidoreductases, transferases, signalling proteins, membrane proteins, transcription, transport proteins, ligases, lyases, ribosome, replication, motor protein/calcium binding protein, protein binding, antiviral protein, PR protein, electron transport, and cytochrome C. The gene model and their function are given in Table 4.2.

Based on the broad category of biological compounds expressed by the cellular defence we have established a cell model to RWA resistance (Figure 4.1)

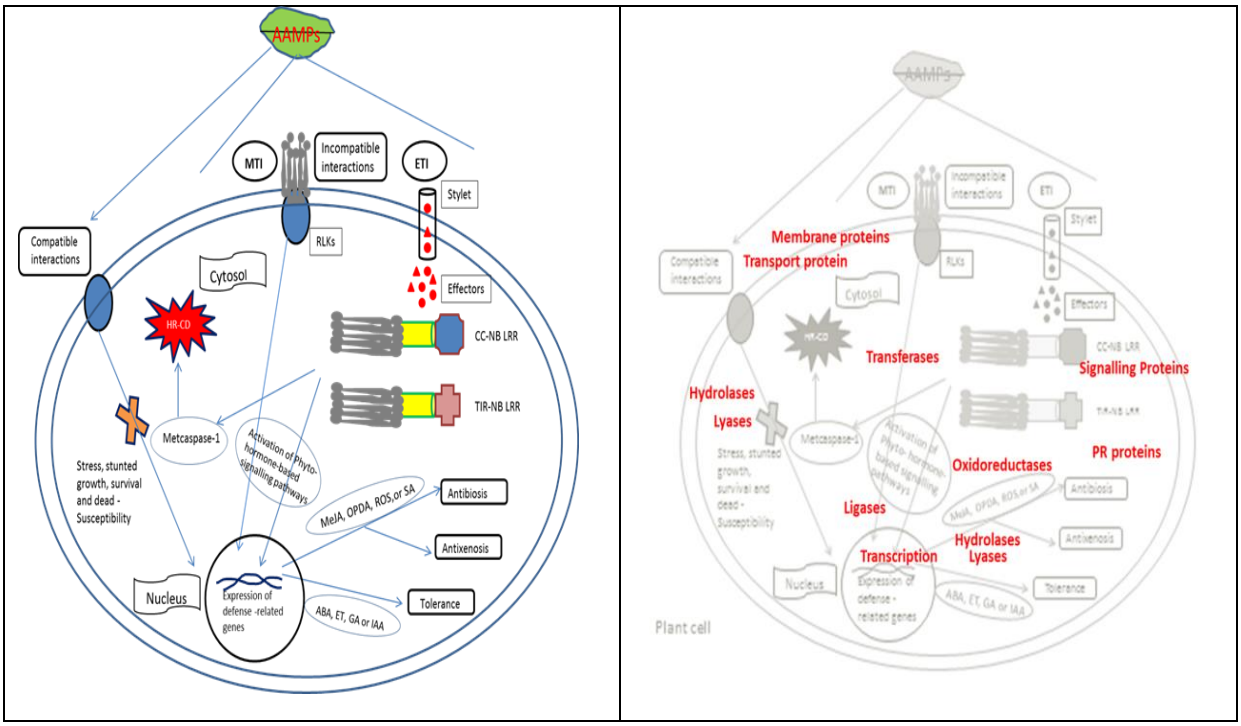

Figure 4.1: Classification of gene models in relation to RWA defence cell biology. The panel on the left is the overall gene network model described in Chapter 2. The panel on the right identifies the categories of genes annotated in this Chapter, in relation to the overall gene network.

Table 4.2: Grouping of possible classification of gene model

Major classification of proteins annotated	Chromosome 1DS	Chromosome 7DS	Chromosome 7BL	Chromosome 4AS	Chromosome 4DL	Chromosome 3B
Hydrolase	Traes_1DS_0DF78825D	Traes_7DS_0B170AFF9	None	Traes_4AS_85B580603	None	Traes_3B_9F3320C78
	Traes_1DS_CD25033C4	Traes_7DS_2F5418BA0				TRAES3BF128500020CFD_g
		Traes_7DS_A2F956FD8				TRAES3BF043600090CFD_g
		Traes_7DS_BCC35B081				TRAES3BF168400230CFD_g
Oxidoreductase	Traes_1DS_27349324C	Traes_7DS_28E2128F3	Traes_7BL_63C1B410D	Traes_4AS_20EAF4CEC	Traes_4DL_B75BA7E6C	TRAES3BF041000020CFD_g
		Traes_7DS_546D3927E	Traes_7BL_0367BBFE6		Traes_4DL_8DBE42AE9	TRAES3BF047400040CFD_g
Signalling protein	Traes_1DS_321E8C254	Traes_7DS_303EC152F	none	none	none	TRAES3BF050800220CFD_g
	Traes_1DS_9696ADD50	Traes_7DS_E1BFD91BA				
	Traes_1DS_BD30088EB					
	Traes_1DS_DBE2058BD					
Membrane protein	Traes_1DS_474BD1144	none	none	none	none	TRAES3BF040500030CFD_g
	Traes_1DS_A171C7D59					
Transcription	Traes_1DS_A6733B734	none	Traes_7BL_74071485F	Traes_4AS_A79A68739	Traes_4DL_D41CB81EA	TRAES3BF109900090CFD_g
				Traes_4AS_2BDA1260C	Traes_4DL_C083C804E	TRAES3BF117700060CFD_g
						TRAES3BF267200010CFD_g
						TRAES3BF001100080CFD_g
Transport protein	none	none	Traes_7BL_CA6B7C9E6	Traes_4AS_7258345F9	Traes_4DL_CFC191A06	TRAES3BF063600170CFD_g
					Traes_4DL_38FBC0AC7	TRAES3BF088300030CFD_g
					Traes_4DL_B81290546	TRAES3BF042900030CFD_g
						TRAES3BF111500010CFD_g
Transferase	Traes_1DS_A373E79EA	Traes_7DS_351943FD9	Traes_7BL_580CFC05F	None	Traes_4DL_1184F6F68	TRAES3BF089500140CFD_g
		Traes_7DS_5A68A26E9	Traes_7BL_660FFDCE2			TRAES3BF111600230CFD_g
		Traes_7DS_E373FDD65				TRAES3BF154700050CFD_g
		Traes_7DS_EC365BE37				TRAES3BF021800050CFD_g
		Traes_7DS_309E71F44				TRAES3BF038300120CFD_g
						TRAES3BF044100020CFD_g
						TRAES3BF061700020CFD_g
Ligase	none	none	Traes_7BL_39451C0EC	none	none	TRAES3BF234900010CFD_g
Lyase						TRAES3BF078400030CFD_g
Ribosome	none	Traes_7DS_52F1E4F62	Traes_7BL_54CCDE40A	Traes_4AS_2D88ED3F8	Traes_4DL_BE50C5130	none
Replication	none	none	Traes_7BL_6A2BED3EA	none	none	none
Motor protein/ calcium binding protein	none	Traes_7DS_3F6DCEAA8	Traes_7BL_AABF91B01	none	none	none
		Traes_7DS_5A98193E8				
Protein binding	Traes_1DS_0D10FE51D	Traes_7DS_80767C575	Traes_7BL_A51BC9795			TRAES3BF186700010CFD_g
Antiviral protein	none	Traes_7DS_0A968BA86	none	none	none	none
PR protein	none	Traes_7DS_10C38526F1	none	none	none	none
Electron transport	none	none	none	Traes_4AS_705FE3DAC	Traes_4DL_4448E934B1	none
cytochrome c	none	none	none	none	none	TRAES3BF086900030CFD_g
						TRAES3BF082100020CFD_g

Although several genes were identified on chromosomes 1DS, 7DS, 7BL, 3BL, 4AS and 4DL where RWA resistance loci were mapped in the DH population generated in this study, the rest of this Discussion focuses of those gene models that could be assigned to the regions of the chromosome where RWA resistance loci mapped. The following is based on the protein models assigned the RWA resistance loci regions.

4.5.1 Hydrolases

Hydrolases are enzymes that catalyse the hydrolysis of a chemical bond. Gene encoding for hydrolysing activity identified on chromosome 1DS, 7DS and 3B among the chromosome RWA resistance loci mapped. Major hydrolases identified in the mapped chromosomes were categorised into esterases, phosphatases, glucanases, glycoside hydrolases, peptidases and proteases. RWA resistance loci were mapped in the region of 12 to 24 cM (POPSEQ distance) on chromosome 1D, 74 to 84 cM on 7D and 55 to 75 cM on 7BL. The gene, Traes_7DS_A2F956FD8 encoding for hydrolase enzyme Endo-alpha-n-acetylgalactosaminidase is in the resistance loci region of 7DS (76.49 cM). The cell surface family of enzymes belong to the GH101 family of glycoside hydrolases. A major function of this enzyme degrades the glycoprotein by removing o-linked disaccharide Gal-β-1, 3-GalNAc-α for glycoproteins. Several biochemical compounds including hydrolytic enzymes (eg. cellulases, pectinases, glucose oxidases), structural proteins (eg. glycoproteins) and other components such volatiles found in the insect elicitors may cause detrimental effects on the host (Botha et al., 2005). Mohase and van der Westhuizen (2002) isolated and confirmed that lectin binding glycoprotein as a elicitors of RWA accumulated in the intercellular spaces of infested resistant 'TugelaDN' wheat plants. Transcript profile profiles shows the gene (Traes_7DS_A2F956FD8) expressed in leaf and root tissues at the early stages of wheat growth (Zadoks 10) where wheat seedling are more vulnerable to RWA infestation (See Chapter 2).

4.5.2 Oxidoreductases

Oxidoreductases are class of enzymes that catalyse oxidation and reduction reactions by transferring electrons from one molecule (the oxidant) to another (the reductant). Genes encoding for the oxidases and dehydrogenases are the two major groups among the chromosomes where RWA resistance loci mapped. Oxidases are the enzymes where oxygen acts an acceptor of hydrogen or electrons whereas dehydrogenases oxidize a substrate by transferring hydrogen to an acceptor that is either NAD+/NADP+ or a flavin enzyme. Among the oxidoreductases, a gene (Traes_7DS_28E2128F3) encoding for FMN-linked oxidoredutases on 7DS (75.353 cM) and a gene encoding for chloroplastic malate dehydrogenase on 7BL (51.193 cM) were mapped in the region of resistance loci. FMN-linked oxidoredutases are the enzymes which require flavin mononucleotide (FMN) for catalytic function. 12-Oxophytodienoate reductase (OPR) is a flavin mononucleotide (FMN) dependant oxidoredutase in plants. OPR involved in bio synthesis of jasmonic acid (JA) in plants. JA plays an important role in plant defence against RWA feeding in wheat plants (Gottwald et al., 2012). RNASeq profile of Traes_7DS_28E2128F3 shows the gene expressed in leaf and root tissues at the early wheat growth stages (Z10).

4.5.3 Transferases

Transferases are class of enzyme performing the transfer of specific functional groups (eg. acyl,methyl, glycosyl or aldehyde group) from one molecule (Donor) to another (acceptor). The following proteins were annotated to the chromosomes where RWA QTLs are mapped: a) Shikimate kinase, b) Sucrose 6-fructosyltransferase, c) Telomerase reverse transcriptase, d) DNA polymerase iii subunit psi, e) Adenylate kinase 2, f) LRR receptor like serine/threonine protein kinase, g) Glycero-3-phosphate (1) - acyltransferase and H) flavonoid 3-o-glucosyltransferase. However the enzymes shikimate kinase, telomerase transcriptase and DNA polymerase iii subunit psi were mapped in the RWA resistance loci on 7DS. The shikimate pathway is a biosynthetic pathway employed by prokaryotes such as bacteria and eukaryotes such as yeast,

fungi, protozoan parasite *Plasmodium falciparum* and plants to generate aromatic amino acids phenylalanine (Phe), tyrosine (Tyr), and tryptophan (Trp) (Herrmann & Weaver, 1999; Roberts et al., 1998) (Figure 4.2). Protein encoded for the genes involved in shikimate pathway possesses a chloroplast transit peptide (cTP) at their NH2 termini indicating the shikimate pathway takes place in plastids (Weaver & Herrmann, 1977). Secondary metabolites such as produced in the shikimate pathway play important roles in defence systems (Dixon & Pativa, 1995; Dixon & Steele, 1999). Pathogen infection (or effectors) and elicitors have been found to affect the expression of plant genes that involved in the pre or post chorismate pathways (Gorlach et al., 1995; Kanno et al., 2004; Keith et al., 1991; Tozawa et al., 2001). Studies by Keith et al. (1991) reported the expression of DHS2 which encodes 3-deoxy-D-arabino-heptulosonate (DAHP) synthase was induced by wounding or pathogen invasion in *Arabidosis thaliana*. Gorlach et al., (1995) also reported expression of genes encoding DAHP synthase, shikimate kinase (SK; 2.7.1.71), 5-enolpyruvylshikimate 3-phosphate (EPSP) synthase (EC 2.5.1.19), chorismate synthase (EC 4.6.1.4), and phenylalanine ammonia-lyase (EC 4.3.1.5) was induced in cultured tomato cells by elicitor treatment. The gene (Traes_7DS_351943FD9) encoding shikimate kinase mapped in the region of RWA resistance loci on the short arm of chromosome 7D at the POPSEQ distance of 77.626cM. The transcript profile of this gene shows the expression of the gene in leaf tissues and root tissues at the early wheat growth stages (Z10).

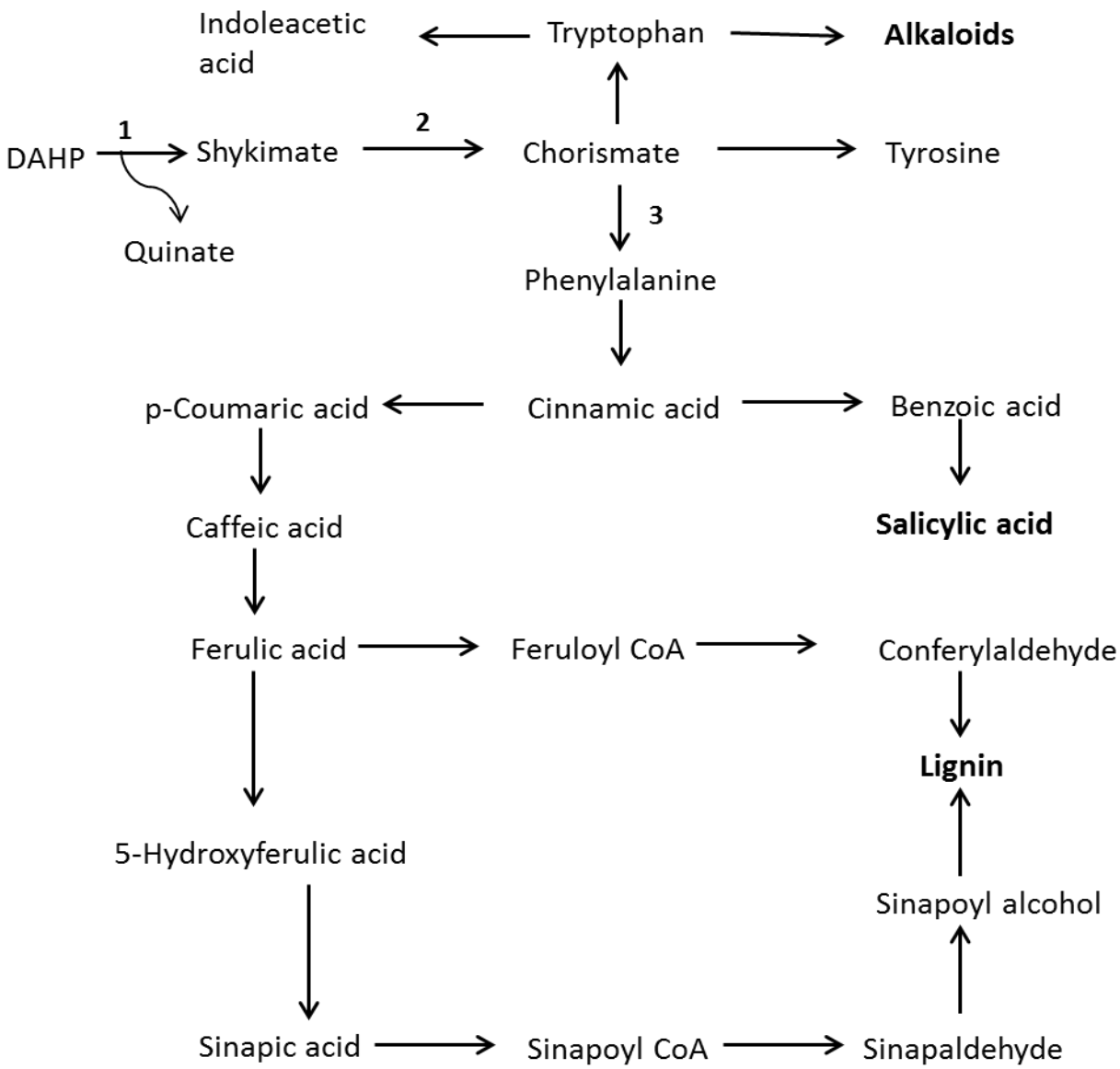

Figure 4.2: The shikimate pathway involving the biosynthesis of aromatic compounds, phenylalanine, alkaloids, sinapic acid, salicylic acid and lignin which play vital role against aphid attack. DAHP: 3-deoxy-D-arabino-heptulosonate. 1. Shikimate kinase; 2. Chorismate synthase; 3. Phenylalanine ammonia-lyase {Modified diagram of Mauch-Mani and Slusarenko (1996)}

Two other genes telomerase transcriptase (Traes_7DS_EC365BE37) and DNA polymerase iii subunit psi (Traes_7DS_309E71F44) mapped in the RWA resistance loci region of 7DS. Structure and integrity of telomeres which protects chromosomal

termini against fusion, degradation and other inappropriate reactions and promotes proper partitioning of chromosomes during mitosis and meiosis is essential for genome stability. Telomerase consists of a reverse transcriptase and an RNA template, which coding for the synthesis of the G-rich strand of telomere terminal repeats and does the maintenance of telomere. The telomerase transcriptase contains unique and variable N- and C- terminal extensions that flank a central RT-like domain. The gene (Traes_7DS_EC365BE37) encoding the telomerase transcriptase mapped in the region of RWA resistance loci on the short arm of chromosome 7D at the POPSEQ distance of 82.173 cM. Smith et al. (2010) reported 2 to 4 fold up regulation of shikimate kinase in *DnX* plants when infested with RWA compared to uninfested control plants. Transcript profile of this gene shows the expression of the genes in leaf and root tissues at the early wheat growth stages (Z10).

Enzyme DNA polymerases are essential for DNA replication. The gene (Traes_7DS_309E71F44) encoding for this protein mapped in the RWA resistance loci region at the POPSEQ distance of 83.31cM. Transcript profiles show the gene express only in the leaf tissues at the early wheat growth stages (Z10).

4.5.4 Transport protein

Traes_7BL_CA6B7C9E6 - divalent metal cation transporter mnth (upregulated in *Dn0* plants)

Cellular organisms require metal transporters to fulfil many essential functions ranging from metal absorption to metal sequestration and storage (Lyons & Eide, 2006). Metal ions includes Cu^{2+}, Zn^{2+}, Mn^{2+}, Fe^{2+}, Ni^{2+} and Co^{2+} are essential micronutrients for plant metabolism but when their present in excess and other non-essential metal ions such as Cd^{2+}, Hg^{2+}, Ag^{2+}, and Pb^{2+}, can become extremely toxic to many cellular functions (Callahan et al., 2006; Williams et al., 2000). Toxicity also resulted in binding of metal ions to sulfhydryl groups in proteins and thereby it inhibits the enzyme activity or protein function or by producing a deficiency by

inhibiting binding of other essentials ions into the transporter proteins (Meharg, 1994; van Assche & Clijsters, 1990). Transporter proteins protect the cells from the toxic effects by lowering the metal ion concentration in the cells. Toxicity effects may also be the results of disruption of cell transport processes and oxidative damage (Meharg, 1994). Roots of the plant are the prime site of the metal ions absorption and absorbed metal ions are then transported to cellular compartments (Guerinot & Salt, 2001). Cellular membranes are effective barriers that prevent movement of metal ions into the cells in order to control the metal ion concentration and prohibit unwanted metal ions from entering into the cytoplasm (Lyons & Eide, 2006). Transport proteins embedded in the cellular membranes facilitate the selective movement of inorganic ions across the barrier (Lyons & Eide, 2006). Cytoplasm consists of metal ion chelators such as soulble proteins, peptides (eg. glutathione) and organic metabolites (eg. citrate) which prevents the movement of the metal ion to the specific target within the cytoplasm by acting as competitive metal ion chelators. Soluble transport proteins (chaperones) found in the cytoplasm facilitate transfer of the metal ions to their specific targets. For example, free Cu (as Cu^{+} or Cu^{2+}) damage biomolecules by adventious binding or by producing radicals but copper chaperones, a specific soluble transport protein facilitate transfer of Cu from the plasma membrane to various copper containing proteins (Finney & O'Halloran, 2003).

A gene, Traes_7BL_CA6B7C9E6 encoding metal ion transport protein was mapped in the RWA resistance loci region of chromosome 7DS. The gene encoding transporter protein homology to the Natural Resistance Associated Macrophage Protein 1 (NRAMP1) was up regulated in infested *Dn0* plants (Smith et al., 2010). NRAMP genes have conserved function as metal transporters among all kingdoms and they are able to transfer several metal ions including iron, manganese and zinc (Thomine and Schroeder- www.ncbi.nlm.gov/books/NBK6452). Transcript expression profiles of Traes_7BL_CA6B7C9E6 shows that the gene is expressed in tissues of leaves and roots at the 2^{nd} wheat growth stage (Z10).

4.5.5 Isomerase: Cyclophilin (Traes_7BL_660FFDCE2)

Isomerases are a ubiquitous class of enzymes which convert a molecule from one isomer molecule to another. The peptidyl-prolyl-cis-trans isomerases (PPI-ases) and the protein dissulfide isomerase (PDI) are protein folding isomerases which catalyse folding of protein by isomerisation of peptide bonds or rearrangements of disulphide bonds (Aviezer et al., 1998). Cyclophilins are ubiquitous proteins found in almost all cellular compartments of prokaryotes and eukaryotes and encode unique functions (Wang & Heitman, 2005). PPIases belong to the cyclophilins and FK506 binding proteins (FKBPs) of monocot and docot plants and the members of the family resided in the cytosol, chloroplast, mitochondria, and endoplasmic reticulum are induced by various stresses such as high salt concentrations and salicylic acid (Marivet et al., 1992; Marivet et al., 1995; Vucich & Gasser, 1996). Cyclophilins were found to be expressed in young and reproductive tissues (Blecher et al., 1996; Gasser et al., 1990; Marivet et al., 1995).

A gene Traes_7BL_660FFDCE2, encoding cyclophilin protein was mapped in the region of RWA resistance loci on chromosome 7BL at the POPSEQ distance of 55.74 cM. Transcript expression profiles of Traes_7BL_660FFDCE2 shows that the gene is expressed in tissues of leaves and roots at the early wheat growth stages (Z10).

4.5.6 Ligase: Homoglutathione synthetase (Traes_7BL_39451C0EC)

Exposure of plants to biotic and abiotic stress diminishes the photosynthetic metabiolism and increases photorespiration, photoreduction of molecular oxygen (O2) and dissipation of excitation energy at photosystem II (Asada, 1999; Ort and Baker, 2002). As a protective measure, the changes in metabolism leads to increase formation of reactive oxygen species (ROS) such as superoxide anion (O_2), singlet O_2 and hydrogen peroxide (H_2O_2) (Asada 1999). The increased level of ROS causes oxidative stress to the plant and the stress is minimise by network of low molecular weight antioxidants, enzymes which keep ROS at reduced level and ROS scavenging enzymes (Karpinski et al., 1997; Asada, 1999). Low molecular weight thiol

glutathione is the key component of the antioxidant network (Ball et al., 2004). Glutathoine regulates the sulphur nutrition by storage and distribution of reduced sulphur within the plant and the precursor of phytochelatins which participates in the sequestration of heavy metals (Noctor, 1998) and it is also an essential component of the plant's defence system against environmental stress, Figure 4.3 (Rennenberg and Brunold, 1994). Glutathione may possibly be involved in activation of regulatory proteins NPR1 and protein phosphatase 2C (ABI2), as both play important roles in salicylic acid (SA) and abscisic acid (ABA) signalling (Meinhard et a., 2002, Mouet al., 2003). Glutathione is synthesised from its constituent amino acids, L-Glu, L-Cys and Gly in an ATP dependant two step pathway catalysed by the enzymes γ-glutamylcysteine synthetase and glutathione synthetase (Ball eta l., 2004; Noctor et al., 2002). A gene, Traes_7BL_39451C0EC was mapped in the RWA resistance loci region on chromosome 7BL at the POPSEC distance of 63.702cM. The transcript profile of this gene shows the expression in leaf and root tissues at the early wheat growth stages (Z10).

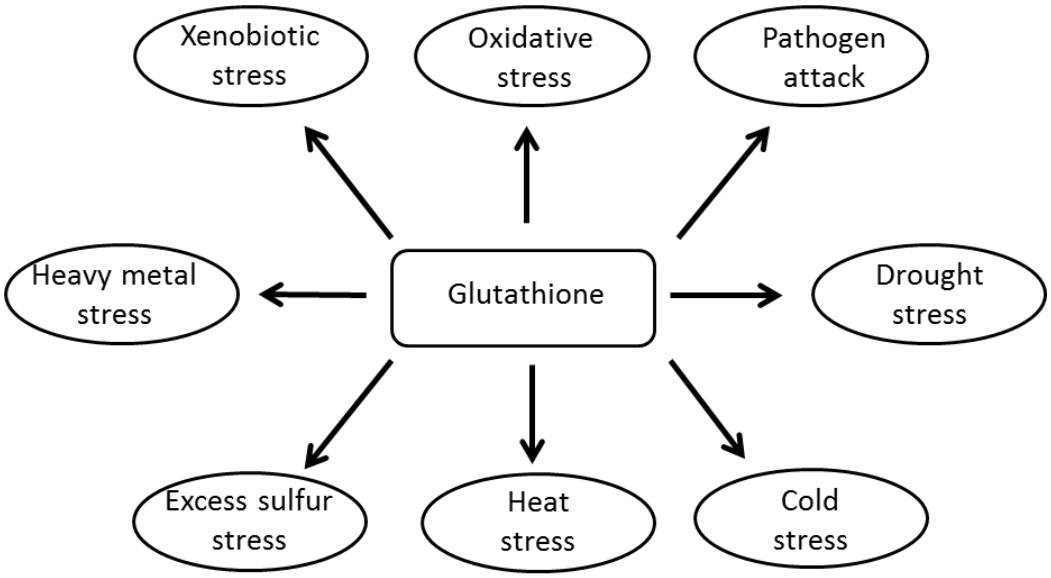

Figure 4.3 : Involvements of glutathione under different stress situations. This figure is taken from Rennenberg and Brunold, 1994

4.5.7 Protein binding: hypothetical protein (Traes_1DS_0D10FE51D)

This hypothetical protein was mapped on the short arm of chromosome 1D at the POPSEC distance of 18.2cM. The transcript profile show the uncharacterised protein expressed at the early wheat growth stage (Z10) of leaf and root tissues. The uncharacterised protein needs to be further investigated.

4.5.8 Pathogenesis related proteins (Traes_7DS_10C38526F1)

In the absence of acquired immunity, pathogenesis related proteins (PR) plays vital roles to protect the plants from biotic attack. PR proteins are the proteins encoded by the host plant to protect against various types of pathogens such as fungi, bacteria and viruses (Bowles, 1990). The PR genes encoded for the PR proteins may be expressed constitutively in various parts of the plants or may be induced by the biotic stress. PR- 2 (β-1-3 glucanase) and PR-3 (Chitinase) are well known PR proteins involved in antifungal activities. Increased inter and intra cellular β-1-3 glucanase activity was seen in resistant wheat cultivars containing the *Dn1* gene with RWA infestation (Van der Westhuizen et al., 1998a). However β-1-3 glucanase catalyse β-1-3 glucan and produce oligomers of 2-6 glucose units and therefore it causes direct detrimental effects to pathogens and possible indirect effects on releasing elicitors which induce defense genes (Van der Westhuizen et al., 1998a). The authors further reported that RWA infestation selectively induced chitinase activity in resistant cultivars, Tugela DN, Molopo DN and Betta DN (Van der Westhuizen et al., 1998b). During feeding, RWA probe through the apoplast where many defence related products such as β-1-3 glucanase, chitinase, peroxidases (Bowles, 1990) accumulate. This might be the possible site that elicits defence responses. A gene (Traes_7DS_10C38526F1) responsible for a PR protein was mapped in the RWA resistance loci region on chromosome 7DS at the POPSEQ distance of 71.94 cM. The transcript profile of the gene shows the expression in leaf and root tissues at the early stages of wheat growth (Z10).

4.5.9 Calcium binding protein

a. Annexin vi - Calcium/Phopholipid binding protein (Traes_7DS_3F6DCEAA8) (76.49cM)
b. Calcium binding pollen allergen Phl p7 (Traes_7DS_3F6DCEAA8)

The first line of defense to the RWA resistance is to recognise aphid landing and transfer the signal to the defense genes via signal transduction pathways. Calcium ions play important roles in the signal transduction and are involved in a wide variety of plant responses and processes (Hepler, 2005; Hetherington & Brownlee, 2004). At least 200 different targets of calcium exist in plant cells, among them the annexin family is an important calcium binding and calcium regulatory protein families (Clark eta l., 2012). The EF-hand motif, the c2 domain and the annexin domain are well characterised Ca^{2+} regulatory protein motifs in plants (Clark 2012). Plant annexins are abundant soluble proteins and are widely spread in the plant kingdom including wheat (Mortimer et al., 2008; Breton et al., 2000). They are capable of CA^{2+} dependant and Ca^{2+} independent binding of phospholipids of endomembrane and plasma membrane (Talukdar, 2009). Annexins are multifunctional lipid–binding proteins and they might cluster together at a membrane, bind membrane receptors, demarcrate membrane domains, regulate traffic, regulate the cytoskeleton or transport proteins or form a transport pathway themselves (Laohavist and Davies, 2010). A model illustrating potential functions of annexins in plants is shown in Figure 4.4.

A gene, Traes_7DS_3F6DCEAA8 encoding annexin motif and a gene, Traes_7DS_5A98193E8 encoding EF hand like motif (calcium binding pollen allergen Phl p7) were mapped in the region of RWA resistance loci on chromosome 7DS. Gene,Traes_7DS_3F6DCEAA8 was mapped at the POPSEQ distance of 76.49 cM and the transcript profile shows it was expressed in both leaf and root tissues at the 2nd wheat growth stage (Z10). The gene, Traes_7DS_5A98193E8 was mapped at the

POPSEQ distance of 83.31cM and the transcript profile shows its expression is only in the stem tissues at the Z66 stage.

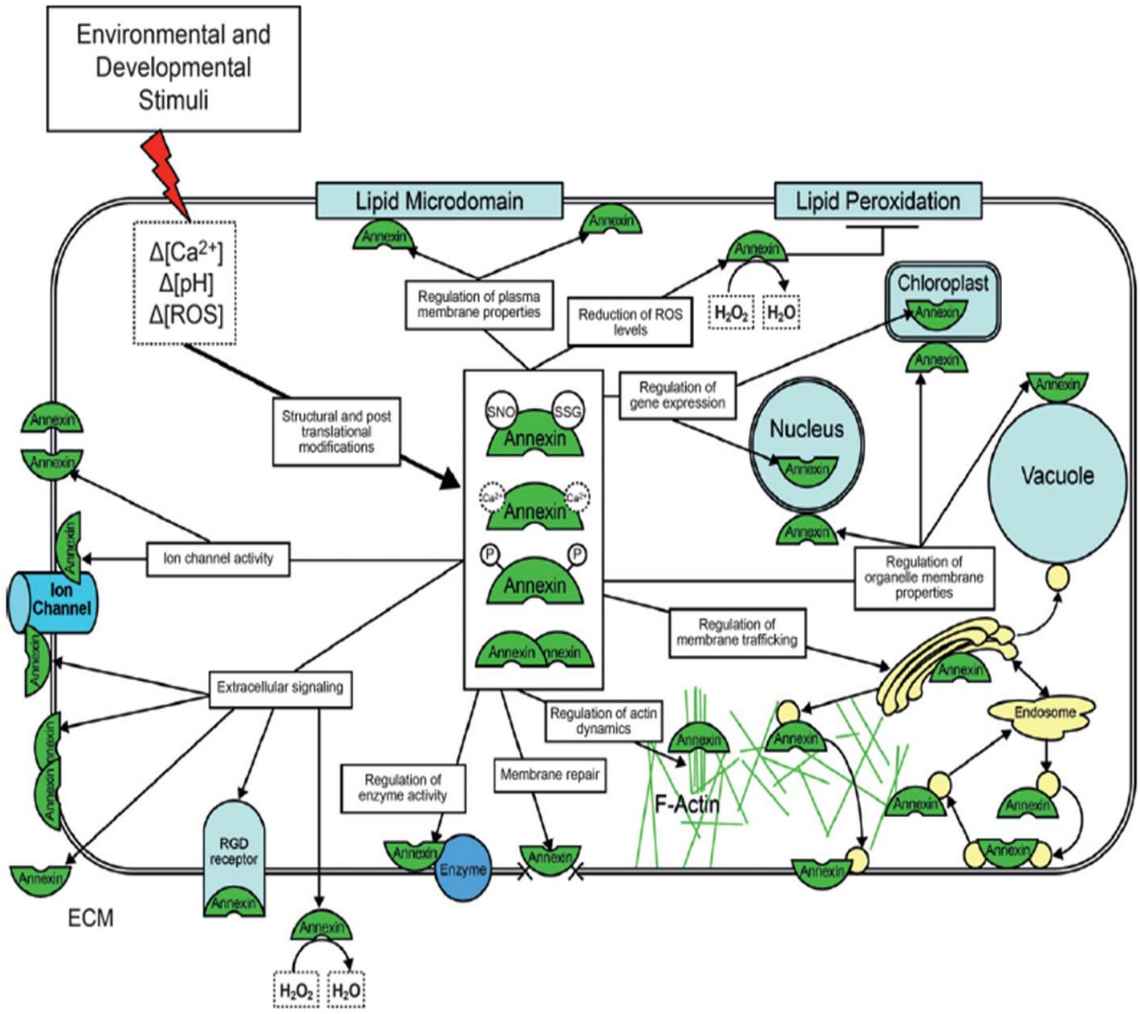

Figure 4.4: Model illustrating potential functions of annexins in plant cells. Development or environmental signals can induce changes in calcium, pH and reactive oxygen species (ROS) which can result in structural and / or post-translational modifications of plant annexins. Specific annexins may function differently and in different cellular locales such as the extracellular matrix (ECM) or in association with different membranes or organelles (Clark et al., 2012).

The transcriptome analysis able us to identify transcripts expressed in tissues from leaf, stem, root, spike and grain. In general, root and root structure of the plants improve assimilation and water uptake and therefore roots could help plants to

tolerate above ground herbivory (Erb et al., 2009). Riedell and Kieckhefer (1995) reported wheat plants infected with RWA, showed significant impacts on root growth. Ennahli et al. (2009) concluded in their study that root measurements in conjunction with measurement of leaf damage symptoms were necessary to identify promising *D. noxia* resistant genotypes. The findings from the above studies suggest that genetics of the root system must be taken into account within the context of the whole-of-plant phenotype and good resistance against RWA. The transcript profiles documenting the expression of genes in different parts of the plant, suggest new areas of study in order to achieve improved protection against RWA as discussed further in Chapter 6.

4.6 Conclusion

The availability of advanced wheat genome sequence data bases has made it possible to annotate the majority of differentially expressed genes directly to the wheat genome and thereby identify possible protein models for those genes. Their expression levels in relation to tissues were also possible using newly available transcript profiles.

These analyses can be put into the context of an overall RWA resistance model as outlined in chapter 6.

Chapter 5: Proteome based approach to characterise genome regions conferring Russian aphid resistance acquired from resistance source PI94365

Chapter contributor:

Proteomics International, Australia: Carrying out iTRAQ experiment and analysis

5.1 Abstract

Constitutive plant genes play a pivotal role in the defence against aphids. RWA is a phloem feeding insect and causes significant damage on wheat production through the injection of elicitors. The model considered for this Chapter is that a resistant plant defends itself by utilizing both induced and constitutive gene expression. In this study, we explored the concept of the constitutive genes involved in the resistance mechanism with an identified group of resistance and susceptible DH wheat lines. Extracted proteins from the leaves at the two leaf stage were separated with 2D gel electrophoresis and iTRAQ technology. We identified ten proteins that were significantly expressed at different levels in between the resistant and susceptible groups of DH lines. The wheat genes encoding to these proteins were identified and chromosomal positions of the some of the genes were identified. This work provides the basis to enhance the development of molecular markers and to understand the resistance mechanism in order to develop RWA resistance cultivars.

5.2 Introduction

Aphids are a major class of insects threatening crop cultivation by causing physical damage and removing nutrients from the plants. Plants protect themselves over the time by evolving new traits comprising direct and indirect defensive responses against aphids attack. Direct defences of the plants include structural barriers such as tissue toughness, glandular and non-glandular trichomes (Ni et al., 2001), and presence of alleochemicals such as alkaloids, terpenoides, lectins, cyanogenic

glycosides and digestive enzyme inhibitors (Agrawal, 2007; Smith et al., 2004). Indirect defences include excreted volatile compounds from the insect-damaged tissues that attract insect predators and parasitoids or repel ovipositions of insect.

Successful aphid resistance cultivars have been developed through plant breeding primarily utilising constitutively expressed defences during the past decades (Forslund et al., 2000). Architecture of the plant also mediates aphid acceptance/rejection. Aphid acceptance depends on ability of the aphid to probe the leaf surface, ability to penetrate through the cells to reach the phloem and the nutritional (taste) quality of the phloem sap (Fartek et al., 2012; Lazzari et al., 2009). The molecular compounds present in the ingested phloem sap may promote or inhibit aphid growth and development; and aphid survival and fecundity (Smith & Chuang, 2014).

Constitutive plant defensive traits are always expressed even in the absence of herbivore attack and many of such traits are also enhanced by herbivore attack (Agrawal, 2007). Aphid resistant cultivars of potato, sorghum, soybean and wheat exhibit over expression of large number of genes that are predicted to contribute to aphid resistance (Boyko et al., 2006; Park et al., 2006; Studham & MacIntosh, 2013; Zaayman et al., 2009). Transcriptome studies of these plants reveal that constitutively expressed R genes, pathogenesis related (PR), ROS, JA, SA, ET, ABA, GA signalling pathway genes, and genes involved in allelochemical and biophysical factors were differentially expressed.

Studies show that levels of allelochemical, and biophysical plant factors (eg. adhesive glandular trichomes) present in the plant correlated significantly with insect resistance and these factors are often governed by constitutive genes (Ciepiela & Sempruch, 1999; Forslund et al., 2000; Kazemi & van Emden, 1992; Ni et al., 2001). When tolerance mechanisms are always expressed regardless of aphid presence they

are regarded as being governed by constitutive genes, often polygenic traits (Smith & Chuang, 2014). Therefore increased photosynthetic rate, growth rate and stored root carbon that were observed in tolerant wheat plants were argued to allow the respective plants to be better able to withstand or recover from the aphid feeding damage (Burd & Elliott, 1996; Haile et al., 1999; Heng-Moss et al., 2003). Tolerance/resistance exists in wheat cultivars against RWA (Du Toit, 1989) and the tolerance mechanisms shown by the resistance plants often produces more biomass than a susceptible plant under similar conditions (Smith, 2005). Also genes involved in photosystem and chlorophyll genes were highly expressed in the canopy of RWA tolerant wheat (Boyko et al., 2006; Gutsche et al., 2009).

Therefore objectives of this study

(i) to identify proteins that are constitutively expressed in the resistance group and differentially expressed between resistance and susceptible double haploid wheat lines with 2D gel electrophoresis and with the iTRAQ experiment

(ii) to annotate differentially expressed proteins into the wheat genome with MIPS model analysis and identify their expression in wheat growth stages (Zadoks) with RNAseq database (Pingault et al., 2015) through Tritigate website (aestivum.accwi.org.au)

(iii) to consider the possible functions of the genes in response to RWA resistance

5.3 Materials and methods

5.3.1 Haplotype analysis

Major QTLs for the RWA resistance were mapped on short arms of chromosomes 1D and 7D and long arm of chromosome 7B as described in Chapter 3. Haplotype analysis of the DH lines was performed by assessing genotypes of the entire

population of doubled haploid lines derived from the PI94365 (RWA resistant) wheat line crossed to the susceptible Australian wheat cultivar EGA Gregory (Pelsart/2*Batavia doubled haploid line) at the chromosomal region of interest (see Chapter 3 for details).

5.3.2 Plant materials

Imbibition of seeds

Seeds (approximately 15 seeds) of resistant and susceptible haplotype lines were placed in a petri-dishes containing Whatman filter paper separately. Thin film of water was applied to wet the filter paper. Petri-dishes were wrapped with aluminium foil and kept at 4^0C for 72 hours in order to imbibe the seeds.
Pots (20 cm diameter round black nursery plastic pots) were filled with potting mix [40 liter Murdoch mix (2 parts of composed pine bark, 2 parts of course river sand and 1 part of coco peat); 20 g dolomite (Multi-Ag Nutrient supplies (Australia); 12 g Calcium carbonate (SIBELCO Australia); 40 g Growers blue (Forte Fertilisers Pty Ltd., Australia); 40 g Osmocote (Osmocote Pro,Low P, pH 8 to 9)]. Imbibed seeds of five were sown in each pot.

Sample collection

Leaf samples were collected at the two-leaf stage of growth when the 3rd leaf was beginning to unfurl [Zadoks Growth Stage 10 (Z 10)].

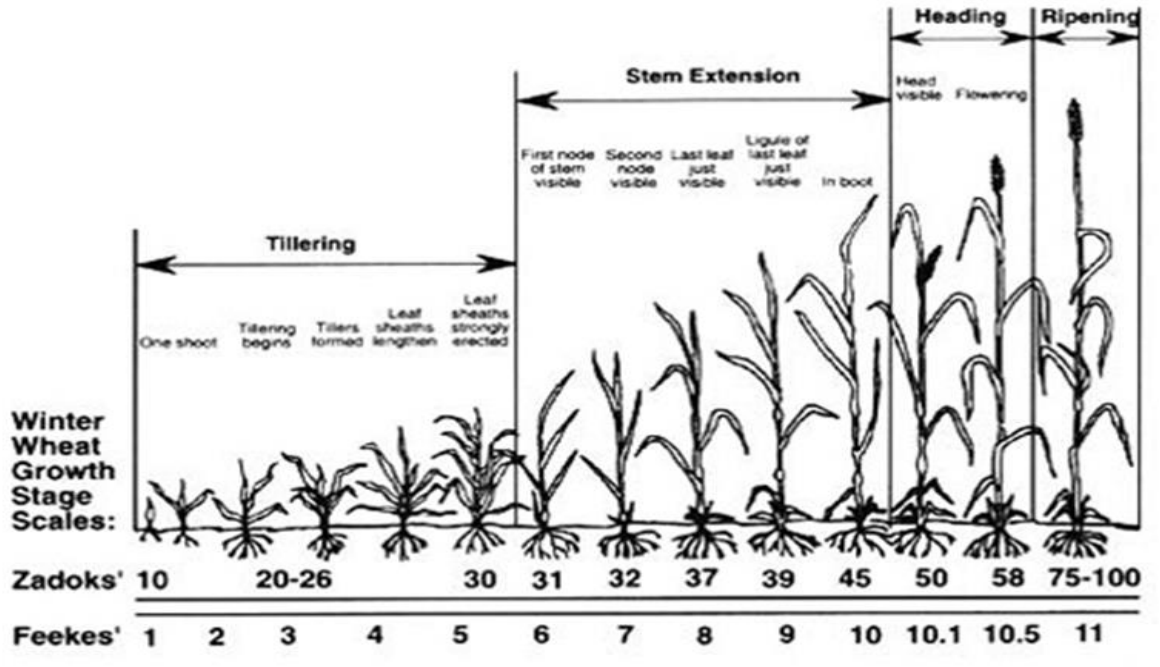

Figure 5.1: Zadoks growth stages of wheat (Zadoks et al., 1974)

Three biological triplicates were chosen (BR1, BR2 and BR3) as shown in figure from single leaf. Pooled tissues from the lines of each triplicate were placed in a 2ml Eppendorf tube, immediately frozen in liquid nitrogen and stored at --80^{0}C prior to protein extraction.

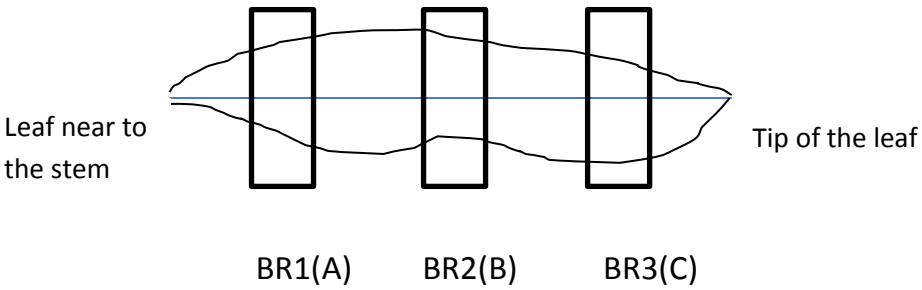

Figure 5.2: Schematic diagram showing location of the leaf tissues collected from each leaf for the protein extraction. BR1: Biological replicate 1; BR2: Biological replicate 2; BR3: Biological replicate 3

5.3.3 Extraction and quantification of protein from leaf tissues

Protein extraction was performed Trichloroacetic acid (TCA) precipitation described by Wang et al. (2008) with modification. Total of 300 mg of frozen leaf tissues from a replicate sample was taken in a pre-chilled clean mortar and pestle and ground with liquid nitrogen until the powder became to the finer the powder. The finer the powder was transferred into 50 ml falcon tube. A total volume of 20 ml of cold (-20^{o}C) extraction buffer (10% w/v TCA/acetone containing 0.07% beta mercaptoethanol (β-ME) was added to the powder. The powder was homogenised with the buffer by vortexing vigorously for 20 sec and the tube was incubated at -20^{0}C overnight to allow complete precipitation of proteins. This procedure was repeated for each replicates of resistant and susceptible groups. After the overnight incubation, the tubes were centrifuged at 5200 x g for 30 minutes at 40^{0}C. Supernatant was removed and acetone wash was performed three times by adding 5 ml of acetone (-20^{0}C) containing 0.07% β-ME, vortexing the tube briefly, centrifuging at 5200 x g for 15 minutes and removing the supernatant. After the 3rd wash, the supernatant was removed and then tube was centrifuged another 10 min and then the remaining removed supernatant using a pipette. The pellet was lyophilized for two hours. The lyophilized samples were stored at -80^{0}C till further use.

Solubilisation of proteins from the lyophilized pellet

To the pellet, 600µl lysis buffer (7M urea/2M Thiourea/4% CHAPS 3-[(3-cholamidopropyl) dimethylammonio]-1-propanesulfonate] and 65mM DTT (Dithiothreitol) was added. The tube were vortexed and incubated at +4^{0}C overnight in a shaker at 200 rpm. After overnight incubation, the tubes were centrifuged at 5200 x g for 5 minutes. The supernatant was transferred into a 1.5 ml Eppendorf tube and the tube was centrifuged at 16000 x g for 5 minutes. The supernatant were removed, aliquoted in to fresh 1.5 ml Eppendorf tubes and stored at -20^{0}C prior to isoelectric focussing (IEF).

Protein Quantitation using Bradford assay

The protein amount in the sample was quantified using the Bradford protein assay (Bradford, 1976) with bovine serum albumin (BSA) as a standard.

Preparing working Bradford solution from the stock solution:

Original stock solution (Bio-Rad Protein Assay Dye reagent concentration - cat# 500-0006) was diluted into 1: 4 dilutions with sterile water and the diluted solution was filtered through Whatman No. 1 filter paper.

Sample dilution:

Protein samples were diluted with lysis buffer (7M urea/2M Thiourea/4% CHAPS). Dilution of the samples was decided based on the colour intensity when Bradford solution was added into the protein solution. Dilution of the original protein sample was 1:10 in many cases and few cases were 1:20 dilution to fit the standard curve.

Preparation of standards by serial dilutions:

A series of BSA protein standards (1.48, 1.00, 0.68., 0.48, 0.36 and 0.2 mg/ml) were made by serial dilution with lysis buffer.

Preparation Standards, protein samples and blank for the quantitation of proteins:

60µl of sterile water and 5ml of Bradford solution were added to 40µl of diluted samples or standards in a 10 ml glass tube. For the bank solution, a glass tube with 60µl water, 40µl lysis buffer and 5 ml of Bradford solution was prepared.

Absorbance reading (Spectrophotometer) at 595 nm wavelength:

All the tubes were incubated at least 15 minutes, to ensure the reaction between protein and Bradford dye solution (Coomassive Brilliant Blue) reached plateau before taking the absorbance readings. Spectrophotometer measurements at 595 nm were normalised with ultra-pure water reading.

Calculation of protein amount of unknown samples:

Standard curve was created with known concentration of standards by plotting concentration on the x-axis and absorbance on the y-axis. The standard curve was used to determine the concentrations of unknown proteins when the r^2 (regression coefficient) value was above 0.990.

5.3.4 Separation of proteins

Proteins were separated by 2-Dimension (2-D) electrophoresis based on Bio-Rad protocols (www.bio-rad.com, Bulletin_6040). The first dimension of 2-D electrophoresis was isoelectric focussing (IEF) where proteins were separated by on the basis of their differences in their isoelectric point (pI) and the second dimension separation was by protein size using SDS-PAGE (Sodium dodecyl sulphate poly acrylamide gel electrophoresis). The proteins separated by first dimension IEF were run again on SDS-PAGE and further separated.

Protein separation by isoelectric focussing (First dimension)

Immobilised pH gradients (IPGs) strips (17cm, pH 3 -10, non-linear (NL) IPG ready strips from Bio-Rad laboratories Pty. Ltd) were used for IEF. Strips were stored at -20^0 C prior to use. IPG strips were rehydrated to original thickness before IEF running in order to achieve efficient absorption of proteins.

Rehydration of immobilised pH gradients (IPGs) strip with protein solution:

Strips were passively rehydrated with rehydration solution containing 1100 µg of proteins. Amount of protein equivalent to 1100 µg was taken in a 1.5 ml of Eppendorf tube. 65mM DTT, 6.6 µl IPG buffer [BIOLYTE 3-10 (Bio-Rad)] and 6.0 µl bromophenol blue (BP) were added to the samples and the final volume was adjusted to 330 µl with lysis buffer. The tube was vortexed and centrifuged for 20 seconds. The entire amount of solution was transferred along the furrow of focusing

tray. Plastic coating of the strip was carefully removed and the strip was placed by keeping gel side down and by maintaining the polarity (+/-). IPG strips were overlayed with 2ml of mineral oil to prevent evaporation and precipitation of urea during rehydration.

IEF running condition:

The following steps were followed for isoelectric focussing of the proteins

Step 1:	Passive run for 12 hours to rehydrate the strips		
Step 2:	1000 V	Rapid	1 hour
Step 3:	10,000 V	Linear	5 hour
Step 4:	10,000 V	Rapid	60000 Voltage hours (~6 hours)
Step 5:	500 V	Rapid	48 hours

Protein separation by size (Second dimension)

Preparation of IEF strips for the second dimension:

A two-step equilibration process was employed to prepare the proteins which are separated by IEF for the SDS-PAGE. Equilibration of the IPG strips was carried out in the equilibration tray. After the rehydration and IEF running, strip was washed with sterile water and equilibrated with equilibration buffer (50mM Tris-HCl (pH 8.8), 6M Urea, 65mM DTT, 30% (v/v) glycerol, 2% (w/v) SDS and 0.02% bromophenol blue) for 15 minutes on the shaker at 200rpm by keeping the gel side up. Similarly strip was washed with sterile water and equilibrated with 2nd equilibration buffer containing 50mM Tris-HCl (pH 8.8), 6M Urea, 135mM iodoacetamide, 30% (v/v) glycerol, 2% (w/v) SDS and 0.02% bromophenol blue).

SDS- Poly Acrylamide Gel Electrophoresis (SDS-PAGE):

12% resolving gel (40% Acrylamide/Bis solutions 31.5:1) was used to separate the proteins in the second dimension. Gel was electrophoresed at 2mA per gel for 2 hours followed by 5mA per gel for 2 hours and 10mA per gel for 15 hours.

Visualising gel image:

Gels were stained with freshly prepared staining solution for 30 minutes (One litre staining solution containing 1g of Coomassie (R) brilliant blue R250, 450 ml of ethanol, 100ml of acetic acid and 450 ml of sterile water). Gels were de-stained with de-staining solution by changing every 10, 20, 30 minutes and then 1 hour (One litre staining solution containing 250 ml of ethanol, 75 ml of acetic acid and 675 ml of sterile water). After staining and destaining the gels were scanned with a BIO-RAD GS-900™ Calibrated densitometer scanner with default setting for the Coomassive blue R (Protocol: Application- Coomassive blue R-250; Filter-Red; Mode- Transmissive; Prescan calibration- yes; Resolution-63.5µ; Gel selection- custom size; Scan area – 24.3 top, 2.8 bottom, 4.6 left, 25.8 right; Highlight saturated pixels – On; Colour- Coomassive). Gel images were analysed with software package PDQuest™ Version 7.4.0, BIO-RAD Laboratories.

5.3.5 isobaric Tags for Relative and Absolute Quantification (iTRAQ™)

Overview of iTRAQ experiment

To further identify and quantify proteins simultaneously, isobaric Tags for Relative and Absolute Quantification (iTRAQ) was carried out to the extracted proteins from biological replicates, BR1, BR2 and BR3 of resistant and susceptible haplotype groups and pool samples of BR1, BR2 and BR3 from resistant and a susceptible groups by the Proteomics International Pty. Ltd., a commercial company providing proteomics services following standard protocols. Briefly, protein samples of biological replicates were diafiltrated, reduced, alkylated and trypsin digested according to the

iTRAQ protocol (AB Sciex). After trypsin digestion and labelled with 8 isobaric tags, the analytical separation and identification of the mixture composed of eight samples were performed by Electrospray ionisation mass spectrometry (ESI-MS/MS).

Statistical analysis of proteome data derived from the iTRAQ experiment

Each of the 6 DH lines had protein expression measurements taken from a leaf divided into 3 equal areas. Each of the 3 leaf measurements were used as biological replicates in calculating a combined score across the 6 lines. Spectral data analysis against the UniProt Viridiplantae database (downloaded August 2015 - 3,353,453 sequences) for each replicate was carried out with the ProteinPilot™ 4.5 Software (AB Sciex). Unused Protscore cut off value of >1.3 was used as measure of the protein confidence (>95%) for a detected protein at the false discovery rate (FDR) of less than 0.1%.

Unused Protoscore was calculated by the software from the peptide confidence for peptides from spectra that had not already been completely used by higher scoring, top ranking, proteins. In addition to the protein-species detection confidence (Unused protoscore) cut off the overall false discovery rate (FDR) was automatically calculated by the Proteomics System Performance Evaluation Pipeline (PSPEP) feature in the ProteinPilot™ software using the reversed version of the protein sequences contained in the search database (reversed hits). The local FDR estimates the "local" error rate around a given identification, which indicates the likelihood that the specific identification is incorrect if FDR value is greater than 0.1%.

The program, ProteinPilot™ 4.5 Software (AB Sciex) calculates a probability value (*p*-value) for each protein reported to decide the changes in protein expression are real or not. A *p*-value of less than 0.05 while comparing biological replicates at FDR <0.1% was regarded as proteins expressed differentially at the significant level. Subsequent analysis with MIPS data base was performed to identify corresponding Traes ID (corresponding to wheat protein models) and chromosome positions for those proteins that had significant differential expression in between resistant and

susceptible groups. Only Traes ID that had all three biological replicates as significant was included for the final assessment comparing biological functionality with aphid damage.

5.4 Results

5.4.1 Haplotype analysis of DH lines

Resistance to RWA is acquired by a gene or group of genes that the progeny inherited from the resistant parent. Major chromosomal regions contributing RWA resistance have been mapped in the chapter 3. Therefore resistant DH lines differ in their genotypes at the QTL regions from the susceptible lines. Major QTLs for RWA resistance in the DH population were mapped on chromosome 1DS, 7DS and 7BL. Both resistance and susceptible haplotypes among the DH lines to the RWA resistance regions were identified by examining genotype data. Six haplotype DH lines for the resistance group (D1-010, D1-019, D1-049, D1-059, D2-091, D2-096) and for the susceptible group (D1-035, D2-107, D1-066, D1-070, D2-081, D1-073) were identified (Appendix-Supplementary Table III). These lines were further used to carry out the proteome study.

5.4.2 Separation of proteins

Extraction of protein from the leaf tissues

Protein extraction from three biological samples (BR1, BR2, and BR3) was carried out in three replications. On average, 15 to 20 mg per ml of protein was consistently obtained from 300mg of leaf tissue. Higher protein yield was achieved by grinding the leaf tissues to a fine powder (finer the powder higher the protein yield) and prolonged incubation (12 hours) of powder in TCA/Acetone extraction buffer at $^{-}20^{0}$C. Figure 5.3 shows a sample gel from resistant and susceptible group and remaining gels from all biological replicates are attached in the Appendix - Supplementary Figure II.

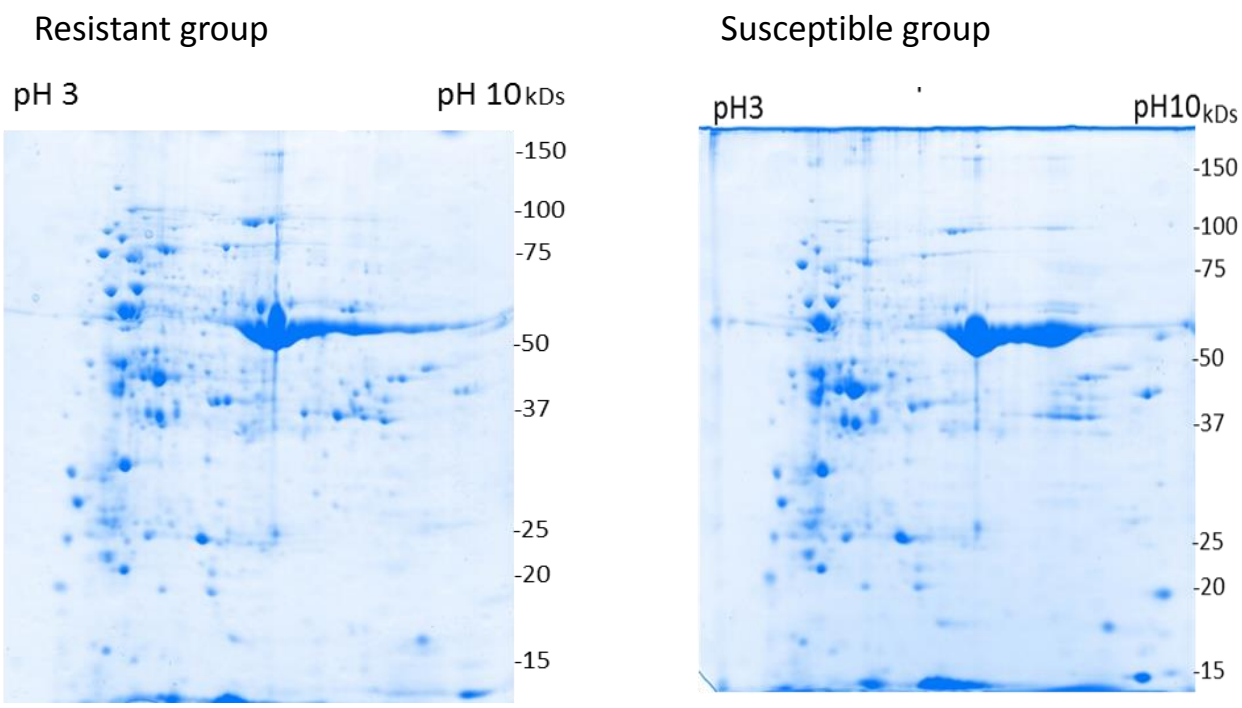

Figure 5.3: 2DE separation of proteins from leaf tissues: Iso-electric focalisation was performed with 1100 µg of proteins using 3-10 pH non linear (NL) IPG strips and 12% poly acrylamide was used for the second dimension. Gels were scanned after staining with Coomassie (R) brilliant blue R250 staining solution

2D gel images were analysed with PDQuest software. Presence /absence variation with protein spots could not be detected in between resistant and susceptible groups. Presence / absence variation of such proteins between two related samples is rarely the case, but more likely that they vary in abundance to different degrees (Fuller & Morris, 2012). Absolute or relative quantification of protein spots between two gels with PDQuest software was not found to be significant.

Isobaric Tags for Relative and Absolute Quantification (iTRAQ^{TM}) have been widely used in health and agricultural research to both identify and quantify differences between total proteins preparations (Fu et al., 2016; Liu et al., 2015; Wiese et al., 2007). Therefore the iTRAQ^{TM} experiment was performed to determine quantitative difference in level of protein expression.

isobaric Tags for Relative and Absolute Quantification (iTRAQ^{TM})

An eight-plex iTRAQ^{TM} experiment was performed with biological replicates of resistant and susceptible groups. 18,888 spectra were detected and a total number of 650 unique proteins were identified. Based on the criteria described in statistical analysis section of 5.3.5 (*p*-value <0.05, Unused protscore >1.3 and FDR <0.1%), 409 proteins were significantly different in their expression between resistant and susceptible group. Traes ID numbers for the unique peptide sequences were retrieved through EnsemblPlants-Tritcum aestivum (plants.ensembl.org/Triticum_aestivum) (Appendix - Supplementary Table IV). Following the MIPS gene model translation, genes that were located in the RWA resistance chromosome regions were searched for. RWA resistance genes in this DH population were mapped on chromosome 1DS, 7DS, 7BL, 3BL, 4AS and 4DL (see Chapter 3). The major QTLs for the SA biotype 1, 2 and 3; Turkey Izmir biotype and Moroccan biotype were in the 1DS, 7DS and 7BL. With respect to significant difference in their expression at least in one of the replicates, 17 proteins from 7DS, 9 from 1DS, 5 from 7BL, 12 from 4A and 33 from 4D were identified (Appendix Supplementary table IV). Based on the consistency with the expression of protein within 3 replicates (BR R1/BR S1; BR R2/BR S2; BR R3/ BR S3), 10 proteins (3 from 1DS; 2 from 7DS; 1 from 4AS; 4 from 4DL) were differentially expressed at the significant level between resistant and susceptible groups, although not located in the major RWA resistance loci. None of the proteins was identified on 7BL. Protein models and predicted functions for those proteins were investigated with Phyre 2 (Protein Homology/Analogy Recognition Engine) annotation (see Chapter 4). Protein expression via the transcriptome [(Pingault et al., 2015); RNAseq] at different growth stages of wheat (Zadoks growth stages) was identified via Tritigate website (aestivum.accwi.org.au, J Nystrom-Persson, Gabriel Keeble-Gagnere, R. Appels manuscript in preparation) (Table 5.1).

Table 5.1: The description of identified protein that were differentially expressed at the significant level between resistant and susceptible groups

Trace ID	Amino acid sequence	Phyre 2 annotation	Expression of protein of Chinese spring at the Zadoks growth stages (Pingault et al., 2015) - aestivum.accwi.org.au	Basic protein structure via Phyre[2] annotation (Kelley et al., 2015)
Traes_1DS_947F6918F Scaffold: IWGSC2:IWGSC_CSS_1DS_scaff_1899380:2770:6754:-1 POPSEQ distance: 49.47cM	MAMASLARRRAAEAVLLRRPHAAAWASAC RGYAASGEESDVVVIGGGPGGDVAAIKAAQ LGLKTTCIEKRGALGGTCLNVGCIPSKALLHSS HMYHEAKSSFAHHGVKFSNLEVDLPAMMA QKDKAVSGLTKGIEGLFKKNKVEYVKGFGKL VSPSEVSVDLVDGGSTIVKGKNIIVATGSDVK SLPGVTIDEKKIVSSTGALALTEIPKKLVVIGAG YIGLEMGSVWNRLGSEVTVVEFAPDIVPSM DGEIRKQFQRMLEKQKFKFMLKTKVVGVDT SGSGVKLTVEPAAGGEQTVIEADVVLVSAGR VPYTAGIGLDAIGVETDKGGRVLVDNRFMT NVKGVYAIGDAIPGPMLAHKAEEDGVACVE FIAGKEGHVDYDTVPGVVYTHPEVASVGKTE EQVKASGVAYQVGKFPLLANSRAKAIDDAEG MVKVISEKETDRILGVHIMSPGAGEIIHEAVL ALQYGASSEDIARTCHAHPTVSEALKEACMN TYDKAIHM	PDB: Oxidoreductase PDB Molecule: Dihydrolipoamide dehydrogenase PDB Title: Dihydrolipoamide dehydrogenase of glycine decarboxylase 2 from *Pisum sativum*	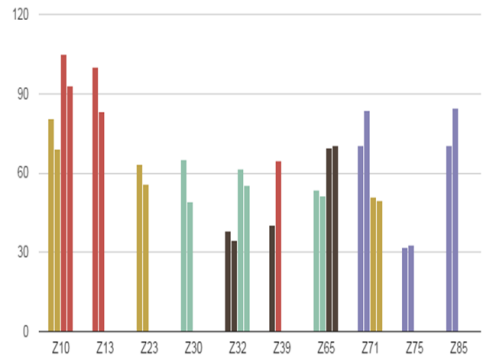	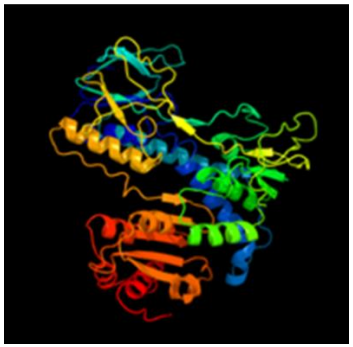
Traes_1DS_D46002062 Scaffold: IWGSC2:IWGSC_CSS_1DS_scaff_1886609:4016:9665:1 POPSEQ distance: Unknown	MHSVSISASASASAIASGGARSKAAAGRRPG EIRFCGLRGDALACASLRASHAAAATRRAVLR AAASANGAAGSGDGFDYDLVIIGAGVGGHG AALHAVEEGLKTAIIEGDVVGGTCVNRGCVP SKALLAVSGRMRELHDEHHMKSLGLQVSST GYDRQAVADHANNLASKIRSNLTNSMKAM GVDILTGFGKIVGKQKVRYGKVGFPEKEITAK NIIIATGSVPFVPKGIEIDGKTVFTSDHALKLES VPDWIAIVGSGYIGLEFSDVYTALGSEVTFVE ALDQLMPGFDPEIAKLAQRVLINTRKIDYHTG VFASKITPAKDGKPVLIELIDAKTKEHKETLEV DAALIATGRAPFTSGLGLENINVVTQRGFIPV DERMQVTDADGNVVPNLFCIGDANGKLML AHAASAQGISVVEQISGRDHILNHLSIPAACF THPEISMVGLTEPQAREKADNEGFEVSVVKT SFKANTKALAENEGDGIAKMIYRPDTGEILGV HILGLHAADLIHEASNAIALGTRLQELKLAVH AHPTLSEVLDELFKAAKLQPKDGQEREPNHP PQPLLKVLSFITSLLSSPQRDRQP	PDB header: Oxidoreductase PDB Molecule: Thioredoxin glutathione reductase PDB Title: structure of schistosoma mansoni thioredoxin-glutathione 2 reductase (smtgr)	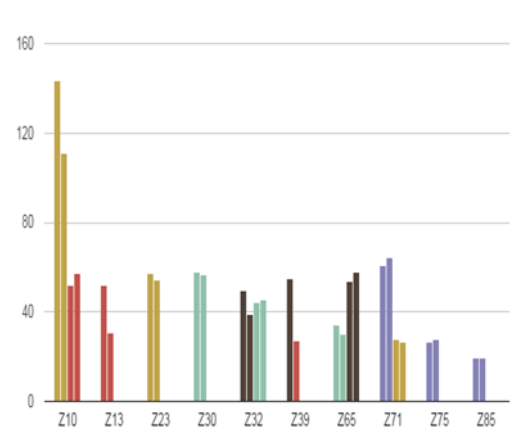	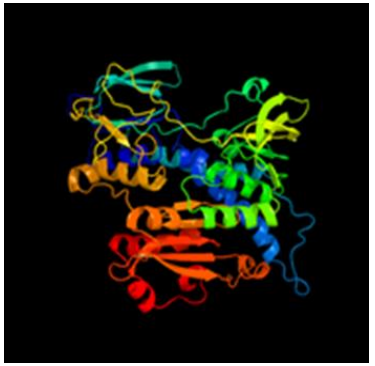

Traes_1DS_ACF9E82D8 Scaffold: IWGSC2:1D:65046590:65050492:1 POPSEQ distance: 1D:47.67cM	MADAKQQQAAAPTGVWKTIKPFVNGGASGMLATCVIQPIDMIKVKIQLGEGSAAQVAKTMYANEGLGSFYKGLSAGLLRQATYTTARLGSFRVLTNKAIEANDGKPLPLVQKAFIGLTAGAIGACVGSPADLALIRMQADSTLPAAQRRHYKNAFHALYRITADEGVLALWKGAGPTVVRAMSLNMGMLASYDQSVELFRDKLGAGEYQTVIGASAISGFCAAACSLPFDYVKTQIQKMQPDATGKYPYTGSLDCAMQTLKTGGPFKFYSGFPVYCVRIAPHVMMTWLFLNQIQKYQKKIGI	PDB header: Transport protein PDB molecule: ADP, ATP carrier protein3 PDB Title: Structure of yeast mitochondrial ADP/ATP carrier isoform 32 inhibited by carboxyactyloside (p21 crystal form)	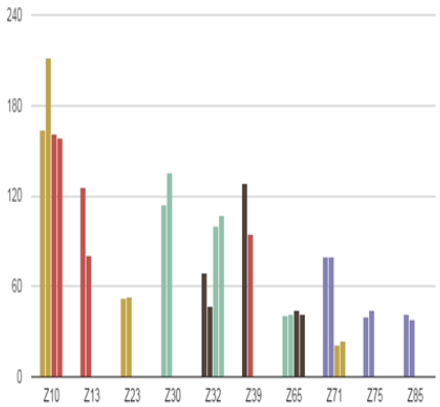	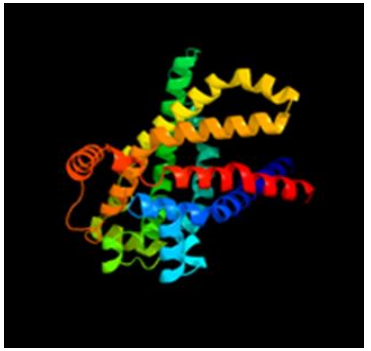
Traes_7DS_FDC2AB87A Scaffold: IWGSC2:IWGSC_CSS_7DS_scaff_3949110:1:3423:1 POPSEQ distance: 7D:19.33cM	LASVAGAALALPFRLGTGLFVLGYSVSLVSADKIPSDQYSLEFLGLKVKETSKIDQCRRPEKPIEIYEFEGCPFCRKVREMVSVLDLDVLFYPCPQKGPTFRPKVLEMGGKKQFPYMVDPNTGVAMYESDAIIKYLADTYGDGTVPIMLSLGLFTTITAGLAMIWRVWKGSSYTVSKLPPQPIEIWAYEGSPFCKIAREALVELELPHLLHSCARGSPKRQEIFKKHGLFQAPYIEDPNTGVKMFESAEIVEYLRATYTLYPQYQNL	PDB header: Transferase PDB molecule: Thioldependent reductase 1 PDB Title: Leishmania tdr 1 – a unique trimeric glutathione transferase	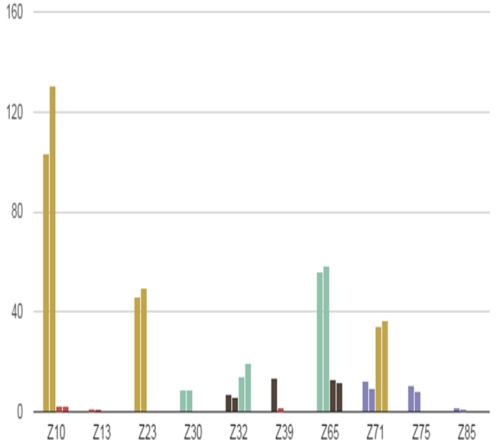	

Traes_7DS_07E6F5FD6 Scaffold: IWGSC2:7D:21263809:21265315:1 POPSEQ distance: 7D:44.60cM	MAATLQFISLLGTSSAHPAPSCSSSXXXXXXXXXXXXXXXXXXXXXXXXXXXXADSETTVEPPSVDFAFVSPRLLPDGTPDVHYRTACGGQKLRDIMLQGYIDLYGPYDKLLLNCSGGGECGTCIVEVVEGGEMLSPKNEVEKEKLKRKPKSWRLACQATVGNPDSTGQMVIQQLPEWKVHKWDK	PDB header: Metal binding protein PDB molecule: Ferredoxin PDB Title: Crystal structure of the isc like ferredoxin from *Pseudomonas putida*	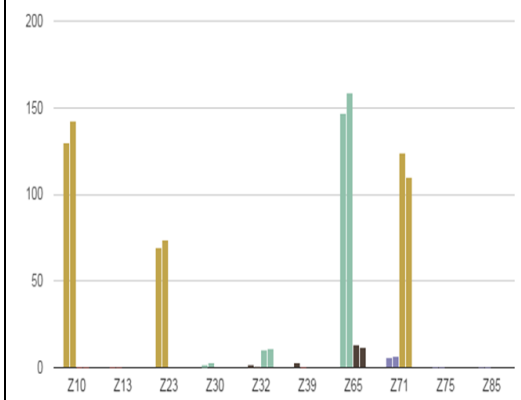	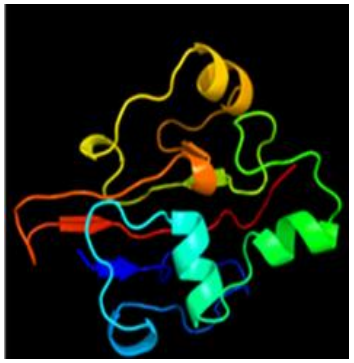
Traes_4AS_90CC29CAA Scaffold: IWGSC2:4A:81039076:81043065:1 POPSEQ distance: 4A:61.02cM	MATACPPLSLPSTSLLRKTTRAGPARQPLPSVRCSAVGEAVAEAAVAGTAEEPLLVSAIKGKKVERPPVWLMRQAGRYMKSYQNLCEKYPLFRERSENVDLVVEISLQPWKVFKPDGVILFSDILTPLPGMNIPFDIVKGKGPVIYDPLRTAAAVNEVREFVPEEWVPYVGQALNLLRGEVKNEAAVLGFVGAPFTLASYCVEGGSSKNFSKIKRMAFAEPAILHNLLQKFTTSMASYIKYQADNGAQAVQIFDSWATELSPVDFEEFSLPYLKQIVDSVKETHPDLPLILYASGSGGLLERLPLTGVDVVSLDWTVDMAEGRKRLGSNIAVQGNVDPGVLFGSKEFITKRIYDTVQKAGSEGHVLNLGHGIKVGTPEENVAHFFEVAKGIRY	Family: Uroporphyrinogen decarboxylase (UROD)	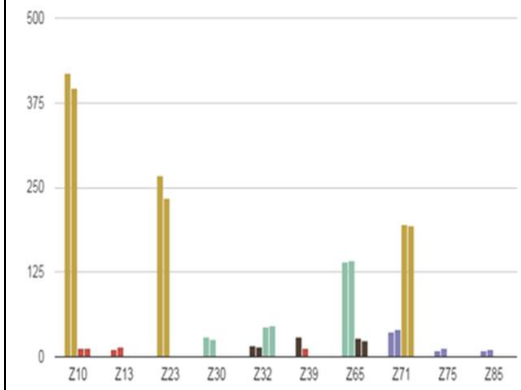	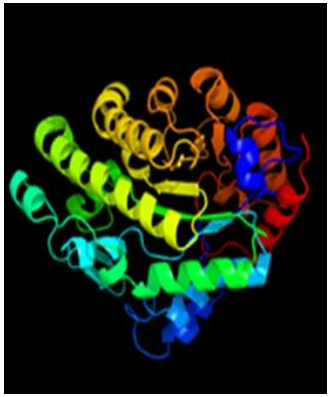

Traes_4DL_3D9786B06 Scaffold: IWGSC2:IWGSC_CSS_4DL_scaff_14354305:1739:6575:-1 POPSEQ distance: Unknown	MLLLRAARRRDLASPLATLTANVQSTYAA ANVCSRWGTFARAFSAKPIGNEVIGIDLGT TNSCVAVMEGKNAKVIENSEGARTTPSVV AFSPKGELLVGIPAKRQAVTNPQNTFFGTK RMIGRRFDDPQTQKEMNMVPYKIVKAPN GDAWVETTDGKQYSPSQIGGFVLTKMKE TAEAYLGKSISKAVITVPAYFNDAQRQATK DAGRIAGLDVQRIINEPTAAALSYGTNNKE GLIAVFDLGGGTFDVSILEISNGVFEVKATN GDTFLGGEDFDNTLLGFLVSEYKNTENIDL SKDRLALQRLREAAEKAKIELSSTTQTEINL PFITADASGAKHLNITLTRSKFESLVNGLIER TREPCKSCLKDAGITTKDVDEVLLVGGMTR VPKVQEIVSEIFGKAPSKGVNPDEAVAMG AAIQGGILRGDVKELLLLDVTPLSLGIETLG GIFTRLISRNTTIPTKKSQVFSTAADNQTQV GIKVLQGEREMATDNKLLGEFDLVGIPPAP RGTPQVEVTFDIDANGIVTVSAKDKATGK EQQITIRSSGGLSEAEIQKMVQEAEVHSHK DQERKALIDVRNTADTTIYSVEKSLGEYRD KVPAEVVSEIESAVADLRAEMASDDAEKIK AKMDAANRAVSKIGQHMSGGEPGSQQG GGGGDEAPEAEYEEVKK	PDB header: Chaperone PDB molecule: Heat shock protein 70 PDB Title: Structure of E.coli hsp 70 (dnak) chaperone (1-605) 2 complexed with adp and substrate	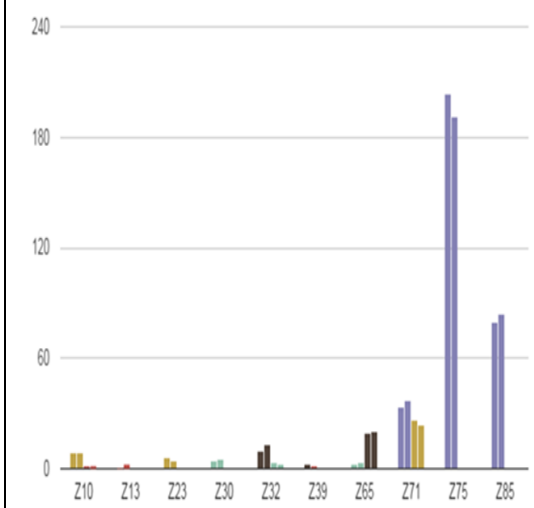	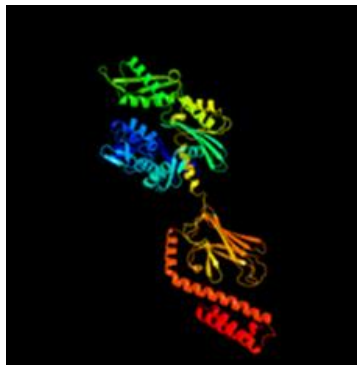
Traes_4DL_E8582A179 Scaffold: IWGSC2:IWGSC_CSS_4DL_scaff_14384722:3183:5439:-1 POPSEQ distance: 45.8-58.7cM	MVAPATLSLRPCATLAPSRAALPRAHAH AGFAPASRPALSVSCPPTRFESLRRAATA VSDRQGSAEPSEKQEGKSRTYYFLVANA KFMLDDEEHFQEQLQEKLRLYEERSKEQ DFWLVIEPKFLDRFPNVAKRLKRPAVAL VSTDRNWIRFMKLRLDRVLAEQFDAET PEEALASNPAELKFDKPDKWTAPYPKYE SGWWEAFLPPKSSNGTA	PDB header: Structural genomics, Unknown function PDB molecule: All 0216 protein PDB Title: X ray structure of all0216 protein from *Nostoc* sp	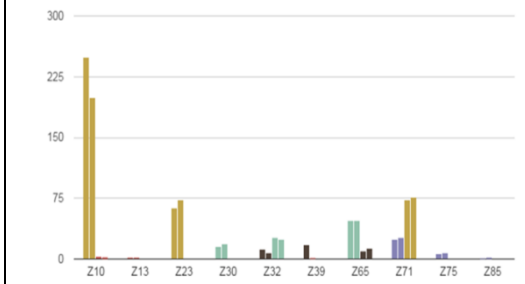	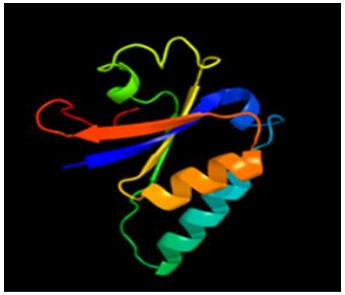

Traes_4DL_D7237EFB9 Scaffold: IWGSC2:4D:58547816:58554314:1 POPSEQ distance: 4D:54.76cM	MATPNGLARIDTTHAEKKAAAKHENGICHDDS SAPVRAQNIDELHSMQRKRSAPTTPIKDTSASP FAVAVSDEDRRKQQLQSISASLASLTRETGPKVV RGDPARKGEAAAKTAPAAAPPPPQPHLAAAKT APAAAPPPPQPHHHHHHHVAPTISVSDSSLKFT HVLYNLSPGELYEQAIKYEKGSFITATGALATLSG AKTGRSPRDKRIVKDEAAAQELWWGKGSPNIE MDEHTFLTNRERAVDYLNSLDKVYVNDQFLN WDPENRIKVRIISARAYHSLFMHNMCIRPTEEEL ESFGTPDFTIYNAGKFPCNRYTHYMTSSTSVDIN LGRREMVILGTQYAGEMKKGLFGVMHYLMPK RRILSLHSGCNMGRDGDVALFFGLSGTGKTTLS TDHNRLLIGDDEHCWSDNGVSNIEGGCYAKCI DLSREKEPDIWNAIKFGTVLENVVFDEHTREVD YTDKSVTENTRAAYPIEYIPNAKIPCVGPHPKNVI LLACDAFGVLPPVSKLNLAQTMYHFISGYTALV AGTEDGIKEPQATFSACFGAAFIMLHPTKYAAM LAEKMQTYGATGWLVNTGWSGGRYGVGKRIK LPYTRKIIDAIHSGELLTANYQKTEVFGLEIPTAIE GVPSEILDPINTWTDKAAYKETLLKLAGLFGKNF EVFASYKIGEDSTLTEEILAAGPKV	PDB header: Lyase PDB molecule: Phosphoenolpyruvate carboxykinase PDB Title: Crystal structure of ATP dependent phosphoenolpyruvate carboxykinase 2 from *Thermus thermophilus* hb 8	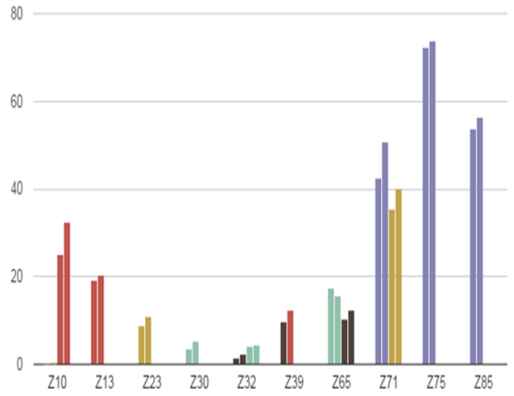	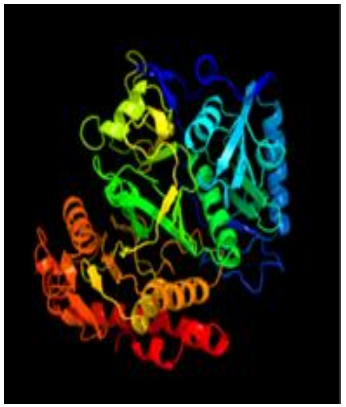
Traes_4DL_8DED0B0C8 Scaffold: IWGSC2:IWGSC_CSS_4DL_scaff_14352871:1:4017:1 POPSEQ distance: Unknown	MLFKGTGTRSAGQLEQEIEDMGGHLNAYTS REQTTYYAKVLDKDVPRAMNVLADILQDSKL EDNRIERERGVILREMEEVQGQSEEVIFDHLH ATAFQYTSLGRPILGSADNVKSITKKNLIDYIQ KHYTASRMVITAAGAVKHEDIVQQAKELFKS LPTDPTTTNMLVAEQPAIFTGSEVRIIDDDM PLAQFAVAFNGASWTDPDSIALMVMQTML GSWNKSAGGGKHMGSELVQRVAINEIAESI MAFNTNYKDTGLFGVYAVAKADCLDDLAFAI MQEMSKLSYRVTEEDVIRARNQLKSSIQLHL DGSTAVVEDIGRQQLIYGRRIPIPELFARIDAV DPSTIRRVANRFIFDQDIAIAAMGPIKSLPDY NWFRRRTYMLRY	PDB header: Oxidoreductase PDB molecule: Ubiquinolcytochrome-c reductase complex core protein 1 PDB Title:Crystal structure analysis of bovine bc 1 with myxothiazol	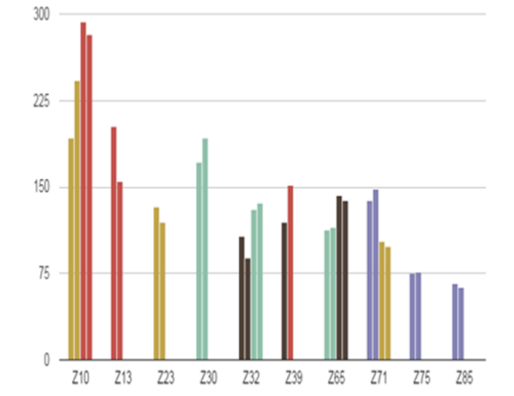	

Expression of Protein: Yellow bars – inra-rna: leaf; Blue bars – inra-rna: grain; Red bars – inra-rna:root; Green bars – inra-rna:stem (Detailed information from aestivum.accwi.org.au.)

5.5 Discussion

Biotic and abiotic stresses are major factors limiting agricultural production and plants have evolved a combination of defensive mechanisms to overcome the stresses caused by the biotic and abiotic factors. Plant resistance to insects is a complex process, often involving numerous plant biochemical pathways (Smith et al., 2010). RWA causes significant yield reduction in susceptible wheat cultivars. Resistant cultivars respond to RWA through constitutive or induced defensive signalling networks or with both (Smith et al., 2014). We have demonstrated in Chapter 3 that the DH mapping populations forming the basis of this thesis, have consistent RWA-resistant and susceptible lines. We hypothesised constitutive genes in the RWA resistant lines are likely to play a vital role in the defence mechanism against RWA. 2DE gel analysis and iTRAQ experiments to identify the expressed proteins were conducted to explore this concept. Although several protein spots were detected in the 2DE gel analysis, presence/absence variation between resistance and susceptible groups was not detected in these studies. Absolute quantification of the detected protein using 2D gel analysis was not accurate enough for the present study due to the detection limit of the technology. The more sensitive iTRAQ experiment shows several proteins differentially expressed at the significant levels between resistance and susceptible groups in chromosome 1DS, 7DS, 3BL, 4AS and 4DL. A total of 10 proteins were consistently differentially expressed in all three biological triplicates. Among them, the gene Traes_4AS_90CC29CAA annotated to uroporphyrinogen decarboxylase (UROD) was down regulated in the RWA resistant group relative to RWA susceptible group. Their functional annotations are as follow:

5.5.1 Oxidoreductase - Dihydrolipoamide dehydrogenase glycine decarboxylase 2 from *Pisum sativum* (Traes_1DS_947F6918F)

Two multigene complexes, the pyruvate dehydrogenase complex (PDC) and the glycine decarboxylase dehydrogenase complex (GDC) play a fundamental role in plant leaf respiration. PDC regulates entry of the carbon into the tricarboxylic acid and related metabolism (Bourguignon et al., 1996) and GDC catalyses the oxidative decarboxylation and deamination of glycine molecules flooding out of peroxisomes during the course of photorespiration (Douce et al., 1994; Oliver et al., 1990). Glycine is the predominant substrate oxidised by leaf mitochondria during the day (Oliver et al., 1990 b). GDC consists of four proteins a) glycine cleavage H protein, b) glycine decarboxylase P protein, c) the dihydrolipoamide dehydrogenase L protein and d) the amino methyl transferase T protein (Figure 5.4).

The overall net reaction is:

$$2\ \text{Glycine} + NAD^+ + H_2O \longrightarrow \text{Serine} + CO_2 + NH_3 + NADH + H^+$$

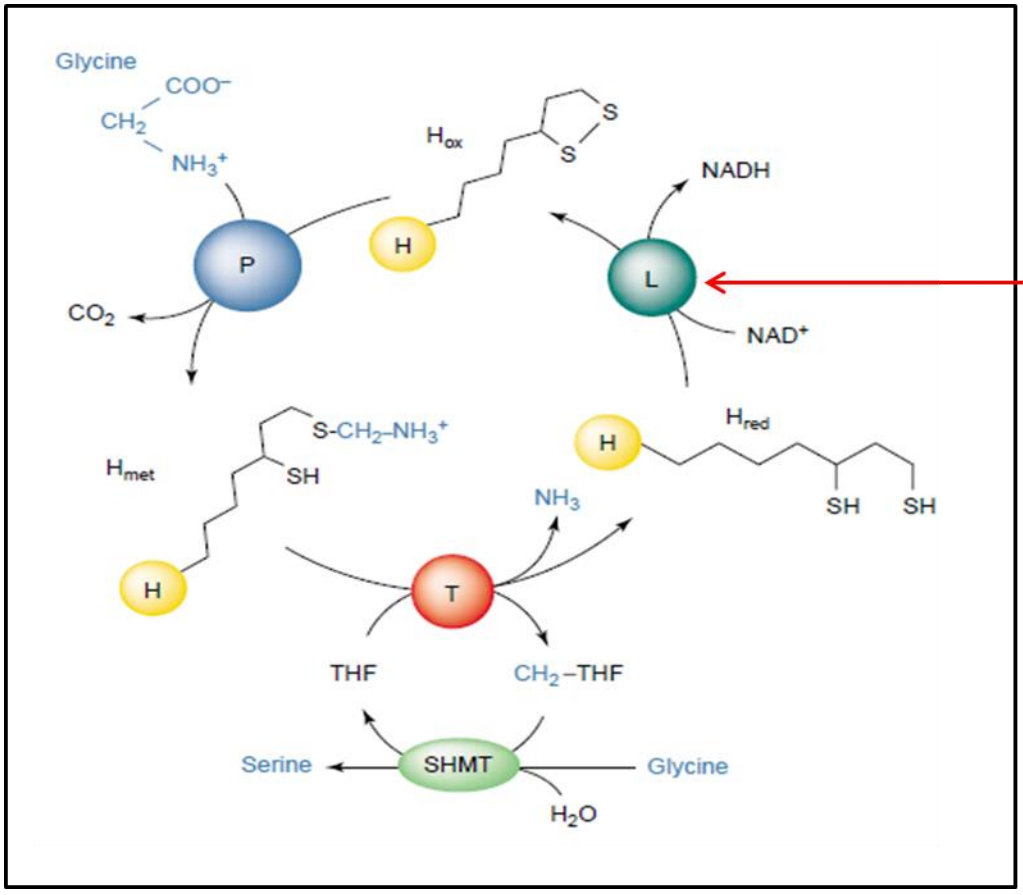

Figure: 5.4 Outline of the reactions involved in oxidative decarboxylation and deamination of glycine in plant mitochondria (text for legend taken from Douce et al. (2001)). P-, H-, T-, and L- are the protein components of the glycine-decarboxylase multienzyme system. The pivotal enzyme in the entire sequence of reactions is the 14000 M lipoamide- containing H protein, which undergoes a cycle of reductive methyamination (Catalysed by the P-protein), methylamine transfer (catalysed by the T- protein) and electron transfer (Catalysed by the L- protein). The lipoyl moiety in the H- protein is attached by an amide linkage to the ε-aminogroup of alysine residue. This linkage provides a rather flexible arm, ~14 Å in length, conveying the reactive dithiolane ring from one catalytic center to another. SHMT: serine hydroxymethyltransferase involved in the conversion of CH2-THF to THF at the expense of a second molecule of glycine. Note that the methylamine moiety deriving from glycine is passed to the distal sulphur of the dithiolane ring. H met, H red and Hox: methylaminated, reduced and oxidised forms of the H protein, respectively (Douce et al., 2001).

Dihydrolipoamide dehydrogenase L protein in this multigene complex plays a pivotal role to convert glycine into serine. Up regulation of this gene found in the RWA resistant group enhance the conversion of glycine produced in the green leaves and therefore possibly indirectly protect the plant from the aphid attack. A transcript profile of the gene shows the expression in the leaf and root tissues at the early stages of wheat growth (Z10).

5.5.2 Oxidoreductase - Thioredoxin glutathione reductase (Traes_1DS_D46002062)

Formation or breakage of a disulfide bond between cysteine moieties in proteins is an important reaction to regulate several biological functions in living organisms (Vieira Dos Santos & Rey, 2006). Reactive oxygen species (ROS) act at subtle levels as signalling molecules during plant development or when the plant is exposed to biotic or abiotic stress. But increasing ROS levels in the cells cause oxidative damage to macromolecules (Mittler et al., 2004) such as proteins which are prone to ROS-induced modification processes particularly at their thiol groups which can be oxidized to sulfinic forms or undergo disulphide formation (Davis, 2005). Thiolredoxins (Trxs) and glutaredoxins (Grxs) are conserved proteins catalysing in-vivo disulphide reduction through a redox-active thiol (Arnér & Holmgren, 2000; Rouhier et al., 2004) and protect the proteins from modification.

A main target of RWA elicitors is the chloroplast since chloroplast is the main site of the ROS production in plant cells because of photosynthetic activity, particularly during environmental constraints (Mittler et al., 2004). Thereby half of plant thioredoxins (Trx) are located in the plastid (Figure 5.4). In several plant species, *Trx* gene expression is often associated with increased level of ROS (Vieira Dos Santos & Rey, 2006). For example, the amount of transcript of Arabidopsis *Trx h5* gene increased significantly during an incompatible interaction with a pathogen and more generally under oxidative stress conditions (Laloi et al., 2004). This indicates that *Trx*

is possibly involved in defence mechanism linked to the oxidative burst resulted in pathogen attack.

The observed significant different levels in thioredoxin glutathione reductase expression between RWA resistant and susceptible group indicates it may be involved in the RWA resistance. ROS may have been produce at higher levels at the early stage of growth since early stages are more vulnerable to RWA infestation. The relatively high level of expression of the gene at the early wheat growth stage (Zadoks growth state 2) in leaf and root tissues as shown in table 5.1 would provide improved protection to the cells.

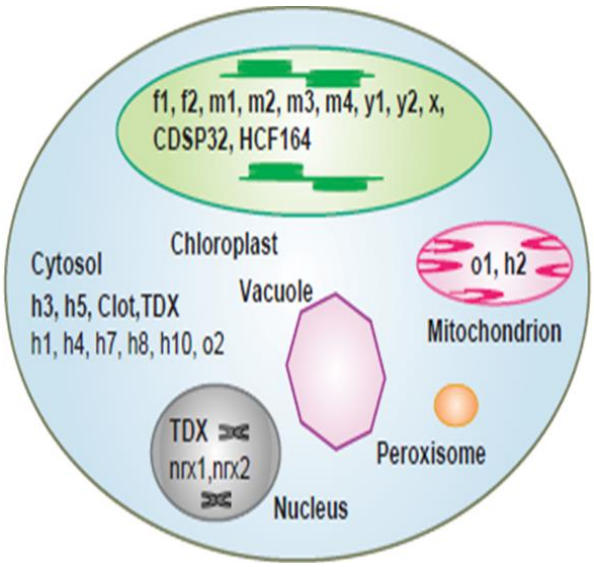

Figure 5.5: Subcellular localisation of the main thioredoxins (Vieira Dos Santos & Rey, 2006)

5.5.3 Transport protein - ADP, ATP carrier protein3 (Traes_1DS_ACF9E82D8)

Mitochondria have been described as a powerhouse of the cells since they produce not only adenosin triphosphate (ATP) as energy source but also carbon compounds necessary for many biosynthetic pathways via respiration (Millar et al., 2001). Respiration also maintains higher photosynthesis rates necessary for maximal plant

growth (Kroemer 1995). ATP is formed inside the mitochondria matrix by oxidative phosphorylation require importation of phosphate and Adenosine diphosphate (ADP) through the inner mitochondrial membrane. Phosphate is transported via a phosphate carrier (PiC) and ADP is exchanged with the ATP produced via adenine nucleotide translocator (ANT), ADP and ATP carrier proteins (Figure 5.5)

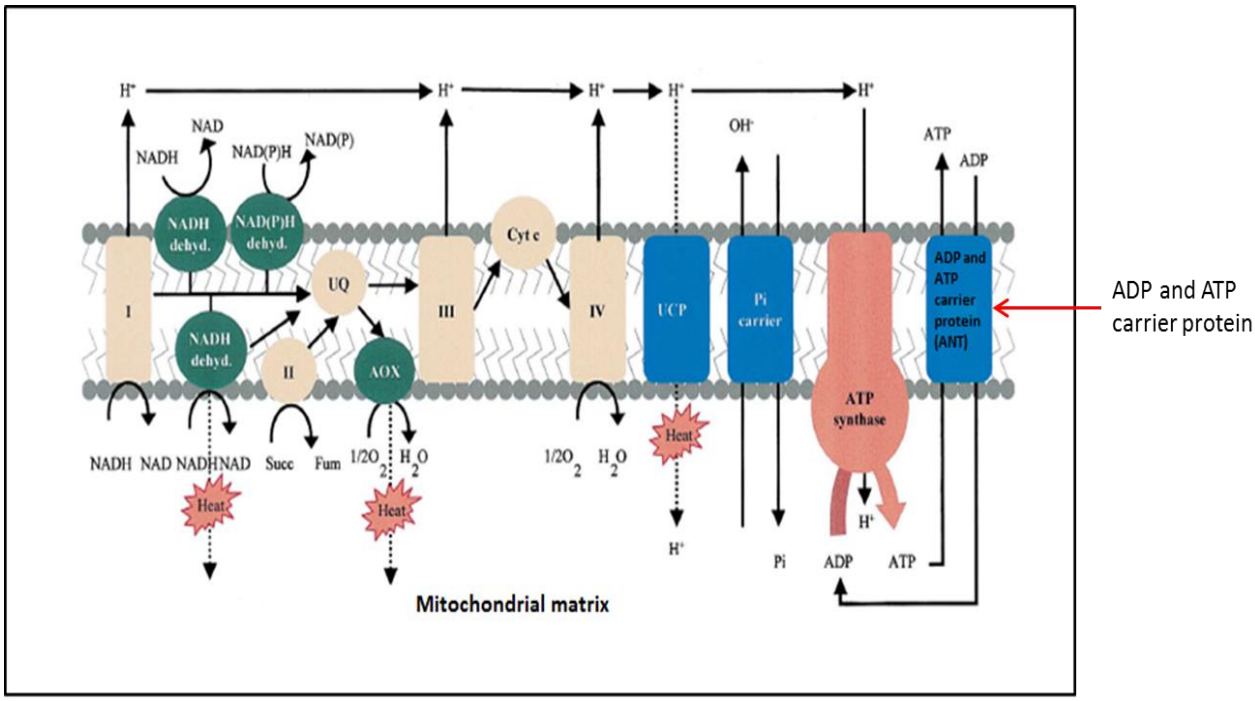

Figure 5.6: Schematic representation of the plant inner mitochondrial membrane (text for legend taken from Laloi (1999)). The diagram shows proteins involved in the electron transfer common to plants and animals in orange, plant-specific proteins in green and mitochondrial carriers involved in oxidative phosphorylation in blue. I, Complex I or NADH dehydrogenase complex; II, complex II or succinate; III, complex III or cytochrome c reductase; IV, complex IV or cytochrome c oxidase; dehyd., dehydrogenase; Succ, succinate; Fum, fumarate; AOX, alternative oxidase; Cyt c, cytochrome c (Laloi, 1999)

The gene, Traes_1DS ACF9E82D8 coding for an adenine nucleotide translocator was up regulated in the resistant group and would thus provide energy for the cell growth and for the bio synthetic pathways. It means plants with higher energy metabolism are able to tolerate or quickly recover from the biotic and abiotic stress.

The transcript profile of the gene shows the expression in the leaf and root tissues at the early stages of wheat growth (Z10).

5.5.4 Transferase – Thioldependent reductase 1 (Traes_7DS_FDC2AB87A)

Glutathione transferases (GST) are soluble proteins and catalyse the transfer of the tripeptide glutathione (γ-glutamyl-cysteinyl-glycine; GSH) to a cosubstrate (R-X) containing a reactive electrophilic center to form a polar S-glutathionylated reaction product (R-SG). It is first reported in maize to be responsible for conjugating the chloro-S_triazine atrazine herbicide and thereby protecting the crop from injury by this herbicide (Edwards & Dixon, 2000). Soluble GSTs in plants are predominantly localised in cytosol (Edwards et al., 2000; Marrs, 1996) where they perform GSH dependant catalytic function. Different GSTs isoforms seem to be expressed in different tissues (Sari-Gorla et al., 1993). Though many plant GSTs have been cloned tau and phi GSTs are known to be induced by abiotic and biotic stress (Marrs, 1996). Primary function of known GST is shown in figure 5.6. Transcript profile of the gene shows the expression primarily in the leaf tissues at the early stages of wheat growth (Z10)

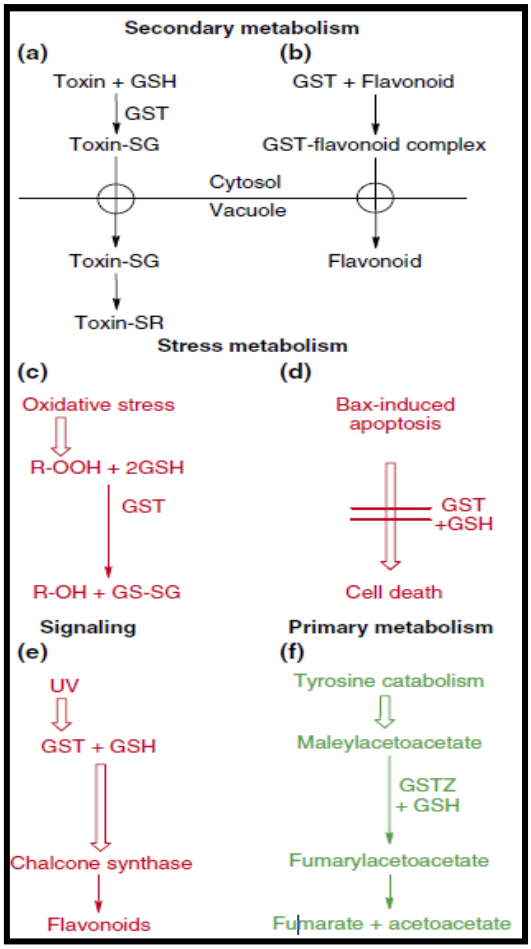

Figure 5.7: Overview of known GST functions in plants (text legend taken from Dixon et al. (2002)). (a) In secondary metabolism, GSTs detoxify toxins by conjugation with GSH; the conjugate (toxin-SG) are then ransported into vacuole by ABC transporters (shown as circles) prior to proteolytic processing. (b) Some phi and tau class enzymes are also required for transport of flavonoid pigments to the vacuole. (c-e) Roles of GSTs in stress metabolism include acting as (c) glutathione peroxidases that can reduce cytotoxicDNA and lipid hydroperoxides; (d) in an antioxidant capacity, protecting against Bax-induced cell death; and (e) in stress signalling, playing a role in the induction of chalcone synthase following exposure to ultraviolet light. (f) zeta GSTs (GSTZ) have a role in primary metabolism as maleylacetoacetate isomerases. Wide arrows denote an induction process; narrow arrows denote enzymatic reactions; thick lines denote inhibition of a reaction; R, an alkyl group (Dixon et al., 2002).

5.5.5 Metal ion binding Ferredoxin (Traes_7DS_07E6F5FD6)

Ferredoxin-1 (Fd-1) is a fundamental protein involved in several important metabolic path ways such as photosynthesis, nitrate reduction and lipid synthesis (Curdt et al., 2000). Ferredoxin exists in isoforms, Fd-I, Fd-II and Fd-III. Fd1 is always found in green tissues often accompanied by Fd-II involved in electrons transfer from photosystem-I to the enzyme NADP+ whereas Fd-III exists in root tissues of the plants (Hanke et al., 2004). The work of Dayakar et al. (2003) demonstrated that sweet pepper ferredoxin-1 (Fd-1) protein (PFLP) was involved with hypersensitive reaction with production of ROS. As FD-1 is a major component of photosynthesis–associated protein and catalyse electron transfer in photosynthesis it may generate ROS under stress full conditions (Tognetti et al., 2006) and therefore plants can activate the defence mechanism by altering the levels of FD-1 when they expose to biotic factors (Huang et al., 2007). The transcript profile of this gene shows the expression only in the leaf tissues at the early stages of wheat growth (Z10).

5.5.6 Uroporphyrinogen decarboxylase (Traes_4AS_90CC29CAA)

The enzyme is responsible for catalysing the conversion of uroporphyrinogen (UROD) to corproporphyrinogen (CPO) by removing of four carboxymethyl side chains. Our results show significant up regulation in the RWA susceptible groups. Studies by Mock et al. (1999) demonstrated UROD or CPO antisense tobacco transgenic plants accumulated considerable amount of scopoline compounds. Scopolin is a glucoside of scopoletin formed by the action of the enzyme, scopoletin glucosyltransferase. Scopoletin and its glucoside scopoline are important secondary metabolites synthesised in plants as a defense mechanism against various environmental stresses (Siwinska et al., 2014). Accumulation of scopoletin and scopoline compounds was also reported in cell suspension cultures of antisense UROD or CPO tobacco (Okazaki et al., 1982). Scopolin and scopoletin compounds play an important role in disease resistance (Mock et al., 1999). A rapid and pronounced synthesis of scopoletin was seen in incompatible plant-pathogen interactions and a slower and reduced

formation was found in compatible interaction (EI Modafar et al., 1995; Valle et al., 1997). Accumulated level of Scopolin was also found during hypersensitive reaction on the leaf of Tobacco mosaic virus (TMV) infected tobacco varieties (Fritig & Hirth, 1971; Tanguy & Martin, 1972). Elevated constitutive levels of scopoletin and scopoline were seen in a disease resistant *Nicotiana* hybrid (Ahl Goy et al., 1993). Observed up regulation of the Uroporphyrinogen decarboxylase gene in RWA susceptible lines may result in accumulated level of UROD and CPO and therefore reduced the level of scopoletin and scopoline compounds which would contribute to a general defensive mechanism against biotic stresses. Transcript profile of the gene shows the expression primarily in the leaf tissues at the early stages of wheat growth (Z10)

5.5.7 Chaperone - Heat shock protein 70 (Traes_4DL_3D9786B06)

The gene Traes_4DL_3D9786B06 was up regulated in the RWA resistant group. Protein modelling and annotation using the nucleic acid databases identified this gene to code for heat shock protein 70. The majority of HSP70 family members perform chaperone functions related to when the cells are exposed to stresses such as heat, cold, UV or biotic stress (Basha et al., 2004; Mayer & Bukau, 2005; Miller & Mittler, 2006). Under these conditions partial denaturation and aggregations of proteins can be reduced by HSP 70 and facilitate their reactivation by allowing them to refold (Ben-Zvi et al., 2004; Diamant et al., 2000). Heat shock protein 70 also prevents incorrect protein folding during post translational import into the mitochondria/ chloroplast (Mayer & Bukau, 2005). RWA causes damage on the wheat plants by injecting elicitors into the host cells. Protein compounds found in the elicitors may interact with host proteins and do partial change in the protein structure. Heat shock protein 70 may recover these altered proteins and protect the plants from the biotic stress. The transcript profile of the gene shows the expression in the leaf and root tissues at the early stages of wheat growth (Z10).

5.5.8 Phosphoenolpyruvate carboxykinase (Traes_4DL_D7237EFB9)

The gene Traes_4DL_D7237EFB9 was up regulated in RWA resistant group and the gene is responsible for the synthesis of the phosphoenolpyruvate carboxykinase enzyme which involved in gluconeogenesis and mapped to the long arm of chromosome 4D at the POPSEQ distance of 45.76cM. Gluconeogenesis is a reverse process of glycolysis that results in the generation of glucose from the breakdown of non-carbohydrate carbon substrates that includes proteins, lipids, pyruvate and lactate (Figure 5.8). Phosphoenolpyruvate carboxykinase (PEP carboxykinase) is a Mn^{2+} dependent enzyme that catalyses oxaloacetate to phosphoenolpyruvate (PEP) in a reversible reaction (Chen et al., 2002).

Oxaloacetate + ATP $\longleftrightarrow$ Phosphoenolpyruvate (PEP) + ADP + Co_2

This reaction lies at an interface between organic acids, amino acids and sugar metabolism. Because of the presence of PEP carboxykinase enzyme, the wide range of plant tissues can have higher contents of oil and resins products which may contribute to repelling aphids. The transcript profile of the gene shows the expression primarily in root tissues at the early stages of wheat growth (Z10).

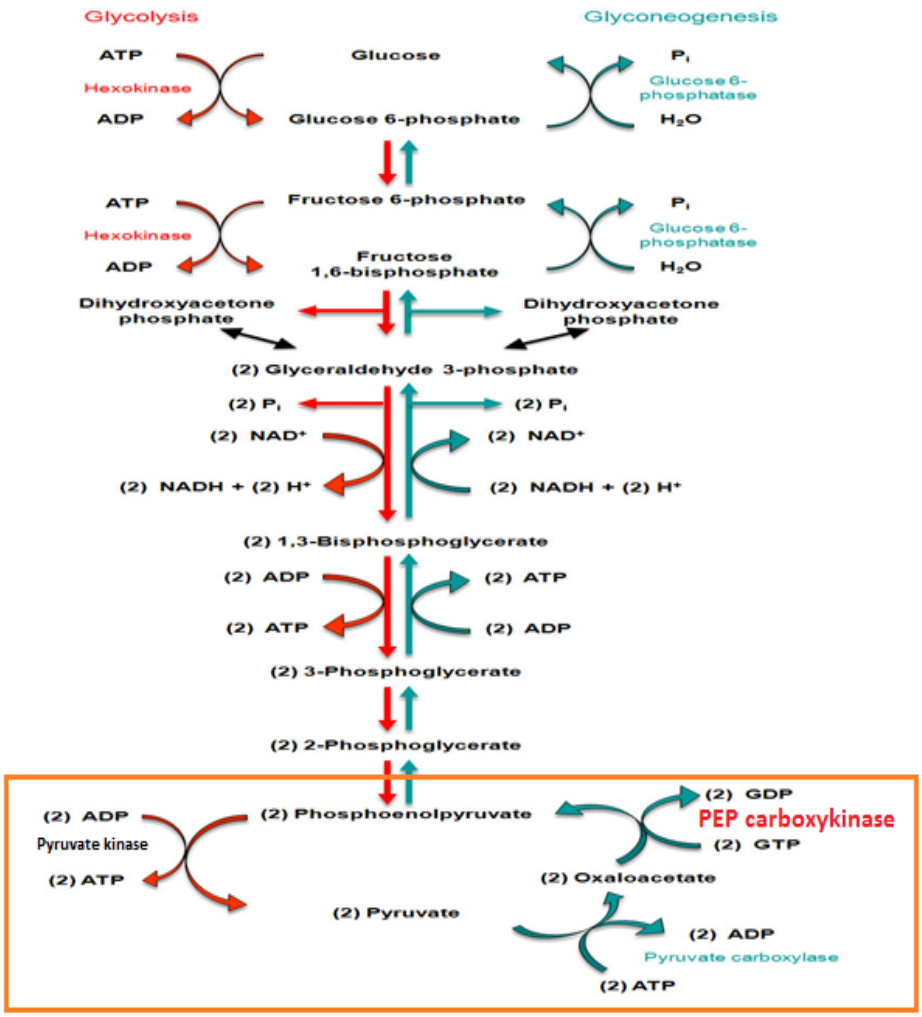

Figure 5.8: Involvement of Phosphoenolpyruvate carboxykinase in glyconeogenesis pathway

5.5.9 Oxidoreductase - Ubiquinolcytochrome-c reductase complex core protein 1 (Traes_4DL_8DED0B0C8)

The main role of the chloroplasts is photosynthesis where chlorophyll molecules capture light energy and convert this energy into stabilised chemical products such as ATP and nicotinamide adenine dinucleotide phosphate (NADPH) while freeing oxygen from water. Chloroplasts are made of smooth outer and inner membranes. These photosynthetic membranes contain a number of integral membrane protein complexes that are involved in energy conversion reactions. In addition to photochemical complexes, all photosynthetic membranes also consist of an electron transfer complex known either as the cytochrome bc_1 or b_6f complex (Malkin, 1992).

The cytochrome b is the central redox catalytic subunit of the quinol:cytochrome c or plastocyanin oxidoreductases. The cytochrome bc_1 or b_6f complex converts the redox energy released during the oxidation of quinols into a gradient proton across the membrane. This proton gradient is a high energy source and this energy is utilised for the synthesis of ATP (Malkin, 1992) .

Cytochrome b is also found in the mitochondria of eukaryotic cells. Function of the cytochrome b protein binds the quinine substrate and release energy by oxidising the quinine substrate. It also responsible for transmembrane electron transfer by which redox energy obtained from oxidising quinone substrate is converted into a protonmotive force (Esposti et al., 1986) .

Significant differential expression of this protein was seen in RWA resistant groups relative to the susceptible genotypes. More energy creation among the RWA resistant lines compared to susceptible lines could help to fight against RWA damage. Transcript profile of the gene shows the expression in the leaf and root tissues at the early stages of wheat growth (Z10).

5.5.10 Unidentified protein (Traes_4DL_E8582A179)

The protein expressed by the gene Traes_4DL_E8582A179 is currently uncharacterised. However it may involve in biosynthesising structural related compounds. It is clearly up regulated in the RWA resistant DH lines and because it is unidentified protein and it needs to be investigated further. The transcript profile of the gene shows the expression only in the leaf at the early stages of wheat growth (Z10).

5.6 Conclusion

We hypothesised that constitutive genes constantly expressed regardless of aphid infestation play an important role in the protection of aphid damage (see also Chapter2). In the present study ten proteins were identified consistently with regards to their significant differential expression between resistant and susceptible double haploid lines using the iTRAQ technology. The ten proteins were annotated to the wheat genome and the corresponding genes and their locations were identified. Although the proteins were not located in the RWA resistance loci, it is reasonable to suggest that the levels of these proteins provide a significant background contribution to the gene networks that forms the basis of the overall RWA resistance phenotype. As discussed in Chapter 6, it is proposed that 10 proteins identified in this Chapter will contribute to identifying RWA resistant wheat varieties through the establishment of new molecular markers.

Chapter 6: General Discussion and Conclusion

The overall experimental approach of this PhD thesis was provided in Chapter 1 and it is reproduced as Figure 6.1

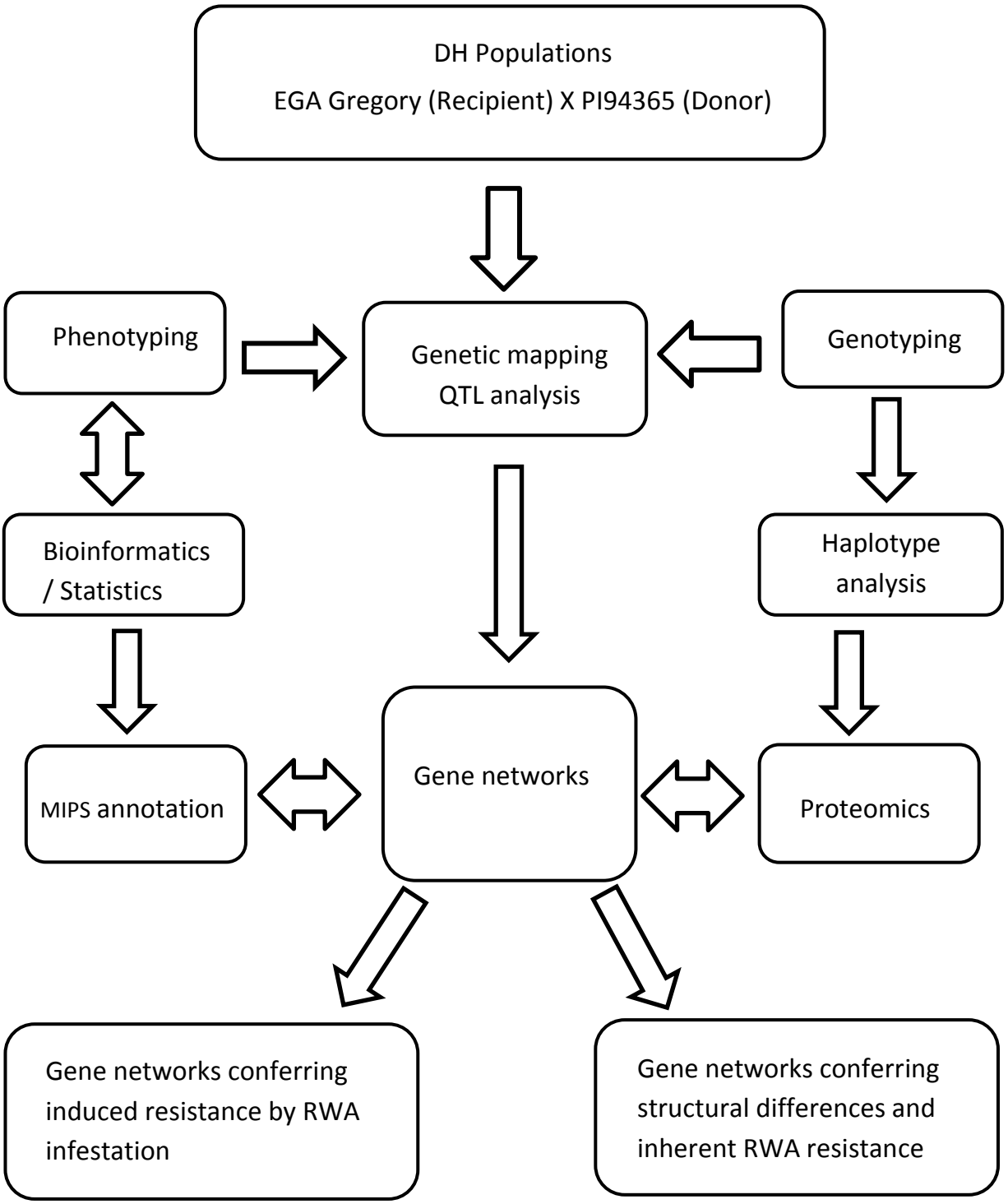

Figure 6.1: Summarises the overall experimental approach used in the thesis to investigate the nature of RWA resistance in DH population derived from EGA Gregory and PI94365.

The aim of the thesis was to develop a RWA resistance wheat population from a novel RWA resistance source and gain an understanding of the genetic mechanisms involved in RWA resistance.

The research in this thesis has achieved the following against the summary provided in Figure 6.1:

6.1 DH Populations [EGA Gregory (Recipient) X PI94365 (Donor)]

A double haploid (DH) population consisting 188 lines were created using a resistant landrace PI94365 as a donor parent and susceptible cultivars EGA Gregory as a recipient parent using the microspore culture technique. Landrace PI94365 was screened against several RWA biotypes found in several countries including South Africa, Turkey, Morocco and Kenya (Chapter 3 section 3.3.1).

6.2 Phenotyping and genotyping

The DH population was screened in South Africa, Turkey and Morocco against their respective RWA biotypes. Screening results identified DH lines showing moderately to good resistant to RWA biotypes. Four thousand and fifty three polymorphic molecular markers including SSR, GBS and DArT were identified in this DH population. The SSR, GBS and DArT markers are genome sequence based markers and hence the respective DNA sequences in the genome contigs in ENSEMBL plants (plants.ensembl.org/triticum_aestivum) could be identified. This capacity allowed the map produced in chapter 3 to be aligned to the very high density POPSEQ map published by Chapman et al. (2015). The technique of using a large number of markers has been made available for the genetic loci of interest. In addition, this study identified SSR markers that can be used in 2% agarose for the DH population screening instead of Poly acrylamide gel electrophoresis (PAGE) screening. The markers and the type of gels used for the screening are listed in the Appendix: Supplementary Table **I** and the gel figures in the appendix: Supplementary Figure I.

6.3 Genetic mapping QTL analysis

This study was able to establish high quality molecular marker genetic maps that defined the chromosomal locations for major RWA resistance loci with phenotype and genotype data. The maps for chromosomes were aligned to new high density molecular marker maps based on the wheat genome sequence assemblies available. Major QTLs for the RWA resistance were identified on chromosome 1DS, 7DS and 7BL. This is the first study to identify a QTL for leaf chlorosis on the long arm of chromosome 7B. Comparative alignment with the POPSEQ map carried out in this study was able to determine the relative POPSEQ distances for the 1DS and 7DS QTLs and therefore many additional molecular marker sequences could be obtained from the sequence data base. This sequence information provides a means to design primer sequences in order to identify molecular markers that can be used in breeding programs for marker assisted selection. A QTL for RWA resistance was mapped on chromosome 7DS, where several *Dn* genes (*Dn1*, *Dn2*, *Dn6*, *Dn8*, *Dnx, Dn626580* and *Dn2401*) from different mapping populations were located in previous studies (see Chapter 3). The 7DS QTL region was explained as a cluster of RWA resistance genes or as a tightly linked location with all the other RWA resistance genes. In Chapter 3 (section 3.5.5), we proposed a model that *Dn* genes at the 7DS locus are possibly within a chromatin loop. In this model we suggested that more genes potentially contributing RWA resistance could be recruited for conferring resistance to emerging RWA biotype. This hypothesis needs to be investigated further.

6.4 Haplotype analysis

The high quality molecular marker genetic map was also used to define groups of lines that were uniform across the RWA loci in terms of molecular marker alleles derived from either the resistant wheat line used in the cross (PI94365) or the susceptible line (EGA Gregory). Identified haplotypes in this population are shown in

the Appendix: Supplementary Table III. These lines were then used to investigate functional proteins that characterized the RWA resistant.

6.5 Gene networks

One of the aims of the thesis was to unravel the genetic mechanism controlling the expression of RWA resistance. Proteomics and bio-informatics approaches were undertaken in an effort to gain an understanding of gene networks underpinning the resistance. In an incompatible interaction, resistant wheat RWA lines respond to RWA infestation by induced or constitutive gene expression (see Chapter 2; Botha et al., 2005; Smith et al., 2010).

By re-examining published data and assigning genes that were demonstrated to respond to the resistance by RWA infection, a total of 287 putative genes were annotated to the current wheat genome assembly. The genes assigned to the region of RWA resistance loci based on the genetic back ground of PI94365 x EGA Gregory cross were determined and the corresponding protein models were identified using updated Phyre2 software. The Phyre2 takes into account the 3-D structures that can be adopted by a string of amino acids forming a protein. By looking at the major QTLs for RWA resistance in the DH population, the gene networks associated with RWA resistance involved in hydrolases, oxidoreductases, transferases, isomerases, ligases, transports, Ca^{2+} binding protein and PR proteins were examined.

Several genes involved in defence related activity were found in the region of RWA resistant loci on 7DS. The genes at the 7DS resistance loci region govern different functions and it is believed they are all involved in the defence network. Genes identified in the RWA resistance loci on 7BL are possibly associated with stress related proteins caused by the disruption of the photosynthetic metabolism. Through the annotation process, genes involved in the broad category of functional classification to RWA defence were identified on chromosomes 1DS, 7DS, 7BL, 4AS,

4DL and 3B where QTLs were mapped for RWA resistance. They are detailed in Chapter 4.

Resistance to RWA may be achieved in conjunction with the expression of constitutive genes (Agrawal, 2007; Forslund et al., 2000; Ni et al., 2001; Smith & Chuang, 2014). Chapter 5 focussed on identifying genes associated with the RWA resistance response. Although none of the genes were found to be located in the RWA resistance loci regions this study identified a total of ten proteins that were consistently differentially expressed in all three biological triplicates. These proteins were annotated to the wheat genome assembly and characterised. They are detailed in Chapter 5 and could represent genes that provide a suitable genetic background for the RWA resistance loci to function.

This study also examined transcript profiles of the genes with newly developed software package (aestivum.accwi.org.au) to study the gene association to RWA resistance (chapter 4 and in chapter 5) and found several entries being expressed in early wheat growth stages (Z10). This is consistent with the possible relationship to RWA infestation at early stages of development as discussed in Chapter 2. Transcript profiles of induced and constitutive genes to RWA resistance were studied and the details of the transcript profiles are provided in Tables 4. 1 and 5.1. The tissue-specific expression of genes identified to be involved in RWA resistance indicated in some cases a root-specific expression pattern which requires further investigation (see also discussed in Chapter 4).

The overall output of this thesis is the release of germplasm carrying RWA resistance that is extremely well characterised at three levels with respect to molecular markers. Based on Chapter 3, the lines carrying RWA resistance have the major loci defined by 1130 markers for the 1DS locus and 14,908 markers for the 7DS locus (predominantly SNPs). Chapter 4 provided a list of twelve genes that responded to

RWA infestation and mapped to the RWA resistance loci on chromosomes 1DS, 7DS and 7BL. These genes included Traes_7DS_A2F956FD8, Traes_7DS_28E2128F3, Traes_7BL_0367BBFE6, Traes_7BL_CA6B7C9E6, Traes_7DS_351943FD9, Traes_7DS_EC365BE37, Traes_7DS_309E71F44, Traes_7BL_660FFDCE2, Traes_7BL_39451C0EC, Traes_7DS_3F6DCEAA8, Traes_7DS_5A98193E8 and Traes_7DS_10C38526F1. In Chapter 5, a set of ten genes were identified as being of broader significance and were argued to be of importance in providing a gene-network capacity capable of responding more efficiently to RWA infestation. The genes included Traes_1DS_947F6918F, Traes_1DS_D46002062, Traes_1DS ACF9E82D8, Traes_7DS_FDC2AB87A, Traes_7DS_07E6F5FD6, Traes_4AS_90CC29CAA, Traes_4DL_3D9786B06, Traes_4DL_E8582A179, Traes_4DL_D7237EFB9 and Traes_4DL_8DED0B0C8.

The three levels of markers provided as a result of the work in this thesis would allow a suite of 100 – 200 markers to be developed for assaying the RWA loci haplotypes in novel germplasm within a breeding program. These haplotypes would be tailored to be distinguishable from the genome sequences of the germplasm in the breeding programs.

The gene-level studies in Chapters 4 and 5 also identified a suite of genes that could be readily placed, based on the annotation studies carried out, into the gene network proposed by Botha et al. (2005) that underpins RWA resistance. Important genes participating in this network of RWA defence included hydrolases, transferases, oxidoreductases, signalling proteins, transport proteins, membrane protein, PR proteins, transcription, lyases and ligases.

The achievements in this thesis include:

- DH lines carrying resistance loci to resistant to Russian wheat aphid that includes biotypes from South Africa, Turkey and Morocco were created from F1 cross. Incorporation of resistance loci from resistant line PI94365 to the Australian susceptible wheat cultivar to RWA paves the way to develop new germplasm for release to breeding programs in anticipating of RWA becoming an issue in Australia.

- Twelve induced genes to RWA infestation were identified in the resistance loci regions through the annotation study. The genes and their functions are listed below.

Major classification	**Gene ID**	**Functional classification**
Hydrolase	Traes_7DS_A2F956FD8	Endo-alpha-n-acetylgalactosaminidase
Oxidoreductase	Traes_7DS_28E2128F3	FMN-linked oxidoredutases
Oxidoreductase	Traes_7BL_0367BBFE6	Chloroplastic malate dehydrogenase
Transport protein	Traes_7BL_CA6B7C9E6	Divalent metal cation transporter mnth
Transferase	Traes_7DS_351943FD9	Shikimate kinase
Transferase	Traes_7DS_EC365BE37	Telomerase reverse transcriptase
Transferase	Traes_7DS_309E71F44	DNA polymerase iii subunit psi
Isomerase	Traes_7BL_660FFDCE2	Cyclophilin
Ligase	Traes_7BL_39451C0EC	Homoglutathione synthetase
Motor protein/ calcium binding protein	Traes_7DS_3F6DCEAA8	Annexin vi
Motor protein/ calcium binding protein	Traes_7DS_5A98193E8	EF Hand-like, Family: Polcalcin; Calcium binding pollen allergen Phl p7
Protein binding	Traes_1DS_0D10FE51D	Hypothetical protein

Differentially expressed ten constitutive genes (without RWA inducement) were identified through the proteomics study. The genes and their functions listed below.

Major classification	**Gene ID**	**Functional classification**
Oxidoreductase	Traes_1DS_947F6918F	Dihydrolipoamide dehydrogenase glycine decarboxylase 2 from *Pisum sativum*
Oxidoreductase	Traes_1DS_D46002062	Thioredoxin glutathione reductase
Transport protein	Traes_1DS ACF9E82D8	ADP, ATP carrier protein3
Transferase	Traes_7DS_FDC2AB87A	Thioldependent reductase 1
Metal ion binding	Traes_7DS_07E6F5FD6	Ferredoxin
Transferase	Traes_4AS_90CC29CAA	Uroporphyrinogen decarboxylase
Chaperone	Traes_4DL_3D9786B06	Heat shock protein 70
Structural genomics	Traes_4DL_E8582A179	Unknown function
Lyase	Traes_4DL_D7237EFB9	Phosphoenolpyruvate carboxykinase
Oxidoreductase	Traes_4DL_8DED0B0C8	Ubiquinolcytochrome-c reductase complex core protein 1

Constitutive genes identified through this study are not in the resistance loci regions. However these genes may be involved in providing fundamental structural support or enhance the induced resistance response.

- The alignment of RWA resistance loci regions into the current wheat genome sequence data base (POPSEQ) provides access many molecular markers that can be employed to identify polymorphic markers in marker assisted selection breeding programs.
- The study ends with an conclusion of bringing germplasm to RWA resistance with an extensive and detailed knowledge of the genome sequences and genes that contribute the RWA resistance loci and the genes mapped to the RWA R loci and the characterization of RWA resistance lines from the mapping population provide some novel insights into the plant response to RWA infestation.

6.6 Future direction

The identification of the gene models provides a sound basis for future studies in delineating further details of the RWA infection process and the responses by the wheat plant:

- Design and develop PCR based marker assay for the high throughput screening for marker assisted selection in breeding programs.

- QTLs were mapped in the chromosome 3BL, 4AS, 4DL and 7BL. POPSEQ alignments of these maps were ambiguous and further work is required to investigate these POPSEQ alignments.

- Identify mode of inheritance of RWA resistance loci incorporated into local cultivars. This can be achieved through screening next generation plants (F2s and F2:3) with the extensive set molecular markers presented in this thesis.

Appendix

Supplementary document 1: Information of resistant line PI94365 (USDA germplasm collection) gathered from http://www.ars-grin.gov/cgi-bin/npgs/acc/display.pl?1126511

94301 to 94762—Continued.

94343. No. 13BSW. Winter wheat from Gonzah, Armenia.

94344 and 94345. *Reasante.* Winter wheat from the original Flemish collection. Collected at Gonzah, Armenia.

94344. No. 14BSW.

94345. No. 15.

94346. No. 17. Siberian spring wheat from Gonzah, Armenia.

94347 and 94348. Winter wheat from a South African collection at Gonzah, Armenia.

94347. No. 19.

94348. No. 20AWS.

94349. No. 22. Winter wheat from Gonzah, Armenia.

94350. No. 33. Winter wheat from Saratov.

94351. No. 36. Winter wheat from Saratov.

94352 to 94354. A collection of black-stripe winter wheat from Armenia.

94352. No. 39Bs.

94353. No. 39BPW.

94354. No. 39BSW.

94355 to 94358. Winter wheat from Erivan, Armenia.

94355. No. 40. *Schroeder.*

94356. No. 41.

94357. No. 48.

94358. No. 51. Originally from Abyssinia.

94359 and 94360. Winter wheat from Odessa.

94359. No. 52ASW.

94360. No. 52BSW.

94361. No. 54. Rust-resistant winter wheat from Kiev.

94362. No. 58. Winter wheat, selection No. 392. The highest-yielding wheat in the District of Krasnodar.

94363 and 94364. Winter wheat, collected at a high altitude near Erivan, Armenia.

94363. No. 59BS. Black stripe.

94364. No. 59BSW.

94365. No. 60. Winter wheat from Erivan, Armenia.

94366. No. 61BSW. Winter wheat, collected at a high altitude near Erivan, Armenia.

94367 and 94368. Winter wheat from Erivan, Armenia.

94367. No. 61 club BP.

94368. No. 61APW.

94369. No. 62. Meister selection of winter wheat from Saratov.

94370 to 94380. Winter wheat from Erivan, Armenia.

94370. No. 63.

94371. No. 65BSW.

94301 to 94762—Continued.

94372. No. 65BPR.

94373. No. 65BPW.

94374. No. 65BSR.

94375. No. 66BPR.

94376. No. 66APR.

94377. No. 66BPW.

94378. No. 66ASW.

94379. No. 66BSW.

94380. No. 66BSR.

94381. No. 67. Bronz winter wheat from Bristol, England.

94382. No. 43. From Erivan, Armenia.

94383 to 94388. From Stanton, England.

94383. No. 68. *Square head.*

94384. No. 69. A collection of rust-resistant varieties.

94385. No. 70. Winter wheat.

94386 to 94388. Mixed types of winter wheat.

94386. No. 71ASW.

94387. No. 71ASR.

94388. No. 71APW.

94389 to 94392. Winter wheat from Bristol, England.

94389. No. 72. *Square head.*

94390 to 94392. A collection of mixed varieties.

94390. No. 73APW.

94391. No. 73ASW.

94392. No. 73ASR.

94393 and 94394. Winter wheat from Stanton, England.

94393. No. 74. *Bronz head.*

94394. No. 75. *Square head.*

94395 to 94413. Winter wheat from Bulgaria.

94395. No. 76.

94396. No. 77.

94397. No. 78. Selection N.

94398. No. 79. Experiment station variety *Silvata.*

94399. No. 80.

94400. No. 81.

94401. No. 82.

94402. No. 83.

94403. No. 84. Variety *Knica.* A selection of winter wheat from the North Bulgaria Experiment Station.

94404. No. 85

94405. No. 86. A mixed sample of wheat and rye.

94406 to 94413. Pure line winter wheat from the North Bulgaria Experiment Station.

94406. No. 87. Experiment Station No. 7.

Supplementary Figure I : PAGE images of parental screening with 7D, 1D, 1B and 7B SSR markers to identify polymorphic markers between parents PI94365 and EGA Gregory

i) Parents PI 94365 (P1) and EGA Gregory (P2): Screening with 7D and 1D SSR markers

1

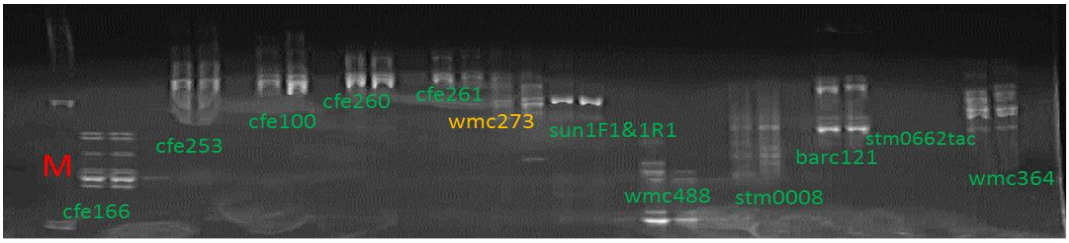

2

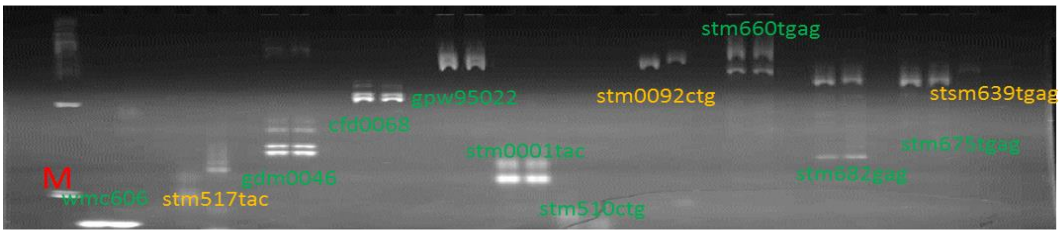

3

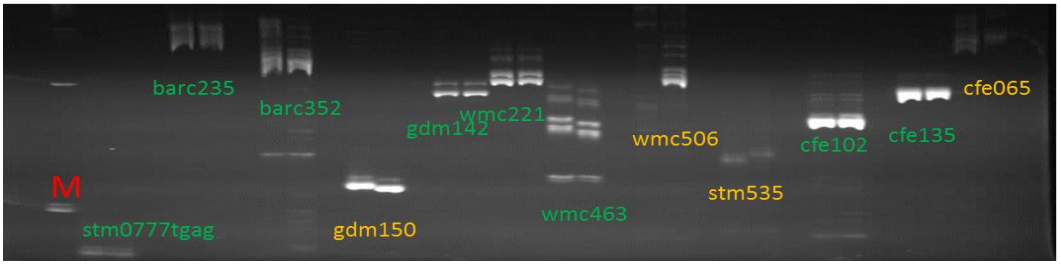

4

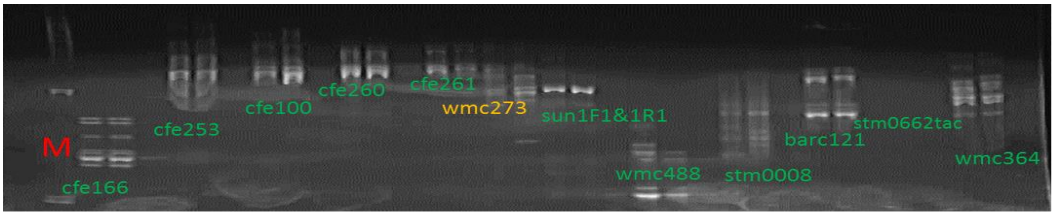
cfe260
cfe261
cfe100
wmc273
sun1F1&1R1
stm0662tac
cfe253
barc121
M
wmc364
wmc488
stm0008
cfe166

5

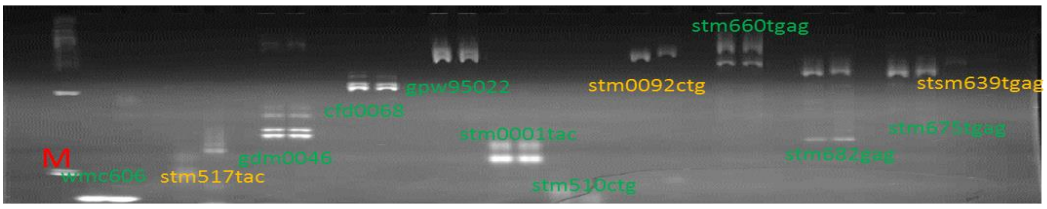
stm660tgag
gpw95022
stm0092ctg
stsm639tgag
cfd0068
stm0001tac
gdm0046
M
stm682gag
wmc606
stm517tac
stm510ctg

6

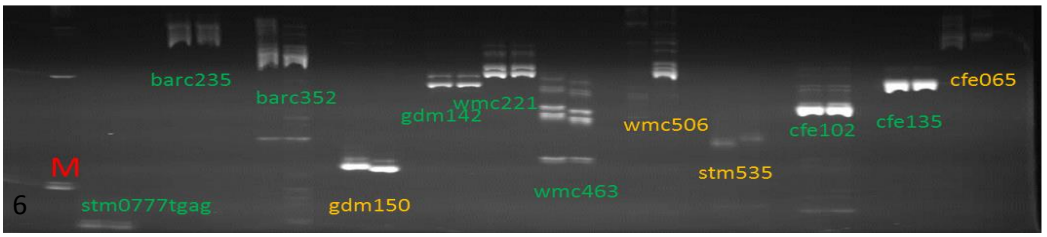
barc235
barc352
cfe065
wmc221
gdm142
wmc506
cfe102
cfe135
M
stm535
wmc463
6
stm0777tgag
gdm150

7

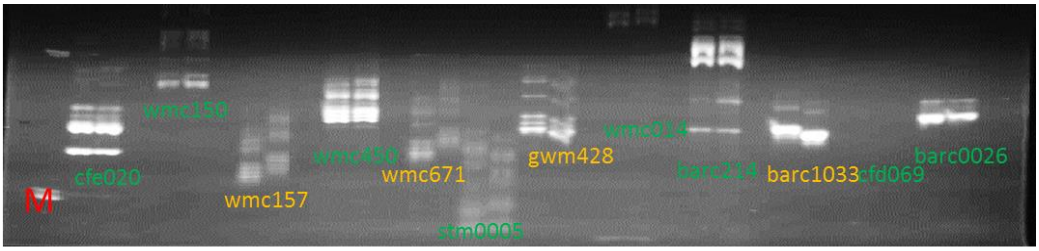
wmc150
wmc314
wmc450
gwm428
barc0026
cfe020
wmc671
barc214
barc1033
cfd069
M
wmc157
stm0005

8

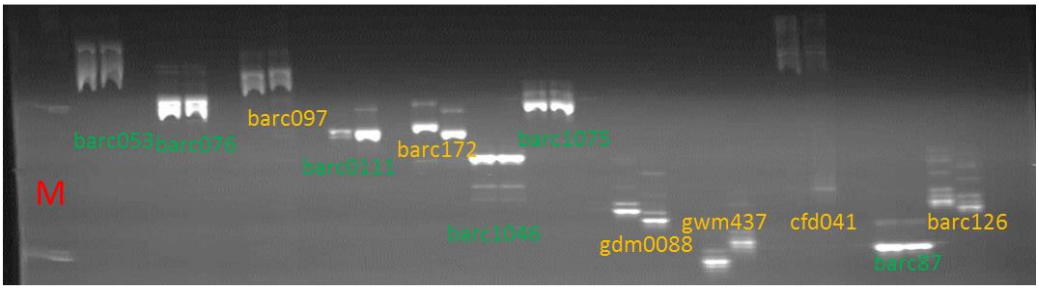
barc097
barc053
barc076
barc172
barc1075
barc0111
M
barc1046
gwm437
cfd041
barc126
gdm0088
barc87

9

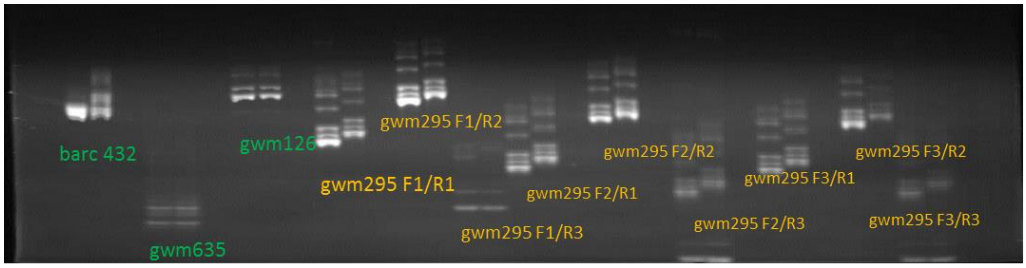

10

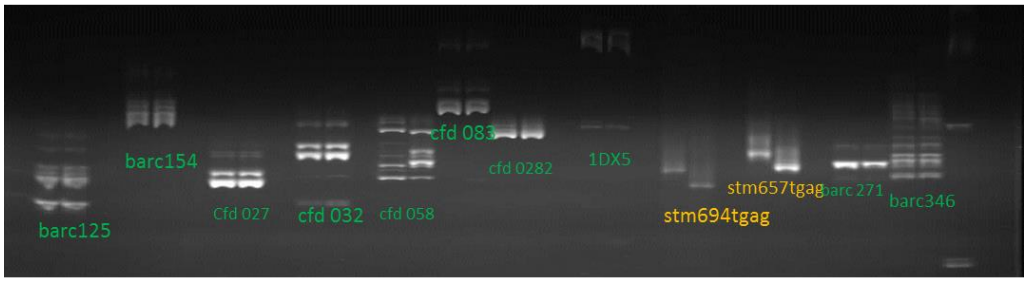

11

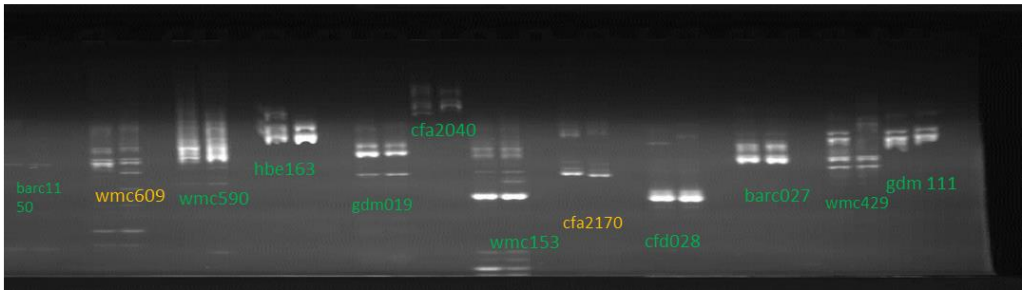

12

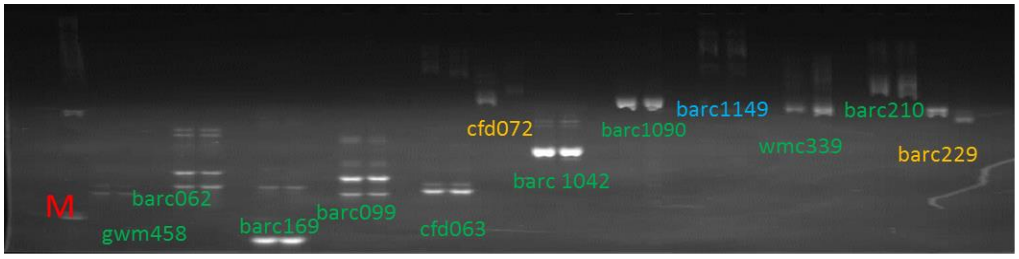

13

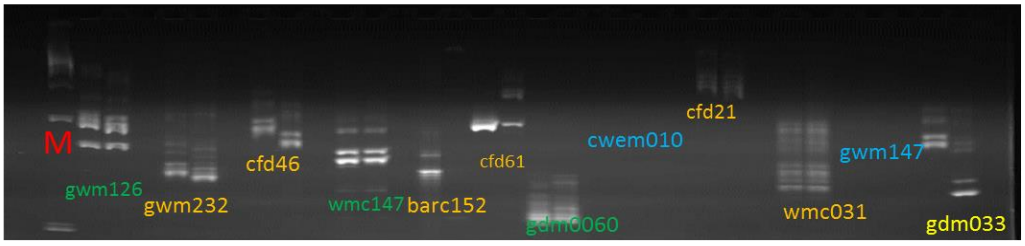

14

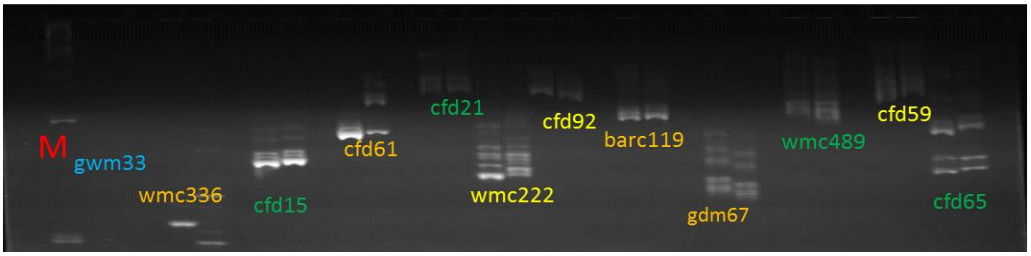

ii) Parents PI 94365 (P1) and EGA Gregory (P2): Screening with 1B SSR markers

15

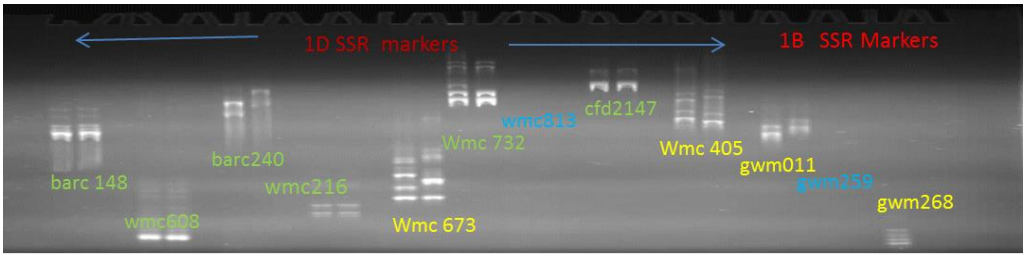

16

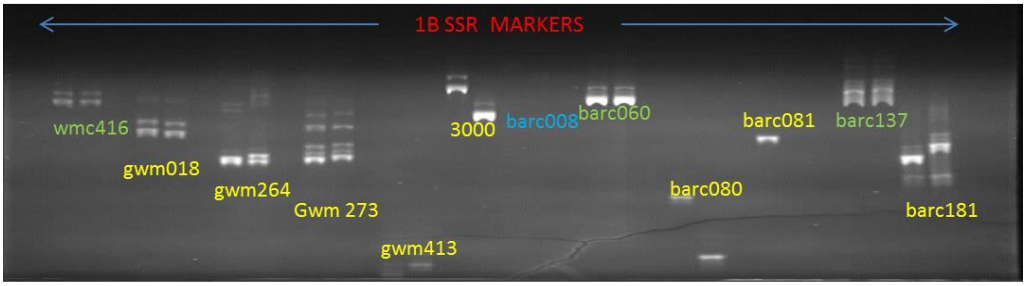

17

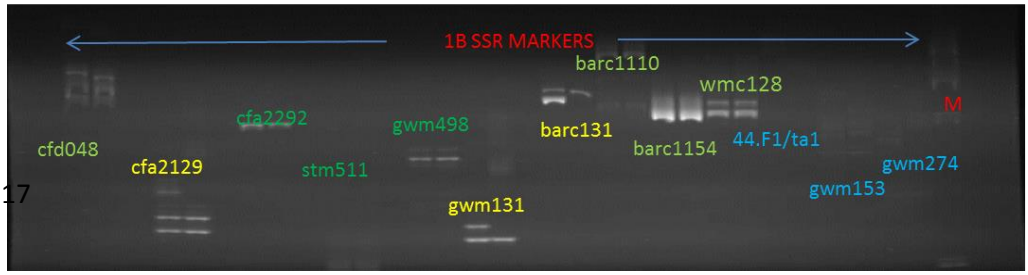

17

iii) Parents PI 94365 (P1) and EGA Gregory (P2): Screening with 7B SSR markers

18

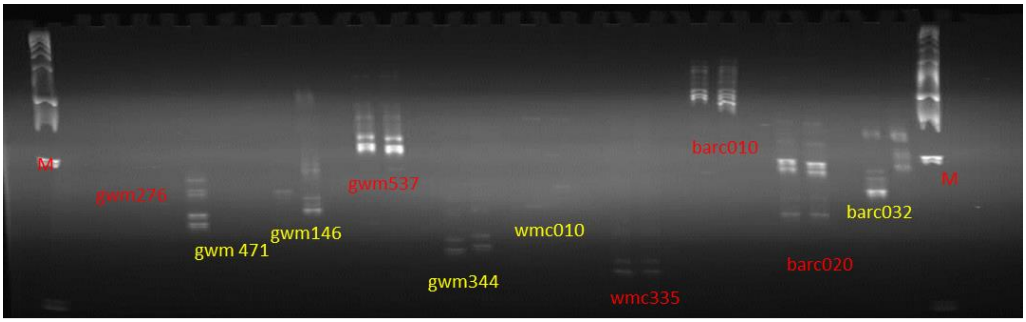

19

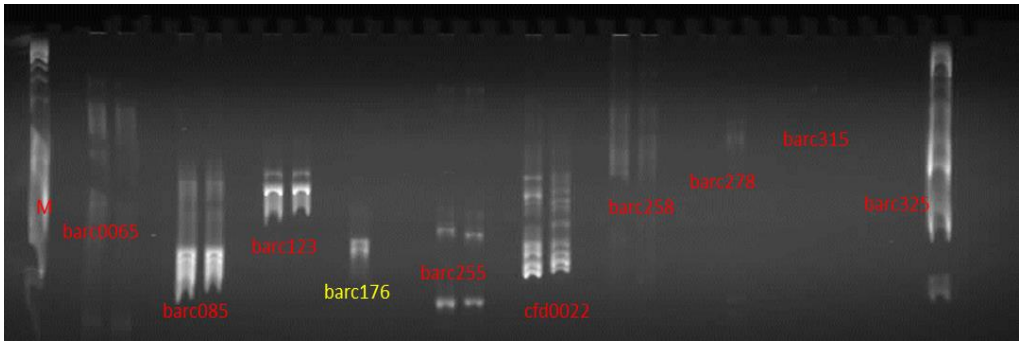
M
barc0065
barc085
barc123
barc176
barc255
cfd0022
barc258
barc278
barc315
barc325

20

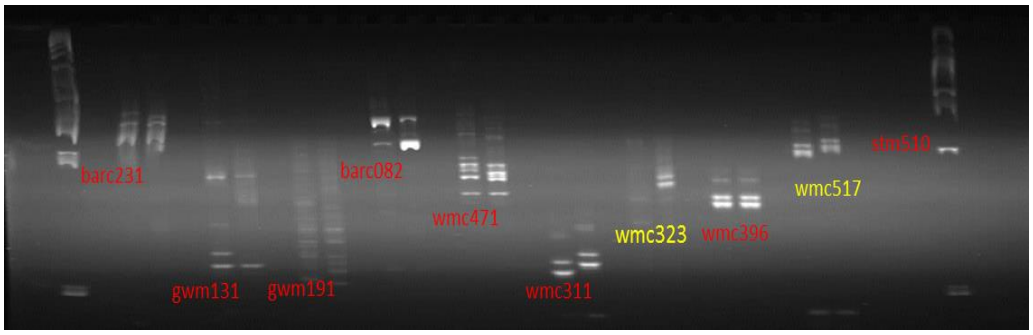
barc231
gwm131
gwm191
barc082
wmc471
wmc311
wmc323
wmc396
wmc517
xlm510

21

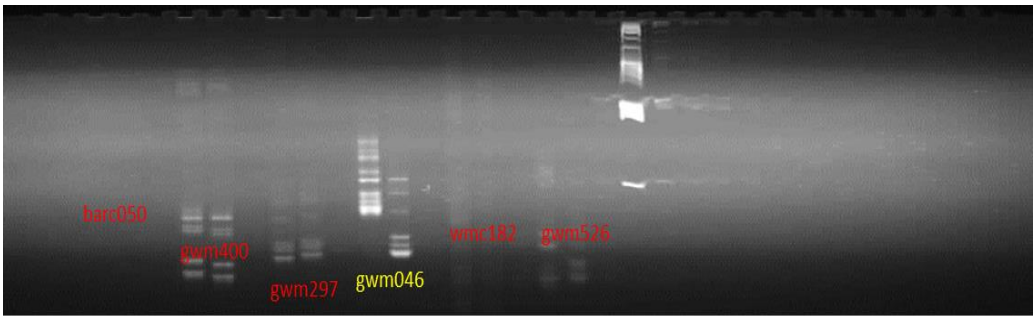
barc050
gwm400
gwm297
gwm046
wmc182
gwm526

Supplementary Table I: Identified polymorphic markers and the type of gels used to screen the DH population

SSR Primers and type of gels used to screen the DH population		
SSR markers	Chromosome	Type of gel
gwm111	7D	PAGE
gwm44	7D	PAGE
cfd 66	7D	Agarose
wmc506	7D	Agarose
barc184	7D	PAGE
wmc698a	7D	PAGE
wmc 698b	7D	PAGE
gwm130	7D	PAGE
barc827	7D	PAGE
wmc 630	7D	PAGE
wmc 473	7D	PAGE
wmc 824	7D	Agarose
wmc797	7D	PAGE
wmc702	7D	PAGE
gwm294	7D	PAGE
cfa2174	7D	PAGE
wmc273	7D	PAGE
gdm145	7D	PAGE
gdm067	7D	PAGE
ta2390	7D	Agarose
stm517a	7D	PAGE
stm517b	7D	PAGE
ta2391a	7D	PAGE
ta2391b	7D	PAGE
stm 92	7D	PAGE
cfd46	7D	Agarose
barc 229 b	1D	PAGE
gwm295	7D	PAGE
gwm106	1D	Agarose
gwm337	1D	PAGE
barc152	1D	Agarose
cfd 72	1D	Agarose
gdm33	1D	Agarose
wmc 336	1D	Agarose
stm 694	1D	Agarose
stm657	1D	Agarose
barc229a	1D	PAGE
gwm232	1D	PAGE
cfa2170	1D	PAGE
gdm067	7D	PAGE
wmc609	1D	Agarose
wmc222	1D	PAGE
barc 080	1B	Agarose
gwm0011	1B	PAGE
gwm273	1B	PAGE
barc 081	1B	Agarose
barc 181	1B	Agarose
cfa2129	1B	PAGE
gwm131a	1B	PAGE
gwm131b	1B	PAGE
psp3000	1B	Agarose
gwm268	1B	Agarose
gwm146	7B	Agarose
barc032	7B	Agarose
gwm471	7B	Agarose
barc176	7B	Agarose
gwm344	7B	PAGE
wmc10	7B	PAGE
wmc517	7B	PAGE
gwm46	7B	Agarose
wmc323	7B	Agarose

Supplementary Table 2: Annotation of putative genes to the wheat genome expressed by RWA infestation at the two leaf wheat growth stages (Z10)

Gene ID	Species	Putative ID	Overlapping Gene(s)	E-val	POPSeq distance (cM)
AB029887	wheat	Sucrose:fructan 6-fructosyltransferase (6-SFT)	Traes_7DS_E373FDD65	0	7D: 0.5685
AB029934	barley	Chitinase	Traes_7BL_265653FAF	0	
AB029934	barley	Chitinase	Traes_1DL_95936DC50	7.2E-138	1D: 48.904
AB029936	wheat	Chitinase III (Chia-3)	Traes_2AL_6162A036E	0	-
AF112966	wheat	Chitinase IV (Chia-4)	Traes_2BL_2D440C559		2B:59.184
AF112967	wheat	β 1,3-glucanase	TRAES3BF043600090CFD_g		
AF384143	wheat	PR protein 1	Traes_5BL_E0E3EC75D	0	
AF384143	wheat	PR protein 1	Traes_5DL_43D95A3FE	0	5D: 30.698
AF384143	wheat	PR protein 1	Traes_7DS_10C38526F1	0	7D: 71.93
AF442967	wheat	Thaumatin-like protein	Traes_5BS_94EB99BCB	0	5B: 14.808
AF442967	wheat	Thaumatin-like protein	Traes_5AS_5EA9F25E9	4.10E-170	
AJ610099	rice	Putative flavanone 3-hydroxylase	Traes_5AL_3C74F0AAC	1.10E-132	5A: 93.664
AJ610099	rice	Putative flavanone 3-hydroxylase	Traes_4BL_09186DE10	5.60E-116	4B: 66.3
AJ611498	rice	Putative phi-1 (PH1)	Traes_7DS_A2F956FD8	0	7D: 76.49
AJ611498	rice	Putative phi-1 (PH1)	Traes_7DS_587BEA50E	2.20E-66	7D: 76.49
AJ611498	rice	Putative phi-1 (PH1)	Traes_7DS_9790B51CE	4.90E-58	7D:76.49
BE424472	rice	Calcium-dependent protein kinase	Traes_6AS_CE8BAAE7A	0	6A: 45.661

BE424472	rice	Calcium-dependent protein kinase	Traes_6BS_814D20B55	2.60E-80	6B: 43.284
BE515437	rice	Glutathione S-transferase (fragment)	Traes_1AL_2103C5913	0	
BE515437	rice	Glutathione S-transferase (fragment)	Traes_1BL_ACE9E7BF8	0	1B: 45.574
BE604247	barley	Putative nematode-resistance protein	TRAES3BF052600030CFD_g	8.90E-80	
BF199967	wheat	Phenylalanine ammonia-lyase	Traes_2AS_958327519	8.60E-59	2A: 59.228
BF199967	wheat	Phenylalanine ammonia-lyase	Traes_2DS_28CA50371	3.00E-49	2D: 64.566
BG606917	barley	Myb4 transcription factor fragment	Traes_2AL_E2F8D46CE	2.30E-133	2A: 58.092
BG606917	barley	Myb4 transcription factor fragment	Traes_2BL_0501BC320	3.50E-92	
BG607332	maize	Roothairless 3	Traes_4AS_85B580603	9.30E-132	4A: 61.05
BG907089	rice	Receptor serine/threonine kinase PR5K-like	TRAES3BF011100130CFD_g	7.10E-85	
BG907089	rice	Receptor serine/threonine kinase PR5K-like	Traes_3AL_B27A64367	1.10E-83	
BJ213107	barley	NBS-LRR disease resistance protein homologue	Traes_5BL_A7C4DAE11	7.80E-83	
BJ213107	barley	NBS-LRR disease resistance protein homologue	Traes_5DL_B89CD8432	7.80E-83	5D: 66.057
BJ214918	barley	NBS-LRR disease resistance protein homologue	Traes_1AS_E6F253266	0	
BJ225818	rice	Putative phi-1 (PH1)	Traes_6AL_635A78EBD	0	6A: 55.893
BJ226189	rice	C2 GRAM domain-containing protein	Traes_6DL_35E566505	0	6D: 52.35
BJ226189	rice	C2 GRAM domain-containing protein	Traes_6BL_17EA654BB	0	6B: 50.104
BJ226189	rice	C2 GRAM domain-containing protein	Traes_6AL_75C0A8A03	0	6A: 52.482
BJ227672	wheat	β 1,3-glucanase (GLG)	TRAES3BF043600010CFD_g	0	

BJ228146	rice	XET precursor		4.20E-110	
BJ229742	rice	Glutathione transferase	Traes_6AS_4FB64483A	0	6A: 30.838
BJ234909	maize	Homocysteine S-methyltransferase 1	Traes_4BL_22522D845	1.30E-139	
BJ239965	rice	ABC transporter permease protein	Traes_2BS_EA016F20A	9.80E-157	2B: 56.91
BJ239965	rice	ABC transporter permease protein	Traes_2AS_D457775D6	8.10E-142	2A: 6.882
BJ243736	rice	Putative phosphatidylinositol phosphatidylcholine transferase protein	Traes_2BL_BA58567071	2.90E-157	2B: 62.594
BJ253690	tulip tree	Laccase (EC 1.10.3.2)	Traes_3DL_CE06741A7	0	3D: 63.905
BJ253690	tulip tree	Laccase (EC 1.10.3.2)	Traes_3B_29C2301AA	9.70E-96	3B: 57.46
BJ254055	wheat	Peroxidase precursor	Traes_2BS_40C683B47	0	2B: 51.794
BJ254055	wheat	Peroxidase precursor	Traes_2AS_BDA6E4F93	5.30E-110	2A: 52.385
BJ264288	rice	Putative potyviral helper protease-interacting protein	Traes_6AL_38CA87B45	0	
BJ264288	rice	Putative potyviral helper protease-interacting protein	Traes_6DL_472B97393	0	
BJ273225	barley	SNAP-34	Traes_7DS_0B170AFF9	0	7D: 13.647
BJ273225	barley	SNAP-35	Traes_4AL_63F62F96F	1.20E-175	4A: 130.505
BJ273225	barley	SNAP-36	Traes_7AS_4393C73C0	7.40E-171	7A: 1.137
BJ281221	wheat	Phenylalanine ammonia-lyase (PAL) fragment	Traes_2BS_88CF42F2E	0	2B: 59.184
BJ281221	wheat	Phenylalanine ammonia-lyase (PAL) fragment	Traes_2DS_28CA50371	4.20E-113	2D: 64.566
BJ281221	wheat	Phenylalanine ammonia-lyase (PAL) fragment	Traes_2AS_958327519	5.60E-100	2A: 59.228
BJ281221	wheat	Phenylalanine ammonia-lyase (PAL) fragment	Traes_1AS_6BDC65775	5.40E-97	1A: 44.512

BJ281221	wheat	Phenylalanine ammonia-lyase (PAL) fragment	Traes_1DS_A171C7D59	1.30E-94	1D: 47.767
BJ281711	rice	Putative UDP-glucose:salicylic acid glucosyltransferase	TRAES3BF154700050CFD_g	0	
BJ285213	rice	Putative polygalacturonase inhibitor		0	
BJ285213	rice	Putative polygalacturonase inhibitor	Traes_7DS_D01759F78	1.90E-41	
BJ285466	rice	AP2 domain-containing transcription factor	Traes_6BL_48B46613A	0	6B: 52.377
BJ285466	rice	AP2 domain-containing transcription factor	Traes_6DL_569FCEEC5	3.80E-132	6D: 59.171
BJ286240	rice	Putative Avr9/Cf-9 rapidly elicited protein	Traes_1BS_C8A500342	0	1B: 44.438
BJ286240	rice	Putative Avr9/Cf-9 rapidly elicited protein	Traes_1DS_A373E79EA	0	1D: 46.631
BJ286240	rice	Putative Avr9/Cf-9 rapidly elicited protein	Traes_1AS_3FCCD2735	0	1A: 44.512
BJ286329	barley	β 1,3-D-glucan glucanohydrolase isoenzyme	TRAES3BF061600100CFD_g	0	
BJ286329	barley	β 1,3-D-glucan glucanohydrolase isoenzyme	Traes_3AL_28186DB96	0	3A: 119.706
BJ296624	barley	UDP-D-glucuronate decarboxylase (fragment)	Traes_1AL_97333ABA1	0	1A: 45.6495
BJ296624	barley	UDP-D-glucuronate decarboxylase (fragment)	Traes_1BL_F439F0D99	0	1B: 45.574
BJ302168	rice	Aucellin-like aspartic protease-like protein)	Traes_2BL_7194A68D3	0	2B: 104.675
BJ306089	rice	Putative cytokinin dehydrogenase		0	
BJ309335	wheat	Putative speckle-type Zn finger domain protein	Traes_3AL_5E1A8E2A9	2.10E-177	3A: 121.979
BJ309335	wheat	Putative speckle-type Zn finger domain protein	TRAES3BF186700010CFD_g	8.20E-140	
BJ321259	rice	Calmodulin-2	Traes_5BS_80C145A13	0	
BJ321259			Traes_5DS_E868D18F7	0	
BQ162134	rice	Shikimate kinase 2	Traes_7AS_069A1FA77	1.30E-113	7AS: 63.946

BQ162134	rice	Shikimate kinase 2	Traes_7BS_32A05019A	6.80E-97	7B: 50.057
BQ162134	rice	Shikimate kinase 2	Traes_7DS_351943FD9	6.80E-60	7D: 77.626
BQ162481	rice	Intramembrane serine protease	Traes_2BL_FAF3BB158	0	2B: 61.457
BQ162481	rice	Intramembrane serine protease	Traes_2DL_8C5162E91	6.10E-69	2D: 67.4075
BQ162481	rice	Intramembrane serine protease	Traes_2AL_B4A22DC4F	9.20E-65	2A: 58.092
BQ165982	wheat	Serine/threonine protein kinase	Traes_2BS_802CF83A9	6.00E-94	
BQ169201	rice	Putative UDP-glucose glucosyltransferase	Traes_6AS_D68761CF8	0	6A: 3.414
BQ169201	rice	Putative UDP-glucose glucosyltransferase	Traes_6DS_EC682031E	0	6D: 9.105
BQ171266	rice	Cell cycle associated protein Mob1-like protein	Traes_6BS_9ADFB4327	4.80E-159	
BQ171266			Traes_6AS_F08087F7F	1.00E-144	6D:27.33
BQ578676	barley	Bowman-Birk type trypsin inhibitor	TRAES3BF168400230CFD_g	1.10E-157	
BT008984	rice	Putative ascorbate oxidase AO4	Traes_7DL_6874E0AF7	0	7D: 83.31
BT008984	rice	Putative ascorbate oxidase AO5	Traes_7AL_BFCA8542E	3.50E-92	
BT008984	rice	Putative ascorbate oxidase AO6	Traes_7BL_BBD987B59	9.80E-65	
BT008992	barley	Lipoxygenase 1	Traes_4BS_63DD9D036	0	
BT008992	barley	Lipoxygenase 1	Traes_4BS_71CB57A0D	0	
BT008992	barley	Lipoxygenase 1	Traes_4AL_AAB70FF2D	0	4A: 62.152
BT008992	barley	Lipoxygenase 1	Traes_4DS_7868A8C2E	0	4D: 43.383
BT009301	rice	Putative sorbitol transporter	Traes_2BS_D5A97B888	0	
BT009301	rice	Putative sorbitol transporter	Traes_2AS_3F30521B9	0	2A: 59.228
BT009301	rice	Putative sorbitol transporter	Traes_2DS_228272C06	0	2D: 63.43
BT009397	rice	Fungal elicitor response gene	TRAES3BF111500010CFD_g	1.40E-163	

BT009397	rice	Fungal elicitor response gene	TRAES3BF104600010CFD_g	1.40E-163	
BT009398	sorghum	LRR-containing glycoprotein precursor	Traes_3AL_CE3238869	1.30E-151	3A: 119.706
BT009398	sorghum	LRR-containing glycoprotein precursor	TRAES3BF047400040CFD_g	2.30E-88	
BT009398	sorghum	LRR-containing glycoprotein precursor	Traes_3DL_CBB57F249	3.40E-81	3D: 93.471
BT0009444	rice	Putative UDP-glucose dehydrogenase	Traes_5BL_7F59B65A3	0	5B: 83.196
BT0009444	rice	Putative UDP-glucose dehydrogenase	Traes_5DL_0A7630D1E	0	5D: 99.049
BT0009444	rice	Putative UDP-glucose dehydrogenase	Traes_4DS_4C6846850	0	4D: 46.794
BT0009444	rice	Putative UDP-glucose dehydrogenase	Traes_4BS_773925576	0	4B: 45.825
BT0009444	rice	Putative UDP-glucose dehydrogenase	Traes_4AL_8845F411B	0	4B: 45.825
BT0009444	rice	Putative UDP-glucose dehydrogenase	Traes_6BL_C22DEC10D	0	6B: 79.672
BT0009444	rice	Putative UDP-glucose dehydrogenase	TRAES3BF041000020CFD_g	0	
BT0009444	rice	Putative UDP-glucose dehydrogenase	Traes_2AL_77DE42E1C	0	
CA599187	rice	Putative Fe-dependent oxidoreductase	Traes_6DL_5EF8EAD26	1.00E-143	6D: 98.054
CA599187	rice	Putative Fe-dependent oxidoreductase	Traes_6DL_915C4E5BF	2.30E-61	6D: 98.055
CA600792	rice	LRR, putative	TRAES3BF072400120CFD_g	1.40E-125	
CA600792	rice	LRR, putative	Traes_3DL_740865E24	3.30E-123	3D: 78.685
CA601808	rice	Putative oxidoreductase	Traes_4DS_D626A2368	0	
CA603417	rice	Putative cytochrome P450	Traes_5BS_007F4E23C	2.70E-122	5B: 4.5509
CA603417	rice	Putative cytochrome P451	Traes_5DS_A8368C6AE	5.60E-108	5D: 2.274
CA603417	rice	Putative cytochrome P452	Traes_5AS_B2C4620E6	3.30E-103	
CA606181	rice	Ankyrin-like protein	Traes_3DL_1652E03C0	1.30E-122	3D: 63.905
CA606181	rice	Ankyrin-like protein	Traes_3AL_1C47C0484	1.20E-110	3A: 64.474
CA606181	rice	Ankyrin-like protein	TRAES3BF117700060CFD_g	1.20E-110	

CA609522	rice	Fiber protein Fb2-like	TRAES3BF154000020CFD_g	1.00E-92	
CA611113	rice	PDR4 ABC transporter	TRAES3BF083100030CFD_g	4.90E-141	
CA611113	rice	PDR4 ABC transporter	TRAES3BF083500030CFD_g	4.90E-141	
CA611113	rice	PDR4 ABC transporter	Traes_3AL_0C1B383C3	2.90E-136	
CA616263	sesame	σ--3 fatty acid desaturase, chloroplast precursor	Traes_4BL_6B4FFC0A8	0	4B: 52.65
CA616263	sesame	σ--3 fatty acid desaturase, chloroplast precursor	Traes_4DL_B75BA7E6C	5.80E-100	4D: 54.756
CA616263	sesame	σ--3 fatty acid desaturase, chloroplast precursor	Traes_4AS_20EAF4CEC	2.00E-90	4A: 57.601
CA623616	rice	LRR-like protein	Traes_6DL_78812C0F5	2.20E-132	
CA623616	rice	LRR-like protein	Traes_6AL_CAC96C59A	1.10E-38	6A: 50.208
CA623872	rice	WRKY10	TRAES3BF003800010CFD_g	6.40E-91	
CA625572	maize	40S ribosomal protein S8	Traes_2BL_7BC3942D6	1.00E-10	4B: 52.65
CA625572	maize	40S ribosomal protein S8	Traes_2AL_1B2CC9926	1.00E-10	2A: 58.66
CA631663	wheat	Endotransglucosylase/hydrolase (XTH5)		0	
CA647624	barley	HGA6 (carbohydrate transport)	TRAES3BF050800220CFD_g	1.10E-144	
CA650490	rice	12-OPDA reductase	Traes_7BS_62CC4CA59	0	7B: 51.193
CA650490	rice	12-OPDA reductase	Traes_7DS_28E2128F3	5.80E-109	7D: 75.353
CA650490	rice	12-OPDA reductase	Traes_7AS_8D22F29A0	2.40E-37	7A: 63.3775
CA651243	rice	Putative flavonol 4'-sulfotransferase	Traes_2BS_D26800667	6.40E-62	
CA652856	wheat	Germin-like protein precursor	Traes_4BL_C77E12A14	0	4B: 84.5
CA652856	wheat	Germin-like protein precursor	Traes_4BL_9965572CD	0	4B: 84.5

CA652948	rice	Glutathione S-transferase	Traes_1BL_A5CC574CF	0	1B: 45.574
CA652948	rice	Glutathione S-transferase	Traes_1DL_645A2ECC0	7.10E-158	1D: 48.904
CA655474	rice	Ethylene-insensitive-3-like protein (EIN3)	Traes_4AS_2BDA1260C	9.40E-158	4A: 61.015
CA655474	rice	Ethylene-insensitive-3-like protein (EIN3)	Traes_4DL_C083C804E	1.20E-104	4D: 54.756
CA662086	rice	Putative SA-binding protein 2	Traes_2BL_3AEB92035	8.70E-81	
CA663807	wheat	Cytochrome P450	Traes_2DS_1E5EB2757	5.00E-152	2D: 0.0
CA663807	wheat	Cytochrome P450	Traes_2AS_ADA59BD4F	4.10E-100	2A: 1.137
CA664763	barley β	glucan endo-1,3- β-glucosidase precursor	TRAES3BF061600100CFD_g	1.20E-26	
CA666521	rice	Putative cytochrome P450	Traes_3DS_90FA62704	1.80E-79	3D: 22.882
CA667998	rice	Putative monoterpene synthase	Traes_6BS_88C7A313B	1.10E-107	6B: 41.01
CA668708	rice	Putative cytochrome P450	Traes_2DL_373A8CB6D	7.60E-44	
CA668708	rice	Putative cytochrome P450	Traes_2AL_53BE4ECB9	1.10E-36	
CA668908	rice	Putative elicitor-inducible cytochrome P450	Traes_5BL_295EE93F9	1.70E-73	5B: 38.2005
CA668908	rice	Putative elicitor-inducible cytochrome P450	Traes_5AL_30D59F68B	3.30E-16	
CA668995	barley	Thaumatin-like protein TLP8	Traes_4AL_586359D761	1.00E-65	4A: 110.042
CA668995	barley	Thaumatin-like protein TLP8	Traes_4BS_3EF8C6FA9	3.70E-56	4B: 19.0935
CA670384	rice	Putative cytochrome P450 monooxygenase	Traes_2AL_53BE4ECB9	7.70E-81	2A: 76.592
CA670445	barley	Methionine synthase 2 enzyme	Traes_4AL_8D0193195	3.70E-76	
CA670456	rice	Glucosyltransferase	Traes_3AS_4B9462BD0	6.80E-104	

CA679100	rice	Oxidoreductase	Traes_2AL_DC3904667	7.30E-103	2A: 58.092
CA679100	rice	Oxidoreductase	Traes_2BL_781BA1506	1.10E-95	2B: 61.457
CA679100	rice	Oxidoreductase	Traes_2DL_F2D3DED15	3.70E-49	2D: 65.703
CA681727	rice	Putative ribosomal protein S29	Traes_4BL_6B4FFC0A8	7.00E-137	4B: 52.65
CA682753	rice	PDR-like ABC transporter	Traes_5BL_AAE5B3832	0	5B: 105.939
CA682753	rice	PDR-like ABC transporter	Traes_5AL_F8FDAC215	5.20E-85	5A: 60.499
CA682753	rice	PDR-like ABC transporter	Traes_5DL_F292F9EA4	1.10E-70	5D: 127.472
CA686606	rice	Putative XET	Traes_7AL_1B1FBCDE4	0	7A: 70.767
CA686606	rice	Putative XET	Traes_7AL_8C4A9BEBF	2.00E-142	7A: 75.315
CA686606	rice	Putative XET	Traes_7DL_AD8F90F24	3.90E-122	7D: 92.408
CA687531	maize	Annexin p33	Traes_7DS_3F6DCEAA8	1.50E-146	7D: 76.49
CA687531	maize	Annexin p33	Traes_7AS_FFB7CAFC3	3.80E-73	7A: 63.946
CA688344	wheat	Hypothet. protein (membrane-attack)	Traes_1DL_CA060EFAD	2.00E-129	1D: 104.613
CA689554	rice	Putative cycloartenol synthase	Traes_5DS_669F20907	6.50E-75	5D: 1.137
CA689554	rice	Putative cycloartenol synthase	Traes_5AS_50A2496B9	3.80E-70	
CA690727	barley	Ent-kaurene synthase-like protein	Traes_2BL_B06E350C2	5.00E-91	2B: 67.141
CA690727	barley	Ent-kaurene synthase-like protein	Traes_2DL_E14B9F774	1.10E-76	2D: 67.976
CA690727	barley	Ent-kaurene synthase-like protein	Traes_2AL_A38A2E415	3.00E-49	2A: 71.9935
CA691758	rice	Putative cytochrome P450	Traes_5AS_44322BC0E	4.40E-57	
CA692409	rice	Sterol 14-demethylase (fragment)	Traes_5DS_E7FDA5B26	5.30E-180	5D: 0.0

CA692789	wheat	PR protein 4	Traes_1AL_ED8C9876C	4.90E-149	1A: 75.781
CA692789	wheat	PR protein 5	Traes_1DL_6EA7A6808	4.50E-106	
CA695230	rice	Putative anthocyanidin hydroxylase	Traes_7AL_9D1BEACC0	4.10E-52	7A: 110.567
CA695230	rice	Putative anthocyanidin hydroxylase	Traes_7DL_A2604A6D5	4.10E-52	7D: 150.625
CA695961	rice	Putative UDP-glucose: flavonoid 7-O-glucosyltransferase	Traes_3DS_9897882C9	4.30E-85	
CA695961	rice	Putative UDP-glucose: flavonoid 7-O-glucosyltransferase	TRAES3BF021800050CFD_g	6.30E-78	
CA695961	rice	Putative UDP-glucose: flavonoid 7-O-glucosyltransferase	TRAES3BF021800030CFD_g	9.80E-77	
CA695961	rice	Putative UDP-glucose: flavonoid 7-O-glucosyltransferase	TRAES3BF022600010CFD_g	7.60E-56	
CA698434	barley	Putative WRKY5 protein	Traes_3AL_AB2BAE660	1.50E-137	
CA698434	barley	Putative WRKY5 protein	TRAES3BF267200010CFD_g	1.30E-125	
CA699183	rice	Cellulose synthase-like A1 (CslA)	Traes_7DL_1A45BDE27	2.60E-102	7D: 84.447
CA699183	rice	Cellulose synthase-like A1 (CslA)	Traes_7AL_FF5852F09	3.70E-95	7A: 68.493
CA699183	rice	Cellulose synthase-like A1 (CslA)	Traes_7BL_D0D116361	1.30E-85	7B: 52.33
CA712411	rice	Hydrolase	Traes_4DS_83607CF31	0	4D: 54.756
CA712411	rice	Hydrolase	Traes_4BS_68EB4B5DA	0	4B: 50.376
CA713419	wheat	Sec61 alpha subunit	Traes_4AS_2D88ED3F8	2.40E-71	4A: 57.601
CA713419	wheat	Sec61 alpha subunit	Traes_4DL_BE50C5130	3.50E-64	
CA715084	rice	UDP-glucuronic acid decarboxylase	Traes_2DS_5AAE4D28E	7.10E-114	2D: 47.514
CA715084	rice	UDP-glucuronic acid decarboxylase	Traes_2BS_170E32572, Traes_2BS_58E7D5315	1.50E-62	2B: 51.226 2B: 51.226

CA717510	Arabidopsis	Receptor protein kinase-like protein	Traes_1AL_7E3623F89	2.30E-130	1A: 50.198
CA717510	Arabidopsis	Receptor protein kinase-like protein	Traes_1DL_53C2C5E14	1.40E-125	1D: 55.725
CA717510	Arabidopsis	Receptor protein kinase-like protein	Traes_1BL_CFD471B75	8.10E-121	1B: 47.847
CA721939	wheat	Thaumatin-like protein	Traes_2AS_84C021B0B	9.00E-170	2A: 52.385
CA721939	wheat	Thaumatin-like protein	Traes_2DL_D267A495A	3.50E-95	
CA732035	wheat	Wall-associated kinase 3	Traes_7DS_E1BFD91BA	0	
CA732035	wheat	Wall-associated kinase 3	Traes_7DS_2F5418BA0	1.90E-152	7D: 44.602
CA732035	wheat	Wall-associated kinase 3	Traes_7DS_303EC152F	3.10E-117	7D: 44.602
CA742640	rice	HGWP repeat containing protein		7.50E-75	
CA744929	rice	Serine/threonine kinase PR5K		1.70E-82	
CA745732	barley	Mlo3	Traes_2BS_DABEABDDC	9.00E-115	2B: 39.274
CD452988	rice	GDSL lipase/acylhydrolase	Traes_1BS_09CBCE13A	0	1B: 44.438
CD452988	rice	GDSL lipase/acylhydrolase	Traes_1AS_C8406F3D5	1.60E-128	1A: 44.512
CD452988	rice	GDSL lipase/acylhydrolase	Traes_1DS_0DF78825D	9.10E-121	
CD863039	wheat	Thaumatin-like protein precursor	Traes_7DL_0FD6D8ED61	0	7D: 157.445
CD863039	wheat	Thaumatin-like protein precursor	Traes_7DL_0FD6D8ED61	4.70E-67	
CD872898	rice	Putative galactosyltransferase	Traes_5DL_3685C6B34	0	5D: 132.591
CD872898	rice	Putative galactosyltransferase	Traes_7AL_8755C994C	0	
CD872898	rice	Putative galactosyltransferase	TRAES3BF083000030CFD_g	0	
CD872898	rice	Putative galactosyltransferase	Traes_6AL_111B6F71F	0	6A: 58.168
CD875437	rice	Putative membrane protein	Traes_4BL_A289962F6	6.60E-133	4B: 58.338

CD883484	rice	Monosaccharide transporter 4	Traes_4DL_CFC191A06	1.20E-153	4D: 54.756
CD883484	rice	Monosaccharide transporter 4	Traes_4BL_2CD045152	1.00E-141	4B: 56.065
CD883484	rice	Monosaccharide transporter 4	Traes_4AS_7258345F9	8.60E-130	4A: 57.601
CD884095	rice	Putative Defective Anther Dehiscence1	Traes_7DL_2A27E826D	5.50E-103	
CD898086	rice	Putative latex-abundant protein	Traes_1DL_F993AE517	2.20E-133	
CD915938	wheat	PR protein 4	PR4B	0	
CD937391	rice	Putat. hydroxyanthranilate hydroxycinnamoyltransferase 3	Traes_6AL_D8A91F983	0	6A: 50.208
CD937391	rice	Putat. hydroxyanthranilate hydroxycinnamoyltransferase 3	Traes_6DL_0D44EDC0E	0	6D: 52.35
CK161752	barley	Putative WRKY1 protein	Traes_7AL_C3FEBECBC	1.30E-176	7A: 103.176
CK161752	barley	Putative WRKY1 protein	Traes_7DL_B09854286	9.50E-150	7D: 130.02
CK163901	rice	NBS-LRR-like protein	Traes_1AS_AAB89883E	0	1A: 19.439
CK163901	rice	NBS-LRR-like protein	Traes_1AS_BF353B963	0	
CK169277	wheat	WIR1A protein (WIR1A)		1.90E-110	
CK93066	rice	Cinnamyl alcohol dehydrogenase (CAD)	Traes_6DS_211935E65	0	6D: 52.35
CK194889	wheat	Nodulin-like protein	Traes_2BS_4EC8C834B	0	2B: 59.184
CK194966	rice	Cellulose synthase-like D2 (CSLD2)		3.60E-167	
CK195830	rice	WRKY12 transcription factor	Traes_1AS_F3EAEC435	0	1A: 39.962

CK195830	rice	WRKY12 transcription factor	Traes_1DS_A6733B734	2.60E-143	1D: 46.631
CK196251	rice	ß-ketoacyl-CoA synthase	Traes_6BS_6ED53953A	0	6B: 48.399
CK196251	rice	ß-ketoacyl-CoA synthase	Traes_6AS_5B857E12F	0	
CK196251	rice	ß-ketoacyl-CoA synthase	Traes_6DS_F359F2588	0	
CK199451	rice	Putative cinnamoyl-CoA reductase	Traes_7BL_63C1B410D	7.80E-153	
CK199508	rice	Peroxidase 3 precursor	Traes_3AS_7E7D5E614	0	
CK199508	rice	Peroxidase 3 precursor	Traes_3DS_1A3A001FA	0	3D: 52.536
CK199508	rice	Peroxidase 3 precursor	TRAES3BF008800150CFD_g	0	
CK205943, FGAS017	barley	Chitinase (Chia)	Traes_1AL_E96C0662D	0	1A: 45.6495
CK205943, FGAS017507	barley	Chitinase (Chia)	Traes_1BL_265653FAF	5.60E-145	1B: 45.574
CK206362	wheat	Sucrose:sucrose 1-fructosytransferase (1-SST)	Traes_7DS_5A68A26E9	6.00E-148	7D: 1.137
CK206362	wheat	Sucrose:sucrose 1-fructosytransferase (1-SST)	Traes_7AS_800D443F5	4.60E-53	7A: 0.0
CK206362	wheat	Sucrose:sucrose 1-fructosytransferase (1-SST)	Traes_7DS_9D51710FD	1.10E-50	7D: 23.88
CK208387	rice	xyloglucan endo-1,4-β-D-glucanase	Traes_6DL_11D060B98	6.20E-108	6D: 52.35
CK208387	rice	xyloglucan endo-1,4-β-D-glucanase	Traes_6AL_E967F4C5D	1.00E-72	6A: 52.482
CK209172	rice	Putative ornithine decarboxylase	Traes_5BL_82626DD6E	0	5B: 62.719
CK209172	rice	Putative ornithine decarboxylase	Traes_5BL_B8424D2E6	2.00E-95	5B: 51.278
CK212487	wheat	Cinnamoyl-CoA reductase (CCR)	Traes_5BL_B007160F8	6.10E-114	5B: 38.769
CK212487	wheat	Cinnamoyl-CoA reductase (CCR)	Traes_5DL_D3F3569E1	1.30E-99	5D: 30.698
CK212487	wheat	Cinnamoyl-CoA reductase (CCR)	Traes_5AL_2DE3A8330	5.80E-74	

CK215460	faba bean	4-coumarate: CoA ligase	Traes_2AS_D86455172	0	2A: 59.228
CK215460	faba bean	4-coumarate: CoA ligase	Traes_2BS_7C174F31D	0	2B: 55.773
CK215460	faba bean	4-coumarate: CoA ligase	Traes_2DS_F6307AF21	0	2D: 58.883
CK215979	rice	Putative phi-1 (PH1)	Traes_7DS_A2F956FD8	5.10E-28	7D: 76.49
CK216158	rice	Putative cupin family protein	Traes_5BL_B92355534	0	5B: 109.35
CK216158	rice	Putative cupin family protein	Traes_5DL_B27E96B65	2.30E-110	5D: 130.316
CK216297	maize	Bet v I allergen	Traes_2DL_BA1B746DF	0	2D: 64.566
CK216297	maize	Bet v I allergen	Traes_2BL_71D9D4D71	2.20E-144	
CK216297	maize	Bet v I allergen	Traes_2AL_71D9D4D71	2.20E-144	
CK216349	rice	Trypsin α-amylase inhibitor	Traes_4BL_251486C33	0	4B: 76.531
CK216349	rice	Trypsin α-amylase inhibitor	Traes_4DL_38FBC0AC7	1.10E-124	
CN009367	Lithospermum	LEDI-5c protein (oxidoreductase)	Traes_6AL_D2DD54576	0	6A: 58.168
CN009367	Lithospermum	LEDI-5c protein (oxidoreductase)	Traes_6BL_5B613F9E5	1.30E-156	
CN009367	Lithospermum	LEDI-5c protein (oxidoreductase)	Traes_6DL_94DCF0B70	5.00E-156	6D: 58.034
CN011869	barley	Xyloglucan endotransglycosylase (XET)	Traes_7DL_0F8CC5C5A	0	7D: 92.408
X85228	human	Super cysteine rich protein (fragment)	Traes_2AS_EE549925C	0	2A: 52.385
X85228	human	Super cysteine rich protein (fragment)	Traes_2DS_2CCCA54C1	0	2D: 47.514
X85228	human	Super cysteine rich protein (fragment)	Traes_2BS_FF5A68083	0	2B: 50.089
Y18212	wheat	glucan endo-1,3- β-glucosidase precursor	Traes_3B_9F3320C78	0	3B: 80.772
Y18212	wheat	glucan endo-1,3- β-glucosidase precursor	TRAES3BF272400060CFD_g	0	
Y18212	wheat	glucan endo-1,3- β-glucosidase precursor	Traes_3B_766459852	8.80E-172	3B: 80.772

AJ613161	rice	Putative phytosulfokine receptor	Traes_6BS_D995329CC	4.30E-131	
AJ613161	rice	Putative phytosulfokine receptor	Traes_6DS_28AC66057	5.00E-106	6D: 49.509
AJ613161	rice	Putative phytosulfokine receptor	Traes_6AS_0A72D3AF5	7.50E-102	
BJ208688	rice	Embryogenesis transmembrane protein-like	Traes_6BL_1753A0518	7.40E-123	
BJ208688	rice	Embryogenesis transmembrane protein-like	Traes_6DL_E00D38C9D	1.10E-115	6D: 94.071
BJ208688	rice	Embryogenesis transmembrane protein-like	Traes_6AL_300B78880	2.50E-73	6A: 86.883
BJ225484	rice	Putative GTP-binding protein	Traes_1DS_CD25033C4	0	1D: 7.36099
BJ225484	rice	Putative GTP-binding protein	Traes_1AS_737669F3E	5.20E-122	1A: 14.7975
BJ229131	rice	Spl7 protein		8.90E-90	
BJ230140	rice	Putative aldose reductase	Traes_1BL_4D2CB33FC	0	
BJ230140	rice	Putative aldose reductase	Traes_1AL_7D7864504	8.90E-106	1A: 49.061
BJ230140	rice	Putative aldose reductase	Traes_1DL_03EFA2FE5	5.10E-61	1D: 54.588
BJ266247	rice	Putative proteophosphoglycan	Traes_3AS_8EA65DABE	0	3A: 33.11
BJ266247	rice	Putative proteophosphoglycan	Traes_3DS_BBC3A1CDB	0	3D: 18.334
BJ272922	rice	Transcription factor	Traes_2DL_DE3909A32	0	2D: 63.998
BJ272922	rice	Transcription factor	Traes_2BL_8FED05903	1.40E-82	2B: 59.184
BJ272922	rice	Transcription factor	Traes_2AL_411B944D6	8.10E-78	
BJ286960	wheat	Blue copper-binding protein homolog	Traes_4AS_705FE3DAC	0	4A: 43.941
BJ286960	wheat	Blue copper-binding protein homolog	Traes_4DL_4448E934B1	0	4D: 53.619
BJ286960	wheat	Blue copper-binding protein homolog	Traes_4BL_CD3262E351	0	4B: 57.7695
BJ292438	rice	BCS1 ATP & nucleotide binding protein	TRAES3BF042900030CFD_g	0	
BJ292438	rice	BCS1 ATP & nucleotide binding protein	Traes_3AL_7658BB10E	0	
BJ292438	rice	BCS1 ATP & nucleotide binding protein	Traes_3DL_71C489A10	0	3D: 53.673

BJ303490	rice	Pectin methylesterase-like protein	Traes_2BL_2A97100CE	0	2B: 62.594
BJ303490	rice	Pectin methylesterase-like protein	Traes_2DL_F4216BDB8	1.40E-144	2D: 66.839
CA486652	rice	Adenylate kinase A (EC 2.7.4.3)	Traes_7BL_580CFC05F	1.40E-19	7B: 52.33
CA486652	rice	Adenylate kinase A (EC 2.7.4.3)	Traes_7DL_A79EE6AAB	1.40E-19	7D: 83.31
CA486652	rice	Adenylate kinase A (EC 2.7.4.3)	Traes_7AL_B7810831E	5.60E-19	
CA593441	timothy	Calcium binding pollen allergen Phl p 7	Traes_7DS_5A98193E8	2.50E-142	7D: 83.31
CA593441	timothy	Calcium binding pollen allergen Phl p 8	Traes_7BS_EF0C06C5F	1.50E-137	7B: 51.193
CA593441	timothy	Calcium binding pollen allergen Phl p 9	Traes_7AS_C8C2CACD2	4.40E-113	
CA598178	barley	Nonspecific lipid-transfer protein precursor	Traes_3AS_5A72CA3A7	5.10E-177	3A: 28.475
CA598178	barley	Nonspecific lipid-transfer protein precursor	Traes_3AS_989FF6506	1.30E-106	
CA598178	barley	Nonspecific lipid-transfer protein precursor	TRAES3BF088300030CFD_g	1.10E-57	
CA606493	rice	Putative Rho GTPase activating protein 2	Traes_2BL_C7941CDEA	2.90E-59	2B: 60.8885
CA606493	rice	Putative Rho GTPase activating protein 2	Traes_2DL_207E2CB39	2.50E-47	2D: 66.271
CA606852	rice	Putative FEG protein	Traes_5DL_00CC4EBD8	7.70E-130	5D: 32.972
CA606852	rice	Putative FEG protein	Traes_5AL_EC434AE0F	1.60E-115	
CA611762	rice	Putative nucleic acid binding protein	Traes_5AL_9831F9D10	1.20E-64	5A: 5.684
CA611762	rice	Putative nucleic acid binding protein	Traes_5BL_660EDC9D6	1.70E-57	5B: 42.18
CA611762	rice	Putative nucleic acid binding protein	Traes_5DL_E5937D0E5	4.20E-55	
CA616450	maize	Physical impedance induced protein e-39,	Traes_4DL_B81290546	3.50E-18	
CA616450	maize	Physical impedance induced protein e-39,	Traes_4DL_8DA9F53C4	3.50E-18	
CA631461	barley	Amino acid selective channel protein	Traes_2AL_1CC5CC248	1.90E-50	
CA631461	barley	Amino acid selective channel protein	Traes_1DS_0D10FE51D	1.90E-50	1D: 18.194

CA631461	barley	Amino acid selective channel protein	Traes_1DS_D1B39A182	4.00E-36	
CA649400	rice	Putative PrMC3	Traes_2DL_CCACAED41	1.20E-137	
CA649400	rice	Putative PrMC3	Traes_2BL_9DBC04D47	1.70E-127	2B: 61.457
CA649400	rice	Putative PrMC3	Traes_2AL_E398F4EFA	2.80E-55	
CA655789	rice	Putative tonoplast membrane integral protein	Traes_4DL_BB4D6F40A	5.10E-146	4D: 87.845
CA683302	rice	Glutathione synthetase	Traes_7DL_CCBA1A1C9	6.00E-66	7D: 95.819
CA683302	rice	Glutathione synthetase	Traes_7BL_39451C0EC	2.10E-56	7B: 63.702
CA683302	rice	Glutathione synthetase	Traes_7AL_E58674B35	5.20E-54	7A: 71.904
CA694274	barley	b-D-glucan exohydrolase isoenzyme	Traes_5BL_5A2634836	1.30E-76	5B: 75.239
CA694274	barley	b-D-glucan exohydrolase isoenzyme	Traes_5BL_2136D403E	1.30E-76	5B: 82.059
CA694274	barley	b-D-glucan exohydrolase isoenzyme	Traes_5BL_8512C24F7	3.30E-74	5B: 82.059
CA694274	barley	b-D-glucan exohydrolase isoenzyme	Traes_5DL_5C048C7F2	8.00E-72	
CA719923	rice	Putative proline-rich protein APG	Traes_6DL_5BA85C611	0	6D: 54.625
CA719923	rice	Putative proline-rich protein APG	Traes_6AL_7589287BA	1.40E-143	
CA731030	rice	OSJNBa0011J08.14 protein	Traes_2BL_7041808D3	1.00E-163	2B: 61.457
CA731030	rice	OSJNBa0011J08.14 protein	Traes_2DL_5D3E73A0C1	2.20E-81	
CA741282	barley	Possible membrane protein LEM1	TRAES3BF078400030CFD_g	6.40E-100	
CK202183	rice	Putative B12D protein	Traes_1BL_72EC293D2	1.80E-82	1B: 92.205
CK212220	sugarcane	Mitochondrial alternative oxidase 1d	Traes_2BL_EA2B95CF0	0	2B: 67.141
CK212220	sugarcane	Mitochondrial alternative oxidase 1d	Traes_2AL_8394449B2	0	2A: 73.182
CK212407	wheat	Putative vacuolar defense protein precursor	Traes_2BL_3F5D23C05	1.60E-157	

CK212407	wheat	Putative vacuolar defense protein precursor	Traes_2DL_83EBEFBDC	8.70E-147	
CK212407	wheat	Putative vacuolar defense protein precursor	Traes_2BL_5FF85C7F2	8.40E-144	2B: 97.854
BJ276052	rice	DNA integration protein	TRAES3BF089500140CFD_g	0	
BJ310258	rye	b-glucosidase (EC 3.2.1.21)	Traes_2BL_5FC6CBB43	0	2B: 103.538
BJ312602	rice	Putative ankyrin-like protein	TRAES3BF109900090CFD_g	1.40E-85	
BQ162573	rice	Putative oxoglutarate-dependent oxygenase	Traes_4BS_1C192AB4C	0	
BQ483424	rice	Putative S-adenosyl-L-methionine:JA	TRAES3BF044100020CFD_g	0	
BQ483424	rice	Putative S-adenosyl-L-methionine:JA	Traes_3AL_0F5702460	2.50E-136	3A: 71.861
BQ483424	rice	Putative S-adenosyl-L-methionine:JA	Traes_3DL_C68E9E205	2.00E-118	3D: 71.864
BQ5789758	maize	Lipoxygenase (Fragment)	Traes_6AS_9557563D1	3.20E-164	
BQ5789758	maize	Lipoxygenase (Fragment)	Traes_6BS_B26FD03C8	3.90E-142	
BU672305	wheat	Jasmonate-induced protein	Traes_2BS_A1F541056	4.80E-172	
BU672305	wheat	Jasmonate-induced protein	Traes_2AS_A14DCEE75	2.80E-167	2A: 32.441
CA600349	rice	Putative tafazzin isoform	TRAES3BF111600230CFD_g	0	
CA610518	rice	O-methyltransferase	Traes_4DS_50708AF98	6.70E-81	4D: 53.6195
CA610518	rice	O-methyltransferase	Traes_4BS_410CDF5FA	1.60E-78	4B: 50.376
CA610518	rice	O-methyltransferase	Traes_4AL_B2F48F9FA	3.40E-64	4A: 63.288
CA614158	rice	Putative glyoxysomal fatty acid	Traes_1AL_792843F86	1.90E-87	1A: 45.6495
CA614158	rice	Putative glyoxysomal fatty acid	Traes_1DL_DD2D363B3	1.40E-63	1D: 52.314
CA615345	rice	Putative oxidase-like	Traes_7DL_106F36D5F	0	7D: 82.7415

CA615345	rice	Putative oxidase-like	Traes_1DS_27349324C	8.30E-102	1D: 0.0
CA620148	rice	Putative NRAMP metal ion transporter 1	Traes_7BL_CA6B7C9E6	4.30E-18	7B: 64.839
CA620148	rice	Putative NRAMP metal ion transporter 1	Traes_7DL_26A2F4353	4.30E-18	7D: 103.825
CA620148	rice	Putative NRAMP metal ion transporter 1	Traes_7AL_08B2A7BB2	1.10E-15	
CA649528	barley	Subtilisin-chymotrypsin inhibitor 2	Traes_2AS_D5CD0FD7B	1.50E-59	2A: 59.228
CA660270	rice	Putative disease resistance response protein		1.40E-60	
CA663614	rice	Putative allergen Amb a I.2 (*Amb a II*)	Traes_2AS_9095E0ACC	2.00E-56	2A: 31.873
CA680802	rice	Putative alpha-mannosidase	Traes_1BS_CDAE82BB5	0	1B: 44.438
CA680802	rice	Putative alpha-mannosidase	Traes_1AS_1D5A1B790	2.20E-149	1A: 44.512
CA694095	wheat	Wali3 protein	Traes_1AL_326B4C863	6.40E-105	1A: 45.6495
CA694095	wheat	Wali3 protein	Traes_1DL_260008870	3.50E-57	1D: 54.588
CA697581	wheat	Xylanase inhibitor (fragment)	Traes_3B_B28A8F1C01	7.70E-109	3B: 77.361
CA725665	rice	Putative flavonol glucosyltransferase	Traes_2BL_DDCBD9F84	2.00E-179	2B: 67.141
CA727746	rice	Ubiquitin conjugating enzyme	Traes_5DL_251556B19	0	5D: 35.245
CA727746	rice	Ubiquitin conjugating enzyme	Traes_2AS_2CCF129C3	0	
CA727746	rice	Ubiquitin conjugating enzyme	Traes_5BL_2BFDDEF4A	0	5B: 39.905
CA729248	rice	Putative regulator of gene silencing	Traes_7BL_AABF91B01	7.80E-65	7B: 109.456
CA744340	Arabidopsis	F8K7.7 protein (zinc ion binding)	Traes_1BL_F95F2B116	0	1B: 47.847
CD490932	maize	Putative glutathione peroxidase	Traes_2DL_1827C450E	3.90E-37	2D: 65.703

CD490932	maize	Putative glutathione peroxidase	Traes_2AL_97834165F	9.50E-35	
CA491198	rice	Putative glutathione peroxidase	Traes_7AS_634102ABF	4.50E-49	7A: 59.4
CA491198	rice	Putative glutathione peroxidase	Traes_7DS_546D3927E	1.10E-46	7D: 68.529
CA491198	rice	Putative glutathione peroxidase	Traes_7BS_8F739045B	6.50E-42	7B: 45.51
CD878492	rice	Putative malate dehydrogenase	Traes_4DL_1184F6F68	4.70E-169	
CD878492	rice	Putative malate dehydrogenase	Traes_4DL_8DBE42AE9	6.00E-42	
CD878492	rice	Putative malate dehydrogenase	Traes_7DS_309E71F44	5.40E-33	7D: 83.31
CD878492	rice	Putative malate dehydrogenase	Traes_7BL_0367BBFE6	1.30E-30	7B: 51.193
CD887052	rice	Plastocyanin-like domain, putative	Traes_4AL_CB363FBCA	0	
CK212638	barley	Putative calcium binding EF-hand protein	Traes_3AL_EEC97C32A	0	3A: 57.08
BJ269262	rice	DNA integration protein	Traes_1DS_474BD1144	0	1D: 47.767
BJ269262	rice	DNA integration protein	Traes_1AL_1DD0385D1	0	1A: 44.512
BJ269262	rice	DNA integration protein	TRAES3BF171400010CFD_g	0	
BJ299555	*C. intestinalis*	Trypsin inhibitor precursor	Traes_7BS_B6D10760B	3.5	7B: 51.193
			Traes_7DS_EC365BE37	3.5	7D: 82.173
BJ309490	rice	Pectin methylesterase-like protein	Traes_2DS_F48543AA3	2.90E-127	2D: 10.231
BJ317014	rice	Putative Aux/IAA protein	Traes_3AL_E77F7C3EE	0	3A: 57.08
BJ317014	rice	Putative Aux/IAA protein	TRAES3BF128700030CFD_g	5.80E-109	
BQ161714	rice	Putative Nt-gh3 Auxin-responsive protein		1.50E-63	
CA485835	rice	F-box family protein-like	Traes_7DS_80767C575	5.30E-42	7D: 54.835
CA485835	rice	F-box family protein-like	Traes_7BS_3353D684C	1.90E-32	7B: 39.828
CA485835	rice	F-box family protein-like	Traes_7DS_DE9D90A75	3.80E-15	7D: 54.835

CA502685	beetle	Ribosomal protein S6e (Fragment)		0.0074	
CA599171	barley	Putative acid phosphatase	Traes_4AL_6A6B3238A	5.70E-106	4A: 133.916
CA6000350	rice	Putative β-N-acetylhexosaminidase	Traes_5BL_9663AB85C	2.40E-85	
CA608970	rice	electron transport protein	Traes_2DS_AF94BF729	4.10E-82	
CA608970	rice	electron transport protein	Traes_2AS_A71D3F635	6.20E-78	
CA609394	wheat	ATP binding factor	Traes_7DL_B4943E029	1.20E-63	7D: 83.31
CA609394	wheat	ATP binding factor	Traes_7AL_B951370C7	7.30E-59	
CA609394	wheat	ATP binding factor	Traes_7BL_6A2BED3EA	4.40E-54	7B: 52.33
CA610415	Arabidopsis	Nuclear protein-like binding protein	Traes_6AS_62FDBBB97	1.20E-70	
CA610415	Arabidopsis	Nuclear protein-like binding protein	Traes_6DS_4362C4E69	1.80E-63	6D: 48.941
CA610415	Arabidopsis	Nuclear protein-like binding protein	Traes_6BS_F5F3DB535	4.30E-61	6B: 46.694
CA623021	rice	Putative gag-pol		6.30E-88	
CA640252	Arabidopsis	At5g19740	Traes_3AL_37C86BCBE	1.20E-73	
CA640252	Arabidopsis	At5g19740	Traes_3DL_A7709BD6A	2.50E-59	3D: 54.81
CA640252	Arabidopsis	At5g19740	TRAES3BF128500020CFD_g	3.60E-52	
CA650443	rice	Putative RNA apurinic site specific lyase		2.00E-56	
CA665172	oat	Aux/IAA1 (Fragment)	Traes_7BL_74071485F	2.50E-59	7B: 51.193
CA665172	oat	Aux/IAA1 (Fragment)	Traes_7AL_354EEE44E	3.70E-52	7A: 66.22
CA701100	rice	Tetratricopeptide repeat protein 2-like	Traes_3AL_7741152E8	2.30E-170	3A: 53.669
CA701100	rice	Tetratricopeptide repeat protein 2-like	Traes_3DL_CBEBE7EF1	2.00E-158	3D: 53.673

CA701100	rice	Tetratricopeptide repeat protein 2-like	TRAES3BF093800050CFD_g	2.00E-158	
CA708090	tobacco	60S ribosomal protein L34	Traes_2BL_26CA9BD3B	2.00E-13	2B: 59.184
CA708090	tobacco	60S ribosomal protein L34	Traes_2DL_65004C5E2	2.00E-13	2D: 64.566
CA708090	tobacco	60S ribosomal protein L34	Traes_7BL_54CCDE40A	1.90E-10	7B: 51.193
CA735785	rice	Putative plastid protein SufE	Traes_5BL_66571C27E	0	5B: 38.769
CA735785	rice	Putative plastid protein SufE	Traes_5AL_C26099CEE	0	
CA735785	rice	Putative plastid protein SufE	Traes_5DL_61509ABD3	0	5D: 30.698
CA741208	rice	Putative 5'-phosphoribosyl-	Traes_5DS_DBCD62DF1	1.30E-85	5D: 28.425
CA741208	rice	Putative 5'-phosphoribosyl-	Traes_5AS_F14DBBA24	3.10E-83	
CD491471	rice	OSJNBb0116K07.9 protein	Traes_2AL_FA2B835E7	1.00E-40	2A: 58.092
CD491471	rice	OSJNBb0116K07.9 protein	Traes_2BL_270665D27	3.70E-34	2B: 59.184
CD491471	rice	OSJNBb0116K07.9 protein	Traes_2DL_0EF1AAF53	1.50E-33	2D: 67.976
CD878492	rice	Putative malate dehydrogenase	Traes_4DL_1184F6F68	100.0 [Alignment]	
CK154333	wheat	S-adenosylmethionine decarboxylase	Traes_2BL_D80441793	1.90E-67	2B: 59.184
CK163272	rice	Growth-regulating factor 1	Traes_6DL_4C3F04219	0	
CK163272	rice	Growth-regulating factor 1	Traes_6AL_F5BFFCA3E	2.30E-76	
CK213306	Arabidopsis	26S proteasome subunit RPN12	Traes_2DL_D5E96F74C	390	
CK213306	Arabidopsis	26S proteasome subunit RPN13	Traes_2BL_F130ED628	222	2B: 66.004
CK215961	rice	Transcription Factor	Traes_2BL_8FED05903	4.40E-127	2B: 59.184
AB107992	wheat	PISTILLATA-like MADS box protein	TRAES3BF021600020CFD_g	0	
AB107992	wheat	PISTILLATA-like MADS box protein	Traes_3DL_D6A294E13	8.40E-73	3D: 71.864

AY280870	wheat	MADS-box protein TaVRT-1 (VRN-B1)	Traes_5BL_5D2D22E67	0	
AY280870	wheat	MADS-box protein TaVRT-1 (VRN-B1)	Traes_5BL_89636D032	0	5B: 82.6275
AY280870	wheat	MADS-box protein TaVRT-1 (VRN-B1)	Traes_5DL_9CC4EC839	0	5D: 99.049
BE430349	rice	Putative UVB-resistance protein (UVR8)	Traes_6AS_ACCBA9D69	4.70E-141	6A: 50.208
BE430349	rice	Putative UVB-resistance protein (UVR8)	Traes_6DS_C1B74A6EC	8.90E-118	6D: 52.35
BE430349	rice	Putative UVB-resistance protein (UVR8)	Traes_6BS_FE73D78BF	1.30E-73	6B: 47.831
BJ259919	rice	OSJNBb0038F03.10 protein (transcription)	Traes_2DL_640A09678	0	2D: 84.4585
BJ259919	rice	OSJNBb0038F03.10 protein (transcription)	Traes_2AL_C3E7F1648	1.90E-174	
BJ259919	rice	OSJNBb0038F03.10 protein (transcription)	Traes_2BL_0C41F5FAB	3.90E-160	
BJ290995	rice	Putative cytochrome P450	Traes_1DL_BD82CC61E	0	
BJ319268	rice	Receptor-like protein kinase-like protein	Traes_2DS_EE4E7DC1E	0	
BJ319268	rice	Receptor-like protein kinase-like protein	Traes_2BS_17EF3E7AE	0	
BJ319268	rice	Receptor-like protein kinase-like protein	Traes_2AS_A17B8569B,	1.50E-162	
BQ161248	rice	Putative cyclopropane synthase	Traes_2AL_A53F5D5BC	5.40E-140	2A: 92.517
BQ161248	rice	Putative cyclopropane synthase	Traes_2BL_5A742B6A6	7.10E-53	
BQ172090	rice	Phospholipase-like	Traes_3DS_74DA6D960	2.20E-138	3D: 38.873
BQ172090	rice	Phospholipase-like	TRAES3BF057900120CFD_g	3.50E-66	
BQ172090	rice	Phospholipase-like	Traes_3AS_C8BDBC0AA	3.30E-60	
BQ806534	wheat	5a2 protein (Fragment)	Traes_1BS_E67B9B190	2.40E-167	1B: 43.301
BQ806534	wheat	5a2 protein (Fragment)	Traes_1AS_9385680A1	5.00E-153	
BQ806534	wheat	5a2 protein (Fragment)	Traes_1DS_321E8C254	1.20E-150	
CA620519	rice	Hypothetical mitochondrial ATP synthase	TRAES3BF086900030CFD_g	6.20E-57	

CA620519	rice	Hypothetical mitochondrial ATP synthase	Traes_3AL_D1E4DF6E4,	4.80E-36	
CA620520	rice	Hypothetical mitochondrial ATP synthase	Traes_3AL_D56D8DC9B	4.80E-36	
CA620519	rice	Hypothetical mitochondrial ATP synthase	Traes_3DL_67E978DB8	4.80E-36	3D: 53.673
CA625310	rice	MutT/nudix protein-like	Traes_7AS_6D3C580F7	1.50E-26	7A: 32.091
CA625310	rice	MutT/nudix protein-like	Traes_7DS_BCC35B081	3.20E-15	7D: 44.602
CA635043	rice	Putative Pollen specific protein C13	Traes_6AL_55EAD553E	9.00E-155	6A: 55.893
CA635043	rice	Putative Pollen specific protein C14	Traes_6DL_81A50FE0F	2.00E-143	6D: 54.625
CA635043	rice	Putative Pollen specific protein C15	Traes_6BL_FFD1C6858	9.70E-124	6B: 50.104
CA641356	rice	Putative cell division control protein 6	Traes_3B_AAF753E78	2.20E-53	
CA641356	rice	Putative cell division control protein 6	Traes_3DL_D292A338C	3.10E-46	3D: 63.905
CA641356	rice	Putative cell division control protein 6	Traes_3AL_B8DBDA3BD	3.10E-46	
CA659851	rice	Putative ADP-ribosylation factor	Traes_2DL_A81EE80A5	7.50E-75	2D: 65.703
CA659851	rice	Putative ADP-ribosylation factor	Traes_2AS_266235910	4.40E-70	
CA659851	rice	Putative ADP-ribosylation factor	Traes_2DL_A00550722	1.00E-61	2D: 66.839
CA693401	rice	Putative response regulator 9	Traes_6AL_9C9D677D4	7.80E-66	6A: 82.334
CA693401	rice	Putative response regulator 9	Traes_6DL_D1C9CE275	7.80E-66	6D: 83.8005
CA742602	rice	OSJNBa0084A10.7 protein	Traes_2AL_7A5A9C6BF,	4.10E-116	2A: 58.66
CA742602	rice	OSJNBa0084A10.7 protein	Traes_2BL_73CE59958	6.00E-109	2B: 59.184
CA742602	rice	OSJNBa0084A10.7 protein	Traes_2DL_79CAEA964	1.50E-106	2D: 64.566
CA743352	rice	OSJNBa0071I13.9 protein	Traes_2BL_343D6F661	6.70E-84	2B: 72.825
CA743352	rice	OSJNBa0071I13.9 protein	Traes_2AL_40EA9EC7F	4.00E-79	2A: 81.15
CA743352	rice	OSJNBa0071I13.9 protein	Traes_2DL_E148EE533	9.70E-77	2D: 78.7745
CD453571	rice	Putative glutathione S-transferase	TRAES3BF061700060CFD_g	7.10E-180	

CD453571	rice	Putative glutathione S-transferase	Traes_3AL_D45F1F789	5.60E-125	
CD453571	rice	Putative glutathione S-transferase	TRAES3BF061700020CFD_g	6.30E-97	
CD453571	rice	Putative glutathione S-transferase	Traes_3DL_1028CA135	9.80E-96	3D: 98.022
CD490640	rice	Putative LRR protein (ER - Golgi transport)	Traes_7BL_A51BC9795	1.80E-29	7B: 55.744
CD490640	rice	Putative LRR protein (ER - Golgi transport)	Traes_7AL_7B680A58E	1.80E-29	7A: 69.63
CD490640	rice	Putative LRR protein (ER - Golgi transport)	Traes_7DL_E9231DFA4	2.70E-22	7D: 90.133
CD491373	rice	Putative ABA-responsive protein	Traes_1DL_23B562CE2	6.50E-42	1D: 45.242
CD491373	rice	Putative ABA-responsive protein	Traes_1AL_EABE06C30	1.00E-40	1A: 44.512
CD491373	rice	Putative ABA-responsive protein	Traes_1BL_D769DF7F5	6.00E-36	1B: 45.574
CD921471	barley	ß-glucosidase	Traes_2DS_65B31416B	3.90E-121	2D: 56.609
CD928919	wheat	Putative b-xylosidase (Fragment)	Traes_6DL_E56964DA7	0	
CK208366	rice	Putative NAC domain protein NAC1	Traes_7AL_BFBB2AD1E	0	7A: 66.22
CK208366	rice	Putative NAC domain protein NAC2	Traes_7DL_BDD45DB24	2.10E-178	7D: 84.447
BJ231486	rice	Putative pectinacetylesterase	Traes_2AS_06B3F30C8	0	2A: 59.228
BJ231486	rice	Putative pectinacetylesterase	Traes_2BS_BEECCA499	4.20E-92	2B: 55.773
BJ231486	rice	Putative pectinacetylesterase	Traes_2DS_0791E6C67	5.20E-73	2D: 58.883
BJ252983	frog	EPAB protein	Traes_4AS_A32530635	1.80E-168	4A: 57.601
BJ252983	frog	EPAB protein	Traes_4DL_CA58A2B49	2.50E-161	4D: 54.756
BJ252983	frog	EPAB protein	Traes_4BL_02C5DD16F	2.50E-161	4B: 57.201
BJ280134	rice	Putative class III peroxidase 106 precursor	TRAES3BF082100020CFD_g	4.90E-147	
BJ315672	rice	Putative kinase-binding protein 1		1.40E-05	

BJ318774	rice	Putative FHA domain	Traes_4BS_01676C7E0	0	4B: 50.376
BJ318774	rice	Putative FHA domain	Traes_4AL_769FF73F6	2.80E-161	4A: 61.5835
BJ318774	rice	Putative FHA domain	Traes_4DS_149AF313B	8.80E-143	4D: 54.756
BQ607159	rice	Putative tuber-specific & sucrose-responsive binding factor	Traes_4AS_A79A68739	1.40E-14	4A: 9.1090
BQ607159	rice	Putative tuber-specific & sucrose-responsive binding factor	Traes_4BL_545A5716E	3.30E-06	4B: 60.612
BQ607159	rice	Putative tuber-specific & sucrose-responsive binding factor	Traes_4DL_D41CB81EA	5.10E-05	4D: 61.58
BT009179	rice	OSJNBb0089B03.6 protein	Traes_2BL_11A4F903B	2.10E-72	2B: 59.184
BT009179	rice	OSJNBb0089B03.6 protein	Traes_2AL_D4BF4AE24	3.00E-65	2A: 58.66
BT009179	rice	OSJNBb0089B03.6 protein	Traes_2DL_8F04980F0	1.30E-70	2D: 64.566
CA598474	rice	OSJNBa0016N04.15 protein	Traes_7DL_F0110933B	3.20E-80	
CA601620	rice	Putative WD repeat domain 45	TRAES3BF063600170CFD_g	7.70E-149	
CA617565	rice	Auxin response factor 2 (fragment)	TRAES3BF001100080CFD_g	9.80E-21	
CA617565	rice	Auxin response factor 2 (fragment)	Traes_3AL_5935773EA	9.50E-18	
CA617565	rice	Auxin response factor 2 (fragment)	Traes_3AL_7A2CED8E7	9.50E-18	
CA617565	rice	Auxin response factor 2 (fragment)	Traes_3DL_1FC3735D9	5.80E-16	3D: 80.3905
CA621406	rice	Putative urease accessory protein G	Traes_1BL_EB3E94642	5.50E-08	1B: 87.658
CA621406	rice	Putative urease accessory protein G	Traes_1AL_287433591	2.20E-07	1A: 108.554
CA623910	rice	Putative mitochondrial receptor subunit	TRAES3BF092600010CFD_g	3.40E-15	
CA623910	rice	Putative mitochondrial receptor subunit	Traes_3DL_2F6E2A1EA	8.10E-10	3D: 74.138
CA623910	rice	Putative mitochondrial receptor subunit	Traes_3AL_BC81D5BF3	2.00E-10	3A: 80.9605

CA638864	rice	OSJNBa0027H09.6 protein	Traes_2AS_E5D366E76	8.20E-132	2A: 11.39
CA682481	rice	Putative serine/threonine kinase protein	Traes_6AS_999DF6AE7	5.20E-76	
CA686860	wheat	TAK33	Traes_1AS_581D331E0	2.00E-81	1A: 18.213
CA686860	wheat	TAK33	Traes_1BS_FBB6C5A981	1.70E-66	1B: 18.7695
CA686860	wheat	TAK33	Traes_1DS_9696ADD50	1.20E-73	1D: 9.0939
CA715067	maize	Ras-related protein Rab-2-B		2.60E-89	
CA722042	rice	Disease resistance response protein	Traes_5BL_D6543DA63	3.90E-160	5B: 38.2005
CA722043	rice	Disease resistance response protein	Traes_5DL_7575B5B36	1.60E-159	5D: 30.698
CA733642	rice	Putative peroxidase	Traes_1BL_34402E888	0	
CA733642	rice	Putative peroxidase	Traes_5BL_0BC865004	0	
CA733642	rice	Putative peroxidase	Traes_1BL_34C4F0EE9	0	
CA735686	rice	Mitogen-activated protein kinase	Traes_5BL_FC28DECD0	1.90E-59	
CA742615	rice	Putative makorin RING finger protein	Traes_7AS_477D676E5	0	7A: 65.083
CA742615	rice	Putative makorin RING finger protein	Traes_7DS_0A968BA86	0	
CA742615	rice	Putative makorin RING finger protein	Traes_7BS_5D60BF43A	0	7B: 51.193
CA624824	barley	Bet3-like protein component	Traes_2BS_4AD0F6412	1.50E-41	2B: 55.773
CA624824	barley	Bet3-like protein component	Traes_2DS_0BDFD6AEE	1.50E-41	2D: 58.883
CA624824	barley	Bet3-like protein component	Traes_2AS_F0D016BD0	9.10E-37	2A: 59.228
CD867734	barley	Metallothionein-like protein (fragment)	Traes_1BL_8B855ABE5	2.90E-120	1B: 45.574
CD867734	barley	Metallothionein-like protein (fragment)	Traes_1AL_55193240C	1.80E-118	1A: 45.6495
CD873926	rice	Rhodanese-like domain-containing protein	Traes_6AL_6CD6A9215	0	

CD873926	rice	Rhodanese-like domain-containing protein	Traes_6DL_71544DFF8	4.40E-83	6D: 52.35
CD890594	rice	Putative phytochelatin synthetase	Traes_2BS_D9A0F1157	0	2B: 56.91
CD890594	rice	Putative phytochelatin synthetase	Traes_2AS_56518836B	0	2A: 59.228
CD890594	rice	Putative phytochelatin synthetase	Traes_2DS_9873F2335	0	2D: 62.293
CK154453	rice	O-methyltransferase	TRAES3BF038300120CFD_g	0	
CK154453	rice	O-methyltransferase	Traes_3DS_B5DCCA6F2	6.00E-55	3D: 12.65
CK154453	rice	O-methyltransferase	Traes_3AS_F5FBB71C6	9.10E-51	3A: 13.665
CK165182	rice	Putative carboxylate oxidase	Traes_4BL_6B601836D	0	4B: 65.163
BJ213208	rice	OSJNBb0079B02.14 protein	Traes_2DL_E324B45FE	3.90E-77	3A: 13.665
BJ213208	rice	OSJNBb0079B02.14 protein	Traes_2DL_E324B45FE	2.20E-69	
BJ260653	rice	Glycerophosphoryl diester phosphodiesterase 2-like protein	Traes_1BL_DA4EE7BDD	2.10E-164	
BJ260653	rice	Glycerophosphoryl diester phosphodiesterase 2-like protein	Traes_1AL_DF9E38C1D	4.30E-150	1A: 74.076
BJ260653	rice	Glycerophosphoryl diester phosphodiesterase 2-like protein	Traes_1DL_7BFA60046	4.30E-150	1D: 83.009
BJ316737	rice	Putative spop	Traes_7DL_AAAA8E765	0	7D: 82.7415
BJ316737	rice	Putative spop	Traes_7BL_AB14BD6B8	0	7B: 51.193
CA595213	rice	Putative SKP1 interacting partner	Traes_6BS_80170D243	0	6B: 27.36
CA595213	rice	Putative SKP1 interacting partner	Traes_6DS_B8E4EAAB5	2.70E-135	6D: 19.376
CA595213	rice	Putative SKP1 interacting partner	Traes_6AS_AF0D795CF	2.70E-135	6A: 25.146
CA604568	beet	Eukaryotic translation initiation factor	Traes_2AS_72EC97B33	4.10E-46	2A: 59.228
CA604568	beet	Eukaryotic translation initiation factor	Traes_2BS_55D17B222	1.00E-43	2B: 55.773

CA604568	beet	Eukaryotic translation initiation factor	Traes_2DS_A6B5DDA37	2.50E-41	2D: 58.883
CA614208	maize	retrotransposon Cinful-1		1.80E-105	
CA616728	rice	PPR protein-like protein	Traes_5BL_B1C98E55D	5.30E-17	5B: 35.9275
CA616728	rice	PPR protein-like protein	Traes_5AL_2C41D7902	5.30E-17	
CA616728	rice	PPR protein-like protein	Traes_5DL_3B088D5061	1.30E-14	5D: 30.698
CA616728			Traes_5BL_B1C98E55D	5.30E-17	5B: 35.9275
CA616728			Traes_5AL_2C41D7902	5.30E-17	
CA616728			Traes_5DL_3B088D5061	1.30E-14	5D: 30.698
CA618012	maize	60S ribosomal protein L17	Traes_7AS_FC0A3A1AC	8.20E-10	
CA618012	maize	60S ribosomal protein L17	Traes_7BS_586D1E6FD	2.00E-07	7B: 51.193
CA618012	maize	60S ribosomal protein L17	Traes_7DS_52F1E4F62	2.00E-07	7D: 83.31
CA619934	rice	Profilin A	TRAES3BF128500040CFD_g	1.50E-20	
CA619934	rice	Profilin A	Traes_1BL_7FFD602EC	3.50E-18	
CA619934	rice	Profilin A	Traes_1DL_8D4911E9F	3.50E-18	
CA619966	Arabidopsis	Guanine nucleotide-exchange-like protein	Traes_2BS_D2A3A5041	8.70E-31	2B: 60.32
CA619966	Arabidopsis	Guanine nucleotide-exchange-like protein	Traes_2AS_A93AB0BA6	8.70E-31	2A: 59.228
CA619966	Arabidopsis	Guanine nucleotide-exchange-like protein	Traes_2DS_C5098AF76	8.70E-31	2D: 64.566
CA624167	rice	BHLH protein family-like	Traes_5DL_E96693018	1.40E-14	5D: 39.793
CA624167	rice	BHLH protein family-like	Traes_5BL_AAC9C7238	1.40E-14	5B: 42.18
CA642777	rice	Putative ATP cell differentiation binding protein	TRAES3BF049000020CFD_g	8.10E-81	
CA642777	rice	Putative ATP cell differentiation binding protein	Traes_3B_E339F3EE4	8.10E-81	

CA642777	rice	Putative ATP cell differentiation binding protein	TRAES3BF049300040CFD_g	8.10E-81	
CA683257	rice	Putative AGO1 homologous protein	Traes_6AL_616161AAB	1.30E-110	6A: 99.391
CA683257	rice	Putative AGO1 homologous protein	Traes_6DL_58620B158	7.80E-106	6D: 119.937
CA729941	rice	Putative linalool synthase	Traes_6AS_C4E616554	2.40E-133	6A: 30.838
CA729941	rice	Putative linalool synthase	Traes_6BS_9C79DB188	1.70E-143	
CD490412	rice	OSJNBa0084A10.13 protein	Traes_2AL_1B22EA0AD	0	
CD490412	rice	OSJNBa0084A10.13 protein	Traes_2BL_B2811EA531	0	2B: 59.184
CD490719	rice	Putative cyclophilin	Traes_7DL_EDE77652A	2.90E-34	7D: 88.997
CD490719	rice	Putative cyclophilin	Traes_7BL_660FFDCE2	7.20E-32	7B: 55.744
CD490719	rice	Putative cyclophilin	Traes_7AL_89E0BA362	7.20E-32	7A: 69.63

Supplementary Table III: Haplotype profiles of resistant and susceptible DH lines on 1DS, 7BL and 7DL. A: Denotes loci from RWA susceptible parent EGA Gregory; B: Denotes loci RWA from Resistant parent PI94365; X: Denotes missing values

			RWA resistant group											RWA susceptible group									
Molecular markers	Chrom-osome No.	Position (cM)	DH7	DH19	DH49	DH52	DH59	DH61	DH79	DH94	DH96	DH100	DH10	DH6	DH8	DH24	DH35	DH66	DH70	DH73	DH81	DH97	DH107
1105980	3	80.8	X	A	A	B	B	B	A	B	B	X	A	A	A	B	A	A	A	A	A	A	A
1200629	3	82.06	B	A	B	B	B	X	A	B	B	B	A	A	A	B	A	A	A	A	A	A	A
100032520	3	83.28	B	A	A	B	B	B	A	B	B	B	A	A	A	B	A	A	A	A	X	X	A
2249179	3	83.28	B	A	A	B	B	B	A	B	B	B	A	A	A	B	A	A	A	A	A	A	A
1237068	3	87.84	B	A	B	B	B	B	A	B	B	B	B	A	A	B	A	A	A	A	A	A	A
2249152	3	89	B	A	B	B	X	X	A	B	X	X	B	A	A	B	A	A	A	A	A	A	A
2299782	3	94.84	B	A	B	B	B	B	A	B	B	B	B	A	A	A	A	A	A	A	A	A	A
100006706	3	107.93	B	B	B	B	B	B	B	B	B	B	B	A	A	A	A	A	X	A	A	A	A
1228408	3	112.59	B	B	B	B	B	B	B	B	B	B	B	A	A	A	A	A	A	A	A	A	A
3027665	3	112.59	B	B	B	B	B	B	B	B	B	B	B	A	A	A	A	A	A	A	A	X	A
wmc336	3	113.75	B	B	B	B	B	B	B	B	B	B	B	A	A	A	A	A	A	A	A	A	A
barc152	3	117.02	B	B	B	B	B	B	B	B	B	B	B	A	A	A	A	A	A	A	A	A	A
984608	3	117.02	B	B	B	B	B	B	B	B	B	B	B	A	A	X	A	A	A	A	A	A	A
3028391	3	117.02	B	B	B	B	B	B	B	B	B	B	B	A	A	A	A	A	A	A	A	A	A
2250495	3	118.14	B	B	B	B	B	B	B	B	B	B	B	A	A	A	A	A	A	A	A	A	A
1076794	3	119.33	B	B	B	B	B	B	B	B	B	B	B	X	A	X	A	A	A	A	A	A	A
1056487	3	120.63	B	B	B	B	B	B	B	B	B	B	B	A	A	X	A	A	X	A	A	A	A
988523	3	121.88	B	B	B	B	B	X	B	B	B	B	B	A	A	A	A	A	A	A	A	A	A
1076039	3	124.13	B	B	B	B	B	B	B	B	B	B	B	A	A	A	A	A	A	A	A	A	A
991664	3	127.67	B	B	B	B	B	B	B	B	B	B	B	A	B	A	A	A	A	A	A	A	A
1012981	3	129.99	B	B	B	B	B	B	B	B	B	B	B	A	A	A	A	A	A	A	A	A	A
stm694	3	131.09	B	B	X	B	B	B	B	B	B	B	B	A	A	A	A	A	A	A	A	A	A
gwm106	3	132.19	B	B	B	B	B	B	B	B	B	B	B	A	A	A	A	A	A	A	A	A	A
100004911	3	133.41	B	B	B	B	B	B	B	B	B	B	B	A	A	A	A	A	A	A	A	A	X
stm657	3	134.63	B	B	B	B	B	B	B	B	B	B	B	A	A	A	A	A	A	A	A	A	A
1090318	3	134.63	B	B	B	B	B	B	B	B	B	B	B	A	A	A	A	A	A	A	A	A	A
981077	3	134.63	B	B	X	X	B	B	B	B	B	B	B	A	A	A	A	A	A	A	A	A	A
wmc222	3	134.63	B	B	B	B	B	B	B	B	B	B	B	A	A	A	A	A	A	A	A	A	A
2243260	3	134.63	B	B	B	B	B	X	B	B	B	B	B	A	A	A	A	A	A	A	A	A	A
985475	3	134.63	B	B	B	B	B	B	B	B	B	B	B	A	A	A	A	A	A	A	A	A	A
gwm337	3	149.86	B	B	B	B	B	B	A	A	B	A	B	B	A	A	A	A	A	A	A	B	B	X
1037975	3	153.48	B	B	B	B	B	X	B	A	A	A	B	B	A	A	A	A	A	A	A	B	B	A
1225267	3	154.67	B	B	B	B	B	B	B	A	A	A	B	B	A	A	A	A	A	A	A	B	B	A
3222548	3	156.92	B	B	B	A	A	B	B	A	A	A	B	B	A	A	A	A	A	A	A	A	B	A
3026807	20	749.16	B	B	A	B	B	B	A	X	B	B	B	B	B	A	A	B	A	A	B	A	A
3024652	20	752.66	B	B	B	B	B	B	A	B	B	B	B	B	B	A	A	B	A	A	B	A	A
3064707	20	755.92	B	B	B	B	B	B	A	B	B	B	B	B	B	A	A	A	A	A	B	A	A
1016559	20	758.10	B	B	B	B	B	B	A	B	B	B	B	B	B	A	A	A	A	A	B	A	A
1215816	20	759.21	B	B	B	B	B	B	A	B	B	B	B	B	B	A	A	A	A	A	B	A	A
1205254	20	759.21	B	B	B	B	B	X	A	B	B	B	B	B	B	A	A	A	A	A	B	A	A
gwm344	20	760.33	B	B	B	B	B	B	A	B	B	B	B	B	B	A	A	A	A	A	B	A	A
1378333	20	762.72	B	B	B	B	B	B	X	B	B	B	B	B	B	X	A	A	A	A	B	A	A
3025080	20	766.43	B	B	B	B	B	X	B	B	B	B	B	B	B	A	A	A	A	A	B	A	A
2303561	20	780.73	B	B	B	B	B	B	B	B	B	B	B	A	A	A	A	A	X	A	A	X	X
1115283	20	781.96	B	X	B	B	B	B	B	B	B	B	B	A	A	A	A	A	A	A	A	A	A
1215832	20	783.06	B	B	B	B	B	B	B	B	B	B	B	A	A	A	A	A	A	A	A	A	A
2271493	20	795.20	B	B	B	B	B	B	B	B	X	B	B	A	A	A	A	A	A	A	A	A	A
2280318	20	797.80	B	B	B	B	B	B	B	B	B	B	B	A	A	A	A	A	A	A	A	A	A
1205012	20	808.63	B	B	B	B	B	B	B	B	B	B	B	A	A	A	A	A	A	A	A	A	A
3021993	20	821.08	B	B	B	B	B	B	B	B	B	B	B	A	A	A	A	A	A	A	A	A	A
1041538	20	825.49	B	B	B	B	B	B	B	B	B	B	B	A	A	A	A	A	A	A	A	A	A
1075525	20	827.69	B	B	B	B	B	B	B	B	B	B	B	A	A	A	A	A	A	A	A	A	A
1113446	20	831.18	B	B	B	X	B	A	B	B	B	B	B	A	A	A	A	A	A	A	A	A	A
1056049	20	832.48	B	B	B	B	X	A	B	B	X	B	B	A	A	A	A	A	A	X	A	A	A
1099421	20	835.15	B	B	B	B	B	A	B	B	X	B	B	A	A	A	X	A	A	A	X	A	A
1058899	20	836.37	B	B	B	B	B	A	B	B	B	B	B	A	A	A	A	A	A	A	A	A	A
100000445	20	836.37	B	B	B	B	B	A	B	B	B	B	B	A	A	A	A	A	A	A	A	A	A
1125929	20	836.37	B	B	B	B	B	A	B	B	B	B	B	A	A	A	A	A	A	A	A	A	A
1228027	20	838.62	B	B	B	B	B	A	B	B	B	B	B	A	A	A	A	A	A	A	A	A	A
1067518	20	839.77	B	B	B	B	X	A	B	A	B	B	B	A	A	A	A	A	A	A	A	A	A
100002031	20	840.96	A	B	B	X	X	A	B	A	B	B	B	A	A	A	A	A	A	A	A	A	A
1252924	20	840.96	A	B	B	B	B	A	B	A	B	B	B	A	A	A	A	A	A	A	A	A	A
1068196	21	171.43	A	B	B	A	B	B	A	B	B	A	B	A	A	A	A	A	A	A	A	A	A
1094740	21	171.43	A	B	B	A	B	B	A	B	B	A	X	A	A	A	A	A	A	A	A	A	A
1121058	21	176.78	A	B	B	A	B	B	X	B	B	A	A	A	A	A	A	A	X	A	A	A	A
1108288	21	180.84	A	B	B	A	B	B	B	B	B	A	B	A	A	A	A	A	A	A	A	A	X
1120507	21	185.99	X	B	B	A	B	B	B	B	B	B	B	X	A	A	A	X	A	A	A	A	A
cfa2174	21	193.27	B	B	B	A	B	B	B	B	B	B	B	A	A	A	A	A	A	A	A	A	A
1062859	21	193.27	B	B	B	A	B	B	B	B	B	B	B	A	A	A	A	A	A	A	A	A	A
wmc702	21	197.88	B	B	B	A	B	B	B	A	B	B	B	A	A	A	A	A	A	A	A	A	A
1078691	21	220.00	B	B	B	B	B	B	B	B	B	B	B	A	B	X	A	A	A	X	A	A	B
1089029	21	234.69	B	B	B	B	B	B	B	B	B	B	X	A	A	X	A	A	A	A	A	A	A
1109327	21	254.07	B	B	B	B	B	B	B	B	B	B	B	X	A	A	A	A	X	X	A	A	X
1010929	21	266.06	B	B	B	B	B	B	B	B	B	B	B	A	A	A	A	A	A	A	A	A	A
1209110	21	266.06	B	B	B	B	B	B	B	B	B	B	B	X	A	A	A	A	A	A	A	A	A
1090476	21	266.06	B	B	B	B	B	B	B	B	B	B	B	A	A	A	A	A	A	A	A	A	A
100002995	21	267.47	B	B	B	B	B	B	B	B	B	B	B	A	A	A	A	A	A	A	A	B	A
987784	21	268.73	B	B	B	B	X	B	B	B	B	B	B	A	A	A	A	A	A	X	A	X	A
100003529	21	272.74	B	B	B	B	B	A	B	X	B	B	X	A	A	A	A	X	X	A	B	X	A
1243355	21	292.36	B	B	B	A	B	A	B	B	A	B	B	A	A	A	A	A	A	A	B	A	A
1208614	21	315.15	X	B	A	A	B	B	B	B	A	B	X	A	X	B	B	A	A	A	B	A	A
wmc797	21	316.45	B	B	A	A	B	B	B	B	A	B	B	A	B	B	B	A	A	A	B	A	A
100003744	21	322.29	X	B	A	A	B	B	B	B	A	B	B	B	X	B	B	A	B	A	B	A	A
2364961	21	326.00	B	B	A	A	B	B	B	B	A	B	B	B	B	B	B	A	A	A	B	A	A
100002157	21	326.00	B	B	A	A	B	B	B	B	A	B	B	B	B	B	B	A	A	A	B	A	A

Supplementary Figure II : Two dimension gels of biological replicates from resistant and susceptible groups (Chapter 5)

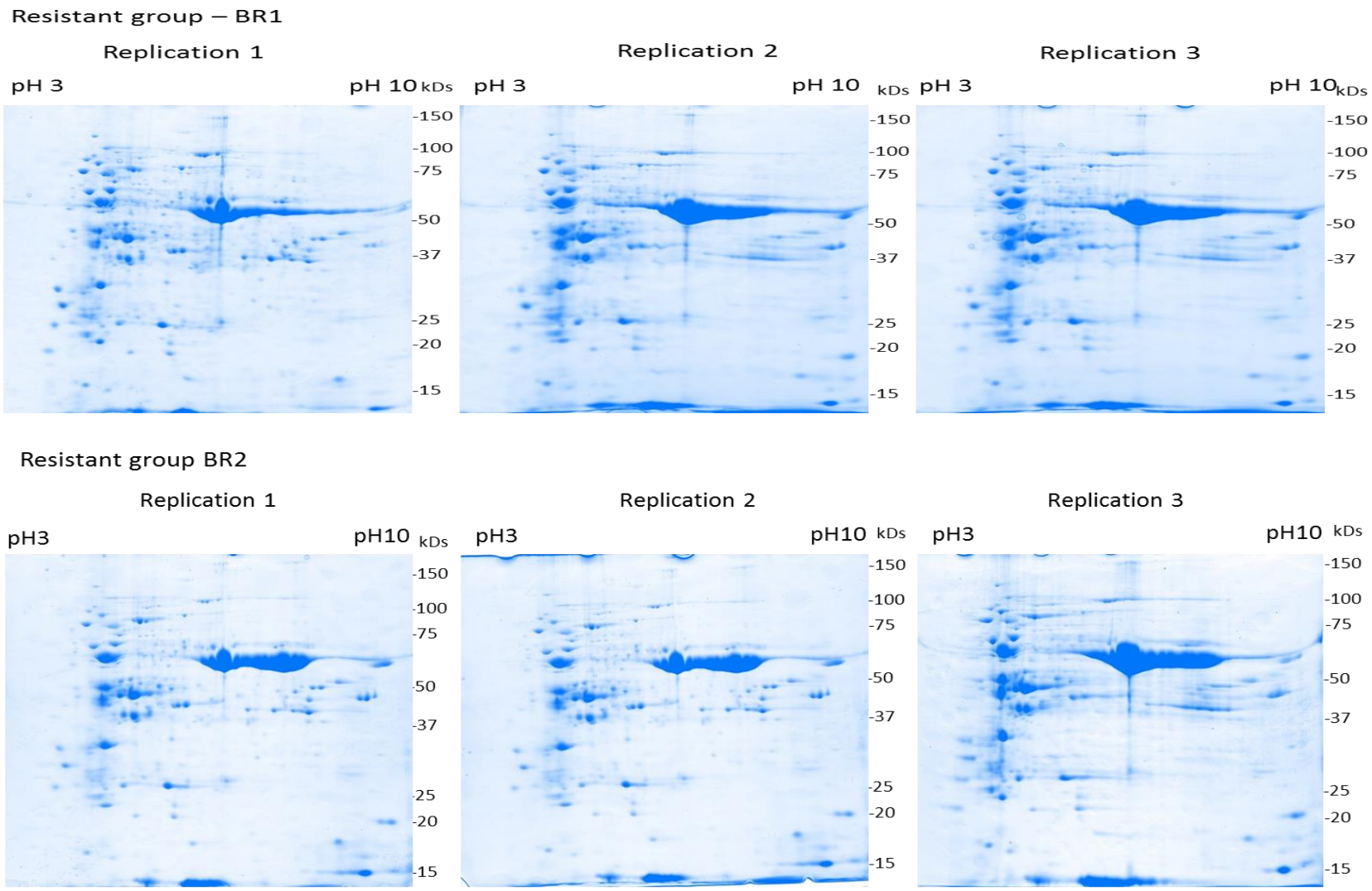

Resistant group - BR3

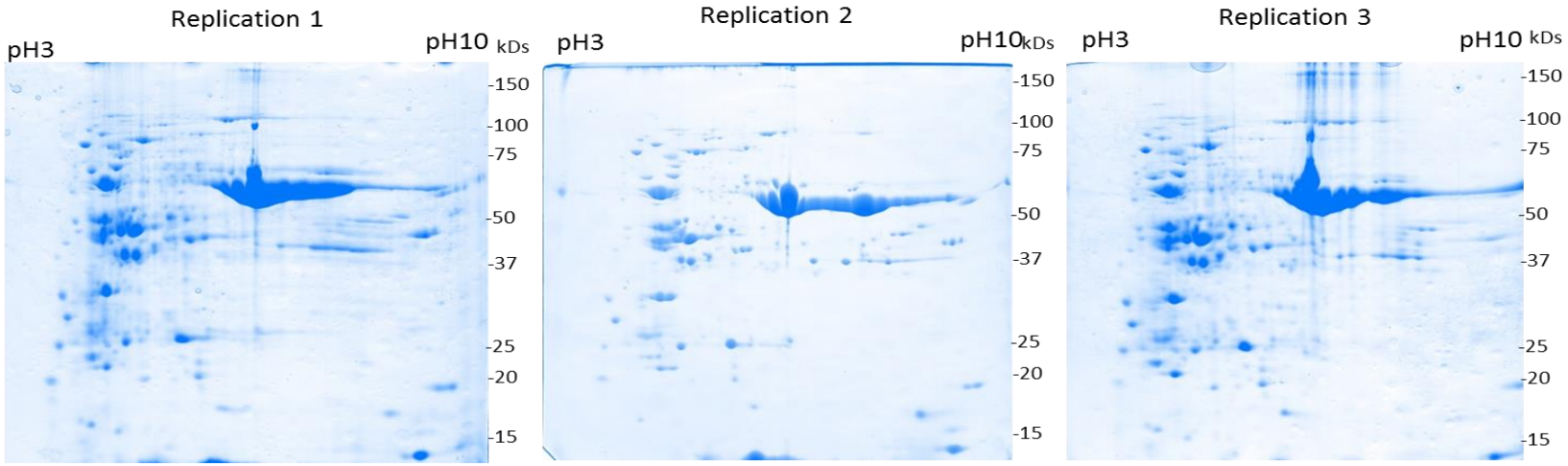

Susceptible group BR1

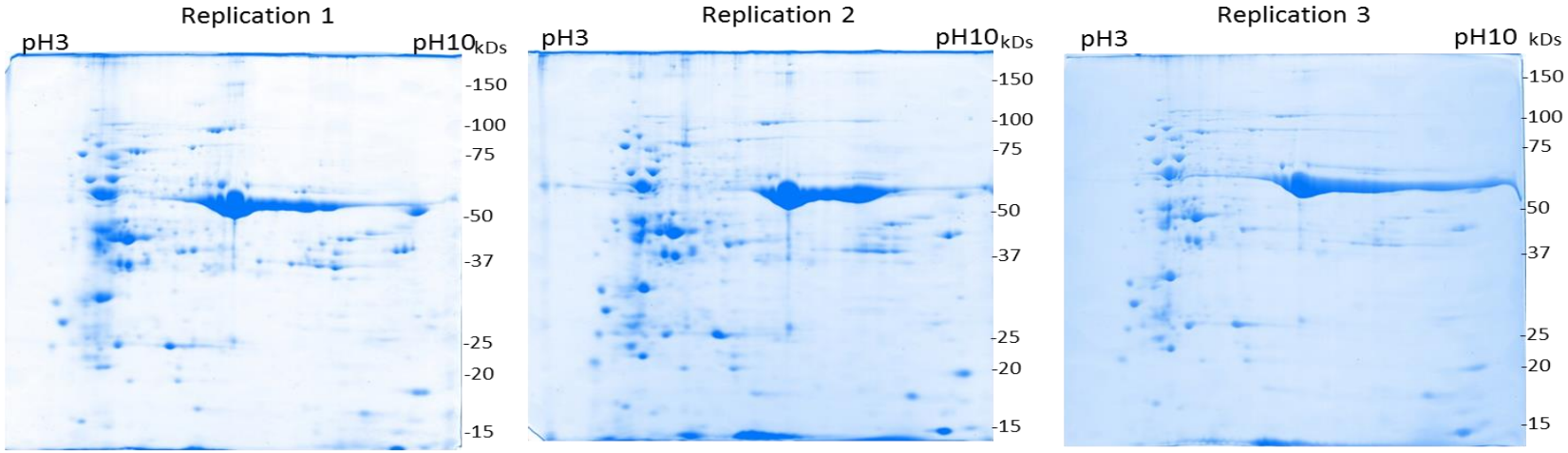

Susceptible BR2

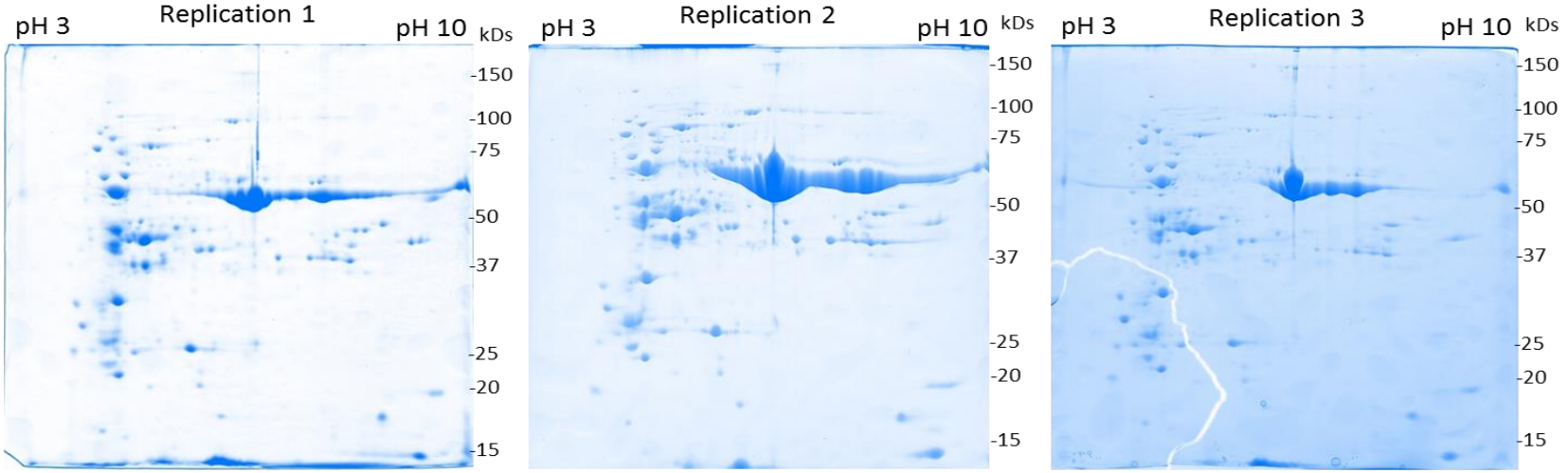

Susceptible group BR 3

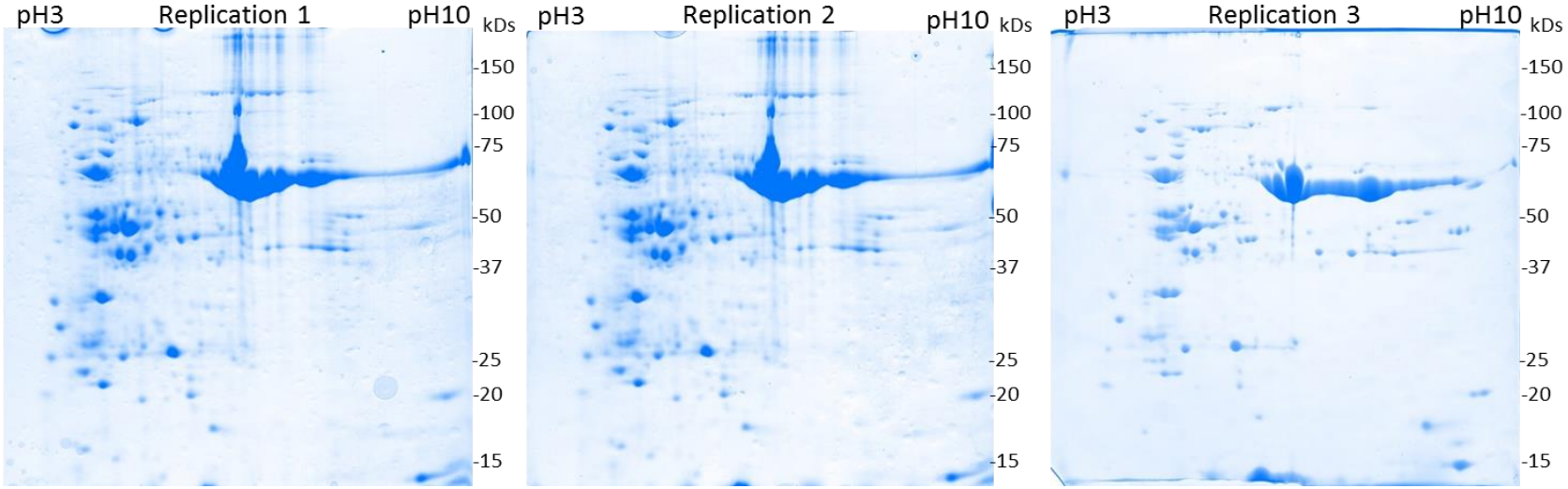

Supplementary Table IV: Annotation of differentially expressed proteins from the iTRAQ experiment (Chapter 5)

Gene ID	Description
EPlTAEP00000010015	pep:known chromosome:IWGSC2:Pt:68325:69851:1 transcript:EPlTAET00000010015 description: “Photosystem II CP47 chlorophyll apoprotein”.
EPlTAEP00000010028	pep:novel chromosome:IWGSC2:Pt:32864:34240:1 transcript:EPlTAET00000010028 description: “ATP synthase subunit b, chloroplastic”.
EPlTAEP00000010030	pep:novel chromosome:IWGSC2:Pt:8657:9718:1 gene:EPlTAEG00000010030 transcript:EPlTAET00000010030 description: “Photosystem II D2 protein”.
EPlTAEP00000010056	pep:novel chromosome:IWGSC2:Pt:76680:77051:-1 gene:EPlTAEG00000010056 transcript:EPlTAET00000010056 description: “50S ribosomal protein L14, chloroplastic”.
EPlTAEP00000010058	pep:novel chromosome:IWGSC2:Pt:34332:35846:1 gene:EPlTAEG00000010058 transcript:EPlTAET00000010058 description: “ATP synthase subunit alpha, chloroplastic”.
Traes_1AL_4F3CAE982.2	pep:novel chromosome:IWGSC2:1A:247743620:247747207:-1 gene:Traes_1AL_4F3CAE982 transcript:Traes_1AL_4F3CAE982.2
Traes_1AL_51CED3DBF.1	pep:novel scaffold:IWGSC2:IWGSC_CSS_1AL_scaff_3933057:288:4412:1 gene:Traes_1AL_51CED3DBF transcript:Traes_1AL_51CED3DBF.1
Traes_1AL_6F2E87864.2	pep:novel chromosome:IWGSC2:1A:199247721:199250553:-1 gene:Traes_1AL_6F2E87864 transcript:Traes_1AL_6F2E87864.2
Traes_1AL_ADC801BEB.1	pep:novel chromosome:IWGSC2:1A:182756196:182758523:1 gene:Traes_1AL_ADC801BEB transcript:Traes_1AL_ADC801BEB.1
Traes_1AL_C42DE440F.1	pep:novel scaffold:IWGSC2:IWGSC_CSS_1AL_scaff_3932547:597:1401:-1 gene:Traes_1AL_C42DE440F transcript:Traes_1AL_C42DE440F.1

Traes_1AL_C4F9F792D.1	pep:novel chromosome:IWGSC2:1A:195907932:195910475:1 gene:Traes_1AL_C4F9F792D transcript:Traes_1AL_C4F9F792D.1
Traes_1AS_C7E294E15.1	pep:novel chromosome:IWGSC2:1A:102735580:102740531:-1 gene:Traes_1AS_C7E294E15 transcript:Traes_1AS_C7E294E15.1
Traes_1AS_FBD1793BD1.2	pep:novel chromosome:IWGSC2:1A:124627496:124628306:-1 gene:Traes_1AS_FBD1793BD1 transcript:Traes_1AS_FBD1793BD1.2
Traes_1BL_714F4E4AC.2	pep:novel chromosome:IWGSC2:1B:196429391:196435152:-1 gene:Traes_1BL_714F4E4AC transcript:Traes_1BL_714F4E4AC.2
Traes_1BL_CAB6FC379.2	pep:novel chromosome:IWGSC2:1B:179895518:179897262:-1 gene:Traes_1BL_CAB6FC379 transcript:Traes_1BL_CAB6FC379.2
Traes_1BL_EE81995CA.1	pep:novel scaffold:IWGSC2:IWGSC_CSS_1BL_scaff_3833717:6550:12545:-1 gene:Traes_1BL_EE81995CA transcript:Traes_1BL_EE81995CA.1
Traes_1BS_15C828137.2	pep:novel scaffold:IWGSC2:IWGSC_CSS_1BS_scaff_3484688:2544:5827:-1 gene:Traes_1BS_15C828137 transcript:Traes_1BS_15C828137.2
Traes_1BS_351490964.2	pep:novel chromosome:IWGSC2:1B:15316007:15316801:1 gene:Traes_1BS_351490964 transcript:Traes_1BS_351490964.2
Traes_1BS_5F9257978.1	pep:novel chromosome:IWGSC2:1B:86395944:86397374:-1 gene:Traes_1BS_5F9257978 transcript:Traes_1BS_5F9257978.1
Traes_1BS_693EBA0AF.1	pep:novel chromosome:IWGSC2:1B:18048455:18050654:1 gene:Traes_1BS_693EBA0AF transcript:Traes_1BS_693EBA0AF.1
Traes_1BS_82B47CBF7.2	pep:novel chromosome:IWGSC2:1B:70351224:70356331:1 gene:Traes_1BS_82B47CBF7 transcript:Traes_1BS_82B47CBF7.2

Traes_1BS_C2B29988C.1	pep:novel scaffold:IWGSC2:IWGSC_CSS_1BS_scaff_3420870:1187:1680:1 gene:Traes_1BS_C2B29988C transcript:Traes_1BS_C2B29988C.1
Traes_1BS_E0A52650C.2	pep:novel chromosome:IWGSC2:1B:5848416:5854850:1 gene:Traes_1BS_E0A52650C transcript:Traes_1BS_E0A52650C.2
Traes_1BS_F226DF9B4.1	pep:novel scaffold:IWGSC2:IWGSC_CSS_1BS_scaff_3459314:1:4896:-1 gene:Traes_1BS_F226DF9B4 transcript:Traes_1BS_F226DF9B4.1
Traes_1DL_14CCD1497.2	pep:novel scaffold:IWGSC2:IWGSC_CSS_1DL_scaff_133840:2123:4287:-1 gene:Traes_1DL_14CCD1497 transcript:Traes_1DL_14CCD1497.2
Traes_1DL_3F4A8E2D6.1	pep:novel chromosome:IWGSC2:1D:62573221:62578921:-1 gene:Traes_1DL_3F4A8E2D6 transcript:Traes_1DL_3F4A8E2D6.1
Traes_1DL_443047168.1	pep:novel chromosome:IWGSC2:1D:128533338:128536062:1 gene:Traes_1DL_443047168 transcript:Traes_1DL_443047168.1
Traes_1DL_583EA9B4A.1	pep:novel scaffold:IWGSC2:IWGSC_CSS_1DL_scaff_2258602:2:6763:1 gene:Traes_1DL_583EA9B4A transcript:Traes_1DL_583EA9B4A.1
Traes_1DL_69D4A3E8B.1	pep:novel chromosome:IWGSC2:1D:91966175:91969968:1 gene:Traes_1DL_69D4A3E8B transcript:Traes_1DL_69D4A3E8B.1
Traes_1DL_729306215.1	pep:novel chromosome:IWGSC2:1D:83422975:83425654:-1 gene:Traes_1DL_729306215 transcript:Traes_1DL_729306215.1
Traes_1DL_7657153A4.1	pep:novel chromosome:IWGSC2:1D:132765113:132767647:1 gene:Traes_1DL_7657153A4 transcript:Traes_1DL_7657153A4.1

Traes_1DL_8298FB2DF.1	pep:novel scaffold:IWGSC2:IWGSC_CSS_1DL_scaff_1244649:1:3014:1 gene:Traes_1DL_8298FB2DF transcript:Traes_1DL_8298FB2DF.1
Traes_1DL_88DD1E468.1	pep:novel chromosome:IWGSC2:1D:129301870:129306583:-1 gene:Traes_1DL_88DD1E468 transcript:Traes_1DL_88DD1E468.1
Traes_1DL_9926BBAE1.1	pep:novel scaffold:IWGSC2:IWGSC_CSS_1DL_scaff_411489:928:3809:-1 gene:Traes_1DL_9926BBAE1 transcript:Traes_1DL_9926BBAE1.1
Traes_1DL_A1E887281.2	pep:novel scaffold:IWGSC2:IWGSC_CSS_1DL_scaff_142930:4:877:-1 gene:Traes_1DL_A1E887281 transcript:Traes_1DL_A1E887281.2
Traes_1DL_AF3FB8142.1	pep:novel chromosome:IWGSC2:1D:112146763:112152945:1 gene:Traes_1DL_AF3FB8142 transcript:Traes_1DL_AF3FB8142.1
Traes_1DL_C100B5557.1	pep:novel chromosome:IWGSC2:1D:93001324:93006452:-1 gene:Traes_1DL_C100B5557 transcript:Traes_1DL_C100B5557.1
Traes_1DL_C172C96CB.1	pep:novel scaffold:IWGSC2:IWGSC_CSS_1DL_scaff_1971366:1:200:-1 gene:Traes_1DL_C172C96CB transcript:Traes_1DL_C172C96CB.1
Traes_1DL_C4BCF25A2.1	pep:novel scaffold:IWGSC2:IWGSC_CSS_1DL_scaff_2230347:4893:7577:-1 gene:Traes_1DL_C4BCF25A2 transcript:Traes_1DL_C4BCF25A2.1
Traes_1DL_C875BF063.1	pep:novel scaffold:IWGSC2:IWGSC_CSS_1DL_scaff_2244937:2201:5079:-1 gene:Traes_1DL_C875BF063 transcript:Traes_1DL_C875BF063.1
Traes_1DL_CFD627F06.1	pep:novel chromosome:IWGSC2:1D:111368551:111371415:-1 gene:Traes_1DL_CFD627F06 transcript:Traes_1DL_CFD627F06.1

Traes_1DL_E31CD9338.1	pep:novel scaffold:IWGSC2:IWGSC_CSS_1DL_scaff_2287265:1300:2881:-1 gene:Traes_1DL_E31CD9338 transcript:Traes_1DL_E31CD9338.1
Traes_1DS_257B630F0.1	pep:novel chromosome:IWGSC2:1D:80795416:80799520:-1 gene:Traes_1DS_257B630F0 transcript:Traes_1DS_257B630F0.1
Traes_1DS_8FE31BBF3.1	pep:novel chromosome:IWGSC2:1D:2172126:2180003:-1 gene:Traes_1DS_8FE31BBF3 transcript:Traes_1DS_8FE31BBF3.1
Traes_1DS_9256376AB.1	pep:novel chromosome:IWGSC2:1D:79435427:79435894:1 gene:Traes_1DS_9256376AB transcript:Traes_1DS_9256376AB.1 description:"Ubiquitin "
Traes_1DS_947F6918F.2	pep:novel scaffold:IWGSC2:IWGSC_CSS_1DS_scaff_1899380:2770:6754:-1 gene:Traes_1DS_947F6918F transcript:Traes_1DS_947F6918F.2
Traes_1DS_ACF9E82D8.1	pep:novel chromosome:IWGSC2:1D:65046590:65050492:1 gene:Traes_1DS_ACF9E82D8 transcript:Traes_1DS_ACF9E82D8.1
Traes_1DS_B74218BA2.1	pep:novel chromosome:IWGSC2:1D:5018996:5021374:1 gene:Traes_1DS_B74218BA2 transcript:Traes_1DS_B74218BA2.1
Traes_1DS_BB9715188.1	pep:novel chromosome:IWGSC2:1D:57723952:57727071:-1 gene:Traes_1DS_BB9715188 transcript:Traes_1DS_BB9715188.1
Traes_1DS_C2DACDAF1.1	pep:novel chromosome:IWGSC2:1D:5897494:5898941:-1 gene:Traes_1DS_C2DACDAF1 transcript:Traes_1DS_C2DACDAF1.1
Traes_1DS_D46002062.2	pep:novel scaffold:IWGSC2:IWGSC_CSS_1DS_scaff_1886609:4016:9665:1 gene:Traes_1DS_D46002062 transcript:Traes_1DS_D46002062.2

Traes_2AL_06A59CD63.2	pep:novel chromosome:IWGSC2:2A:73489691:73493584:1 gene:Traes_2AL_06A59CD63 transcript:Traes_2AL_06A59CD63.2
Traes_2AL_1F6605694.2	pep:novel scaffold:IWGSC2:IWGSC_CSS_2AL_scaff_6369578:4540:5525:1 gene:Traes_2AL_1F6605694 transcript:Traes_2AL_1F6605694.2
Traes_2AL_21B8BCA9C.1	pep:novel scaffold:IWGSC2:IWGSC_CSS_2AL_scaff_6438930:2595:5191:-1 gene:Traes_2AL_21B8BCA9C transcript:Traes_2AL_21B8BCA9C.1
Traes_2AL_2E2DFB904.1	pep:novel chromosome:IWGSC2:2A:222464922:222467467:-1 gene:Traes_2AL_2E2DFB904 transcript:Traes_2AL_2E2DFB904.1
Traes_2AL_783420E8B.1	pep:novel scaffold:IWGSC2:IWGSC_CSS_2AL_scaff_6402211:3324:9084:-1 gene:Traes_2AL_783420E8B transcript:Traes_2AL_783420E8B.1
Traes_2AL_783CF383F.1	pep:novel chromosome:IWGSC2:2A:75021621:75023101:1 gene:Traes_2AL_783CF383F transcript:Traes_2AL_783CF383F.1
Traes_2AL_7EABAC855.1	pep:novel scaffold:IWGSC2:IWGSC_CSS_2AL_scaff_6330236:2114:5328:1 gene:Traes_2AL_7EABAC855 transcript:Traes_2AL_7EABAC855.1
Traes_2AL_8CBEE2F6B.2	pep:novel chromosome:IWGSC2:2A:245087947:245089194:1 gene:Traes_2AL_8CBEE2F6B transcript:Traes_2AL_8CBEE2F6B.2
Traes_2AL_DF262E611.1	pep:novel scaffold:IWGSC2:IWGSC_CSS_2AL_scaff_6374692:1544:5744:1 gene:Traes_2AL_DF262E611 transcript:Traes_2AL_DF262E611.1
Traes_2AL_E5A33D194.1	pep:novel chromosome:IWGSC2:2A:225248619:225250919:1 gene:Traes_2AL_E5A33D194 transcript:Traes_2AL_E5A33D194.1

Traes_2AS_1475F8BDB.1	pep:known scaffold:IWGSC2:IWGSC_CSS_2AS_scaff_5241293:1353:3254:-1 gene:Traes_2AS_1475F8BDB transcript:Traes_2AS_1475F8BDB.1 description:"Cytochrome b6-f complex iron-sulfur subunit, chloroplastic "
Traes_2AS_18BA58F8D.1	pep:novel chromosome:IWGSC2:2A:70403846:70410156:1 gene:Traes_2AS_18BA58F8D transcript:Traes_2AS_18BA58F8D.1
Traes_2AS_57C9CAC3C.2	pep:novel chromosome:IWGSC2:2A:187500406:187515729:1 gene:Traes_2AS_57C9CAC3C transcript:Traes_2AS_57C9CAC3C.2
Traes_2AS_5A5258192.1	pep:novel chromosome:IWGSC2:2A:10042559:10056482:1 gene:Traes_2AS_5A5258192 transcript:Traes_2AS_5A5258192.1
Traes_2AS_67F19428A.1	pep:novel chromosome:IWGSC2:2A:144718477:144720292:-1 gene:Traes_2AS_67F19428A transcript:Traes_2AS_67F19428A.1
Traes_2AS_84EA9C6091.1	pep:novel scaffold:IWGSC2:IWGSC_CSS_2AS_scaff_5198125:4095:5333:-1 gene:Traes_2AS_84EA9C6091 transcript:Traes_2AS_84EA9C6091.1
Traes_2AS_D23AA7200.1	pep:novel scaffold:IWGSC2:IWGSC_CSS_2AS_scaff_5256125:584:2174:-1 gene:Traes_2AS_D23AA7200 transcript:Traes_2AS_D23AA7200.1
Traes_2BL_047344CB6.1	pep:novel scaffold:IWGSC2:IWGSC_CSS_2BL_scaff_8090499:12421:18963:1 gene:Traes_2BL_047344CB6 transcript:Traes_2BL_047344CB6.1
Traes_2BL_2825A3D0F.1	pep:known chromosome:IWGSC2:2B:311457446:311459824:-1 gene:Traes_2BL_2825A3D0F transcript:Traes_2BL_2825A3D0F.1 description:"Adenosylhomocysteinase "
Traes_2BL_312F06C61.1	pep:novel chromosome:IWGSC2:2B:326394611:326399045:1 gene:Traes_2BL_312F06C61 transcript:Traes_2BL_312F06C61.1

Traes_2BL_4AEA2109C.2	pep:novel chromosome:IWGSC2:2B:306622394:306628496:1 gene:Traes_2BL_4AEA2109C transcript:Traes_2BL_4AEA2109C.2
Traes_2BL_4B8B77E73.1	pep:known chromosome:IWGSC2:2B:223450975:223452603:-1 gene:Traes_2BL_4B8B77E73 transcript:Traes_2BL_4B8B77E73.1 description:"Oxygen-evolving enhancer protein 1, chloroplastic "
Traes_2BL_4EA417A3A.1	pep:novel scaffold:IWGSC2:IWGSC_CSS_2BL_scaff_7967496:3315:5226:1 gene:Traes_2BL_4EA417A3A transcript:Traes_2BL_4EA417A3A.1
Traes_2BL_5D64E8C87.1	pep:novel scaffold:IWGSC2:IWGSC_CSS_2BL_scaff_7993541:535:2017:1 gene:Traes_2BL_5D64E8C87 transcript:Traes_2BL_5D64E8C87.1
Traes_2BL_6552196A1.1	pep:novel scaffold:IWGSC2:IWGSC_CSS_2BL_scaff_8014036:92:3400:-1 gene:Traes_2BL_6552196A1 transcript:Traes_2BL_6552196A1.1
Traes_2BL_931FB03D1.1	pep:novel chromosome:IWGSC2:2B:329651771:329654161:1 gene:Traes_2BL_931FB03D1 transcript:Traes_2BL_931FB03D1.1
Traes_2BL_964FC881C.1	pep:novel chromosome:IWGSC2:2B:160555652:160561574:1 gene:Traes_2BL_964FC881C transcript:Traes_2BL_964FC881C.1
Traes_2BL_A35156C50.2	pep:novel chromosome:IWGSC2:2B:322852998:322854397:-1 gene:Traes_2BL_A35156C50 transcript:Traes_2BL_A35156C50.2
Traes_2BL_AC69B36DF.1	pep:novel chromosome:IWGSC2:2B:187477712:187481471:-1 gene:Traes_2BL_AC69B36DF transcript:Traes_2BL_AC69B36DF.1
Traes_2BL_AEEA273E2.1	pep:novel chromosome:IWGSC2:2B:181633540:181636300:1 gene:Traes_2BL_AEEA273E2 transcript:Traes_2BL_AEEA273E2.1

Traes_2BL_E198EA9E0.1	pep:novel chromosome:IWGSC2:2B:94262855:94264635:-1 gene:Traes_2BL_E198EA9E0 transcript:Traes_2BL_E198EA9E0.1
Traes_2BL_E3222439E.1	pep:novel chromosome:IWGSC2:2B:290549637:290551965:-1 gene:Traes_2BL_E3222439E transcript:Traes_2BL_E3222439E.1
Traes_2BL_E4D78CECE.2	pep:novel chromosome:IWGSC2:2B:171132897:171141333:1 gene:Traes_2BL_E4D78CECE transcript:Traes_2BL_E4D78CECE.2
Traes_2BL_E6F86DAFA.1	pep:novel chromosome:IWGSC2:2B:173229654:173232672:-1 gene:Traes_2BL_E6F86DAFA transcript:Traes_2BL_E6F86DAFA.1
Traes_2BS_4AE914BE2.1	pep:novel chromosome:IWGSC2:2B:84561279:84563106:1 gene:Traes_2BS_4AE914BE2 transcript:Traes_2BS_4AE914BE2.1
Traes_2BS_51E9E0AD1.2	pep:novel chromosome:IWGSC2:2B:36633216:36634082:-1 gene:Traes_2BS_51E9E0AD1 transcript:Traes_2BS_51E9E0AD1.2
Traes_2BS_62E19AC5C.2	pep:novel chromosome:IWGSC2:2B:157008666:157009484:-1 gene:Traes_2BS_62E19AC5C transcript:Traes_2BS_62E19AC5C.2
Traes_2BS_6DEC6A223.1	pep:novel chromosome:IWGSC2:2B:46680172:46681832:1 gene:Traes_2BS_6DEC6A223 transcript:Traes_2BS_6DEC6A223.1
Traes_2BS_7F29300C6.2	pep:novel chromosome:IWGSC2:2B:38639648:38641067:1 gene:Traes_2BS_7F29300C6 transcript:Traes_2BS_7F29300C6.2
Traes_2BS_90255A78E.2	pep:novel chromosome:IWGSC2:2B:68778513:68779487:1 gene:Traes_2BS_90255A78E transcript:Traes_2BS_90255A78E.2
Traes_2BS_9F9F7AC781.1	pep:novel scaffold:IWGSC2:IWGSC_CSS_2BS_scaff_5187596:9401:9910:-1 gene:Traes_2BS_9F9F7AC781 transcript:Traes_2BS_9F9F7AC781.1

Traes_2BS_CB79BAFB1.1	pep:novel chromosome:IWGSC2:2B:32773127:32775107:1 gene:Traes_2BS_CB79BAFB1 transcript:Traes_2BS_CB79BAFB1.1
Traes_2BS_DFC825EBF.1	pep:novel chromosome:IWGSC2:2B:4920242:4922312:1 gene:Traes_2BS_DFC825EBF transcript:Traes_2BS_DFC825EBF.1
Traes_2BS_E67494A11.1	pep:novel chromosome:IWGSC2:2B:40922260:40927210:-1 gene:Traes_2BS_E67494A11 transcript:Traes_2BS_E67494A11.1
Traes_2BS_F4E831A77.2	pep:novel scaffold:IWGSC2:IWGSC_CSS_2BS_scaff_5173322:465:3139:1 gene:Traes_2BS_F4E831A77 transcript:Traes_2BS_F4E831A77.2 description:"RuBisCO large subunit-binding protein subunit alpha, chloroplastic "
Traes_2BS_F66779538.1	pep:novel scaffold:IWGSC2:IWGSC_CSS_2BS_scaff_5242225:4257:8587:1 gene:Traes_2BS_F66779538 transcript:Traes_2BS_F66779538.1
Traes_2DL_00F25E85E.1	pep:novel chromosome:IWGSC2:2D:137529097:137531310:-1 gene:Traes_2DL_00F25E85E transcript:Traes_2DL_00F25E85E.1
Traes_2DL_053E73CFE.1	pep:novel scaffold:IWGSC2:IWGSC_CSS_2DL_scaff_9838569:2575:11002:-1 gene:Traes_2DL_053E73CFE transcript:Traes_2DL_053E73CFE.1
Traes_2DL_0B13E5B2D.1	pep:novel scaffold:IWGSC2:IWGSC_CSS_2DL_scaff_326339:1:212:1 gene:Traes_2DL_0B13E5B2D transcript:Traes_2DL_0B13E5B2D.1
Traes_2DL_0FADBEC03.2	pep:novel scaffold:IWGSC2:IWGSC_CSS_2DL_scaff_9725919:2:2503:1 gene:Traes_2DL_0FADBEC03 transcript:Traes_2DL_0FADBEC03.2
Traes_2DL_330051E531.1	pep:novel scaffold:IWGSC2:IWGSC_CSS_2DL_scaff_9840306:5543:6665:-

	1 gene:Traes_2DL_330051E531 transcript:Traes_2DL_330051E531.1
Traes_2DL_50F662E15.1	pep:novel chromosome:IWGSC2:2D:140005754:140007594:-1 gene:Traes_2DL_50F662E15 transcript:Traes_2DL_50F662E15.1
Traes_2DL_62ACB7134.1	pep:novel chromosome:IWGSC2:2D:141065359:141068372:1 gene:Traes_2DL_62ACB7134 transcript:Traes_2DL_62ACB7134.1
Traes_2DL_66736A596.1	pep:novel scaffold:IWGSC2:IWGSC_CSS_2DL_scaff_9908488:9410:12983: -1 gene:Traes_2DL_66736A596 transcript:Traes_2DL_66736A596.1
Traes_2DL_893AC06B8.1	pep:novel chromosome:IWGSC2:2D:136934295:136935713:-1 gene:Traes_2DL_893AC06B8 transcript:Traes_2DL_893AC06B8.1
Traes_2DL_9BDB78425.1	pep:novel chromosome:IWGSC2:2D:112789493:112791350:-1 gene:Traes_2DL_9BDB78425 transcript:Traes_2DL_9BDB78425.1
Traes_2DL_A5EEC27EC.1	pep:novel scaffold:IWGSC2:IWGSC_CSS_2DL_scaff_9835536:2240:7002:- 1 gene:Traes_2DL_A5EEC27EC transcript:Traes_2DL_A5EEC27EC.1
Traes_2DL_AA319AB9D.1	pep:novel chromosome:IWGSC2:2D:78947683:78950636:1 gene:Traes_2DL_AA319AB9D transcript:Traes_2DL_AA319AB9D.1
Traes_2DL_ABC309A2B.1	pep:novel scaffold:IWGSC2:IWGSC_CSS_2DL_scaff_9883942:119:2162:1 gene:Traes_2DL_ABC309A2B transcript:Traes_2DL_ABC309A2B.1
Traes_2DL_B5B62EE11.1	pep:novel chromosome:IWGSC2:2D:148663689:148666471:1 gene:Traes_2DL_B5B62EE11 transcript:Traes_2DL_B5B62EE11.1
Traes_2DL_B7F8FFEB9.1	pep:novel chromosome:IWGSC2:2D:81692269:81694472:1 gene:Traes_2DL_B7F8FFEB9 transcript:Traes_2DL_B7F8FFEB9.1

Traes_2DL_E1C8AA27A.2	pep:novel scaffold:IWGSC2:IWGSC_CSS_2DL_scaff_9841975:3661:5980:-1 gene:Traes_2DL_E1C8AA27A transcript:Traes_2DL_E1C8AA27A.2
Traes_2DL_EE47AFA8C.1	pep:novel chromosome:IWGSC2:2D:26669882:26673351:1 gene:Traes_2DL_EE47AFA8C transcript:Traes_2DL_EE47AFA8C.1
Traes_2DL_F311FFC60.1	pep:novel chromosome:IWGSC2:2D:74152562:74154217:-1 gene:Traes_2DL_F311FFC60 transcript:Traes_2DL_F311FFC60.1
Traes_2DL_F48387F4E.1	pep:novel scaffold:IWGSC2:IWGSC_CSS_2DL_scaff_9909099:1:4470:-1 gene:Traes_2DL_F48387F4E transcript:Traes_2DL_F48387F4E.1
Traes_2DL_FEA38CB04.1	pep:novel scaffold:IWGSC2:IWGSC_CSS_2DL_scaff_9757923:1:552:1 gene:Traes_2DL_FEA38CB04 transcript:Traes_2DL_FEA38CB04.1
Traes_2DS_169409753.1	pep:novel chromosome:IWGSC2:2D:21695559:21697076:1 gene:Traes_2DS_169409753 transcript:Traes_2DS_169409753.1
Traes_2DS_18C7044FA1.1	pep:novel chromosome:IWGSC2:2D:43218068:43221285:1 gene:Traes_2DS_18C7044FA1 transcript:Traes_2DS_18C7044FA1.1
Traes_2DS_270EB3BAE.1	pep:novel scaffold:IWGSC2:IWGSC_CSS_2DS_scaff_5331527:2601:3715:1 gene:Traes_2DS_270EB3BAE transcript:Traes_2DS_270EB3BAE.1
Traes_2DS_46C9F8F5F.1	pep:novel scaffold:IWGSC2:IWGSC_CSS_2DS_scaff_5390113:774:2223:1 gene:Traes_2DS_46C9F8F5F transcript:Traes_2DS_46C9F8F5F.1
Traes_2DS_47717E715.1	pep:novel scaffold:IWGSC2:IWGSC_CSS_2DS_scaff_5384461:9206:10812:1 gene:Traes_2DS_47717E715 transcript:Traes_2DS_47717E715.1

Traes_2DS_5814764C5.1	pep:novel chromosome:IWGSC2:2D:15075041:15076133:-1 gene:Traes_2DS_5814764C5 transcript:Traes_2DS_5814764C5.1
Traes_2DS_5A62799DD.1	pep:novel chromosome:IWGSC2:2D:2736546:2738988:1 gene:Traes_2DS_5A62799DD transcript:Traes_2DS_5A62799DD.1
Traes_2DS_698DAD811.1	pep:novel chromosome:IWGSC2:2D:10249258:10252154:-1 gene:Traes_2DS_698DAD811 transcript:Traes_2DS_698DAD811.1
Traes_2DS_7FA2B76541.1	pep:novel chromosome:IWGSC2:2D:3968505:3970474:-1 gene:Traes_2DS_7FA2B76541 transcript:Traes_2DS_7FA2B76541.1
Traes_2DS_A32E0CCF5.1	pep:known chromosome:IWGSC2:2D:11161680:11163828:-1 gene:Traes_2DS_A32E0CCF5 transcript:Traes_2DS_A32E0CCF5.1 description:"Elongation factor 1-alpha "
Traes_2DS_E72225729.1	pep:novel chromosome:IWGSC2:2D:61127514:61128244:-1 gene:Traes_2DS_E72225729 transcript:Traes_2DS_E72225729.1
Traes_2DS_EB3269FEE.1	pep:novel chromosome:IWGSC2:2D:21187891:21190860:-1 gene:Traes_2DS_EB3269FEE transcript:Traes_2DS_EB3269FEE.1
Traes_2DS_F661EA0C4.2	pep:novel chromosome:IWGSC2:2D:4819295:4820625:-1 gene:Traes_2DS_F661EA0C4 transcript:Traes_2DS_F661EA0C4.2
Traes_3AL_3D5C860FD.1	pep:novel chromosome:IWGSC2:3A:80680017:80682618:-1 gene:Traes_3AL_3D5C860FD transcript:Traes_3AL_3D5C860FD.1
Traes_3AL_5027B584C.1	pep:novel chromosome:IWGSC2:3A:62921465:62925964:-1 gene:Traes_3AL_5027B584C transcript:Traes_3AL_5027B584C.1
Traes_3AL_84EE0045F.1	pep:novel scaffold:IWGSC2:IWGSC_CSS_3AL_scaff_2200751:27:637:-1 gene:Traes_3AL_84EE0045F transcript:Traes_3AL_84EE0045F.1

Traes_3AS_12D74A531.2	pep:novel chromosome:IWGSC2:3A:110639097:110639834:1 gene:Traes_3AS_12D74A531 transcript:Traes_3AS_12D74A531.2
Traes_3AS_BF0DE4B3D.1	pep:novel chromosome:IWGSC2:3A:72435203:72441235:-1 gene:Traes_3AS_BF0DE4B3D transcript:Traes_3AS_BF0DE4B3D.1
Traes_3AS_D1E1079AA.1	pep:novel scaffold:IWGSC2:IWGSC_CSS_3AS_scaff_3376107:2118:4545:1 gene:Traes_3AS_D1E1079AA transcript:Traes_3AS_D1E1079AA.1
Traes_3DL_003F4B87B.2	pep:novel chromosome:IWGSC2:3D:99035729:99039537:1 gene:Traes_3DL_003F4B87B transcript:Traes_3DL_003F4B87B.2
Traes_3DL_082C9DD8D.2	pep:novel chromosome:IWGSC2:3D:36988614:36989634:1 gene:Traes_3DL_082C9DD8D transcript:Traes_3DL_082C9DD8D.2
Traes_3DL_12C93715D.1	pep:novel chromosome:IWGSC2:3D:101498465:101503205:-1 gene:Traes_3DL_12C93715D transcript:Traes_3DL_12C93715D.1
Traes_3DL_1D3995356.1	pep:novel chromosome:IWGSC2:3D:74881172:74884864:1 gene:Traes_3DL_1D3995356 transcript:Traes_3DL_1D3995356.1
Traes_3DL_2323F05CB.1	pep:novel chromosome:IWGSC2:3D:80288703:80292919:-1 gene:Traes_3DL_2323F05CB transcript:Traes_3DL_2323F05CB.1
Traes_3DL_3561481BA.1	pep:novel chromosome:IWGSC2:3D:97587523:97590935:-1 gene:Traes_3DL_3561481BA transcript:Traes_3DL_3561481BA.1
Traes_3DL_43F4381AA.1	pep:novel scaffold:IWGSC2:IWGSC_CSS_3DL_scaff_6823422:1:2055:1 gene:Traes_3DL_43F4381AA transcript:Traes_3DL_43F4381AA.1
Traes_3DL_4B8AB34A9.1	pep:novel chromosome:IWGSC2:3D:76264245:76267780:-1 gene:Traes_3DL_4B8AB34A9 transcript:Traes_3DL_4B8AB34A9.1

Traes_3DL_750FC4166.2	pep:novel scaffold:IWGSC2:IWGSC_CSS_3DL_scaff_6872894:98:3767:1 gene:Traes_3DL_750FC4166 transcript:Traes_3DL_750FC4166.2
Traes_3DL_A82AE80FE.2	pep:novel scaffold:IWGSC2:IWGSC_CSS_3DL_scaff_6950880:410:5149:1 gene:Traes_3DL_A82AE80FE transcript:Traes_3DL_A82AE80FE.2
Traes_3DL_D174E1D63.2	pep:novel chromosome:IWGSC2:3D:56302105:56303807:1 gene:Traes_3DL_D174E1D63 transcript:Traes_3DL_D174E1D63.2
Traes_3DL_D348D37B0.2	pep:novel scaffold:IWGSC2:IWGSC_CSS_3DL_scaff_6894312:600:1767:1 gene:Traes_3DL_D348D37B0 transcript:Traes_3DL_D348D37B0.2
Traes_3DL_E6B71D302.2	pep:novel scaffold:IWGSC2:IWGSC_CSS_3DL_scaff_6904150:1:3452:1 gene:Traes_3DL_E6B71D302 transcript:Traes_3DL_E6B71D302.2
Traes_3DL_F2E4FF6E6.2	pep:novel chromosome:IWGSC2:3D:98242486:98244470:-1 gene:Traes_3DL_F2E4FF6E6 transcript:Traes_3DL_F2E4FF6E6.2
Traes_3DL_F5BA39EAE.1	pep:novel chromosome:IWGSC2:3D:117376805:117379660:1 gene:Traes_3DL_F5BA39EAE transcript:Traes_3DL_F5BA39EAE.1
Traes_3DS_0A1F1EDD5.1	pep:novel chromosome:IWGSC2:3D:61699320:61705787:-1 gene:Traes_3DS_0A1F1EDD5 transcript:Traes_3DS_0A1F1EDD5.1
Traes_3DS_312B5AE1B.1	pep:novel chromosome:IWGSC2:3D:53672244:53677357:-1 gene:Traes_3DS_312B5AE1B transcript:Traes_3DS_312B5AE1B.1
Traes_3DS_4F10C95FB.1	pep:novel scaffold:IWGSC2:IWGSC_CSS_3DS_scaff_1329786:2:1559:1 gene:Traes_3DS_4F10C95FB transcript:Traes_3DS_4F10C95FB.1

Traes_3DS_9C173AB38.1	pep:novel chromosome:IWGSC2:3D:6777497:6780728:1 gene:Traes_3DS_9C173AB38 transcript:Traes_3DS_9C173AB38.1
Traes_3DS_D1031AFC6.2	pep:novel chromosome:IWGSC2:3D:18428619:18433895:-1 gene:Traes_3DS_D1031AFC6 transcript:Traes_3DS_D1031AFC6.2
Traes_3DS_F409FCA80.1	pep:novel chromosome:IWGSC2:3D:17368772:17372220:1 gene:Traes_3DS_F409FCA80 transcript:Traes_3DS_F409FCA80.1
Traes_4AL_0DF0B6152.1	pep:novel chromosome:IWGSC2:4A:207737042:207748109:-1 gene:Traes_4AL_0DF0B6152 transcript:Traes_4AL_0DF0B6152.1
Traes_4AL_205E88570.1	pep:novel chromosome:IWGSC2:4A:212245427:212247448:1 gene:Traes_4AL_205E88570 transcript:Traes_4AL_205E88570.1
Traes_4AL_2EC6083D7.2	pep:novel chromosome:IWGSC2:4A:40674012:40678786:1 gene:Traes_4AL_2EC6083D7 transcript:Traes_4AL_2EC6083D7.2
Traes_4AL_49A8E719D.2	pep:novel chromosome:IWGSC2:4A:172582660:172584772:-1 gene:Traes_4AL_49A8E719D transcript:Traes_4AL_49A8E719D.2
Traes_4AL_4C396387E.1	pep:novel chromosome:IWGSC2:4A:215541263:215554880:1 gene:Traes_4AL_4C396387E transcript:Traes_4AL_4C396387E.1
Traes_4AL_7B8E7660A.2	pep:novel chromosome:IWGSC2:4A:205542171:205543663:-1 gene:Traes_4AL_7B8E7660A transcript:Traes_4AL_7B8E7660A.2
Traes_4AL_82CACD170.1	pep:novel chromosome:IWGSC2:4A:114414247:114422027:-1 gene:Traes_4AL_82CACD170 transcript:Traes_4AL_82CACD170.1
Traes_4AL_8BCE46958.1	pep:novel chromosome:IWGSC2:4A:158846730:158851219:1 gene:Traes_4AL_8BCE46958 transcript:Traes_4AL_8BCE46958.1

Traes_4AL_B6C20BAB9.2	pep:novel chromosome:IWGSC2:4A:209013476:209018509:1 gene:Traes_4AL_B6C20BAB9 transcript:Traes_4AL_B6C20BAB9.2
Traes_4AS_508327B36.1	pep:novel chromosome:IWGSC2:4A:95541083:95542408:1 gene:Traes_4AS_508327B36 transcript:Traes_4AS_508327B36.1
Traes_4AS_757DD8D72.1	pep:novel chromosome:IWGSC2:4A:45226573:45227897:1 gene:Traes_4AS_757DD8D72 transcript:Traes_4AS_757DD8D72.1
Traes_4AS_90CC29CAA.2	pep:novel chromosome:IWGSC2:4A:81039076:81043065:1 gene:Traes_4AS_90CC29CAA transcript:Traes_4AS_90CC29CAA.2
Traes_4BL_3C28FA35B.2	pep:novel chromosome:IWGSC2:4B:101225201:101241875:1 gene:Traes_4BL_3C28FA35B transcript:Traes_4BL_3C28FA35B.2
Traes_4BL_6CC64A7F2.1	pep:novel scaffold:IWGSC2:IWGSC_CSS_4BL_scaff_6996296:1:3540:1 gene:Traes_4BL_6CC64A7F2 transcript:Traes_4BL_6CC64A7F2.1
Traes_4BL_8B3E9186C.1	pep:novel chromosome:IWGSC2:4B:300557419:300558471:-1 gene:Traes_4BL_8B3E9186C transcript:Traes_4BL_8B3E9186C.1
Traes_4BS_15014415A.1	pep:novel chromosome:IWGSC2:4B:145751155:145752912:-1 gene:Traes_4BS_15014415A transcript:Traes_4BS_15014415A.1
Traes_4BS_4682CEE151.1	pep:novel scaffold:IWGSC2:IWGSC_CSS_4BS_scaff_4877284:8165:13388:-1 gene:Traes_4BS_4682CEE151 transcript:Traes_4BS_4682CEE151.1
Traes_4BS_67A99EB9A.2	pep:novel scaffold:IWGSC2:IWGSC_CSS_4BS_scaff_4897488:2765:10114:1 gene:Traes_4BS_67A99EB9A transcript:Traes_4BS_67A99EB9A.2

Traes_4BS_A0F08C214.2	pep:novel chromosome:IWGSC2:4B:220133802:220138523:1 gene:Traes_4BS_A0F08C214 transcript:Traes_4BS_A0F08C214.2
Traes_4DL_0B1ABB56F.2	pep:novel scaffold:IWGSC2:IWGSC_CSS_4DL_scaff_14342299:662:5863:-1 gene:Traes_4DL_0B1ABB56F transcript:Traes_4DL_0B1ABB56F.2
Traes_4DL_18ABDFE0C.1	pep:novel scaffold:IWGSC2:IWGSC_CSS_4DL_scaff_14469005:3208:6966:-1 gene:Traes_4DL_18ABDFE0C transcript:Traes_4DL_18ABDFE0C.1
Traes_4DL_1BB54C850.1	pep:novel chromosome:IWGSC2:4D:89196033:89198381:1 gene:Traes_4DL_1BB54C850 transcript:Traes_4DL_1BB54C850.1
Traes_4DL_31D6228F5.1	pep:novel chromosome:IWGSC2:4D:28519558:28520499:1 gene:Traes_4DL_31D6228F5 transcript:Traes_4DL_31D6228F5.1
Traes_4DL_37654F435.2	pep:novel scaffold:IWGSC2:IWGSC_CSS_4DL_scaff_14335678:3816:7292:-1 gene:Traes_4DL_37654F435 transcript:Traes_4DL_37654F435.2
Traes_4DL_3D9786B06.1	pep:novel scaffold:IWGSC2:IWGSC_CSS_4DL_scaff_14354305:1739:6575:-1 gene:Traes_4DL_3D9786B06 transcript:Traes_4DL_3D9786B06.1
Traes_4DL_3E829438C.1	pep:novel chromosome:IWGSC2:4D:116087437:116088491:1 gene:Traes_4DL_3E829438C transcript:Traes_4DL_3E829438C.1
Traes_4DL_42EA23191.1	pep:novel chromosome:IWGSC2:4D:28914899:28916730:-1 gene:Traes_4DL_42EA23191 transcript:Traes_4DL_42EA23191.1
Traes_4DL_4FC0D4B27.1	pep:known scaffold:IWGSC2:IWGSC_CSS_4DL_scaff_14471396:7429:11355:1 gene:Traes_4DL_4FC0D4B27 transcript:Traes_4DL_4FC0D4B27.1 description:"Catalase-1 "

Traes_4DL_5612CF456.2	pep:novel scaffold:IWGSC2:IWGSC_CSS_4DL_scaff_14375590:1:1745:-1 gene:Traes_4DL_5612CF456 transcript:Traes_4DL_5612CF456.2
Traes_4DL_65CDCF95A.1	pep:novel chromosome:IWGSC2:4D:67330119:67332048:-1 gene:Traes_4DL_65CDCF95A transcript:Traes_4DL_65CDCF95A.1
Traes_4DL_6EE5DD07E.1	pep:novel scaffold:IWGSC2:IWGSC_CSS_4DL_scaff_14470349:373:2736:1 gene:Traes_4DL_6EE5DD07E transcript:Traes_4DL_6EE5DD07E.1
Traes_4DL_75D8BD9F0.1	pep:novel chromosome:IWGSC2:4D:57778936:57780999:1 gene:Traes_4DL_75D8BD9F0 transcript:Traes_4DL_75D8BD9F0.1
Traes_4DL_7D5AF81A6.2	pep:novel scaffold:IWGSC2:IWGSC_CSS_4DL_scaff_14380328:302:3614:1 gene:Traes_4DL_7D5AF81A6 transcript:Traes_4DL_7D5AF81A6.2
Traes_4DL_875174B05.1	pep:novel chromosome:IWGSC2:4D:114104049:114105812:1 gene:Traes_4DL_875174B05 transcript:Traes_4DL_875174B05.1
Traes_4DL_8DED0B0C8.1	pep:novel scaffold:IWGSC2:IWGSC_CSS_4DL_scaff_14352871:1:4017:1 gene:Traes_4DL_8DED0B0C8 transcript:Traes_4DL_8DED0B0C8.1
Traes_4DL_9FBA93015.2	pep:novel chromosome:IWGSC2:4D:119868233:119869062:-1 gene:Traes_4DL_9FBA93015 transcript:Traes_4DL_9FBA93015.2
Traes_4DL_D7237EFB9.2	pep:novel chromosome:IWGSC2:4D:58547816:58554314:1 gene:Traes_4DL_D7237EFB9 transcript:Traes_4DL_D7237EFB9.2
Traes_4DL_E8582A179.1	pep:novel scaffold:IWGSC2:IWGSC_CSS_4DL_scaff_14384722:3183:5439:-1 gene:Traes_4DL_E8582A179 transcript:Traes_4DL_E8582A179.1

Traes_4DL_F394FF94A.1	pep:novel scaffold:IWGSC2:IWGSC_CSS_4DL_scaff_14365832:3207:4095:-1 gene:Traes_4DL_F394FF94A transcript:Traes_4DL_F394FF94A.1
Traes_4DL_FB5D1C901.1	pep:novel chromosome:IWGSC2:4D:115055308:115057680:1 gene:Traes_4DL_FB5D1C901 transcript:Traes_4DL_FB5D1C901.1
Traes_4DS_0A7E021B3.2	pep:novel scaffold:IWGSC2:IWGSC_CSS_4DS_scaff_2304504:22600:33335:-1 gene:Traes_4DS_0A7E021B3 transcript:Traes_4DS_0A7E021B3.2
Traes_4DS_3A7960FAC.2	pep:novel chromosome:IWGSC2:4D:1132471:1134908:1 gene:Traes_4DS_3A7960FAC transcript:Traes_4DS_3A7960FAC.2
Traes_4DS_557846977.1	pep:novel scaffold:IWGSC2:IWGSC_CSS_4DS_scaff_859071:996:3405:-1 gene:Traes_4DS_557846977 transcript:Traes_4DS_557846977.1
Traes_4DS_80C6168FE.1	pep:novel scaffold:IWGSC2:IWGSC_CSS_4DS_scaff_2301348:9340:11846:1 gene:Traes_4DS_80C6168FE transcript:Traes_4DS_80C6168FE.1
Traes_4DS_83BA620C6.1	pep:novel scaffold:IWGSC2:IWGSC_CSS_4DS_scaff_2318442:2729:6282:1 gene:Traes_4DS_83BA620C6 transcript:Traes_4DS_83BA620C6.1
Traes_4DS_8D47B4C37.1	pep:novel scaffold:IWGSC2:IWGSC_CSS_4DS_scaff_2293108:1:3133:1 gene:Traes_4DS_8D47B4C37 transcript:Traes_4DS_8D47B4C37.1
Traes_4DS_9179FF158.2	pep:novel chromosome:IWGSC2:4D:57736015:57743120:1 gene:Traes_4DS_9179FF158 transcript:Traes_4DS_9179FF158.2
Traes_4DS_92264B9F4.1	pep:novel scaffold:IWGSC2:IWGSC_CSS_4DS_scaff_2323695:19473:2301

	6:-1 gene:Traes_4DS_92264B9F4 transcript:Traes_4DS_92264B9F4.1
Traes_4DS_9E574D445.1	pep:novel chromosome:IWGSC2:4D:5928339:5931059:1 gene:Traes_4DS_9E574D445 transcript:Traes_4DS_9E574D445.1
Traes_4DS_AEB645E0A.1	pep:novel chromosome:IWGSC2:4D:57002987:57007488:-1 gene:Traes_4DS_AEB645E0A transcript:Traes_4DS_AEB645E0A.1
Traes_4DS_C5E6E623F.2	pep:novel scaffold:IWGSC2:IWGSC_CSS_4DS_scaff_145236:5678:6790:1 gene:Traes_4DS_C5E6E623F transcript:Traes_4DS_C5E6E623F.2
Traes_4DS_CC9F9317E.2	pep:novel chromosome:IWGSC2:4D:41931093:41933224:-1 gene:Traes_4DS_CC9F9317E transcript:Traes_4DS_CC9F9317E.2
Traes_5AL_12D9258B4.1	pep:novel scaffold:IWGSC2:IWGSC_CSS_5AL_scaff_2747805:5018:5771:1 gene:Traes_5AL_12D9258B4 transcript:Traes_5AL_12D9258B4.1
Traes_5AL_3AB38DAAD.1	pep:novel chromosome:IWGSC2:5A:105307252:105308852:-1 gene:Traes_5AL_3AB38DAAD transcript:Traes_5AL_3AB38DAAD.1
Traes_5AL_4E0638B3E.1	pep:novel chromosome:IWGSC2:5A:77737438:77740472:1 gene:Traes_5AL_4E0638B3E transcript:Traes_5AL_4E0638B3E.1
Traes_5AL_5A3A592D9.1	pep:novel chromosome:IWGSC2:5A:133527813:133532521:-1 gene:Traes_5AL_5A3A592D9 transcript:Traes_5AL_5A3A592D9.1
Traes_5AL_D24A24C13.1	pep:novel chromosome:IWGSC2:5A:142932784:142935230:1 gene:Traes_5AL_D24A24C13 transcript:Traes_5AL_D24A24C13.1
Traes_5AL_E153CEC65.1	pep:novel scaffold:IWGSC2:IWGSC_CSS_5AL_scaff_2462358:563:4753:1 gene:Traes_5AL_E153CEC65 transcript:Traes_5AL_E153CEC65.1

Traes_5AL_E4C37F0BC.1	pep:novel chromosome:IWGSC2:5A:123008159:123010942:-1 gene:Traes_5AL_E4C37F0BC transcript:Traes_5AL_E4C37F0BC.1
Traes_5AS_116663495.1	pep:novel scaffold:IWGSC2:IWGSC_CSS_5AS_scaff_1517360:1210:4899:-1 gene:Traes_5AS_116663495 transcript:Traes_5AS_116663495.1
Traes_5AS_BABE20FBA.1	pep:novel scaffold:IWGSC2:IWGSC_CSS_5AS_scaff_1463256:14:2385:1 gene:Traes_5AS_BABE20FBA transcript:Traes_5AS_BABE20FBA.1
Traes_5AS_E2C5A9DF3.2	pep:novel scaffold:IWGSC2:IWGSC_CSS_5AS_scaff_1551021:666:17193:-1 gene:Traes_5AS_E2C5A9DF3 transcript:Traes_5AS_E2C5A9DF3.2
Traes_5AS_F0A90707C.1	pep:novel scaffold:IWGSC2:IWGSC_CSS_5AS_scaff_1538930:2:1894:-1 gene:Traes_5AS_F0A90707C transcript:Traes_5AS_F0A90707C.1
Traes_5BL_051A88B95.2	pep:novel chromosome:IWGSC2:5B:234599438:234600755:1 gene:Traes_5BL_051A88B95 transcript:Traes_5BL_051A88B95.2
Traes_5BL_1D07AA86C.2	pep:novel chromosome:IWGSC2:5B:248956252:248958026:1 gene:Traes_5BL_1D07AA86C transcript:Traes_5BL_1D07AA86C.2
Traes_5BL_28CCE5325.2	pep:novel chromosome:IWGSC2:5B:186694260:186696945:1 gene:Traes_5BL_28CCE5325 transcript:Traes_5BL_28CCE5325.2
Traes_5BL_29847C42C.1	pep:novel chromosome:IWGSC2:5B:199900569:199901879:-1 gene:Traes_5BL_29847C42C transcript:Traes_5BL_29847C42C.1
Traes_5BL_60D1A74BA.1	pep:novel scaffold:IWGSC2:IWGSC_CSS_5BL_scaff_10910873:636:1111:-1 gene:Traes_5BL_60D1A74BA transcript:Traes_5BL_60D1A74BA.1

Traes_5BL_66571C27E.1	pep:novel chromosome:IWGSC2:5B:80120601:80123141:1 gene:Traes_5BL_66571C27E transcript:Traes_5BL_66571C27E.1
Traes_5BL_7EDE873F5.1	pep:novel chromosome:IWGSC2:5B:228335145:228336502:-1 gene:Traes_5BL_7EDE873F5 transcript:Traes_5BL_7EDE873F5.1
Traes_5BL_885C2757D.2	pep:novel scaffold:IWGSC2:IWGSC_CSS_5BL_scaff_10916006:1974:3110:1 gene:Traes_5BL_885C2757D transcript:Traes_5BL_885C2757D.2
Traes_5BL_8A99D83A5.1	pep:novel chromosome:IWGSC2:5B:230539559:230543157:1 gene:Traes_5BL_8A99D83A5 transcript:Traes_5BL_8A99D83A5.1
Traes_5BL_8F2E81CCA.1	pep:novel chromosome:IWGSC2:5B:214145377:214151131:1 gene:Traes_5BL_8F2E81CCA transcript:Traes_5BL_8F2E81CCA.1
Traes_5BL_AEEB6621B.1	pep:novel chromosome:IWGSC2:5B:208787869:208798915:1 gene:Traes_5BL_AEEB6621B transcript:Traes_5BL_AEEB6621B.1
Traes_5BL_AF99993E8.2	pep:novel scaffold:IWGSC2:IWGSC_CSS_5BL_scaff_10919685:2:511:1 gene:Traes_5BL_AF99993E8 transcript:Traes_5BL_AF99993E8.2
Traes_5BL_C99C99B3C.1	pep:novel chromosome:IWGSC2:5B:207960322:207963332:-1 gene:Traes_5BL_C99C99B3C transcript:Traes_5BL_C99C99B3C.1
Traes_5BL_D4C452B20.2	pep:novel scaffold:IWGSC2:IWGSC_CSS_5BL_scaff_10887236:324:4851:1 gene:Traes_5BL_D4C452B20 transcript:Traes_5BL_D4C452B20.2
Traes_5BL_DECE49DFC.1	pep:novel chromosome:IWGSC2:5B:76802946:76806368:-1 gene:Traes_5BL_DECE49DFC transcript:Traes_5BL_DECE49DFC.1
Traes_5BL_E3BC16326.4	pep:novel scaffold:IWGSC2:IWGSC_CSS_5BL_scaff_10804278:2363:3801:

	-1 gene:Traes_5BL_E3BC16326 transcript:Traes_5BL_E3BC16326.4
Traes_5BS_017F8702A.1	pep:novel chromosome:IWGSC2:5B:77788045:77789904:1 gene:Traes_5BS_017F8702A transcript:Traes_5BS_017F8702A.1
Traes_5BS_2A3494CEF.1	pep:novel chromosome:IWGSC2:5B:152720067:152725060:-1 gene:Traes_5BS_2A3494CEF transcript:Traes_5BS_2A3494CEF.1
Traes_5BS_3EE61E0AC.1	pep:novel scaffold:IWGSC2:IWGSC_CSS_5BS_scaff_504662:191:1669:1 gene:Traes_5BS_3EE61E0AC transcript:Traes_5BS_3EE61E0AC.1
Traes_5BS_4D44AE9D6.2	pep:novel chromosome:IWGSC2:5B:17130500:17134445:-1 gene:Traes_5BS_4D44AE9D6 transcript:Traes_5BS_4D44AE9D6.2
Traes_5BS_8ECE54AC4.1	pep:novel chromosome:IWGSC2:5B:4046797:4047237:1 gene:Traes_5BS_8ECE54AC4 transcript:Traes_5BS_8ECE54AC4.1
Traes_5BS_9AD74E09C.2	pep:novel chromosome:IWGSC2:5B:38765086:38767934:-1 gene:Traes_5BS_9AD74E09C transcript:Traes_5BS_9AD74E09C.2
Traes_5BS_DCB2B616C.1	pep:novel chromosome:IWGSC2:5B:5540458:5541426:-1 gene:Traes_5BS_DCB2B616C transcript:Traes_5BS_DCB2B616C.1
Traes_5DL_07DD04321.1	pep:novel scaffold:IWGSC2:IWGSC_CSS_5DL_scaff_4518099:605:2754:-1 gene:Traes_5DL_07DD04321 transcript:Traes_5DL_07DD04321.1
Traes_5DL_1A322A379.1	pep:novel scaffold:IWGSC2:IWGSC_CSS_5DL_scaff_4585754:387:910:-1 gene:Traes_5DL_1A322A379 transcript:Traes_5DL_1A322A379.1
Traes_5DL_21FAEB45B.2	pep:novel chromosome:IWGSC2:5D:154030571:154037280:1 gene:Traes_5DL_21FAEB45B transcript:Traes_5DL_21FAEB45B.2

Traes_5DL_343F3EE59.1	pep:novel chromosome:IWGSC2:5D:123821287:123822659:-1 gene:Traes_5DL_343F3EE59 transcript:Traes_5DL_343F3EE59.1
Traes_5DL_3FF985F30.1	pep:novel chromosome:IWGSC2:5D:64623929:64628716:-1 gene:Traes_5DL_3FF985F30 transcript:Traes_5DL_3FF985F30.1
Traes_5DL_4072FF10D.1	pep:novel chromosome:IWGSC2:5D:153373241:153376585:-1 gene:Traes_5DL_4072FF10D transcript:Traes_5DL_4072FF10D.1
Traes_5DL_469B4E877.1	pep:known chromosome:IWGSC2:5D:49419246:49426032:-1 gene:Traes_5DL_469B4E877 transcript:Traes_5DL_469B4E877.1 description:"Mitochondrial outer membrane porin "
Traes_5DL_546404AFD.1	pep:novel scaffold:IWGSC2:IWGSC_CSS_5DL_scaff_4603491:4599:10349:1 gene:Traes_5DL_546404AFD transcript:Traes_5DL_546404AFD.1
Traes_5DL_60C61B6C0.1	pep:novel scaffold:IWGSC2:IWGSC_CSS_5DL_scaff_4512353:1910:2993:1 gene:Traes_5DL_60C61B6C0 transcript:Traes_5DL_60C61B6C0.1
Traes_5DL_64C6A2250.1	pep:novel chromosome:IWGSC2:5D:136843689:136846720:1 gene:Traes_5DL_64C6A2250 transcript:Traes_5DL_64C6A2250.1
Traes_5DL_6A497D966.2	pep:novel chromosome:IWGSC2:5D:120847076:120851217:-1 gene:Traes_5DL_6A497D966 transcript:Traes_5DL_6A497D966.2
Traes_5DL_6CDEEA6A6.1	pep:novel chromosome:IWGSC2:5D:143070475:143075383:1 gene:Traes_5DL_6CDEEA6A6 transcript:Traes_5DL_6CDEEA6A6.1
Traes_5DL_7156326D7.1	pep:novel scaffold:IWGSC2:IWGSC_CSS_5DL_scaff_4537629:1:3787:1 gene:Traes_5DL_7156326D7 transcript:Traes_5DL_7156326D7.1

Traes_5DL_7575B5B363.1	pep:novel scaffold:IWGSC2:IWGSC_CSS_5DL_scaff_4507210:78:743:-1 gene:Traes_5DL_7575B5B363 transcript:Traes_5DL_7575B5B363.1
Traes_5DL_7907FFE85.1	pep:novel chromosome:IWGSC2:5D:42327610:42341262:1 gene:Traes_5DL_7907FFE85 transcript:Traes_5DL_7907FFE85.1
Traes_5DL_91F71E89E.1	pep:novel scaffold:IWGSC2:IWGSC_CSS_5DL_scaff_1872853:4192:5363:1 gene:Traes_5DL_91F71E89E transcript:Traes_5DL_91F71E89E.1
Traes_5DL_983E3EDB0.1	pep:novel chromosome:IWGSC2:5D:149018151:149020814:-1 gene:Traes_5DL_983E3EDB0 transcript:Traes_5DL_983E3EDB0.1
Traes_5DL_9865B22EC.1	pep:novel chromosome:IWGSC2:5D:65562420:65565137:1 gene:Traes_5DL_9865B22EC transcript:Traes_5DL_9865B22EC.1
Traes_5DL_A4D36A69C.1	pep:novel chromosome:IWGSC2:5D:135084397:135087439:-1 gene:Traes_5DL_A4D36A69C transcript:Traes_5DL_A4D36A69C.1
Traes_5DL_AC7C885A0.1	pep:novel chromosome:IWGSC2:5D:70445248:70448479:1 gene:Traes_5DL_AC7C885A0 transcript:Traes_5DL_AC7C885A0.1
Traes_5DL_BB2DEEC83.1	pep:novel chromosome:IWGSC2:5D:94084061:94086207:-1 gene:Traes_5DL_BB2DEEC83 transcript:Traes_5DL_BB2DEEC83.1
Traes_5DL_BFB4552D3.1	pep:novel chromosome:IWGSC2:5D:151934348:151940177:1 gene:Traes_5DL_BFB4552D3 transcript:Traes_5DL_BFB4552D3.1
Traes_5DL_C51E9ECBB.1	pep:novel chromosome:IWGSC2:5D:65750724:65752070:1 gene:Traes_5DL_C51E9ECBB transcript:Traes_5DL_C51E9ECBB.1
Traes_5DL_D3AA8B440.1	pep:novel chromosome:IWGSC2:5D:100174818:100180610:-1 gene:Traes_5DL_D3AA8B440 transcript:Traes_5DL_D3AA8B440.1

Traes_5DL_D62C30008.1	pep:novel chromosome:IWGSC2:5D:126278083:126280660:-1 gene:Traes_5DL_D62C30008 transcript:Traes_5DL_D62C30008.1
Traes_5DL_D6E35133A.1	pep:novel chromosome:IWGSC2:5D:136890994:136891992:-1 gene:Traes_5DL_D6E35133A transcript:Traes_5DL_D6E35133A.1
Traes_5DL_D994DF96F.1	pep:novel chromosome:IWGSC2:5D:137251302:137253704:1 gene:Traes_5DL_D994DF96F transcript:Traes_5DL_D994DF96F.1
Traes_5DL_D9FB8D10D.1	pep:novel chromosome:IWGSC2:5D:148457338:148458709:-1 gene:Traes_5DL_D9FB8D10D transcript:Traes_5DL_D9FB8D10D.1
Traes_5DL_E209B0EDE.1	pep:novel chromosome:IWGSC2:5D:112278238:112282234:-1 gene:Traes_5DL_E209B0EDE transcript:Traes_5DL_E209B0EDE.1
Traes_5DL_EED5188AC.2	pep:novel chromosome:IWGSC2:5D:138578315:138585003:1 gene:Traes_5DL_EED5188AC transcript:Traes_5DL_EED5188AC.2
Traes_5DS_1BD5492E6.1	pep:novel chromosome:IWGSC2:5D:12462500:12468265:1 gene:Traes_5DS_1BD5492E6 transcript:Traes_5DS_1BD5492E6.1
Traes_5DS_554AEC0FE.1	pep:novel chromosome:IWGSC2:5D:19118311:19120621:1 gene:Traes_5DS_554AEC0FE transcript:Traes_5DS_554AEC0FE.1
Traes_5DS_5C96A0023.2	pep:novel scaffold:IWGSC2:IWGSC_CSS_5DS_scaff_532277:2736:6635:-1 gene:Traes_5DS_5C96A0023 transcript:Traes_5DS_5C96A0023.2
Traes_5DS_81917280C.1	pep:novel scaffold:IWGSC2:IWGSC_CSS_5DS_scaff_2768592:2968:7688:1 gene:Traes_5DS_81917280C transcript:Traes_5DS_81917280C.1
Traes_5DS_90C6C5521.1	pep:novel chromosome:IWGSC2:5D:40904652:40908623:-1 gene:Traes_5DS_90C6C5521 transcript:Traes_5DS_90C6C5521.1

Traes_5DS_C12EE1942.1	pep:novel scaffold:IWGSC2:IWGSC_CSS_5DS_scaff_2759991:5909:7333:1 gene:Traes_5DS_C12EE1942 transcript:Traes_5DS_C12EE1942.1
Traes_6AL_1DAFF2711.2	pep:novel chromosome:IWGSC2:6A:39776193:39782022:-1 gene:Traes_6AL_1DAFF2711 transcript:Traes_6AL_1DAFF2711.2
Traes_6AL_23918FB79.1	pep:novel chromosome:IWGSC2:6A:159051631:159073638:-1 gene:Traes_6AL_23918FB79 transcript:Traes_6AL_23918FB79.1
Traes_6AL_80FD46553.1	pep:novel chromosome:IWGSC2:6A:204589683:204593693:1 gene:Traes_6AL_80FD46553 transcript:Traes_6AL_80FD46553.1
Traes_6AL_8360ABFA1.1	pep:novel chromosome:IWGSC2:6A:182111755:182113872:-1 gene:Traes_6AL_8360ABFA1 transcript:Traes_6AL_8360ABFA1.1
Traes_6AL_E0594BF4C.2	pep:novel chromosome:IWGSC2:6A:197619573:197629664:-1 gene:Traes_6AL_E0594BF4C transcript:Traes_6AL_E0594BF4C.2
Traes_6AS_1E3D8BB5A.1	pep:novel chromosome:IWGSC2:6A:29914446:29917551:1 gene:Traes_6AS_1E3D8BB5A transcript:Traes_6AS_1E3D8BB5A.1
Traes_6AS_24E61E96B.2	pep:novel chromosome:IWGSC2:6A:2797510:2799379:1 gene:Traes_6AS_24E61E96B transcript:Traes_6AS_24E61E96B.2
Traes_6AS_2E324E361.1	pep:novel chromosome:IWGSC2:6A:50431368:50435579:-1 gene:Traes_6AS_2E324E361 transcript:Traes_6AS_2E324E361.1
Traes_6AS_5BAD56BB6.1	pep:novel scaffold:IWGSC2:IWGSC_CSS_6AS_scaff_3483094:12099:13711:-1 gene:Traes_6AS_5BAD56BB6 transcript:Traes_6AS_5BAD56BB6.1
Traes_6AS_6FE528AD1.2	pep:novel chromosome:IWGSC2:6A:19582916:19583455:1 gene:Traes_6AS_6FE528AD1 transcript:Traes_6AS_6FE528AD1.2

Traes_6BL_22DCB4C2A.1	pep:known scaffold:IWGSC2:IWGSC_CSS_6BL_scaff_4363722:2328:4902:-1 gene:Traes_6BL_22DCB4C2A transcript:Traes_6BL_22DCB4C2A.1 description:"50S ribosomal protein L9, chloroplastic "
Traes_6BL_54182EEB2.1	pep:novel scaffold:IWGSC2:IWGSC_CSS_6BL_scaff_2271874:126:2562:-1 gene:Traes_6BL_54182EEB2 transcript:Traes_6BL_54182EEB2.1
Traes_6BL_98C66424D.1	pep:novel chromosome:IWGSC2:6B:189321762:189324848:-1 gene:Traes_6BL_98C66424D transcript:Traes_6BL_98C66424D.1
Traes_6BL_CFC9B6ACB.1	pep:novel chromosome:IWGSC2:6B:188406858:188411597:1 gene:Traes_6BL_CFC9B6ACB transcript:Traes_6BL_CFC9B6ACB.1
Traes_6BS_259A7E1D3.1	pep:novel chromosome:IWGSC2:6B:100498586:100503543:-1 gene:Traes_6BS_259A7E1D3 transcript:Traes_6BS_259A7E1D3.1
Traes_6BS_5500E7783.1	pep:novel chromosome:IWGSC2:6B:25994368:25996523:1 gene:Traes_6BS_5500E7783 transcript:Traes_6BS_5500E7783.1
Traes_6BS_61205C056.1	pep:novel scaffold:IWGSC2:IWGSC_CSS_6BS_scaff_1263376:13:2685:1 gene:Traes_6BS_61205C056 transcript:Traes_6BS_61205C056.1
Traes_6BS_6D87FC5DE.1	pep:novel scaffold:IWGSC2:IWGSC_CSS_6BS_scaff_2994924:50:3639:1 gene:Traes_6BS_6D87FC5DE transcript:Traes_6BS_6D87FC5DE.1
Traes_6BS_6F8DEF103.1	pep:novel chromosome:IWGSC2:6B:35986570:35989560:-1 gene:Traes_6BS_6F8DEF103 transcript:Traes_6BS_6F8DEF103.1
Traes_6DL_066298459.1	pep:novel chromosome:IWGSC2:6D:99077530:99079736:1 gene:Traes_6DL_066298459 transcript:Traes_6DL_066298459.1

Traes_6DL_11374490D.1	pep:novel chromosome:IWGSC2:6D:159610115:159614253:-1 gene:Traes_6DL_11374490D transcript:Traes_6DL_11374490D.1
Traes_6DL_1B50CCE2A.1	pep:novel chromosome:IWGSC2:6D:116422771:116423472:1 gene:Traes_6DL_1B50CCE2A transcript:Traes_6DL_1B50CCE2A.1
Traes_6DL_1B9FBE0921.1	pep:novel chromosome:IWGSC2:6D:126578838:126582531:-1 gene:Traes_6DL_1B9FBE0921 transcript:Traes_6DL_1B9FBE0921.1
Traes_6DL_1BCF08167.1	pep:novel chromosome:IWGSC2:6D:169221476:169223385:-1 gene:Traes_6DL_1BCF08167 transcript:Traes_6DL_1BCF08167.1
Traes_6DL_241D10DDA.1	pep:novel chromosome:IWGSC2:6D:61206832:61212034:1 gene:Traes_6DL_241D10DDA transcript:Traes_6DL_241D10DDA.1
Traes_6DL_256D92F8A.1	pep:novel chromosome:IWGSC2:6D:93849454:93853204:-1 gene:Traes_6DL_256D92F8A transcript:Traes_6DL_256D92F8A.1
Traes_6DL_29F3EDA86.1	pep:novel chromosome:IWGSC2:6D:39771515:39773238:1 gene:Traes_6DL_29F3EDA86 transcript:Traes_6DL_29F3EDA86.1
Traes_6DL_3CACA0BAE.1	pep:novel chromosome:IWGSC2:6D:147142361:147149855:-1 gene:Traes_6DL_3CACA0BAE transcript:Traes_6DL_3CACA0BAE.1
Traes_6DL_53C8D0FAA.1	pep:novel chromosome:IWGSC2:6D:46301725:46306452:1 gene:Traes_6DL_53C8D0FAA transcript:Traes_6DL_53C8D0FAA.1
Traes_6DL_565B3D7EC.2	pep:novel chromosome:IWGSC2:6D:140852356:140855715:-1 gene:Traes_6DL_565B3D7EC transcript:Traes_6DL_565B3D7EC.2
Traes_6DL_7960654CF.2	pep:novel chromosome:IWGSC2:6D:174755146:174758682:-1 gene:Traes_6DL_7960654CF transcript:Traes_6DL_7960654CF.2
Traes_6DL_8716BB379.1	pep:novel scaffold:IWGSC2:IWGSC_CSS_6DL_scaff_1708026:47:1038:-1

	gene:Traes_6DL_8716BB379 transcript:Traes_6DL_8716BB379.1
Traes_6DL_8E776FEBA.2	pep:novel scaffold:IWGSC2:IWGSC_CSS_6DL_scaff_3223232:1:2986:-1 gene:Traes_6DL_8E776FEBA transcript:Traes_6DL_8E776FEBA.2
Traes_6DL_961B6AFC5.1	pep:novel chromosome:IWGSC2:6D:166362120:166366041:1 gene:Traes_6DL_961B6AFC5 transcript:Traes_6DL_961B6AFC5.1
Traes_6DL_98DC00BA3.2	pep:novel chromosome:IWGSC2:6D:140487004:140489484:-1 gene:Traes_6DL_98DC00BA3 transcript:Traes_6DL_98DC00BA3.2
Traes_6DL_A2EEFE47E.1	pep:novel scaffold:IWGSC2:IWGSC_CSS_6DL_scaff_1001990:1:3022:1 gene:Traes_6DL_A2EEFE47E transcript:Traes_6DL_A2EEFE47E.1
Traes_6DL_A4CE8D26B.1	pep:novel chromosome:IWGSC2:6D:150032810:150035047:-1 gene:Traes_6DL_A4CE8D26B transcript:Traes_6DL_A4CE8D26B.1
Traes_6DL_AB806B5E5.1	pep:novel chromosome:IWGSC2:6D:138886071:138890483:1 gene:Traes_6DL_AB806B5E5 transcript:Traes_6DL_AB806B5E5.1
Traes_6DL_B3FFF94B1.2	pep:novel chromosome:IWGSC2:6D:111604755:111610616:1 gene:Traes_6DL_B3FFF94B1 transcript:Traes_6DL_B3FFF94B1.2
Traes_6DL_C1571283B.1	pep:novel chromosome:IWGSC2:6D:130833289:130837565:-1 gene:Traes_6DL_C1571283B transcript:Traes_6DL_C1571283B.1
Traes_6DL_C6E63ED1C.1	pep:novel chromosome:IWGSC2:6D:168434815:168436507:-1 gene:Traes_6DL_C6E63ED1C transcript:Traes_6DL_C6E63ED1C.1
Traes_6DL_D3A3D1384.2	pep:novel chromosome:IWGSC2:6D:175746506:175752533:-1 gene:Traes_6DL_D3A3D1384 transcript:Traes_6DL_D3A3D1384.2

Traes_6DL_DC91E760F.1	pep:novel chromosome:IWGSC2:6D:132516561:132520963:-1 gene:Traes_6DL_DC91E760F transcript:Traes_6DL_DC91E760F.1
Traes_6DL_EAF694645.1	pep:novel chromosome:IWGSC2:6D:172163876:172165185:1 gene:Traes_6DL_EAF694645 transcript:Traes_6DL_EAF694645.1
Traes_6DL_EDF973683.1	pep:novel scaffold:IWGSC2:IWGSC_CSS_6DL_scaff_1184127:1:2277:1 gene:Traes_6DL_EDF973683 transcript:Traes_6DL_EDF973683.1
Traes_6DL_F980A7D9A.1	pep:novel scaffold:IWGSC2:IWGSC_CSS_6DL_scaff_3257870:2:1473:1 gene:Traes_6DL_F980A7D9A transcript:Traes_6DL_F980A7D9A.1
Traes_6DL_FF2824756.1	pep:novel chromosome:IWGSC2:6D:171558064:171563696:1 gene:Traes_6DL_FF2824756 transcript:Traes_6DL_FF2824756.1
Traes_6DL_FFB7A30B0.1	pep:novel chromosome:IWGSC2:6D:169224621:169228291:1 gene:Traes_6DL_FFB7A30B0 transcript:Traes_6DL_FFB7A30B0.1
Traes_6DS_350AB7B02.1	pep:novel chromosome:IWGSC2:6D:6519150:6520035:-1 gene:Traes_6DS_350AB7B02 transcript:Traes_6DS_350AB7B02.1
Traes_6DS_577BE9937.2	pep:known scaffold:IWGSC2:IWGSC_CSS_6DS_scaff_49860:369:1823:-1 gene:Traes_6DS_577BE9937 transcript:Traes_6DS_577BE9937.2 description:"Ribulose bisphosphate carboxylase large chain "
Traes_6DS_752205EA5.1	pep:novel chromosome:IWGSC2:6D:57651561:57658097:-1 gene:Traes_6DS_752205EA5 transcript:Traes_6DS_752205EA5.1
Traes_6DS_81AA78A29.1	pep:novel chromosome:IWGSC2:6D:102820485:102821347:1 gene:Traes_6DS_81AA78A29 transcript:Traes_6DS_81AA78A29.1

Traes_6DS_B551E20EA.1	pep:novel chromosome:IWGSC2:6D:15669252:15670707:1 gene:Traes_6DS_B551E20EA transcript:Traes_6DS_B551E20EA.1
Traes_6DS_CDB16CE3F.1	pep:novel chromosome:IWGSC2:6D:53812731:53816155:-1 gene:Traes_6DS_CDB16CE3F transcript:Traes_6DS_CDB16CE3F.1 description:"Phosphoglycerate kinase, cytosolic "
Traes_6DS_CDCAD6797.1	pep:novel scaffold:IWGSC2:IWGSC_CSS_6DS_scaff_2089497:3724:11771:-1 gene:Traes_6DS_CDCAD6797 transcript:Traes_6DS_CDCAD6797.1
Traes_7AL_45DF415001.1	pep:novel scaffold:IWGSC2:IWGSC_CSS_7AL_scaff_4555371:11174:12670:-1 gene:Traes_7AL_45DF415001 transcript:Traes_7AL_45DF415001.1 description: ATP synthase subunit beta, chloroplastic.
Traes_7AL_CA3D296A7.1	pep:novel chromosome:IWGSC2:7A:136746513:136748377:1 gene:Traes_7AL_CA3D296A7 transcript:Traes_7AL_CA3D296A7.1
Traes_7AS_CB60FA3AE.1	pep:novel scaffold:IWGSC2:IWGSC_CSS_7AS_scaff_4246109:1:1872:-1 gene:Traes_7AS_CB60FA3AE transcript:Traes_7AS_CB60FA3AE.1
Traes_7BL_44D3E9E5B.2	pep:novel scaffold:IWGSC2:IWGSC_CSS_7BL_scaff_6635401:25:4440:1 gene:Traes_7BL_44D3E9E5B transcript:Traes_7BL_44D3E9E5B.2
Traes_7BL_70F07C889.1	pep:novel chromosome:IWGSC2:7B:100680820:100681627:-1 gene:Traes_7BL_70F07C889 transcript:Traes_7BL_70F07C889.1
Traes_7BL_A42D6C984.1	pep:novel chromosome:IWGSC2:7B:66206631:66207673:1 gene:Traes_7BL_A42D6C984 transcript:Traes_7BL_A42D6C984.1
Traes_7BL_A7120C76A.1	pep:novel chromosome:IWGSC2:7B:113070060:113072533:1 gene:Traes_7BL_A7120C76A transcript:Traes_7BL_A7120C76A.1

Traes_7BL_C35CD97E7.1	pep:novel chromosome:IWGSC2:7B:206611056:206614829:-1 gene:Traes_7BL_C35CD97E7 transcript:Traes_7BL_C35CD97E7.1
Traes_7BS_3082E5A3C.1	pep:novel chromosome:IWGSC2:7B:32793246:32802100:-1 gene:Traes_7BS_3082E5A3C transcript:Traes_7BS_3082E5A3C.1
Traes_7BS_B18D7717E.1	pep:novel chromosome:IWGSC2:7B:69879983:69885899:1 gene:Traes_7BS_B18D7717E transcript:Traes_7BS_B18D7717E.1
Traes_7BS_CA543D479.1	pep:novel chromosome:IWGSC2:7B:101786522:101787098:1 gene:Traes_7BS_CA543D479 transcript:Traes_7BS_CA543D479.1
Traes_7BS_EF1042AE9.1	pep:novel scaffold:IWGSC2:IWGSC_CSS_7BS_scaff_3013535:6:382:1 gene:Traes_7BS_EF1042AE9 transcript:Traes_7BS_EF1042AE9.1
Traes_7DL_0E95F6220.1	pep:novel chromosome:IWGSC2:7D:119531893:119534295:-1 gene:Traes_7DL_0E95F6220 transcript:Traes_7DL_0E95F6220.1
Traes_7DL_186A707C8.1	pep:novel scaffold:IWGSC2:IWGSC_CSS_7DL_scaff_1585152:1:3365:1 gene:Traes_7DL_186A707C8 transcript:Traes_7DL_186A707C8.1
Traes_7DL_1CBD5E967.1	pep:novel chromosome:IWGSC2:7D:83923008:83926500:1 gene:Traes_7DL_1CBD5E967 transcript:Traes_7DL_1CBD5E967.1
Traes_7DL_300C570AD.2	
Traes_7DL_3632B8F7B.1	pep:novel scaffold:IWGSC2:IWGSC_CSS_7DL_scaff_3393461:3415:10618:1 gene:Traes_7DL_3632B8F7B transcript:Traes_7DL_3632B8F7B.1
Traes_7DL_439F5CB72.1	pep:novel chromosome:IWGSC2:7D:74597633:74599339:-1 gene:Traes_7DL_439F5CB72 transcript:Traes_7DL_439F5CB72.1

Traes_7DL_4B6FAFD6B.1	pep:novel chromosome:IWGSC2:7D:59935454:59938463:1 gene:Traes_7DL_4B6FAFD6B transcript:Traes_7DL_4B6FAFD6B.1
Traes_7DL_51CA70B80.1	pep:novel chromosome:IWGSC2:7D:149456187:149457807:1 gene:Traes_7DL_51CA70B80 transcript:Traes_7DL_51CA70B80.1
Traes_7DL_574A91F0E.1	pep:novel chromosome:IWGSC2:7D:172296383:172299314:-1 gene:Traes_7DL_574A91F0E transcript:Traes_7DL_574A91F0E.1
Traes_7DL_58217D4F3.2	pep:novel chromosome:IWGSC2:7D:198364746:198370656:-1 gene:Traes_7DL_58217D4F3 transcript:Traes_7DL_58217D4F3.2
Traes_7DL_64905FA8B.1	pep:novel scaffold:IWGSC2:IWGSC_CSS_7DL_scaff_3321526:4378:5888:-1 gene:Traes_7DL_64905FA8B transcript:Traes_7DL_64905FA8B.1
Traes_7DL_6AC3E4622.2	pep:novel chromosome:IWGSC2:7D:203261743:203265119:-1 gene:Traes_7DL_6AC3E4622 transcript:Traes_7DL_6AC3E4622.2 description:"Eukaryotic initiation factor 4A "
Traes_7DL_7803A2E53.2	pep:novel chromosome:IWGSC2:7D:69348155:69358414:-1 gene:Traes_7DL_7803A2E53 transcript:Traes_7DL_7803A2E53.2
Traes_7DL_930094B08.1	pep:known chromosome:IWGSC2:7D:70899004:70901125:-1 gene:Traes_7DL_930094B08 transcript:Traes_7DL_930094B08.1 description:"Flavone O-methyltransferase 1 "
Traes_7DL_9521D3D43.2	pep:novel chromosome:IWGSC2:7D:67208159:67220765:1 gene:Traes_7DL_9521D3D43 transcript:Traes_7DL_9521D3D43.2
Traes_7DL_961822B36.2	pep:novel chromosome:IWGSC2:7D:67277057:67280381:-1 gene:Traes_7DL_961822B36 transcript:Traes_7DL_961822B36.2

Traes_7DL_96D46C529.1	pep:novel chromosome:IWGSC2:7D:215407673:215411775:-1 gene:Traes_7DL_96D46C529 transcript:Traes_7DL_96D46C529.1
Traes_7DL_994CA11011.2	pep:novel scaffold:IWGSC2:IWGSC_CSS_7DL_scaff_3290387:661:783:-1 gene:Traes_7DL_994CA11011 transcript:Traes_7DL_994CA11011.2
Traes_7DL_A79EE6AAB.2	pep:novel chromosome:IWGSC2:7D:55243996:55247418:1 gene:Traes_7DL_A79EE6AAB transcript:Traes_7DL_A79EE6AAB.2
Traes_7DL_BC3073792.1	pep:novel chromosome:IWGSC2:7D:171609261:171612076:-1 gene:Traes_7DL_BC3073792 transcript:Traes_7DL_BC3073792.1
Traes_7DL_D4B6FF473.1	pep:novel chromosome:IWGSC2:7D:217862451:217869207:1 gene:Traes_7DL_D4B6FF473 transcript:Traes_7DL_D4B6FF473.1
Traes_7DL_EDE77652A.1	pep:novel chromosome:IWGSC2:7D:198663402:198666324:-1 gene:Traes_7DL_EDE77652A transcript:Traes_7DL_EDE77652A.1
Traes_7DL_F3868C6C1.1	pep:novel scaffold:IWGSC2:IWGSC_CSS_7DL_scaff_1762516:10:246:-1 gene:Traes_7DL_F3868C6C1 transcript:Traes_7DL_F3868C6C1.1
Traes_7DL_FE457F7CD.1	pep:novel chromosome:IWGSC2:7D:69660136:69665884:-1 gene:Traes_7DL_FE457F7CD transcript:Traes_7DL_FE457F7CD.1
Traes_7DL_FED4780F5.2	pep:novel chromosome:IWGSC2:7D:159809687:159813123:1 gene:Traes_7DL_FED4780F5 transcript:Traes_7DL_FED4780F5.2
Traes_7DS_0141922EC.2	pep:novel scaffold:IWGSC2:IWGSC_CSS_7DS_scaff_3933113:3:2773:1 gene:Traes_7DS_0141922EC transcript:Traes_7DS_0141922EC.2
Traes_7DS_02539EB3B.1	pep:known chromosome:IWGSC2:7D:134890236:134896174:-1 gene:Traes_7DS_02539EB3B

	transcript:Traes_7DS_02539EB3B.1 description:"Glucose-1-phosphate adenylyltransferase small subunit, chloroplastic/amyloplastic "
Traes_7DS_07E6F5FD6.1	pep:novel chromosome:IWGSC2:7D:21263809:21265315:1 gene:Traes_7DS_07E6F5FD6 transcript:Traes_7DS_07E6F5FD6.1
Traes_7DS_295BC9B39.2	pep:novel scaffold:IWGSC2:IWGSC_CSS_7DS_scaff_3889498:5:3681:1 gene:Traes_7DS_295BC9B39 transcript:Traes_7DS_295BC9B39.2
Traes_7DS_304EAFD6B.1	pep:novel chromosome:IWGSC2:7D:13030093:13031858:-1 gene:Traes_7DS_304EAFD6B transcript:Traes_7DS_304EAFD6B.1
Traes_7DS_310C9A814.1	pep:novel scaffold:IWGSC2:IWGSC_CSS_7DS_scaff_361157:1:4954:1 gene:Traes_7DS_310C9A814 transcript:Traes_7DS_310C9A814.1
Traes_7DS_42F8FD2BD.1	pep:novel scaffold:IWGSC2:IWGSC_CSS_7DS_scaff_3876909:4220:6871:-1 gene:Traes_7DS_42F8FD2BD transcript:Traes_7DS_42F8FD2BD.1
Traes_7DS_51D42FCC4.1	pep:novel chromosome:IWGSC2:7D:96866107:96868792:-1 gene:Traes_7DS_51D42FCC4 transcript:Traes_7DS_51D42FCC4.1
Traes_7DS_595FB94A0.1	pep:novel scaffold:IWGSC2:IWGSC_CSS_7DS_scaff_3967356:3800:5420:-1 gene:Traes_7DS_595FB94A0 transcript:Traes_7DS_595FB94A0.1
Traes_7DS_659C88744.1	pep:novel chromosome:IWGSC2:7D:21122843:21126651:1 gene:Traes_7DS_659C88744 transcript:Traes_7DS_659C88744.1
Traes_7DS_7254A96B4.1	pep:novel scaffold:IWGSC2:IWGSC_CSS_7DS_scaff_3900112:3241:8363:1 gene:Traes_7DS_7254A96B4 transcript:Traes_7DS_7254A96B4.1

Traes_7DS_833BCFCAF.1	pep:novel chromosome:IWGSC2:7D:101940023:101941576:1 gene:Traes_7DS_833BCFCAF transcript:Traes_7DS_833BCFCAF.1
Traes_7DS_A033CB10E.1	pep:novel chromosome:IWGSC2:7D:37267706:37273646:1 gene:Traes_7DS_A033CB10E transcript:Traes_7DS_A033CB10E.1
Traes_7DS_A97F032B8.1	pep:novel scaffold:IWGSC2:IWGSC_CSS_7DS_scaff_3854538:2:1821:1 gene:Traes_7DS_A97F032B8 transcript:Traes_7DS_A97F032B8.1
Traes_7DS_A9BD8001C.1	pep:known scaffold:IWGSC2:IWGSC_CSS_7DS_scaff_3919168:2262:5853:1 gene:Traes_7DS_A9BD8001C transcript:Traes_7DS_A9BD8001C.1 description:"Peroxiredoxin Q, chloroplastic "
Traes_7DS_D05C22D58.1	pep:novel scaffold:IWGSC2:IWGSC_CSS_7DS_scaff_3884772:247:945:1 gene:Traes_7DS_D05C22D58 transcript:Traes_7DS_D05C22D58.1 description:"Cytochrome b6”
Traes_7DS_F7A4607C5.2	pep:novel chromosome:IWGSC2:7D:32370248:32370854:-1 gene:Traes_7DS_F7A4607C5 transcript:Traes_7DS_F7A4607C5.2
Traes_7DS_FDC2AB87A.1	pep:novel scaffold:IWGSC2:IWGSC_CSS_7DS_scaff_3949110:1:3423:1 gene:Traes_7DS_FDC2AB87A transcript:Traes_7DS_FDC2AB87A.1
TRAES3BF007900030CFD_t1	pep:novel chromosome:IWGSC2:3B:473734374:473736019:-1 gene:TRAES3BF007900030CFD_g transcript:TRAES3BF007900030CFD_t1
TRAES3BF023000010CFD_t1	pep:novel chromosome:IWGSC2:3B:530444897:530448805:1 gene:TRAES3BF023000010CFD_g transcript:TRAES3BF023000010CFD_t1
TRAES3BF026200060CFD_t1	pep:novel chromosome:IWGSC2:3B:421870112:421876791:1 gene:TRAES3BF026200060CFD_g transcript:TRAES3BF026200060CFD_t1

TRAES3BF028000060CFD_t1 pep:novel chromosome:IWGSC2:3B:444553027:444553557:1
gene:TRAES3BF028000060CFD_g
transcript:TRAES3BF028000060CFD_t1

TRAES3BF036000280CFD_t1 pep:novel chromosome:IWGSC2:3B:747238104:747239726:1
gene:TRAES3BF036000280CFD_g
transcript:TRAES3BF036000280CFD_t1

TRAES3BF044200210CFD_t1 pep:novel chromosome:IWGSC2:3B:631651011:631653178:1
gene:TRAES3BF044200210CFD_g
transcript:TRAES3BF044200210CFD_t1

TRAES3BF049800100CFD_t1 pep:novel chromosome:IWGSC2:3B:183956930:183961312:1
gene:TRAES3BF049800100CFD_g
transcript:TRAES3BF049800100CFD_t1

TRAES3BF050800360CFD_t1 pep:novel chromosome:IWGSC2:3B:17306999:17310145:1
gene:TRAES3BF050800360CFD_g
transcript:TRAES3BF050800360CFD_t1

TRAES3BF055400010CFD_t1 pep:novel chromosome:IWGSC2:3B:414167525:414171407:-1
gene:TRAES3BF055400010CFD_g
transcript:TRAES3BF055400010CFD_t1

TRAES3BF063600070CFD_t1 pep:novel chromosome:IWGSC2:3B:707277291:707278459:-1
gene:TRAES3BF063600070CFD_g
transcript:TRAES3BF063600070CFD_t1

TRAES3BF065400180CFD_t1 pep:novel chromosome:IWGSC2:3B:772944026:772944656:1
gene:TRAES3BF065400180CFD_g
transcript:TRAES3BF065400180CFD_t1

TRAES3BF073600070CFD_t1 pep:novel chromosome:IWGSC2:3B:488666860:488667555:-1
gene:TRAES3BF073600070CFD_g
transcript:TRAES3BF073600070CFD_t1

TRAES3BF091200110CFD_t1 pep:novel chromosome:IWGSC2:3B:93292908:93295419:1
gene:TRAES3BF091200110CFD_g
transcript:TRAES3BF091200110CFD_t1

TRAES3BF099800020CFD_t1 pep:novel chromosome:IWGSC2:3B:120524258:120528780:1
gene:TRAES3BF099800020CFD_g
transcript:TRAES3BF099800020CFD_t1

TRAES3BF117900070CFD_t1 pep:novel chromosome:IWGSC2:3B:172991553:172995174:1
gene:TRAES3BF117900070CFD_g
transcript:TRAES3BF117900070CFD_t1

TRAES3BF142500040CFD_t1 pep:novel chromosome:IWGSC2:3B:615240428:615243431:1
gene:TRAES3BF142500040CFD_g
transcript:TRAES3BF142500040CFD_t1
description:"Sedoheptulose-1,7-bisphosphatase, chloroplastic
"

TRAES3BF154700090CFD_t1 pep:novel scaffold:IWGSC2:v443_1547:419192:420184:-1
gene:TRAES3BF154700090CFD_g
transcript:TRAES3BF154700090CFD_t1

TRAES3BF155200010CFD_t1 pep:novel chromosome:IWGSC2:3B:669974415:669988816:-1
gene:TRAES3BF155200010CFD_g
transcript:TRAES3BF155200010CFD_t1

TRAES3BF167600010CFD_t1 pep:novel chromosome:IWGSC2:3B:58499772:58501464:1
gene:TRAES3BF167600010CFD_g
transcript:TRAES3BF167600010CFD_t1

TRAES3BF177200020CFD_t1 pep:novel chromosome:IWGSC2:3B:75516878:75517484:1
gene:TRAES3BF177200020CFD_g
transcript:TRAES3BF177200020CFD_t1

References

ABARES. (2015). December 2015 Quarterly Report. *Australian Bureau of Agricultural and Resource Economics and Science (ABARES)*.

Agrawal, A. A. (2007). Macroevolution of plant defense strategies. *Trends Ecol Evol, 22*(2), 103-109.

Ahl Goy, P., Signer, H., Reist, R., Aichholz, R., Blum, W., Schmidt, E., & Kessmann, H. (1993). Accumulation of scopoletin is associated with the high disease resistance of the hybrid *Nicotiana glutinosa* x *Nicotiana debneyi*. *Planta, 191*, 200-206.

Alfaro, A. (1947). Notas sobre *Brachycolus noxius* Mordw., nueva plaga para nuestros trigos y cebadas. *Boletin de Patologia Vegetal y Entomologia Agricola 15*, 125-130.

Amulaka, F. O., Maling'a, J. N., Pathak, R. S., Cakir, M., & Mulwa, R. M. S. (2013). Yield evaluation of a wheat line with combined resistance to Russian wheat aphid and stem rust race "Ug99" in Kenya. *American Journal of Plant Sciences, 04*(07), 1494-1499.

Anderson, G. R., Papa, D., Peng, J., Tahir, M., & Lapitan, N. L. (2003). Genetic mapping of *Dn7*, a rye gene conferring resistance to the Russian wheat aphid in wheat. *Theor Appl Genet, 107*(7), 1297-1303.

Anna Urbanska, Bogumil Leszcynski, Tjallingii, Willem F., & Matok, Henryk. (2002). Probing behaviour and enzymatic defence of the grain aphid against cereal phenolics *Electronic Journal of Polish Agricultural Universities, 5*(2).

Appels, R., Morris, R., & Gill, B. S. (1998). A Book: Chromosome Biology. *DOI 10.1007/978-1-4615-5409-7, ISBN 978-1-4615-5409-7 (eBook), ISBN 978-1-4613-7470-1.*

Arnér, Elias S. J., & Holmgren, A. (2000). Physiological functions of thioredoxin and thioredoxin reductase. *European Journal of Biochemistry, 267*(20), 6102-6109.

Arumuganathan, K., & Earle, E. D. (1991). Nuclear DNA content of some important plant species *Plant Molecular Biology Reporter, 9*(3), 208-218.

Arzani, A., Peng, J. H., & Lapitan, N. L. V. (2004). DNA and morphological markers for a Russian wheat aphid resistance gene. *Euphytica, 139*, 167-172.

Aviezer, K., Kurek, I., Erel, N., Blecher, O., Devos, K. , & Breiman, A. (1998). Studies on the expression of the wheat prolyl isomerase FKBP73 during plant development. *Plant Science*, 149-158.

Baird, N. A., Etter, P. D., Atwood, T. S., Currey, M. C., Shiver, A. L., Lewis, Z. A., . . . Johnson, E. A. (2008). Rapid SNP discovery and genetic mapping using sequenced RAD markers. *PLoS One, 3*(10), 1-7.

Basha, E., Lee, G. J., Demeler, B., & Vierling, E. (2004). Chaperone activity of cytosolic small heat shock proteins from wheat. *Eur J Biochem, 271*(8), 1426-1436.

Bately, J., Barker, G., O'Sullivan, H., Edwards, K. J., & Edwards, D. (2003). Mining for single nucleotide polymorphisms and insertions/deletions in maize expressed sequence tag data. *Plant Phsiology, 132*(1), 84-91.

Beales, J., Laurie, D. A. , & Devos, K. M. (2005). Allelic variation at the linked AP1 and PhyC loci in hexaploid wheat is associated but not perfectly correlated with vernalization response. *Theor Appl Genet, 110*, 1099–1107.

Ben-Zvi, A., De Los Rios, P., Dietler, G., & Goloubinoff, P. (2004). Active solubilization and refolding of stable protein aggregates by cooperative unfolding action of individual hsp70 chaperones. *J Biol Chem, 279*(36), 37298-37303.

Blackman, R. L., & Eastop, V. F. (1984). Aphids on the World's crops: an Ientification and information guide. *Wiley, Chichester, U. K.*

Blecher, O., Erel, N., Callebaut, I., Aviezer, K., & Breiman, A. (1996). A novel wheat peptidyal-prolyl-cis-trans isomerase: cDNA isolation, structure, enzymatic activity, and expression. *Plant Mol. Biol, 32*, 493-504.

Botha-Oberholster, A. M., Matisioloko, M. T., Du Preez, F. B., Van Eck, L., & Walter, R. (2004). Russian wheat aphid-mediated elicitation of the wheat defense-transcriptome. *Plant Biology 2004 Program, Lake Buena Vista, Florida, USA.*, 126.

Botha, A. M., Lacock, L., van Niekerk, C., Matsioloko, M. T., du Preez, F. B., Loots, S., . . . Cullis, C. A. (2006). Is photosynthetic transcriptional regulation in *Triticum aestivum* L. cv. 'TugelaDN' a contributing factor for tolerance to *Diuraphis noxia* (Homoptera: Aphididae)? *Plant Cell Rep, 25*(1), 41-54.

Botha, Anna-Maria, Li, Youchun, & Lapitan, Nora L. V. (2005). Cereal host interactions with Russian wheat aphid: A review. *Journal of Plant Interactions, 1*(4), 211-222.

Botstein, D. R., White, R. L., Skolnick, M., & Davis, R. W. (1980). Construction of a genetic linkage map in man using restriction fragment length polymorphism. *Am. J. Hum. Genet., 32*, 314-331.

Bourguignon, J., Merand, V., Rawsthorne, S., Forest, E., & Douce, R. (1996). Glycine decarboxylase and pyruvate dehydrogenase complexes share the same dihydrolipoamide dehydrogenase in pea leaf mitochondria: evidence from mass spectrometry and primary-structure analysis. *Biochem. J., 313*, 229-234.

Bowles, D. J. (1990). Defense related proteins in higher plants - Annu. Rev. . *Biochem. , 59*, 873-907.

Boyko, E. V. , Smith, C. M. , Thara, V. K. , Bruno, J. M. , Deng, Y. , Starkey, S. R., & Klaahsen, D. L. . (2006). Molecular basis of plant gene expression during aphid invasion: Wheat Pto- and Pti-Like sequences are involved in interactions between wheat and Russian wheat aphid (Homoptera: Aphididae). *J. Econ. Entomol., 99*(4), 1430-1445.

Bradford, M. M. (1976). A rapid and sensitive method for the quantitation of microgram quantities of protein utilizing the principle of protein-dye binding. *Analytical Biochemistry, 72*, 248-254.

Brenchley, R., Spannagl, M., Pfeifer, M., Barker, G. L., D'Amore, R., Allen, A. M., . . . Hall, N. (2012). Analysis of the bread wheat genome using whole-genome shotgun sequencing. *Nature, 491*(7426), 705-710.

Broughton, Sue. (2011). The application of n-butanol improves embryo and green plant production in anther culture of Australian wheat (*Triticum aestivum* L.) genotypes. *Crop and Pasture Science, 62*(10), 813-822.

Burd, J. D., & Burton, R. L. (1992). Characterization of plant damage caused by Russian wheat aphid (Homoptera: Aphididae). *Jounal of Economic Entomology, 85*(5), 2017-2022.

Burd, J. D., & Elliott, N. C. (1996). Changes in chlorophyll a fluorescence induction kinetics in cereals infested with Russian wheat aphid (Homopetra: Aphididea) *Jounal of Economic Entomology, 89*(5), 787-794.

Burd, J. D., Porter, D. R., Puterka, G. J., Haley, S. D., & Peairs, B. F. (2006). Biotypic variation among North American Russian wheat Aphid (Homoptera- Aphididae) populations. *J. Econ. Entomol. , 99*(5), 1862-1866.

Callahan, D. L., Baker, A. J., Kolev, S. D., & Wedd, A. G. (2006). Metal ion ligands in hyperaccumulating plants. *J Biol Inorg Chem, 11*(1), 2-12.

Carolan, J. C., Fitzroy, C. I., Ashton, P. D., Douglas, A. E., & Wilkinson, T. L. (2009). The secreted salivary proteome of the pea aphid *Acyrthosiphon pisum* characterised by mass spectrometry. *Proteomics, 9*(9), 2457-2467.

Castro, A. M., Ramos, S, Vasicek, A., Worland, A. J., Giménez, D. O, Clua, A. A, & Suarez, E. (2001). Identification of wheat chromosomes involved with different types of resistance against greenbug (*Schizaphis graminum*, Rond.) and the Russian wheat aphid (*Diuraphis noxia*, Mordvilko). *Euphytica, 118*, 321-330.

Castro, A. M., Vasicek, A., Ellerbrook, C., Giménez, D. O, Tocho, E., Tacaliti, M. S., . . . Snape, J. W. (2004). Mapping quantitative trait loci in wheat for resistance against greenbug and Russian wheat aphid. *Plant Breeding, 123*(4), 361-365.

Castro, A. M., Vasicek, A., Manifiesto, D. O., Giménez, D. O, Tacaliti, M. S., Dobrovolskaya, O., . . . Borner, A. (2005). Mapping antixenosis genes on chromosome 6A of wheat to greenbug and to a new biotype of Russian wheat aphid. *Plant Breeding, 124*, 229-233.

Chao, S. P., Sharp, P. J., Worland, A. J., Warham, E. J., Koebner, R. M. D., & Gale, M. D. (1989). RFLP-based genetic maps of wheat homoeologous group 7 chromosomes. *Theor Appl Genet, 78*, 493-504.

Chapman, J. A., Mascher, M., Buluc, A., Barry, K., Georganas, E., Session, A., . . . Rokhsar, D. S. (2015). A whole-genome shotgun approach for assembling and anchoring the hexaploid bread wheat genome. *Genome Biol, 16*, 26.

Chen, ZH., Walker, R. P., Acheson, R. M., & Leegood, R. C. (2002). Phosphoenolpyruvate carboxykinase assayed at physiological concentrations of metal ions has ahigh affininity for Co_2. *Plant Phsiology, 128*(1), 160-164.

Cherqui, Anas, & Tjallingii, W. Fred. (2000). Salivary proteins of aphids, a pilot study on identification, separation and immunolocalisation *Journal of Insect Physiology, 46*, 1177-1186.

Choe, L., D'Ascenzo, M., Relkin, N. R., Pappin, D. J., Ross, P. L., Williamson, B., . . . Lee, K. H. (2007). 8-plex quantitation of changes in cerebropinal fluid protein expression in subjects undergoing intravenous immunoglobulin treatment for Alzheimer's disease. *Proteomics, 7*(20), 3651-3660.

Choi, I. Y., Hyten, D. L., & Matukumalli, L. K. et al. (2007). A soybean transcript map: gene distribution, haplotype and single nucleotide polymorphism analysis. *Genetics, 176*(1), 685-696.

Choulet, F., Wicker, T., Rustenholz, C., Paux, E., Salse, J., Leroy, P., . . . Feuillet, C. (2010). Megabase level sequencing reveals contrasted organization and evolution patterns of the wheat gene and transposable element spaces. *Plant Cell, 22*(6), 1686-1701.

Ciepiela, A., & Sempruch, C. (1999). Effect of L-3, 4-dihydroxyphenylalanine, ornithine and $^{\gamma}$-aminonutyric acid on winter wheat resistance to grain aphid. *Journal of Applied Entomology, 123*, 285-288.

Clark, G. B., Morgan, R. O., Fernandez, M. P., & Roux, S. J. (2012). Evolutionary adaptation of plant annexins has diversified their molecular structures, interactions and functional roles. *New Phytol, 196*(3), 695-712.

Coll, N. S., Epple, P., & Dangl, J. L. (2011). Programmed cell death in the plant immune system. *Cell Death Differ, 18*(8), 1247-1256.

Collard, B. C., & Mackill, D. J. (2008). Marker-assisted selection: an approach for precision plant breeding in the twenty-first century. *Phil. Trans. R. Soc. B, 363*, 557-572.

Cooper, W. R., Dillwith, J. W., & Puterka, G. J. (2010). Salivary proteins of Russian wheat aphid (Hemiptera: Aphididae). *Environ Entomol, 39*(1), 223-231.

Corthals, G. L., Wasinger, V. C., Houchstrasser, D. F., & Sanchez, J. C. (2000). The dynamic range of protein expression: a challenge for proteomic research. *Electrophoresis, 21*, 1104-1115.

Curdt, I., Singh, B. B., Jakoby, M., Hachtel, W., & Bohme, H. (2000). Identification of aminoacid residues of nitrite reductase from *Anabaena* sp. PCC 7120 involved in ferredoxin binding. *Biochim. Biophys. Acta., 1543*, 60-68.

Davis, M. J. (2005). The oxidative environment and protein damage *Biochim. Biophys. Acta., 1703*, 93-109.

Dayakar, B. V., Lin, H. J., Chen, C. H., Ger, M. J., Lee, B. H., Pai, C. H., . . . Feng, T. Y. (2003). Ferredoxin from sweet pepper (*Capsicum annum* L.) intensifying hairpin(pss) - mediated hypersensitive response shows an enhanced production of active oxygen species (AOS). *Plant Mol. Biol, 51*, 913-924.

Diamant, S., Peres Ben-Zvi, A., Bukau, B., & Goloubinoff, P. (2000). Size - dependent disaggregation of stable protein aggregates by the DnaK chaperone machinery. *J Biol Chem, 275*, 21107-21113.

Dixon, D. P., Lapthorn, A., & Edwards, R. (2002). Plant glutathione transferases. *Genome Biol, 3*(3), 1-10.

Dixon, R. A., & Pativa, N. L. (1995). Stress-induced phenylpropanoid metabolism. *Plant Cell, 7*, 1085-1097.

Dixon, R. A., & Steele, C. L. (1999). Flavonoids and isoflavonoids: a gold mine for metabolic engineering. *Trends Plant Sci, 4*, 394-400.

Dogimont, C., Bendahmane, A., Chovelon, V., & Boissot, N. (2010). Host plant resistance to aphids in cultivated crops: genetic and molecular bases, and interactions with aphid populations. *C R Biol, 333*(6-7), 566-573.

Dogimont, C., Chovelon, V., Tual, S., Boissot, N., Rittener, V., Giovinazzo, N., & Bendahmane, A. (2008). Molecular diversity at the *Vat/Pm-W* resistance locus in melon. *Cucurbitaceae 2008, Proceedings of the IXth EUCARPIA meeting on genetics and breeding of Cucurbitaceae (Pitrat M, ed), INRA, Avignon (France), May 21-24th, 2008* 219-227.

Dong, H., Quick, J. S, & Zhang, Y. (1997). Inheritance and allelism lines of Russian wheat aphid resistance in several wheat lines. *Plant Breeding, 116*, 449-453.

Douce, R., Bourguignon, J., Macherel, J., & Neuburger, M. (1994). The glycine decarboxylase system in higher plant mitochondria: Structure, Function and biogenesis. *Biochem. Soc. Trans., 22*, 184-188.

Douce, R., Bourguignon, J., Neuburger, M., & Rebeille, F. (2001). The glycine decarboxylase system: a fascinating complex. *Trends in Plant Science, 6*(4), 167-176.

Du Toit, F. (1987). Resistance in wheat (*Triticum aestivum*) to *Diuraphis noxia* (Homoptera: Aphididae). *Cereal Res. Commun., 15*, 175-179.

Du Toit, F. (1989). Inheritance of resistance in two *Triticum aestivum* lines to Russian wheat aphid (Homoptera: Apididae). *Jounal of Economic Entomology, 82*(4), 1251-1253.

Edwards, R., & Dixon, D. P. (2000). The role of glutathione transferases in herbicide metabolism. In herbicides and their mechanism of action. *Sheffield Academic Press*, 33-71.

Edwards, R., Dixon, D. P., & Walbot, V. (2000). Plant glutathione S-transferases: enzyme with multiple functions in sickness and in health. *Trends Plant Sci, 5*, 193-198.

EI Bouhssini, M., Ogbonnaya, F. C., Chen, M., Lhaloui, S., Rihawi, F., & Dabbous, A. (2012). Sources of resistance in primary synthetic hexaploid wheat (*Triticum aestivum* L.) to insect pests: Hessian fly, Russian wheat aphid and Sunn pest in the fertile crescent. *Genetic Resources and Crop Evolution, 60*(2), 621-627.

EI Bouhssini, M., Ogbonnaya, F. C., Ketata, H., Mosaad, M. M., Street, K., Amri, A., . . . Smith, C. M. (2011). Progress in host plant resistance in wheat to Russian wheat aphid (Hemiptera: Aphididae) in North Africa and West Asia. *Australian Journal of Crop science, 5*(9), 1108-1113.

EI Modafar, C., Clerivet, A., Vigouroux, A., & Macheix, J. J. (1995). Accumulation of phytoalexins in leaves of plane tree (*Platanus* spp.) expressing susceptibility or resistance to *Ceratocystis fimbriata* f. sp.*platani*. *European Journal of Plant Pathology, 101*, 503-509.

El Bouhssini, M., Ogbonnaya, F. C., Ketata, H., Mosaad, M. M., Street, K., Amri, A., . . . Smith, C. M. (2011). Progress in host plant resistance in wheat to Russian wheat aphid (Hemiptera: Aphididae) in North Africa and West Asia. *Australian Journal of Crop Science, 5*(9), 1108-1113.

Elzinga, D. A., & Jander, G. (2013). The role of protein effectors in plant-aphid interactions. *Curr Opin Plant Biol, 16*(4), 451-456.

Ennahli, Said, Bouhssini, Mustapha El, Grando, Stefania, Anathakrishnan, Radhika, Niide, Terutaka, Starkus, Laura, . . . Smith, C. Michael. (2009). Comparison of categories of resistance in wheat and barley genotypes against biotype 2 of the Russian wheat aphid, *Diuraphis noxia* (Kurdjumov). *Arthropod-Plant Interactions, 3*(1), 45-53.

Erb, M., Lenk, C., Degenhardt, J., & Turlings, T. C. (2009). The underestimated role of roots in defense against leaf attackers. *Trends Plant Sci, 14*(12), 653-659.
Esposti, M. D., Avitabile, E., Barilli, M., Schiavo, G., Montecucco, C., & Lenaz, G. (1986). Comparative biochemistry of the ubiquinol cytochrome *c* oxidoreductase (EC 1.10.2.2) isolated from different heart mitochondria. *Comp. Bichem. Physiol., 85B*(3), 543-552.
Evert, R. F. (1990). Dicotyledons. In Sieve Elements: Comparative Structure, induction and development (ed. H. D. Behnke and R. D. Sjolund). *Berlin: Springer*, 103-138.
Fartek, B., Nibouche, S., Turpin, P., Costet, L., & Reynaud, B. (2012). Resistance to *Melanaphis sacchari* in the sugarcane cultivar R 365. *Entomologia Experimentalis et Applicata, 144*(3), 270-278.
Fazel-Najafabadi, M., Peng, J., Peairs, F. B., Simkova, H., Kilian, A., & Lapitan, N. L. V. (2014). Genetic mapping of resistance to *Diuraphis noxia* (Kurdjumov) biotype 2 in wheat (*Triticum aestivum* L.) accession CI2401. *Euphytica, 203*(3), 607-614.
Feuillet, C., Stein, N., Rossini, L., Praud, S., Mayer, K., Schulman, A., . . . Appels, R. (2012). Integrating cereal genomics to support innovation in the Triticeae. *Funct Integr Genomics, 12*(4), 573-583.
Finney, L. A., & O'Halloran, T. V. (2003). Transition metal speciation in the cell: Insights from the chemistry of metal ion receptors. *Science, 300*(5621), 931-936.
Forslund, K., Pettersson, J., Bryngelsson, T., & Jonsson, L. (2000). Aphid infestation induces PR proteins differentially in barley susceptible or resistance to the bird cherry-oat aphid. *Physiol Plant, 110*, 496-502.
Fritig, B., & Hirth, L. (1971). Biosynthesis of phenylpropanoids and coumarins in TMV-infected tobacco leaves and tobacco tissue culture. *Acta Phytopathol. acad. Sci. Hung, 6*, 21-29.
Fu, Y., Zhang, H., Mandal, S. N., Wang, C., Chen, C., & Ji, W. (2016). Quantitative proteomics reveals the central changes of wheat in response to powdery mildew. *J Proteomics, 130*, 108-119.
Fuller, H. R., & Morris, G. E. (2012). Quantitative Proteomics Using iTRAQ Labeling and Mass Spectrometry. *Integrative Proteomics, Dr. Hon-Chiu Leung (Ed.), ISBN: 978-953-51-0070-6, InTech, Available from: http://www.intechopen.com/books/integrative-proteomics/quantitative-proteomics-using-itraq-labeling-andmass-spectrometry*.
Ganal, M. W., Altmann, T. , & Roder, M. S. (2009). SNP identification in crop plants. *Current Opinion in Plant Biology, 12*(2), 211-217.
Garcia-Brugger, A., Lamotte, O., Vandelle, E., Bourque, S., Lecourieux, D., Poinssot, B., . . . Pugin, A. (2006). Early signalling events induced by

elicitors of plant defenses. *The American Phytopathological Society, 7*, 711-724.
Gasser, C. S., Gunning, D. A., Budelier, K. A., & Brown, S. M. (1990). Structure and expression of cytosolic cyclophilin/peptidyl prolyl-cis-trans Isomerase of higher plants and production of active tomato cyclphilin in *Escherichia coli*. *Proc. Natl. Acad. Sci. USA, 87*, 9519-9523.
Gilchrist, L., Rodriguez, R., & Burnett, P. A. (1984). The extent of Freestate streak and *Diuraphis noxia* in Mexico. *In: P. A. Burnett (Ed.), Barley Yellow Dwarf, a Proceedings of the Workshop, CIMMYT, Mexico. D. F.*, 157-163.
Gill, B. S., Appels, R., Botha-Oberholster, A. M., Buell, C. R., Bennetzen, J. L., Chalhoub, B., . . . Sasaki, T. (2004). A workshop report on wheat genome sequencing: International Genome Research on Wheat Consortium. *Genetics, 168*(2), 1087-1096.
Goggin, F. L. (2007). Plant-aphid interactions: molecular and ecological perspectives. *Curr Opin Plant Biol, 10*(4), 399-408.
Gorlach, J., Raesecke, H. R., Rentsch, D., Regenass, M., Roy, P., Zala, M., . . . Schmid, J. (1995). Temporally distinct accumulation of transcripts encoding enzymes of the prechorismate pathway in elicitor treated, culture tomato cells. *Proc Natl Acad Sci USA, 92*, 3166-3170.
Gottwald, S., Samans, B., Luck, S., & Friedt, W. (2012). Jasmonate and ethylene dependent defence gene expression and suppression of fungal virulance factors: Two essential mechanisms of Fusarium head blight resistance in wheat? *BMC Genomics, 13*, 369-391.
Guerinot, M. L., & Salt, D. E. (2001). Fortified foods and phytoremediation. Two sides of the same coin. *Plant Phsiology, 125*, 164-167.
Gupta, K., & Varshney, R. K. (2000). The development and use of microsatellite markers for genetic analysis and plant breeding with emphasis on bread wheat. *Euphytica, 113*, 163-185.
Gupta, P. K, Varshney, R. K., Sharma, P. C., & Ramesh, B. (1999). Molecular markers and their applications in wheat breeding. *Plant Breeding, 118*, 369-390.
Gutsche, A., Heng-Moss, T., Sarath, G., Twigg, P., & Xia, Y. (2009). Gene expression profiling of tolerant barley in response to *Diurapohis noxia* (Hemiptera: Aphididae) feeding. *Bulletin of Entomological Research, 99*, 163-173.
Gygi, S. P., Corthals, G. L., Zhang, Y., Rochon, Y., & Aebersold, R. (2000). Evaluation of two-dimensional gel electrophoresis based proteome analysis technology. *Proc. Natl. Acad. Sci. USA, 97*, 9390-9395.
Gygi, S. P., Rist, B., Gerber, S. A., Turecek, F., Gelb, M. H., & Aebersold, R. (1999). Quantitative analysis of complex protein mixtures using isotope-coded affiniity tags. *Nature Biotechnology, 17*(10), 994-999.

Haile, A., & Megenasa, T. (1987). Survey of the aphids in parts of Shewa, Welo and Tigrai, Ethiopia. *Ethiop. J. Agric. Sci, 9*, 39-53.

Haile, F. J., Higley, L. G., Ni, X., & Quisenberry, S. S. (1999). Physiological and growth tolerance in wheat to Russian wheat aphid (Homoptera: Aphididae) Injury. *Environmental Entomology, 28*(5), 787-794.

Haley, S. D. (2004). Registration of 'Ankor' wheat. *Crop Science, 44*, 1025-1026.

Hanke, G. T., Kimata-Ariga, Y., Taniguchi, I., & Hase, T. (2004). A post genomic characterisation of Arabidosis ferredixins. *Plant Phsiology, 134*, 255-264.

Harvey, J. (2011). Australian Grain Focus 2010-2011- Report. *Grains Research & Development Corporation (GRDC)*.

Helentjaris, T. , King, G., Slocum, M., Sidenstrang, C., & Wegman, S. (1985). Restriction fragment length polymorphism as probes for plant diversity and their development as tools for applied plant breeding. *Plant Mol. Biol, 5*, 109-118.

Heng-Moss, T., Ni, X., Macedo, T., Markwell, J. P., Baxendale, F. P., Quisenberry, S. S., & Tolmay, V. (2003). Comparison of chlorophyll and carotenoid concentrations among Russian wheat aphid (Homoptera: Aphididae) - Infested wheat isolines *Jounal of Economic Entomology, 96*(2), 475-481.

Heng, H. H., Krawetz, S. A., Lu, W., Bremer, S. W., Liu, G., & Ye, C. J. (2001). Re-defining the chromatin loop domain. *Cytogenet. Cell Genet.*(93), 155-161.

Heng, H. H. Q., Goetze, S., J., Ye C., Liu, G., Stevens, J. B., Bremer, S. W., . . . Krawetz, S. A. (2004). Chromatin loops are selectively anchored using scaffold/matrix-attachment regions. *Journal of Cell Science, 117*, 999-1008.

Hepler, P. K. (2005). Calcium: A central regulator of plant growth and development. *Plant Cell, 17*, 2141-2155.

Herrmann, K. M., & Weaver, L. M. (1999). The shikimate pathway. *Annu Rev Plant Physiol Plant Mol Biol, 50*, 473-503.

Hetherington, A. M., & Brownlee, C. (2004). The generation of Ca^{2+} signals in plants. *Annual Review of Plant Biology, 55*, 401-427.

Hewitt, P. H., Van Niekerk, G. J. J., Walters, M. C., Kriel, C. F., & Fouche, A. (1984). Russian aphid (*Diuraphis noxia*) feeding damage on wheat, related cereals, and a *Bromus* grass species. *In M. C. Walters [ed.] Progress in Russian wheat aphid (Diuraphis noxia Mordw.) research in the Republic of South Africa. Republic of South Africa Department of Agriculture Technical Communication No. 191*, 23-33.

Heyns, I., Groenewald, E., Marais, F., Du Toit, F., & Tolmay, V. (2006). Chromosomal location of the Russian wheat aphid resistance gene, Dn5. *Crop Science, 46*, 630-636.

Hill, C. B., Yan, L., & Hartman, G. L. (2004). Resistance to the soybean aphid in soybean germplasm. *Crop Science, 44*, 98-106.

Hodges, E., Xuan, Z., Balija, V., Kramer, M., Molla, M. N., Smith, S. W., . . . McCombie, W. R. (2007). Genome-wide in situ exon capture for selective resequencing. *Nat Genet, 39*(12), 1522-1527.

Hopfenberg, R., & Pimentel, D. (2001). Human population numbers as a function of food supply. *Environment, Development and Sustainability, 3*, 1-15.

Huang, H. E., Ger, M. J., Chen, C. Y., Pandey, A. K., Yip, M. K., Chou, H. W., & Feng, T. Y. (2007). Disease resistance to bacterial pathogens affected by the amount of ferredoxin-I protein in plants. *Mol Plant Pathol, 8*(1), 129-137.

Huang, Q., Borner, A., Roder, S., & Ganal, W. (2002). Assessing genetic diversity of wheat (*Triticum aestivum* L.) germplasm using microsatellite markers. *Theor Appl Genet, 105*(5), 699-707.

Hughes, R. D., & Maywald, G. F. (1990). Forecasting the favourableness of the Australian environment for the Russian wheat aphid, *Diuraphis noxia* (Homoptera: Aphididae), and its potential impact on Australian wheat yields. *Bulletin of Entomological Research, 80*(2), 165-175.

Issaq, H. , & Veenstra, T. (2008). Two-dimensional polyacrylamide gel electrophoresis (2D-PAGE): Advances and perspectives. *Biotechniques, 44*(5), 697-700.

Jacobs, D. I., van der Heijden, R., & Verpoorte, R. . (2000). Proteomics in plant biotechnology and secondary metabolism research *Phytochem. Anal, 11*, 277-287.

Jankielsohn, Astrid. (2011). Distribution and diversity of Russian wheat aphid (Hemiptera: Aphididae) biotypes in South Africa and Lesotho. *Journal of Economic Entomology, 104*(5), 1736-1741.

Jaouannet, M., Rodriguez, P. A., Thorpe, P., Lenoir, C. J., MacLeod, R., Escudero-Martinez, C., & Bos, J. I. (2014). Plant immunity in plant-aphid interactions. *Front Plant Sci, 5*, 663.

Jeffery, L. D., & Jonathan, D. G. Jones. (2001). Plant pathogens and integrated defence responses to infection *Nature, 411*, 826-833.

Jia, J., Devos, K. M., Chao, S., Miller, T. E., Reader, S. M. , & Gale, M. D. (1996). RFLP based maps of the homoeologous group 6 chromosomes of wheat and their application in the tagging of *Pm12*, a powdery mildew resistance gene transferred from *Aegilops speltoides* to wheat. *Theor Appl Genet, 92*, 559-565.

Juliana, P., Rutkoski, J. E., Poland, J. A., Singh, R. P., Murugasamy, S., Natesan, S., . . . Sorrells, M. E. (2015). Genome-wide association mapping for leaf tip necrosis and pseudo-black chaff in relation to durable rust resistance in wheat. *The Plant Genome, 8*(2).

Jyoti, J. L., Qureshi, J. P., Michaud, J. P., & Martin, T. J. (2006). Virulance of two Russian what aphid biotypes to eight wheat cultivars at two temperatures. *Crop Science, 46*, 774-780.

Kanno, T., Kasai, K., Ikejiri-Kanno, Y., Wakasa, K., & Tozawa, Y. (2004). In vitro reconstitution of rice anthranilate synthase: distinct functional properties of the alpha subunits OASA1 and OASA2. *Plant Mol. Biol, 54*, 11-22.

Kauss, H., Kohle, H. and Jeblick, W. (1983). Proteolytic activation and stimulation by Ca2+ of glucan synthase from soybean cells. *FEBS Lett., 158*, 84-88.

Kazemi, M., & van Emden, H. (1992). Parial antibiosis to *Rhopalosiphum padi* in wheat and some phytochemical correlations. *Ann Appl Biol, 121*, 1-9.

Keith, B., Dong, H., Ausubel, F. M., & Fink, G. R. (1991). Differential induction of 3-deoxy-D-arabino-heptulosonate 7-phosphate synthase genes in *Arabidopsis thaliana* by wounding and pathogenic attack. *Proc Natl Acad Sci USA, 88*, 8821-8825.

Kelley, L. A., Mezulis, S., Yates, C. M., Wass, M. N., & Sternberg, M. J. (2015). The Phyre2 web portal for protein modeling, prediction and analysis. *Nat Protoc, 10*(6), 845-858.

Kellogg, E. A. (2001). Evolutionary history of the grasses. *Plant Phsiology, 125*, 1198-1205.

Knoblauch, M., Peters, W. S., Ehlers, K. and van Bel, A. J.E. (2001). Reversible calcium-regulated stopcocks in legumw sieve tubes. *Plant Cell, 13*, 1221-1230.

Koebner, R. M. D., Miller, T. E., Snape, J. W. , & Law, C. N. (1988). Wheat endopeptidase: genetic control, polymorphism, intra chromosomal gene location and alien variation. *Genome 30*, 186-192.

Konishi, S., Izawa, T. , Lin, S. Y., Ebana, K., Fukuta, Y., Sasaki, T. , & Yano, M. (2006). A SNP caused loss of seed shattering during rice domestication. *Science, 312*, 1392–1396.

Kosambi, D. D. (1944). The estimation of map distances from recombination values. *Ann. Eugen, 12*, 172-175.

Kovalev, O. V., Poprawski, T. J., Stekolshchikov, A. V., Vereshchagina, A. B., & Gandrabur., S. A. (1991). *Diuraphis* Aizenberg (Hom., Aphididae): key to apterous viviparous females, and a review of Russian language literature on the natural history of *Diuraphis noxia* (Kurdjumov 1913). . *j. Appl. Ent., 112*, 425-436.

Kriel, C. F., Hewitt, P. H., De Jager, J, Walters, M. C., Fouche, A., & Van der Westhuizen, A. J. (1984). Aspects of the ecology of the Russian wheat aphid, *Diuraphis noxia*, in the Bloemfontein District. II. Population dynamics. *In M. C. Walters [ed.] Progress in Russian wheat aphid (Diuraphis noxia Mordw.) research in the Republic of South Africa. Republic of South Africa Department of Agriculture Technical Communication No. 191, 49*, 14-21.

Lacock, L., van Niekerk, C., Loots, S., Du Preez, F. B., & Botha, A. M. (2003). Functional and comparative analysis of expressed sequences from *Diuraphis noxia* infested wheat obtained utilizing the conserved Nucleotide Binding Site. *African Journal of Biotechnology, 2*, 75-81.

Lai, K., Duran, C., Berkman, P. J., Lorenc, M. T., Stiller, J., Manoli, S., . . . Edwards, D. (2012). Single nucleotide polymorphism discovery from wheat next-generation sequence data. *Plant Biotechnol J, 10*(6), 743-749.

Laloi, C., Mestres-Ortega, D., Marco, Y., Meyer, Y., & Reichheld, J. P. (2004). The Arabidopsis cytosolic thioredoxin *h5* gene induction by oxidative stress and its W-box-mediated response to pathogen elicitor. *Plant Physiol, 134*(3), 1006-1016.

Laloi, M. (1999). Plant mitochondrial carriers: an overview. *Cell. Mol. Life Sci., 56*, 918-944.

Lapitan, N. L. V., Peng, J., & Sharma, V. (2007). A high-density map and PCR markers for Russian wheat aphid resistance gene on chromosome 1RS/1BL. *Crop Science, 47*(2), 811-820.

Lazzari, S., Starkey, S., Reese, J., Ray-Chandler, A., McCubrey, R., & Smith, C. M. (2009). Feeding behavior of Russian wheat aphid (Hemiptera: Aphididae) biotype 2 in response to wheat genotypes exhibiting antibiosis and tolerance resistance. *J. Econ. Entomol., 102*(3), 1291-1300.

Lecourieux-Ouaked, F., Pugin, A., & Lebrun-Garcia, A. (2000). Phospho-proteins involved in the signal transduction of crytogein, an elicitor of defense reactions in tobacco. *Mol. Plant-Microbe Interact, 13*, 821-829.

Liu, H., Sun, W. B., Liang, R. B., Huang, L., Hou, J. L., & Liu, J. H. (2015). iTRAQ-based quantitative proteomic analysis of *Pseudomonas aeruginosa* SJTD-1: A global response to n-octadecane induced stress. *J Proteomics, 123*, 14-28.

Liu, M., Smith, M., & Gill, S. (2002). Identification of microsatellite markers linked to Russian wheat aphid resistance genes *Dn4* and *Dn6*. *Theor Appl Genet, 104*(6-7), 1042-1048.

Liu, X. M., Smith, C. M, Gill, B. S., & Tolmay, V. L. (2001). Microsatellite markers linked to six Russian wheat aphid resistance genes in wheat *Thero App Genet, 102*, 504-510.

Liu, X. M., Smith, C. M., Friebe, B. R., & Gill, B. S. (2005). Molecular mapping and allelic relationships of Russian wheat aphid resistance Genes. *Crop Science, 45*(6), 2273-2280.

Liu, X., Meng, J., Starkey, S., & Smith, M. (2011). Wheat gene expression is differentially affected by a virulent Russian wheat aphid biotype. *J Chem Ecol, 37*(5), 472-482.

Liu, Xiang, Marshall, Jeremy L., Stary, Petr, Edwards, Owain, Puterka, Gary, Dolatti, L., . . . Smith, C. Michael. (2010). Global Phylogenetics of *Diuraphis noxia* (Hemiptera: Aphididae), an Invasive Aphid Species: Evidence for Multiple Invasions Into North America. *Journal of Economic Entomology, 103*(3), 958-965.

Livak, K. J., Flood, S. J. A., Marmaro, J., Giusti, W., & Deetz, K. (1995). Oligonucleotides with fluorescent dyes at opposite ends provide a quenched probe system useful for detecting PCR product and nucleic acid hybridization. *Genome Res, 4*(6), 357-362.

Lyons, T. J., & Eide, D. J. (2006). Chapter 5: Transport and storage of metal ions in biology. *A Book: Metal Ion Bioavailability, 2*, 57-78.

Malkin, R. (1992). Cytochrome bc_1 and b_6f complexes of photosynthetic membranes. *Photosynthesis Research, 33*(2), 121-136.

Mammadov, J., Aggarwal, R., Buyyarapu, R., & Kumpatla, S. (2012). SNP markers and their impact on plant breeding. *Int J Plant Genomics*, 11p.

Manosalva, P. M., Davidson, R. M., Liu, B., Zhu, X., Hulbert, S. H., Leung, H., & Leach, J. E. (2009). A germin-like protein gene family functions as a complex quantitative trait locus conferring broad-spectrum disease resistance in rice. *Plant Physiol, 149*(1), 286-296.

Marais, G. F., Boshoff, W., & du Toit, F. (2007). Effect of segregation distortion on genetic mapping of a PI 294994-derived Russian wheat aphid resistance gene. *South African Journal of Plant and Soil, 24*(3), 178-180.

Marais, G. F., & Du Toit, F. (1993). A monosomic analysis of Russian wheat aphid resistance in the common wheat PI 294994. *Plant Breeding, 111*, 246-248.

Marais, G. F., Horn, M., & Du Toit, F. (1994). Intergeneric transfer (rye towheat) of gene(s) for Russian wheat aphid resistance. *Plant Breeding, 113*, 265-271.

Marais, G. F., Wessels, W. G., Horn, M., & du Toit, F. (1998). Association of a stem rust resistance gene (*Sr45*) and two Russian wheat aphid

resistance genes (*Dn5* and *Dn7*) with mapped structural loci in common wheat. *South African Journal of Plant and Soil, 15*(2), 67-71.
Marivet, J., Fredo, P., & Bukard, G. (1992). Effects of abiotic stresses on cyclophilin gene expression in maize and bean and sequence analysis of bean cyclophilin cDNA. *Plant Science, 84*, 171-178.
Marivet, J., Frendo, P., & Burkard, G. (1995). DNA sequence analysis of a cyclophilin gene from maize: developmental expression and regulation by salicylic acid. *Mol. Gen. Genet, 247*, 222-228.
Marrs, K. A. (1996). The functions and regulation of glutathione S-Transferases in plants. *Plant Physiol. Plant Mol. Biol., 47*(127-158).
Martin, B., Collar, J. L., Tjallingii, W. F., & Fereres, A. (1997). Intracellular ingestion and salivation by aphids may cause the acquisition and inoculation of non-persistently tranmitted plant viruses *Journal of general virology, 78*, 2701-2705.
Martínez-Pérez, E., Shaw, P., Reader, S., Aragón-Alcaide, L. , Miller, T. , & Moore, G. (1999). Homologous chromosome pairing in wheat. *Journal of Cell Science, 112*, 1761-1769.
Mauch-Mani, B., & Slusarenko, A. J. (1996). Production of salicylic acid precursors is a major function of phenylalanine ammonia-lyase in the resistance of Arabidopsis to *Peronospora parasitica*. *The Plant Cell, 8*, 203-212.
Mayer, M. P., & Bukau, B. (2005). Hsp70 chaperones: cellular functions and molecular mechanism. *Cell Mol Life Sci, 62*(6), 670-684.
Meharg, A. A. (1994). Integrated tolerance mechanisms: constitutive and adaptive plant responses to elevated metal concentrations in the environment. *Plant , Cell & Environ., 17*, 989-993.
Mensah, Clarice, DiFonzo, Christina, & Wang, Dechun. (2008). Inheritance of soybean aphid resistance in PI 567541B and PI 567598B. *Crop Science, 48, 5p*.
Miles, Peter W. (1999). Aphid Saliva *Biol. Rev., 74*, 41-85.
Millar, A. H., Liddell, A., & Leaver, C. J. (2001). Isolation and Subfractionation of Mitochondria from Plants. *A Book: Methods in Cell Biology, 65*.
Miller, G., & Mittler, R. (2006). Could heat shock transcription factors function as hydrogen peroxide sensors in plants? *Ann Bot, 98*(2), 279-288.
Mirik, M., Ansley, J., Michels, J., & Elliott, N. . (2009). Grain and vegetative biomass reduction by the Russian wheat aphid in winter wheat. *Southwestern Entomologist, 34*(2), 131-139.
Mittler, R., Vanderauwera, S., Gollery, M., & Van Breusegem, F. (2004). Reactive oxygen gene network of plants. *Trends Plant Sci, 9*(10), 490-498.

Mock, HP., Heller, W., Molina, A., Neubohn, B., Sandermann, H., & Grimm, B. (1999). Expression of uroporphyrinogen decarboxylase or coproporphyrinogen oxidase antisense RNA in tobacco induces pathogen defense responses conferring increased resistance to tobacco mosaic virus. *The Journal of Biological Chemistry, 274*(7), 4231-4238.

Morozova, O., & Marra, M. A. (2008). Application of next generation sequencing technologies in functional genomics. *Genomics, 92*(5), 255-264.

Morrison, W. P., & Peairs, F. B. (1998). Response model concept and economic impact. *In: Quisenberry SS, Peairs FB (eds). Response model for an introduced pest—the Russian wheat aphid. Thomas Say Publications in Entomology: Proceedings Entomological Society of America, Lanham, MD*, 1-11.

Mysore, K. S., & Ryu, C. M. (2004). Nonhost resistance: How much do we know? *Trends Plant Sci, 9*(2), 97-104.

Nesbitt, M. (2001). Wheat evolution: integrating archaeological and biological evidence. *Book: Wheat Taxonomy*, 37-55.

Ni, X., Quisenberry, S. S., Heng-Moss, T., Markwell, J., Sarath, G., Klucas, R., & Baxendale, F. (2001). Oxidative responses of reistant and susceptible cereal leaves to symptomatic and nonsymtomatic cereal aphid (Hemiptera: Aphididae) feeding. *J. Econ. Entomol., 94*(3), 743-751.

Nibouche, S., Fartek, B., Mississipi, S., Delatte, H., Reynaud, B., & Costet, L. (2014). Low genetic diversity in *Melanaphis sacchari* aphid populations at the worldwide scale. *PLoS One, 9*(8).

Nicholson, S. J., Hartson, S. D., & Puterka, G. J. (2012). Proteomic analysis of secreted saliva from Russian wheat aphid (*Diuraphis noxia* Kurd.) biotypes that differ in virulence to wheat. *J Proteomics, 75*(7), 2252-2268.

Nkongolo, K. K, Quick, J. S, Limin, A. E, & Fowler, D. B. (1991b). Sources of inheritanceof resistance to Russian wheat aphid in Triticum species amphiploids and *Triticum tauschii.* . *Can J Plant Sci, 71*, 703-708.

Nkongolo, K. K, Quick, J. S, Peairs, F. B., & Meyer, W. L. (1991a). Inheritance of resistance of PI373129 wheat to the Russian wheat aphid. *Crop Science, 31*, 905-906.

Novotna, J., Havelka, J., Stary, P., Koutecky, P., & Vitkova, M. (2011). Karyotype analysis of the Russian wheat aphid, *Diuraphis noxia* (Kurdjumov) (Hemiptera: Aphididae) reveals a large X chromosome with rRNA and histone gene families. *Genetica, 139*(3), 281-289.

O'Farrell, P. H. (1975). High resolution two-dimensional electrophoresis of proteins. *J Biol Chem, 250*, 4007-4021.

Okazaki, M., Hino, F. , Nagasawa, K. , & Miura, Y. (1982). Effects of nutritional factors on formation of scopoletin and scopolin in tobacco tissue cultures. *Agric. Biol. Chem, 46*(3), 601-607.

Oliver, D. J., Neuburger, M., Bourguignon, J., & Douce, R. (1990). Interaction between the component enzymes of the glycine decarboxilase multienzyme complex. *Plant Phsiology, 94*, 833-839.

Oliver, D. J., Neuburger, M., Bourguignon, J., & Douce, R. (1990 b). Glycine metabolism by plant mitochondria. *Physiologia Plantarum, 80*, 487-491.

Ong, S. E., Blagoev, B., Kratchmarova, I., Kristensen, D. B., Steen, H., Pandey, A., & Mann, M. (2002). Stable isotope labeling by amino acids in cell culture, SILAC, as a simple and accurate approach to expression proteomics. *Molecuar and Cellular Proteomics, 1*(5), 376-386.

Ozkan, H., Levy, A. A., & Feldman, M. (2001). Allopolyploidy-induced rapid genome evolution in the wheat (*Agilops-Triticum*) group. *The Plant Cell, 13*, 1735-1747.

Painter, R. H. (1951). Insect resistance in crop plants. *The macmillan Co., New York*, Pp 520.

Painter, R. H. (1958). Resistance of plants to insects. *Annual Review of Entomology, 3*, 267-290.

Park, O. K. (2004). Proteomic studies in plants. *Journal of Biochemistry and Molecular Biology, 37*(1), 133-138.

Park, S. J., Huang, Y., & Ayoubi, P. (2006). Identification of expression profiles of sorghum genes in response to greenbug phloem-feeding using cDNA subtraction and microarray analysis. *Planta, 223*, 932-947.

Pathak, R. S., Kinduiwa, K. J., Kinyua, M. G., & Malinga, J. (2007). Evidence of duplicate gene loci for resistance to Russian wheat aphid (*Diuraphis noxia* Mordvilko) in bread wheat. *African Crop Science Conference Proceedings, 8*, 703-708.

Peng, J., Wang, H., Haley, S. D., Peairs, F. B., & Lapitan, N. L. V. (2007). Molecular mapping of the Russian wheat aphid resistance gene *Dn2414* in wheat. *Crop Science, 47*(6), 2418-2429.

Perez-Ortin, J. E., Alepuz, P. M., & Moreno, J. (2007). Genomics and gene transcription kinetics in yeast. *Trends Genet, 23*(5), 250-257.

Peterson, B. K., Weber, J. N., Kay, E. H., Fisher, H. S., & Hoekstra, H. E. (2012). Double digest RADseq: An inexpensive method for de novo SNP discovery and genotyping in model and non-model species. *PLoS One, 7*(5), 11p.

Pingault, L., Choulet, F., Alberti, A., Glover, N., Wincker, P., Feuillet, C., & Paux, E. (2015). Deep transcriptome sequencing provides new

insights into the structural and functional organization of the wheat genome. *Genome Biol, 16*, 1-29.
Plaschke, J., Ganal, M. W., & Roder, M. S. (1995). Detection of genetic diversity in closely related bread wheat using microsatellite markers. *Theor Appl Genet, 91*, 1001-1007.
Poehlman, J. M., & Sleper, D. E. (1995). Breeding Field Crops, Ames, lowa, USA.
Poland, J. A., & Rife, T. W. (2012). Genotyping-by-sequencing for plant breeding and genetics. *The Plant Genome Journal, 5*(3), 92.
Powell, G., Tosh, C. R., & Hardie, J. (2006). Host plant selection by aphids: Behavioral, evolutionary, and applied perspectives. *Annu Rev Entomol, 51*, 309-330.
Pozniak, C. J., Clarke, J. M., & Clarke, F. R. (2012). Potential for detection of marker–trait associations in durum wheat using unbalanced, historical phenotypic datasets. *Molecular Breeding, 30*(4), 1537-1550.
Puterka, G. J., Giles, K. L., Brown, M. J., Nicholson, S. J., Hammon, R. W., Peairs, F. B., . . . Mornhinweg, D. W. (2015). Change in biotypic diversity of Russian wheat aphid (Hemiptera: Aphididae) populations in the United States. *J Econ Entomol, 108*(2), 798-804.
Quick, J. S, Stromberger, J. A., Clayshulte, S., Clifford, B. L., Johnson, J. J., Peairs, F. B., . . . Lorenz, K. (2001). Registration of Prairie Red Wheat. *Crop Science, 41*, 1362.
Quick, J. S., Ellis, G. E., Norman, R. M., Stromberger, J. A., Shanahan, J. F., Peairs, F. B., . . . Lorenz, K. (1996). Registration of 'Halt' wheat. *Crop Science, 36*, 210.
Randolph, T. L., Peairs, B. F., Weiland, A. A, Rudolph, J. B., & Puterka, G. J. (2009). Plant responses to seven Russian wheat (Hemiptera: Aphididae) biotypes found in the Unites States. *Jounal of Economic Entomology, 102*(5), 1954-1959.
Ratnadass, A., Fernandes, P., Avelino, J. , & Habib, R. (2011). Plant species diversity for sustainable management of crop pests and diseases in agroecosystems: a review. *Agronomy for Sustainable Development, 32*(1), 273-303.
Ricciardi, M., Tocho, E., Tacaliti, M. S., Vasicek, A., Giménez, D. O, A. Paglione, A., . . . Castro, A. M. (2010). Mapping quantitative trait loci for reisitance against Russian wheat aphid (*Diuraphis noxia*) in wheat (*Triticum aestivum* L.) *Crop & Pasture Science, 61*, 970-977.
Riedell, W. E., & Kieckhefer, R. W. (1995). Feeding damage effects of three aphid species on wheat root growth. *Plant Nutrition, 18*(9), 1995.
Roberts, F., Roberts, C. W., Johnson, J. J., Kyle, D. E., Krell, T., Coggins, J. R., . . . McLeod, R. (1998). Evidence for the shikimate pathway in apicomplexan parasites. *Nature, 393*, 801-805.

Robinson, J. (1994). Identification and characterization of resistance to the Russian wheat aphid in small-grain cereals: Investigations at CIMMYT, 1990-92. *CIMMYT Research Report No. 3, Mexico, D.F.: CIMMYT*.

Roder, M. S., Plaschke, J., Konig, S. U., Borner, A., Sorrells, M. E., Tanksley, S. D., & Ganal, M. W. (1995). Abundance, variability and chromosomal location of microsatellites in wheat. *Mol Gen Genet., 246*, 327-333.

Ronald, F. (2015). World Agricultural Production - Circular Series WAP 11-15, November 2015. *United States Department of Agriculture (http://www.pecad.fas.usda.gov)*.

Ross, P. L., Huang, Y. N., Marchese, J. N., Williamson, B., Parker, K., Hattan, S., . . . Pappin, D. J. (2004). Multiplexed protein quantitation in *Saccharomyces cerevisiae* using amine reactive Isobaric Tagging Reagents. *Molecuar and Cellular Proteomics, 13*(12), 1154-1169.

Rouhier, N., Gelhaye, E., & Jacquot, J. P. (2004). Plant glutaredoxins: Still mysterious reducing systems. *Cell Mol Life Sci, 61*(11), 1266-1277.

Saheed, S. A., Botha, C. E. J., Liu, L., & Jonsson, L. (2006). Comparison of structural damage caused by Russian wheat aphid (*Diuraphis noxia*) and Bird cherry-oat aphid (*Rhopalosiphum padi*) in a susceptible barley cultivar, *Hordeum vulgare* cv. Clipper. . *Physiologia Plantarum, 129*(2), 429-435.

Saidi, A., & Quick, J. S. (1996). Inheritance and allelic relationships among Russian wheat aphid resistance genes in winter wheat. *Crop Science, 36*, 256-258.

Sari-Gorla, M., Ferrario, S., Rossini, L., Frova, C., & Villa, M. (1993). Developmental expression of glutathione S-transferase in maize and its possible connection with herbicide tolerance. *Euphytica, 67*, 221-230.

Shevchenko, A. , N., Jensen O., Podtelejnikov, A. V. , Sagliocco, F., Wilm, M., Vorm, O. , . . . Mann, M. (1996). Linking genome and proteome by mass spectrometry: Large-scale identification of yeast proteins from two dimensional gels. *Proc Natl Acad Sci USA, 93*, 14440-14445.

Simkova, H., Safar, J., Kubalakova, M., Suchankova, P., Cihalikova, J., Robert-Quatre, H., . . . Dolezel, J. (2011). BAC libraries from wheat chromosome 7D: Efficient tool for positional cloning of aphid resistance genes. *J Biomed Biotechnol, 2011*, 11p.

Siwinska, J., Kadzinski, L., Banasiuk, R., Gwizdek-Wisniewska, A., Olry, A., Banecki, B., . . . Ihnatowicz, A. (2014). Identification of QTLs affecting scopolin and scopoletin biosynthesis in *Arabidopsis thaliana*. *BMC Plant Biol, 280*, 1-14.

Sjolund, R. D. , & Shih, C. Y. (1983). Freeze-fracture analysis of phloem structure in plant tissue culture. I. The sieve element reticulum. . *J.Ultrastruct. Res., 82*, 111-121.

Smith, C. M. (2005). Book - Plant Resistance to Arthropods: Molecular and Conventional Approaches.

Smith, C. M., Belay, T., Stauffer, C., Stary, P., Kubeckova, I., & Starkey, S. (2004). Identification of Russian wheat aphid (Homoptera: Aphididae) populations virulent to the *Dn4* resistance gene. *Jounal of Economic Entomology, 97*, 1112-1117.

Smith, C. M., & Boyko, E. V. (2007). The molecular bases of plant resistance and defense responses to aphid feeding: Current status. *Entomologia Experimentalis et Applicata, 122*(1), 1-16.

Smith, C. M., & Chuang, W. P. (2014). Plant resistance to aphid feeding: behavioral, physiological, genetic and molecular cues regulate aphid host selection and feeding. *Pest Manag Sci, 70*(4), 528-540.

Smith, C. M., & Clement, S. L. (2012). Molecular bases of plant resistance to arthropods. *Annu Rev Entomol, 57*, 309-328.

Smith, C. M., Liu, X., Wang, L. J., Liu, X., Chen, M. S., Starkey, S., & Bai, J. (2010). Aphid feeding activates expression of a transcriptome of oxylipin-based defense signals in wheat involved in resistance to herbivory. *J Chem Ecol, 36*(3), 260-276.

Smith, C. M., Schotzko, D., Zemetra, R. S., Souza, E. J., & Schroeder-Teeter, S. (1991). Identification of Russian wheat aphid (Homoptera:Aphididae) resistance in wheat. *Jounal of Economic Entomology, 84*(1), 328-332.

Smith, M. C., Schotzko, D. J., Zemetra, R. S., & Souza, E. J. (1992). Categories of resistance in plant introductions of wheat resistant to the Russian wheat aphid (Homoptera: Aphididae). *Journal of Economic Entomology, 85*(4), 1480-1484.

Somers, D. J., Issac, P., & Edwards, K. (2004). A high-density microsatellite consensus map for bread wheat (*Triticum aestivum* L.) *Theor Appl Genet, 109*, 1105-1114.

Sorrells, M. E., La Rota, M., Bermudez-Kandianis, C. E., Greene, R. A., Kantety, R., Munkvold, J. D., . . . Qualset, C. O. (2003). Comparative DNA sequence analysis of wheat and rice genomes. *Genome Res, 13*(8), 1818-1827. doi: 10.1101/gr.1113003

Stankova, H., Valarik, M., Lapitan, N. L., Berkman, P. J., Batley, J., Edwards, D., . . . Simkova, H. (2015). Chromosomal genomics facilitates fine mapping of a Russian wheat aphid resistance gene. *Theor Appl Genet, 128*(7), 1373-1383.

Steemers, F. J., & Gunderson, K. L. (2007). Whole genome genotyping technologieson the BeadArray platform. *Biotechnology Journal, 2*(1), 41-49.

Stein, G. S., van Wijnen, A. J., Stein, J. L., & Lian, J. B. (1999). Interrelationships of transcriptional machinery with nuclear architecture. *Crit. Rev. Eukaryotic Gene Expr., 9*, 183-190.

Studham, M. E. , & MacIntosh, G. C. (2013). Multiple phytohormone signals control the transcriptional response to soybean aphid infestation in susceptible and resistant soybean plants. *Molecular Plant-Microbe interactions, 26*(1), 116-119.

Sumer, H., Craig, J. M., Sibson, M., & Choo, K. H. (2003). A rapid method of genomic array analysis of scaffold/matrix attachment regions (S/MARs) identifies a 2.5-Mb region of enhanced scaffold/matrix attachment at a human neocentromere. *Genome Res, 13*, 1737-1743.

Summers, C. G., & Godfrey, L. D. (www.ipm.ucdavis.edu). UC IPM Pestmangement Guidelines: Small Grains. *UC ANR Publication 3466: Insects and mites (www.ipm.ucdavis.edu)*.

Tanguy, J., & Martin, C. (1972). Phenolic compounds and the hypersensitivity reaction in *Nicotiana tabacum* infected with Tobacco mosaic virus. *Phytochemistry, 11*, 19-28.

Tanigoshi, L. K., Miller, R. H., Miller, T.D., & Allison, D. (1995). Search for, and release of, parasitoids for the biological control of Russian wheat aphid in Washington state (USA). *Agriculture, Ecosystems and Environment, 52, 25-30, 52*, 25-30.

Tanksley, S. D. (1983). Molecular markers in plant breeding. *Plant Mol. Biol, 1*, 1-3.

Tanksley, S. D., & Rick, C. M. (1980). Isozyme gene linkage map of the tomato: Applications in genetics and breeding. *Theor Appl Genet, 92*, 191-203.

Thomas, J. G. (1986). The Russian wheat aphid, *Diuraphis noxia* (Mordvilko): A new pest of Texas grain crops (memo) Extension Entomologist, Texas A &M University, College Station, TX.

Thomine, S., & Schroeder, J. I. Plant metal transporters with homology to proteins of the NRAMP Family. *Madame Curie Bioscience Database (www.ncbi.nlm.gov/books/NBK6452)*.

Thompson, D. C. (1987). Russian wheat aphid news. 3 April, 5 June, 19 June, 2 July, and 22 July issues. State Survey Coordinator, Department of Entomology, Colorado State University, Fort Collins, CO 80523.

Tingey, W. M. , & Laubengayer, J. E. (1981). Defense against the green peach aphid and potato leafhopper by glandular trichomes of *Solanum berthaultii*. *Journal of Economic Entomology, 74*(6), 721-725.

Tjallingii, W. F. (2006). Salivary secretions by aphids interacting with proteins of phloem wound responses. *J Exp Bot, 57*(4), 739-745.
Tjallingii, W. F., & Hogen Esch, T. H. (1993). Fine structure of aphid stylet routes in plant tissues in correlation with EPG signals. *Physiological Entomology, 18*, 317-328.
Tognetti, V. B., Palatnik, J. F., Fillat, M. F., Melzer, M., Hajirezaei, M. R., Valle, E. M., & Carrillo, N. (2006). Functional replacement of ferredoxin by a cyanobacterial flavodoxin in tobacco confers broad-range stress tolerance. *Plant Cell, 18*, 2035-2050.
Tolmay, V. L., & Booyse, M. (2016). Valuable Russian wheat aphid-resistant bread wheat accessions identified using four South African *Diuraphis noxia* biotypes. *South African Journal of Plant and Soil*, 1-6.
Tolmay, V. L., Jankielsohn, A., & Sydenham, S. L. (2012). Resistance evaluation of wheat germplasm containing *Dn4* or *Dny* against Russian wheat aphid biotype RWASA3. *Journal of Applied Entomology, 137*(6), 476-480.
Tozawa, Y., Hasegawa, H., Terakawa, T., & Wakasa, K. (2001). Characterizationof rice anthranilate synthase alpha-subunit genes OASA1 and OASA2. Tryptophan accumulation in transgenic rice expressing a feedback-insensitive mutant of OASA1. *Plant Phsiology, 126*, 1493-1506.
Turanli, F., Ilker, E., Ersin Dogan, F., Askan, L., & Istipliler, D. (2012). Inheritance of resistance to Russian wheat aphid (*Diuraphis noxia* Kurdjumov) in bread wheat (*Triticum aestivum* L.). *Turkish Journal of Field Crops, 17*(2), 171-176.
Valdez, V. A., Byrne, P. F., Lapitan, N. L. V., Peairs, F. B., Bernardo, A. N., Bai, G., & Haley, S. D. (2012). Inheritance and genetic mapping of Russian wheat aphid resistance in Iranian wheat landrace accession PI 626580. *Crop Science, 52*(2), 676-682.
Valle, T., Lopez, J. L., Hernandez, J. M., & Corchete, P. (1997). Antifungal activity of scopoletin and its differential accumulation in *Ulmus pumila* and *Ulmus campestris* cell suspension cultures infected with *Ophiostoma ulmi* spores. *Plant Science, 125*(1), 97-101.
van Assche, F., & Clijsters, H. (1990). Effects of metals on enzyme activity in plants. *Plant, Cell & Enviorn., 13*(3), 195-206.
Van der Westhuizen, A. J., Qian, X.M., & Botha, A. M. (1998a). β-1-3-glucanases in wheat and resistance to the Russian wheat aphid. *Physiol Plant, 103*, 125-131.
Van der Westhuizen, A. J., Qian, X.M., & Botha, A. M. (1998b). Differential induction of apoplastic peroxidase and chitinase activities in susceptible and resistant wheat cultivars by Russian wheat aphid infestation. *Plant Cell Reports, 18*, 132-137.

Vieira Dos Santos, C., & Rey, P. (2006). Plant thioredoxins are key actors in the oxidative stress response. *Trends Plant Sci, 11*(7), 329-334.
Vos, P., Hogers, R. , Reijans, M. , van de Lee, T., Hornes, M., Friters, A., . . . Zabeau, M. (1995). AFLP: a new technique for DNA fingerprinting. *Nucl. Acids Res., 23*, 4407-4414.
Vucich, V. A., & Gasser, C. S. (1996). Novel structure of a high molecular wight FK506 binding protein from *Arabidopsis thaliana Mol. Gen. Genet, 252*, 510-517.
Walters, M. C., Penn, F., Du Toit, F., Botha, T. C., Aalbersberg, K., Hewitt, P. H., & Broodryk, S. W. (1980). The Russian wheat aphid. *Farming in South Africa, Leaflet Series, Wheat C3, Government Printer, Pretoria*, 1-6.
Walters, M. C., Penn, F., Du Toit, F., Botha, T. C., Aalbersberg, K., Hewitt, P. H., & Broodryk, S. W. (1984). The Russian wheat aphid. . *In M. C. Walters (ed): Progress in Russian wheat aphid (Diuraphis noxia Mordw.) research in the Republic of South Africa. Republic of South Africa Department of Agriculture Technical Communication No. 191, 72-78, 191*, 72-78.
Wang, J., Li, H., Zhang, L., & Meng, L. (2014). Users' Manual of QTL IcIMapping. Version 4.0, revised May 2014. http://www.isbreeding.net.
Wang, P., & Heitman, J. (2005). The cyclophilins. *Genome Biol, 6*(7), 226.
Wang, W., Tai, F., & Chen, S. (2008). Optimizing protein extraction from plant tissues for enhanced proteomics analysis. *J Sep Sci, 31*(11), 2032-2039.
Weaver, L. M., & Herrmann, K. M. (1977). Dynamics of the shikimate pathway in plants. *Trends Plant Sci, 2*, 346-351.
Webster, J. A., & Starks, K. J. (1987). Fecundity of *Schizaphis graminum* and *Diuraphis noxia* (Homoptera:Aphididae) at three temperature regimes *Journal of the Kansas Entomological Society, 60*(4), 580-582.
Weining, S., & Langridge, P. (1991). Identification and mapping of polymorphisms in cereals based on the polymerase chain reaction. *Theor Appl Genet, 82*(2), 209-216.
Wiese, S., Reidegeld, K. A., Meyer, H. E., & Warscheid, B. (2007). Protein labeling by iTRAQ: A new tool for quantitative mass spectrometry in proteome research. *Proteomics, 7*(3), 340-350.
Will, T., Kornemann, S. R., Furch, A. C., Tjallingii, W. F., & van Bel, A. J. (2009). Aphid watery saliva counteracts sieve-tube occlusion: a universal phenomenon? *J Exp Biol, 212*(20), 3305-3312.
Will, T., Tjallingii, W. F., Thonnessen, A. , & van Bel, A. J. (2007). Molecular sabotage of plant defense by aphid saliva. *Proc Natl Acad Sci USA, 104*(25), 10536-11041.

Will, T., & van Bel, A. J (2006). Physical and chemical interactions between aphids and plants. *J. Exp. Bot. , 57*, 729-735.
Williams, J. G. K., Kubelik, A. R. K., Livak, J. L., Rafalski, J. A., & Tingey, S. V. (1990). DNA polymorphisms amplified by random primers are useful as genetic markers. *Nucl. Acids Res., 18*, 6531-6535.
Williams, L. E., Pittman, J. K., & Hall, J. L. (2000). Emerging mechanisms for heavy metal transport in plants. *Biochim. Biophys. Acta., 1465*, 104-126.
Wittstock, U., & Gershenzon, J. (2002). Constitutive plant toxins and their role in defense against herbivores and pathogens. *Plant Biology 5*, 1-8.
Wright, B. D. (2012). International grain reserves and other instruments to address volatility in grain markets. *The World Bank Research Observer, Published by Oxford University press, doi:10.1093/wbro/lkr016*, 1-39.
Wright, S. I., Bi, I. V., Schroeder, S. G., Yamasaki, M., Doebley, J. F., McMullen, M. D., & Gaut, B. S. (2005). The effects of artificial selection on the maize genome. *Science, 308*(5726), 1310-1314.
Xu, Y., & Crouch, J. H. (2008). Marker-Assisted selection in Plant breeding: From Publication to Practice *Crop Science, 48*, 391-407.
Zaayman, D., Lapitan, N. L., & Botha, A. M. (2009). Dissimilar molecular defense responses are elicited in *Triticum aestivum* after infestation by different *Diuraphis noxia* biotypes. *Physiol Plant, 136*(2), 209-222.
Zadoks, J. C., Chang, T. T., & Konzak, C. F. (1974). A decimal code for the growth stages of cereals. *Water Research, 14*, 415-421.
Zerene, Z. M., Caglevich, M. D., & Ramirez, L. R. (1988). Un neuvo afido de los cereals detectado en Chile. . *Agricultura Tecnica (Chile), 48*, 60-61.
Zhang, B., Edwards, O. R., Kang, L., & Fuller, S. J. (2012). Russian wheat aphids (*Diuraphis noxia*) in China: Native range expansion or recent introduction? *Mol Ecol, 21*(9), 2130-2144.
Zhang, G. (1991). Russian wheat aphid (RWA) in China. . *In: Proceedings of aphid-plant interactions: populations to molecules, August 12-17, 1990. Stillwater, Oklahoma, USA*, 327-328.
Zhang, Z., Guo, X., Liu, B., Tang, L., & Chen, F. (2011). Genetic diversity and genetic relationship of Jatropha curcas between China and Southwest Asian revealed by amplified fragment length polymorphisms. *African Journal of Biotechnology, 10*(15), 2825-2832.